Biochemical and cellular consequences of lumiflavin-induced riboflavin depletion in human intestinal epithelial cells

EUN-SOOK LEE

Human Nutrition Unit

Department of Oncology

The Faculty of Medicine, Dentistry and Health

University of Sheffield

A thesis submitted for the degree of Doctor of Philosophy

August, 2014

ACKNOWLEDGEMENT

STATEMENT OF INVOLVEMENT

Some measurements were made by others due to limited access to required facilities. These were High performance liquid chromatography (HPLC) for intracellular flavin assay, which was done by Mrs. Marilyn Hill in the Human Nutrition Unit, the Department of Oncology at the University of Sheffield; high content analysis, which was carried out by Dr. Gareth Griffiths at Imagen Biotech, Cheshire, UK, and HILIC fractionation and mass spectrometry, which were carried out by Dr. Caroline Evans in the Department of Chemical and Biological Engineering at the University of Sheffield.

ABSTRACT

Riboflavin is an essential component of the human diet, with an established role for its derivative cofactors, flavin mononucleotide (FMN) and flavin adenine dinucleotide (FAD), in oxidative metabolism. It has previously been demonstrated that luminal but not systemic riboflavin depletion leads to a dysregulation of normal gastrointestinal development. It is hypothesised that riboflavin depletion of intestinal cells in culture interrupts cell signalling pathways, with associated adverse functional effects. The overall aim was to develop and characterise an intestinal cell model of riboflavin depletion using the structural analogue of riboflavin, lumiflavin, which inhibits riboflavin uptake, and to assess the role of riboflavin on cell signalling.

A model of riboflavin depletion was established in three intestinal cell lines, (Caco-2, HCT116 and HT29) through treatment with lumiflavin. Intracellular flavin concentrations and glutathione reductase activation coefficient (GRAC) were measured as markers of riboflavin status. Intracellular ATP concentration, the generation of reactive oxygen species (ROS), clonogenicity and apoptotic DNA fragmentation were determined. Effects of riboflavin depletion on cell signalling were examined in only Caco-2 cells. Changes in the phosphorylation of amino acid residues were determined as an indicator of effects on cell signalling, using western blot and high content analysis (HCA). Isobaric tagging for relative and absolute quantitation (iTRAQ) was used for phosphoprotein profiling, followed by validation of the findings by western blot. HCA and flow cytometry were used to determine changes in the cell cycle.

Cell growth was inhibited by lumiflavin in all three cell lines, in a concentration-dependent manner. Intracellular flavin status was significantly decreased in all cell lines by 48 hours. Riboflavin depletion by lumiflavin led to a significant reduction in intracellular ATP concentration and an enhanced generation of ROS in all cell lines. A cell-specific irreversible loss of proliferative ability was observed. The effect of riboflavin depletion on oxidative stress and disruption of energy generation may have contributed to the observed effects on cell proliferation. There was no effect of lumiflavin on apoptotic DNA fragmentation in any cell line. Lumiflavin resulted in changes in the global phosphorylation of tyrosine by 3-6 hours, before biochemical riboflavin depletion was evident. Significant changes in mRNA processing and apoptosis pathways were found. Lumiflavin seemed to suppress cell signalling. Lumiflavin also caused arrest of cells in S phase with a subsequent G2/M phase block.

In conclusion, riboflavin depletion of intestinal cells by lumiflavin had biochemical and functional consequences. Alterations in cell signalling and arrest in S phase with induction of apoptosis in response to lumiflavin may be causative of adverse consequences on intestinal cell proliferation.

CONTENTS

LIST OF FIGURES

LIST OF TABLES

LIST OF APPENDIX

ABBREVIATIONS

APS	Ammonium persulfate
AspM	Abnormal spindle homolog, the human ortholog of the Drosophila melanogaster asp.
ADP	Adenosine diphosphate
AMP	Adenosine monophosphate
ANOVA	Analysis of variance
ATP	Adenosine triphosphate
BIRC5	Baculoviral IAP repeat-containing 5, IAP (Survivin)
BrdU	Bromodeoxyuridine
BSA	Bovine serum albumin
CCNG2	Cyclin G2
Cdc25 phosphatase	Cell division cycle 25 phosphatase
CDCA2	Cell division cycle associated 2
CDK	Cyclin-dependent kinase
CHAPS	3-[(3-cholamidopropyl) dimethylammonio]-1-propanesulfonate
CKIs	Cyclin-dependent kinase inhibitors
DCFDA	2',7'-dichlorodihydrofluorescein diacetate
ddH$_2$O	Deionised distilled H$_2$O
DMEM	Dulbecco's minimum essential medium
DMSO	Dimethyl sulfoxide
DNA	Deoxyribonucleic acid
ECL	Enhanced chemiluminescence
EDTA	Ethylene diamine tetraacetic acid disodium salt solution
EGRAC	Erythrocyte glutathione reductase activation coefficient
EGTA	Ethylene glycol-bis(2-aminoethylether)-N,N,N',N'-tetraacetic acid
FAD	Flavin adenine dinucleotide
FCS	Foetal calf serum
FMN	Flavin mononucleotide
G1 / G2	Gap1 / gap2 phase
GI tract	Gastrointestinal tract
GR	Glutathione reductase

GRAC	Glutathione reductase activation coefficient
GSH	Reduced glutathione
GSSG	Oxidised glutathione
HBSS	Hank's balanced salt solution
HCA	High content analysis
HILIC	Hydrophilic interaction liquid chromatography
HPLC	High performance liquid chromatography
iTRAQ	Isobaric tag for relative and absolute quantitation
LC-MS/MS	Liquid chromatography tandem mass spectrometry
LF	Lumiflavin
LRNI	Lower reference nutrient intakes
M	Mitosis phase
MMTS	Methyl methane ethiosulfonate
MPF	Mitosis promoting factor
MS	Mass spectrometry
MTT	3-(4,5-Dimethylthiazol-2-yl)-2,5-diphynyltetrazolium bromide
NADPH oxidase	Nicotinamide adenine dinucleotide phosphate-oxidase
NaF	Sodium floride
NaVO$_4$	Sodium orthovanadate
NDNS	The National Diet and Nutritional Survey
P	Probability
PI	Propidium iodide
PBS	Phosphate buffered saline
PBST	Phosphate buffered saline with tween 20
pHH3	Phosphorylated histone H3
PMSF	Phenylmethanesulfonyl fluoride
PVDF	Polyvinylidene fluoride
QC	Quality control
RFVT	Riboflavin transporter
RNA / mRNA	Ribonucleic acid / messenger Ribonucleic acid
RNI	Reference nutrient intakes
ROS	Reactive oxygen species
S	DNA synthesis phase
SCX	Strong cation exchange

SDS	Sodium dodecyl sulphate
SDS-PAGE	Sodium dodecyl sulfate-polyacrylamide gel electrophoresis
SEM	Standard error of mean
SR	Serine/arginine-rich splicing factor proteins family
SRSF	Serine/arginine-rich splicing factor
TCA	Trichloroacetic acid
TBST	Tris buffered saline with tween 20
TCEP	Tris-(2-carboxyethyl)phosphine hydrochloride
TEAB	Triethylammonium bicarbonate buffer
TEMED	Tetramethylenediamine
THF	Tetrahydrofolate
TNF	Tumour necrosis factor
TNFR1	Tumour necrosis factor receptor 1
TOF	Time of flight

CHAPTER 1

INTRODUCTION

1.1.   Introduction

The human body is maintained by reproducing cells through the cycle of cells' duplication and division. Eukaryotic cells divide to form two genetically identical daughter cells through the cell cycle, and the process repeatedly occurs thus maintaining functioning organs of the human body (Alberts, 2008). Abnormal cell proliferation and cell death through mis-controlling of the cell cycle can affect tissue maintenance and development which are critically important for tissues in which cells are rapidly renewed and replaced such as the gastrointestinal tract (GI tract) (Heath, 1996).

Macronutrients i.e. carbohydrates, proteins, and fatty acids are essential for cell proliferation as sources of cellular fuel, and micronutrients also contribute to proper control of the cell cycle however this function is less well understood (Bohnsack and Hirschi, 2004). This study has a particular focus on the role of riboflavin in regulation of intestinal cell proliferation through an effect on cell signalling. This is a key process for cells to initiate and conduct various processes involved in metabolism, proliferation, differentiation, cell death and so on.

This thesis explores effects of cellular riboflavin deficiency on functions relevant to the cell cycle and the effect of an inhibitor of riboflavin uptake into cells on cell signalling.

1.1.1.   Riboflavin

1.1.1.1. Riboflavin

Riboflavin is a water-soluble vitamin, also known as vitamin B2, obtained from human diet or bacterial synthesis in large intestine. Free riboflavin (7,8-dimethyl-10-ribityl-isoalloxazine) consists of a conjugated isoalloxazine ring and the sugar alcohol ribitol as shown in Figure 1. Riboflavin is a precursor of metabolically active forms, FMN (flavin mononucleotide) and FAD (flavin adenine dinucleotide),

Riboflavin   Ribityl chain

Isoalloxazine ring

**Flavin mononucleotide
(FMN)**

**Flavin adenine dinucleotide
(FAD)**
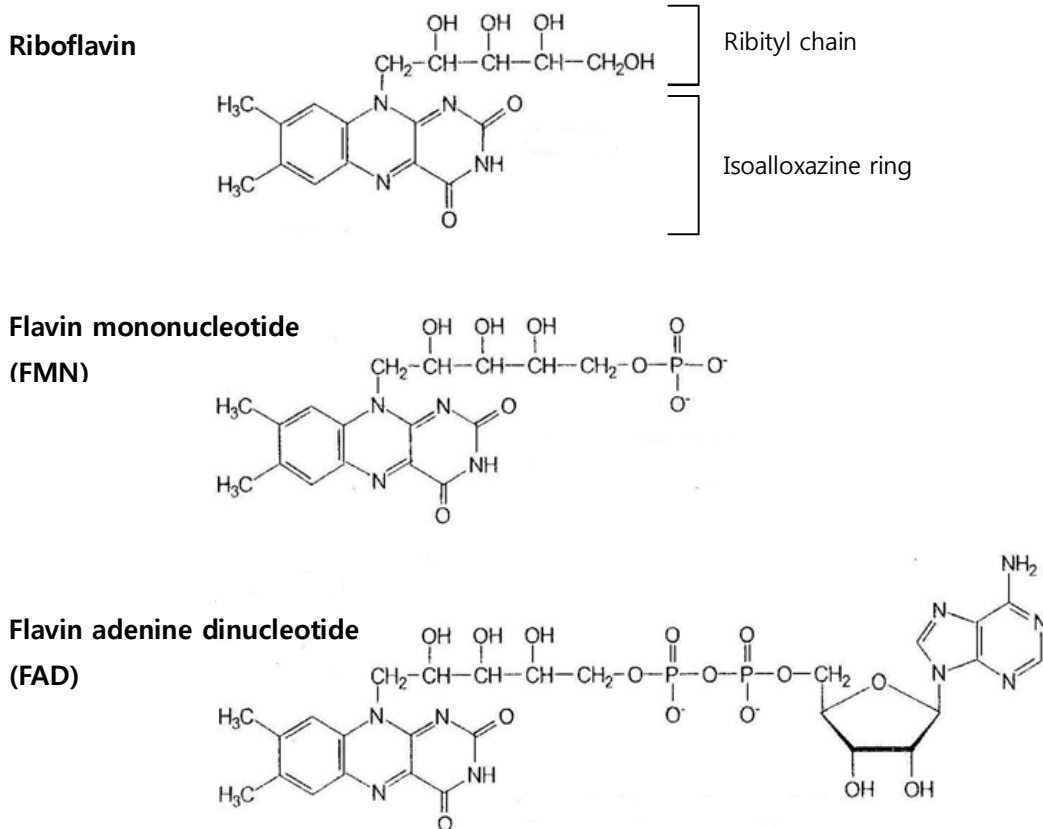
Figure 1 *Structure of riboflavin and the flavin coenzymes*

Riboflavin and its derivatives; FMN and FAD consist of an isoalloxazine ring and ribityl chain. Riboflavin is converted to FMN by adding a phosphate to ribityl chain. FMN is converted to FAD by covalent bind of adenosine monophosphate (AMP) to ribityl chain (Bender, 2003).

1.1.1.2. Absorption of riboflavin

The absorption of riboflavin mainly occurs in the proximal small intestine, the duodenum and jejunum. Transport mechanism of riboflavin is not fully understood. It was reported that uptake of riboflavin into enterocytes involved passive diffusion at high concentration of riboflavin (e.g. over 95μM), and an active transporter at low concentration of riboflavin (e.g. 25 and 42μM) (Zielinska-Dawidziak *et al.*, 2008). In a range of concentration; 25, 42, 95μM that was studied, the lower concentration of riboflavin that was studied, the higher apparent permeability coefficient was observed in human intestinal cells, Caco-2. Also difference in uptake of riboflavin between apical-basolateral direction and basolateral-apical direction was observed. It suggests that an active transporter worked for apical-basolateral uptake of

riboflavin at low concentration. Additionally, studied concentrations were considerably higher level than in human plasma (i.e. >12nM which is considered as physiological level)(Preedy, 2013) and in ordinary growth medium (i.e. 1.1μM which is a concentration in pharmacologically supplemented condition in human) (Nakano *et al.*, 2011). Thus, uptake of riboflavin by an active transporter is thought to dominate in human who take dietary riboflavin or supplement.

Said et al. (1994) firstly suggested the presence of carrier-mediated transport system of riboflavin in the human-derived intestinal cell line Caco-2, which was saturable and pH and Na$^-$ dependent (Said and Ma, 1994). Recently riboflavin transporter family has been identified, consisting of RFVT1 (SLC52A1 or also named as RFT1 (GPR172B)), RFVT2 (SLC52A2 or RFT3 (GPR172A)) and RFVT3 (SLC52A3 or RFT2 (C20orf54)). The active transporters of riboflavin are saturable and Na+ and ATP-dependent. Riboflavin uptake by the transporters is significantly inhibited by some structural analogues of riboflavin such as lumiflavin. (Yonezawa *et al.*, 2008). Each type of the transporters were expressed and localised on the different site of the intestinal cell membrane (Subramanian *et al.*, 2011b; Subramanian *et al.*, 2011a). RFVT3 was predominantly expressed at the apical membrane, while RFVT1 was at the basolateral membrane and RFVT2 was inside cells or basolateral membrane. The intestinal uptake of riboflavin is mainly depending on RFVT3 as it appeared that the level of RFVT3 mRNA expression was higher than the other two types of transporters and also RFVT3 was more efficient in riboflavin uptake than the other two (Subramanian *et al.*, 2011b). In addition, recent in vivo studies examined the response in expression of RFVT3 to riboflavin levels (Fujimura *et al.*, 2010; Ainiwaer *et al.*, 2013). Fujimura et al. (2010) showed that feeding a riboflavin-deficient diet in rats resulted in up-regulated expression of RFVT3 mRNA in the small intestine. Ainiwaer et al. (2013) reported a decrease in expression of RFVT3 mRNA and the protein in tumour tissue in oesophageal squamous cell carcinoma patients who showed lower plasma riboflavin concentration than healthy controls.

Huang and Swaan (2000) revealed involvement of a receptor-mediated endocytosis in uptake of riboflavin in the nanomolar range of concentration. They examined human intestinal epithelial cell model (Caco-2) and rat intestinal tissue, using an inhibitor of endocytosis, nocodazole. This compound caused a decrease in apical uptake of riboflavin in severe riboflavin-deficiency (Huang and Swaan, 2000).

1.1.1.3. Metabolism of riboflavin

Transported riboflavin is intracellularly converted into FMN by flavokinase and then FAD by FAD synthetase as shown in Figure 2.

Figure 2 *Conversion of riboflavin to FMN and FAD*

Riboflavin is phosphorylated by flavokinase (EC 2.7.1.26), to form FMN also called riboflavin monophosphate. FAD synthetase (alternative names are FAD pyrophosphorylase and ATP:FMN adenylyltransferase, EC 2.7.7.2) adenylates FMN to FAD. (Bender, 2003).

There is evidence of effective conservation of FAD availability in response to riboflavin deficiency (Fass and Rivlin, 1969). In severely riboflavin-deficient or chronic marginal deficiency status, the activity of such flavin-metabolising enzymes is changed to conserve FAD concentration at the expense of riboflavin and FMN. In riboflavin-deficient animals, the activity of flavokinase decreases to 60% of normal, while the activity of FAD synthetase is elevated to 150% of normal. However, there is no store of riboflavin or its derivatives; thus inadequate intake of dietary riboflavin causes a fall in the concentration of plasma riboflavin, FMN and FAD (Bates *et al.*, 1982) and also in tissue flavins (Burch *et al.*, 1970).

1.1.1.4. Involvement in metabolic biochemistry
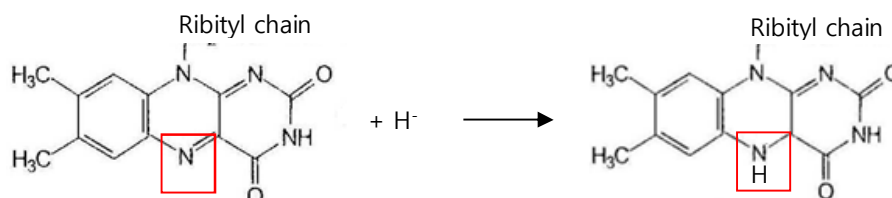
Figure 3 *Example of the role of the isoalloxazine ring in flavins as an electron acceptor*

N expressed in a red box is a binding or unbinding site for an electron.

5

The isoalloxazine ring of the flavins has the ability to lose or gain electrons. Flavins thus act as electron carriers in a range of redox reactions such as oxidative metabolism of carbohydrate, amino acids and fatty acids and the electron transport chain (Powers, 2003; Bender, 2003). Riboflavin deficiency leads to a reduction in activity of flavin-dependent enzymes involved in such energy-yielding reactions, including succinate dehydrogenase(EC 1.3.99.1) and acyl CoA dehydrogenase (EC 1.3.99.2) (Prentice and Bates, 1981b; Olpin and Bates, 1982). Succinate dehydrogenase forms reduced FAD, converting succinate to fumarate and the reduced FAD donates electrons to complex II of the electron transport chain. The activity of this flavoprotein in riboflavin-deficient rats appeared tissue-specific as it sharply declined in the liver while there were smaller changes in brain, skin and intestine (Prentice and Bates, 1981b). Acyl CoA dehydrogenase is also FAD-dependent and active at the first step of beta-oxidation of fatty acids. Thus, diminished activity of the enzyme in riboflavin deficient rats leads to an altered fatty acid profile in hepatic lipids (Olpin and Bates, 1982). A reduction in activity of these enzymes should lead to a reduction of ATP synthesis in the electron transport chain.

1.1.1.5. Riboflavin requirements and effects of deficiency

Riboflavin is present in a wide variety of foodstuffs. Milk and dairy products are the most contributable food sources to riboflavin intake in Western diets. National dietary surveys in the UK reported a high contribution of milk and dairy products to riboflavin intake, which was 51% of riboflavin intake in preschool children, 35% in school children, 27% in adults, and 36% in the elderly (Powers, 2003). Meats, fish and certain fruit and dark-green leafy vegetables are also good sources of riboflavin. The proportional contribution to riboflavin intake from the different food source was approximate 35% from milk and milk products, about 32% from breakfast cereal and about 11% from meat (Gregory *et al.*, 2000).

Reference Nutrient Intakes (RNI) and lower RNI (LRNI) in the UK for riboflavin are presented in Table 1. RNI is defined as the amount of the nutrient, which is sufficient for 97.5% of people in the group who are thus considered to have very small risk of deficiency. LRNI is defined as the amount of the nutrient, which meets requirement of the nutrient for only 2.5% of people (Bates *et al.*, 2011).

Table 1 *Reference Nutrient Intakes (RNIs) and Lower RNI (LRNIs) for riboflavin, by sex and age*

(mg/day)	Age group (Years)					
	1-3	4-6	7-10	11-14	15-18	19+
Males						
RNI	0.6	0.8	1.0	1.2	1.3	1.3
LRNI	0.3	0.4	0.5	0.8	0.8	0.8
Females						
RNI	0.6	0.8	1.0	1.1	1.1	1.1
LRNI	0.3	0.4	0.5	0.8	0.8	0.8

The recent National Diet and Nutritional Surveys (NDNS) (2008-2011) reported that a high proportion of screened people in the UK have riboflavin intakes below LRNI, and whose intake is therefore likely to be insufficient for their needs. The proportion with total riboflavin intakes below the LRNI were 21% of adolescent girls and 8% of adolescent boys aged 11 to 18 years, 7% in adults and 2% in the elderly. Low intakes might be attributable to low consumption of milk, which overall was reduced compared with past surveys (1997-2001) for all age groups (Bates *et al.*, 2011). For example, consumption of milk for girls aged 11 to 18 years was reduced from 131ml per day on average in 1997 to 103ml per day in the recent survey; consumption for boys of the same age was 201ml per day and 166ml per day. There were larger decreases in adults, for women from 188ml per day in 2000/01 to 116ml per day in the recent survey and for men from 217ml to 159ml per day.

The preferred method for determining riboflavin status in animal and human studies is by measuring the activity of the FAD-dependent enzyme, erythrocyte glutathione reductase, in the presence (stimulated) and absence (unstimulated) of added FAD. The ratio of the stimulated to unstimulated activities is expressed as an activation coefficient (EGRAC). EGRAC >1.3 is considered to indicate functional riboflavin deficiency (Powers, 2003). Riboflavin deficiency determined biochemically is prevalent across all age groups in the UK (Gregory *et al.*, 2000; Bates *et al.*, 1999; Weichselbaum and Buttriss, 2014). Particularly schoolchildren were a vulnerable group as 89.2% of adolescent girls and 73.7% of boys in 11-18 years age in the

NDNS (2008-2011) had levels of over 1.3 EGRAC. Approximately 65% of adults aged 19 to 64 years and 40% of the free-living elderly showed evidence of riboflavin deficiency.

In spite of a high prevalence of riboflavin deficiency, since there is no clear functional disturbance, there has been little attention paid to the effects of riboflavin deficiency on human health. However, the literature suggests there may be a number of adverse effects on human health, including cancer, cardiovascular disease and anaemia.

Riboflavin deficiency may be associated with carcinogenesis in the oesophagus, the cervix and the colon (Blot *et al.*, 1993; Liu *et al.*, 1993; de Vogel *et al.*, 2008). This may be mediated by increased DNA strand breakage, genomic instability, aberrant regulation of the cell cycle and apoptosis, partly associated with a role of riboflavin as a cofactor in folate metabolism (van den Donk *et al.*, 2005). This will be addressed further in section 1.1.3.3.

Riboflavin deficiency is also associated with an increase in plasma homocysteine concentration which may increase risk of cardiovascular disease (Moat *et al.*, 2003; Poddar *et al.*, 2001). Riboflavin is involved in remethylation of homocysteine to methionine as a cofactor for MTHFR (methylenetetrahydrofolate reductase, EC1.7.99.5). The enzyme metabolises folate to the methyl tetrahydrofolate, the form used in homocysteine methylation, and is dependent on FAD, thus this contributes to homocysteine homeostasis.

The literature has suggested that riboflavin deficiency may cause low iron status (Rohner *et al.*, 2007) possibly increasing a risk of anaemia. A cohort study recently showed that low riboflavin intake was associated with low plasma ferritin and with an increased risk of anaemia at five-years follow-up (Shi *et al.*, 2014). The study suggests the importance of regular adequate intake of riboflavin particularly in women at risk of anaemia. Plausible mechanisms include a role for riboflavin in iron handling, namely the mobilization of iron from the intracellular store, ferritin (Powers *et al.*, 1983). Also, iron absorption may be impaired and loss of iron from turnover of cells in gastrointestinal (GI) tract may be enhanced (Powers *et al.*, 1991). An animal study proposed that riboflavin deficiency may enhance iron loss in the GI tract by accelerating small-intestinal epithelial cell turnover (Powers *et al.*, 1993). In this context, animal studies have shown that riboflavin is an important nutrient for normal development of the GI tract during the postnatal period (Williams *et al.*, 1995; 1996b; Yates *et al.*, 2001; 2003). Intestinal epithelial cells along the crypts and villi undergo strictly controlled cell proliferation, differentiation and apoptosis, processes responsible for normal development and maintenance of the integrity and absorptive function of the gastro-intestinal system (Jankowski *et al.*, 1994).

In the next section, the role of riboflavin in the normal development of the small intestine will be discussed.

1.1.2. Riboflavin and structure and development of the small intestine

1.1.2.1. Structure and normal development of the intestine

Differentiation from stem cells is not restricted to embryogenesis but is an important feature of normal development for early life as well as maintenance and repair in adult organs such as the intestinal tract. The intestinal epithelium is organised into invasions called the crypts of Lieberkühn and protrusions called villi and covered with a monolayer of the intestinal epithelial cells which migrate up along the crypt-villus axis (van der Flier and Clevers, 2009).
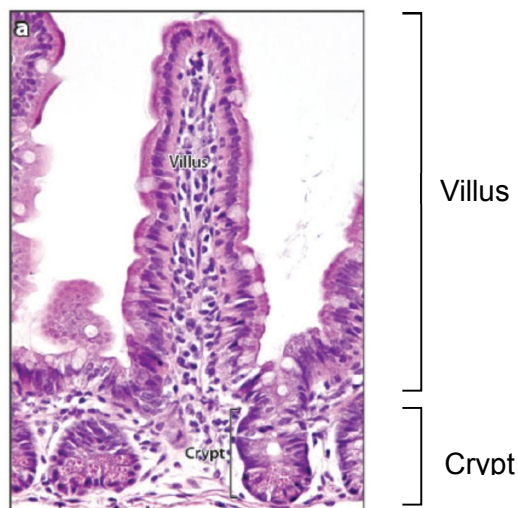
Figure 4 *The intestinal epithelium.*

H&E-stained the mouse intestine (van der Flier and Clevers, 2009).

Stem cells housed in the crypts differentiate to more specialised cells. The stem cells produce progenitors of four cell types of differentiated intestinal epithelial cells; the absorptive enterocytes, mucous-secreting goblet cells, and hormone-secreting enteroendocrine cells which migrate up and cover the villi, and Paneth cells which always are located at the bottom of the crypts. Enterocytes having absorptive function consist of up to 80% of all epithelial cells thus are characteristic of the small intestine (de Santa Barbara *et al.*, 2003).

Crypt stem cells divide near the bottom of the crypt and then the transit-amplifying progeny divide, migrate up to the crypt-villous junction and leave the cell cycle to undergo terminal differentiation. Migrating up along the crypt-villus axis, reaching the tip of the villus, the cells are shed into the intestinal lumen (Wong and Wright, 1999; Yen and Wright, 2006). Under normal circumstances most cells are shed by exfoliation into the lumen and some cells undergo apoptosis (Jankowski *et al.*, 1994). However, in certain circumstances, the number of enterocytes lost by increased apoptosis may increase. Absence of luminal nutrients via total parenteral nutrition (TPN) in rats resulted in a decreased enterocyte population and increased apoptosis throughout the crypt and villus in the adult rat jejunum (Dahly *et al.*, 2002).

Newly produced intestinal epithelial cells replenish lost cells and support normal turnover of cells on the villi. This secures a sufficient absorptive surface of the epithelium and establishes the absorptive function of the intestine (Smith, 1985).

The structure of the small intestine develops differently during the neonatal period in animals even under normal condition. Incidence of crypt bifurcation (fission) occurs more in early life and decreases in adulthood. Animals fed a complete diet showed increased crypt bifurcation during weaning period (Yates *et al.*, 2001). Another animal study showed that the percentage of crypts in fission in the small intestine was decreased 25% to 7% from 21days postparturition to adult, and the number of crypts was increased but villus number was not changed by aging (St Clair and Osborne, 1985). Crypt bifurcation represents the formation of new crypts, which contributes to the intestinal development (Totafurno *et al.*, 1987). Crypt division may occur if crypt stem cells are produced in excess. Crypt cellularity can thereby be kept constant by crypt bifurcation (Jankowski *et al.*, 1994).

1.1.2.2. Role of riboflavin in development of the small intestine

Animal studies of riboflavin deficiency have revealed that the crypts are the first target of riboflavin deficiency in the weaning period. Four days of feeding a riboflavin-deficient diet to weanling rats resulted in no increase in incidence of crypt bifurcation but an increase in the depth and cellularity of the duodenal crypts with a decrease in the proliferative index (DNA synthesis index BrdU), compared with controls (Yates *et al.*, 2001). In contrast, control rats fed a complete diet showed increased crypt bifurcation over the same period. These findings of Yates and colleagues suggest an inhibitory effect of riboflavin depletion on proliferation of the crypt stem cells associated with an interruption of the normal increase in crypt bifurcation of

weaning. The decrease in the duodenal BrdU labelling index in riboflavin-deficient rats implies an association of riboflavin depletion with impairment of the cell cycle. Since BrdU injected intraperitoneally into the animals is incorporated into DNA during S phase of the cell cycle, the BrdU-labelling index is used as a marker of proliferation (Kee *et al.*, 2002).

Prolonged riboflavin depletion for 3 weeks in weanling rats resulted in villus hypertrophy, associated with lower villus number but increase in villus length. Increase in villus length is thought to represent an adaptive response to prolonged depletion of riboflavin. The authors suggest that such adaptatory response would increase the absorptive cell population. They also observed increased transit rate of enterocytes along the villi (Williams *et al.*, 1996a) implying hyperproliferative status but shorter life span of enterocytes. This implies changes in the cell cycle and in regulation of apoptosis induced by riboflavin deficiency. Furthermore, the observed changes in morphology and cytokinetics of the small intestine of weanling rats fed riboflavin-depleted diet for 5 weeks were irreversible following 21 days a repletion with riboflavin despite biochemical evidence showing correction of the deficiency (Williams *et al.*, 1996b).

A subsequent study examined the effects of luminal depletion of riboflavin on intestinal development in the weaning rat (Yates *et al.*, 2003). Weaning rats were fed a riboflavin-deficient diet, but riboflavin was provided in the form of FMN by intraperitoneal injection. This maintained normal systemic riboflavin status. There thus was no difference in the EGRAC and liver flavin concentration between luminally riboflavin-deficient rats and control rats fed a complete diet. Nevertheless, the absence of luminal riboflavin induced abnormal GI development characteristic of dietary riboflavin depletion. Luminal riboflavin-deficient rats exhibited duodenum crypt hypertrophy associated with increased crypt depth and cellularity and also reduced crypt bifurcation by about 6 days of luminal riboflavin deprivation. These cytokinetic and morphological changes in luminally riboflavin-deficient rats are consistent with the characteristics of impaired intestinal development in dietary riboflavin depletion in weanling rats (Yates *et al.*, 2003). The authors proposed the presence of an apical transporter, which may play a key role on GI development. They suggested that riboflavin in the lumen may behave like a signalling molecule for the expression of riboflavin transporter gene and/or certain genes involved in crypt fission.

1.1.3.　The cell cycle and its regulation by riboflavin

1.1.3.1. The cell cycle

The human body is maintained by reproducing cells through the cycle of cell duplication and division. Eukaryotic cells divide to form two genetically identical daughter cells through the cell cycle, and the process occurs repeatedly to maintain normal function of tissues (Alberts, 2008). The cell cycle can be divided into four phases which are G1 (gap 1), S (synthesis), G2 (gap 2), and M phase (mitosis) (Figure 5). Eukaryotic cell begins growth to prepare S phase for DNA replication in G1 phase, and the chromosomes are duplicated during S phase. The cell then enters to G2 phase for preparation of mitosis. The copied chromosomes are segregated into two daughter nuclei following five mitotic phases which are prophase, prometaphase, metaphase, anaphase and telophase as shown in Figure 6. The duplicated DNA molecules in chromosomes are disentangled and condensed into sister chromatids (prophase), and the sister chromatids are attached to microtubules of the mitotic spindle, and then the sister chromatids are pulled to opposite poles of the mitotic spindle by shortening the microtubules (prometaphase, metaphase, and anaphase). The separated chromosomes are decondensed and surrounded by nuclear membranes (telophase), and cytoplasmic division or cytokinesis finally completes the cell cycle producing two separated daughter cells.
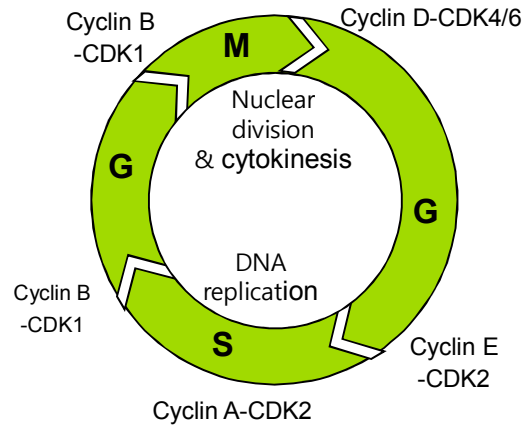
Figure 5 *Overview of the eukaryotic cell cycle.*

G1,Gap 1; S, DNA synthesis; G2, Gap 2; M, Mitosis. The eukaryotic cell begins growth at G1 phase in order to prepare S phase. When ready, DNA replication starts. G2 is a phase to prepare and check the proper condition for mitosis. Mitosis is the process of nuclear division, and the last phase of mitosis is followed by cytokinesis which is the division of the cytoplasm of a mother cell. Details of mitosis are shown in Figure 6.
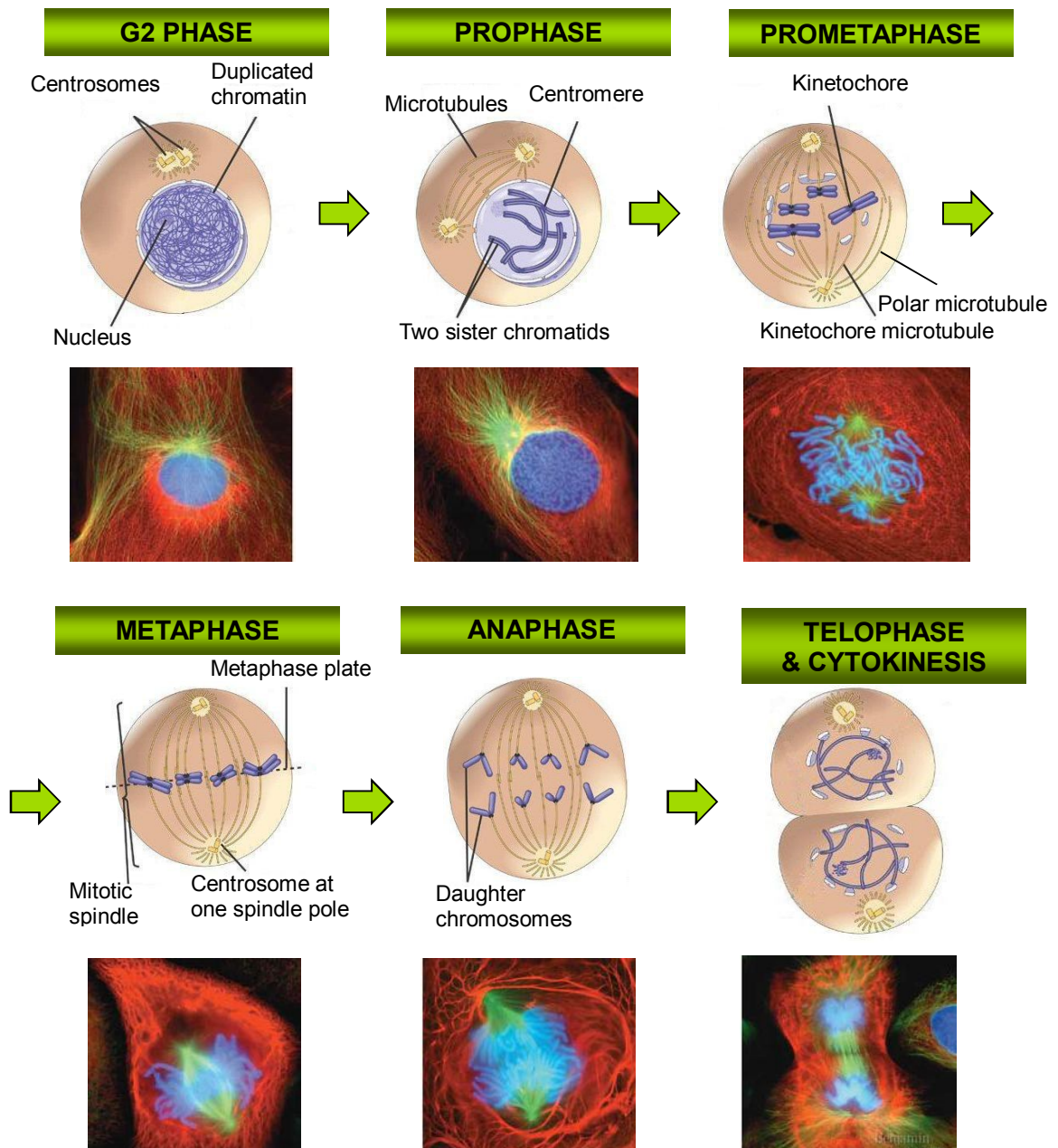
Figure 6 *Overview of mitosis*

Modified from two sources(Pasteur, 2008; Pearson-Education, 2009). Prophase; the chromatin slowly condenses into well-defined chromosomes which consist of two sister chromatids. The early spindle microtubules form outside the nucleus between separating centrosomes. Prometaphase; the nuclear envelope breaks down. The spindle microtubules enter the nuclear region. Mature kinetochores on each centromere attach to some of the spindle microtubules. Metaphase; the kinetochore microtubules align the chromosomes in metaphase plate. Anaphase; the kinetochore microtubule pulls each daughter chromosomes toward the spindle pole. Telophase; the separated daughter chromosomes arrive at the poles and a new nuclear envelope forms around each daughter chromosomes. Cytokinesis; the cytoplasm divides, and two daughter cells separate.

The cell cycle progresses only when the events of each phase are accurately completed and ready for the cell to enter into the next phase. Many cell cycle checkpoints monitor the progression, and they may inhibit the cell cycle proteins if necessary to prevent abnormal progress of the cell cycle (Johnson and Walker, 1999; Shackelford *et al.*, 2000). Some specific micronutrients function as regulators through direct regulation of cell cycle or relevant metabolic pathways and this is briefly presented in Figure 7. In spite of their contribution to regulating the cell cycle progression, the role of micronutrients and the mechanism are not well understood.
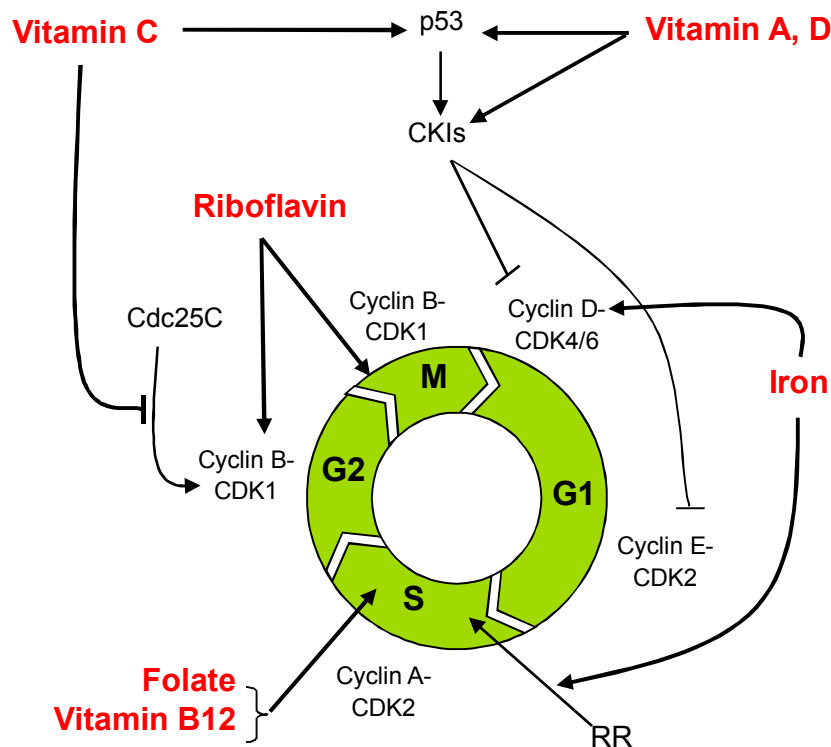
Figure 7 *Regulation of cell cycle by some specific micronutrients; Vitamin A, vitamin D, vitamin C, riboflavin, folate, vitamin B12, and iron.*

In general Vitamin A induces G1 phase arrest by upregulating tumour suppressor p53 and CKIs including cip/wafs; p21 and p27. Vitamin D also induces G1 arrest by upregulating p53 and CKIs including cip/wafs; p21 and p27 and INK4s; p15, p16, and p18. Vitamin C induces transient arrests in S phase and G2/M transit by inhibiting localisation of Cdc25C thus by delaying the activation of CDK1 of cyclin B-CDK1 complex. Folate serves as a methyl carrier to purines synthesis (ATP, GTP), pyrimidines synthesis (dTTP), and methionine synthesis. Vitamin B12 acts as a coenzyme of methionine synthetase. Iron is a cofactor of ribonuleotide reductase (RR) which forms deoxyribonucleotides (dNTPs) and also affects G1/S phase by regulating cyclin D. Riboflavin in an intestinal cell line may involve in the regulation of genes modulating to mitotic progression such as Aspm, Aurora kinase B, CDCA2 and 3, cyclin B1, BIRC5, CCNG2, CK2, and Kif23 (Bohnsack and Hirschi, 2004; Li and Clagett-Dame, 2009; Thomas et al., 2005; Nakano et al., 2011)

1.1.3.2. Role of riboflavin in cell cycle regulation

Several in vitro studies using HepG2 human hepatocarcinoma cells reported that riboflavin depletion led to arrest in G1 phase of the cell cycle, associated with a reduction in cell proliferation (Werner *et al.*, 2005; 2006; Manthey *et al.*, 2005). Riboflavin deficiency may impair the activity of glutathione reductase (EC 1.6.4.2), causing oxidative damage which can mediate cell cycle arrest (Werner *et al.*, 2005; Manthey *et al.*, 2005). Reduced glutathione is a product of glutathione reductase activity, and this compound plays a role as an antioxidant (Hayes and McLellan, 1999). There is evidence that riboflavin deficiency induces decreased cellular concentrations of reduced glutathione (Camporeale and Zempleni, 2003; Manthey *et al.*, 2005). The activity of glutathione reductase was inversely related to reactive oxygen species (ROS) generation and ROS-induced apoptosis in human hepatoma cells (Kim *et al.*, 2010). It was also reported that riboflavin deficiency leads to an increased oxidative damage in proteins and DNA. Presumably due to increased oxidative stress, the level of GADD153 is increased. This is a stress-related transcription factor and a mediator of cell cycle arrest (Manthey *et al.*, 2006). Thus, it is thought that riboflavin deficiency in human hepatoma cells drives cell cycle arrest to avoid cellular damage induced by uncontrolled oxidative stress. However, effects of riboflavin depletion on cell proliferation and regulation of the cell cycle in intestinal cell lines has hardly been investigated.

Nakano and colleagues carried out an investigation into effects of riboflavin depletion on the cell cycle in a human intestinal cell line. Caco-2 human intestinal epithelial cells were cultured in riboflavin–deficient medium (riboflavin-free medium and 10% dialysed FCS), resulting in a final riboflavin concentration of 5.5nM. Severe riboflavin depletion resulted in a two fold increase in cell doubling time with a significant fall in concentrations of intracellular riboflavin, FMN and FAD. The impaired cell growth proceeded to loss of clonogenic ability. A clonogenicity assay showed that following 4 days of culture in a riboflavin deficient medium, Caco-2 cells showed an irreversible loss of proliferative ability when reintroduced to complete medium. Riboflavin depletion also led to cell cycle arrest in mitosis and accumulation of aneuploid cells. These observations were given further support by findings of dysregulated profile of gene expression involved in mitosis regulation. These included downregulation of AspM, Aurora Kinase B, BIRC5, CDCA2 and cyclin B1, and upregulation of CCNG2 (Nakano *et al.*, 2011).

These genes will be briefly introduced here. Firstly, AspM (abnormal spindle-like microcephaly-associated) protein is asymmetrically localised to spindle poles throughout all mitotic stages and required to focus the spindle microtubules. Its mutation or downregulation results in abnormal spindle structure and metaphase arrest (do Carmo Avides and Glover, 1999; Ripoll *et al.*, 1985) which is consistent with mitosis arrest in riboflavin deficient cells.

Aurora kinase B (Aurora-B) associates along chromosomes during prophase and phosphorylates histone H3 which is linked to mitotic chromatin condensation. Additionally, Aurora-A also phosphorylates histone H3 (Crosio *et al.*, 2002). Then, Aurora-B is concentrated to inner centromeres during metaphase, regulating bidirectional movement of centromeres and stable association of kinetochore-microtubule (Murata-Hori and Wang, 2002). Afterwards at anaphase onset, Aurora-B transfers to the spindle midzone. Here, Aurora-B is associated with formation and contraction of the cleavage furrow and thus completion of cytokinesis (Katayama *et al.*, 2003). Ablation of Aurora-B causes monopolar spindles due to unidirectional movement of centromeres, inhibited cleavage furrow formation and uncompleted cytokinesis resulting in cell polyploidy (Terada *et al.*, 1998; Adams *et al.*, 2001). BIRC5 is also known as survivin which is associated with roles and activity of Aurora-B, thus disruption of BIRC5 causes a decline in activity of Aurora-B leading to defects in chromosome alignment and cytokinesis (Katayama *et al.*, 2003).

CDCA2 cooperates with condensin for anaphase chromosome segregation. Condensin depletion causes loss of compact architecture of chromosomes during anaphase, but CDCA2 rescues the characteristic architecture of chromosomes in condensing-depleted cells (Vagnarelli *et al.*, 2006). Thus, down regulated CDCA2 observed in Nakano and colleagues' study may be associated with instability of chromosome structure during anaphase, suggesting the possibility of mis-segregation of chromosomes and aneuploidy.

During G2 phase, cyclin B accumulates and binds to CDK1, but cyclin B-CDK1 complex also known as MPF is at first inactivated. Cdc25 phosphatase activates MPF. Active cyclin B-CDK1 complex initiates transition from G2 to mitosis, and it phosphorylates nuclear substrates thus promoting nuclear envelope breakdown. It is also responsible for the formation of the mitotic spindle. Expression of cyclin B peaks during metaphase transition, afterwards, degradation of cyclin B starts leading to inactivation of CDK1 and initiates mitotic exit. Thus, downregulation of cyclin B is associated with G2 phase arrest and impaired formation of mitotic spindle leading to declined transition from metaphase to anaphase (Lindqvist *et al.*, 2005; Takizawa and Morgan, 2000; Gavet and Pines, 2010).

CCNG2, also known as cyclin G2 is associated with p53-dependent cell cycle inhibition. It is expressed at modest levels in proliferating cells and peaks during the late S or early G2 phase promoting cell cycle exit. It is significantly upregulated in response to DNA damage and growth inhibitory signals such as oxidative stress and differentiation. Ectopically expressed cyclin G2 promotes the formation of aberrant nuclei and inhibition of microtubule growth and depolymerisation (Arachchige Don *et al.*, 2006). Additionally, p53 is known as a tumour suppressor, regulating CKIs (cyclin-dependent kinase inhibitor proteins. The formation and activity of cyclin and CDKs are inhibited by CKIs. p53 consequently induces cell cycle arrest and apoptosis in response to DNA damage (Galderisi *et al.*, 2003).

Taken together, these findings suggest that riboflavin depletion alters the expression of genes important for regulation of mitosis. This dysregulation of gene expression is associated with the following impairments according to the literature.

- Impaired chromatin condensation,
- Monopolar spindles, unfocused spindle microtubules,
- Impaired chromosome alignment,
- Mis-segregation of chromosomes,
- Inhibited cleavage furrow formation and uncompleted cytokinesis.

These aberrations lead to arrest in mitosis with a particularly impaired metaphase transition but increased number of aneuploid cells.

A recent cross-sectional study investigated the association between riboflavin status and GI morphology in duodenal biopsies of adult gastroscopy patients (Nakano *et al.*, 2011). Thirty volunteers recruited in this study comprised 9 male and 21 female subjects, and their age range was 36-46 year in males and 36-78year in females. Riboflavin status was measured using the erythrocyte glutathione reductase activation coefficient (EGRAC). EGRAC values of the subjects ranged between 1.11-1.87. Glutathione reductase is a FAD-dependent enzyme and its activation coefficient which is a measure of the saturation of the enzyme with FAD, provides a sensitive assessment of riboflavin status. EGRAC values are inversely related to concentrations of intracellular FAD and values >1.30 are conventionally considered as biochemical, functional riboflavin deficiency (Powers, 1999). Subjects in the lowest quartile of riboflavin status determined as EGRAC values >1.35 were compared with subjects in the highest quartile (EGRAC <1.24) for proliferative (Ki-67) and mitotic indices (pHH3) and crypt length and cellularity. These were used to demonstrate altered proliferation leading to the changes in total

crypt cell numbers and the consequence of altered proliferation via changes in the crypts. The proliferation index was assessed as the Ki-67 labelling index, and total positive pHH3 by immunohistochemistry was used to assess cells in mitosis. The markers reflect the size of the proliferative compartment relative to the size of the crypt.

Subjects with the poorest riboflavin status showed fewer crypt cells in mitosis and a lower crypt cell proliferation than subjects with the highest riboflavin status (Nakano *et al.*, 2011). Also it appeared that low riboflavin status is associated with significantly decreased crypt length and cellularity. Thus, decreased crypt cell proliferation and mitosis might have proceeded to a decrease in crypt cellularity, and this may reflect a decreased number of progenitor cells entering the cell cycle.

1.1.3.3. Implications for colon cancer

There have been some reports of an association between low intake of riboflavin and increased risk of colorectal cancer (van den Donk *et al.*, 2005; de Vogel *et al.*, 2008). However, the evidence is still weak and the mechanism remains unclear. Riboflavin deficiency may exert an effect on colon cancer risk through interactions with depletion of other B vitamins. Mild depletion of dietary B vitamins, riboflavin, folate, vitamin B6 and B12 in mice for 10 weeks significantly increased DNA strand breaks within the Apc mutation cluster region and decreased expression of the tumour suppressor. Apoptosis was suppressed in B vitamin-depleted mouse colon (Liu *et al.*, 2007). These findings suggest an increased risk of development of aneuploidy which is an early event frequently observed in human colorectal cancers (Fodde *et al.*, 2001). Additionally, aneuploidy implies loss of gain of chromosome leading to chromosomal instability (Rao and Yamada, 2013), which will be addressed later of this section. Such B vitamins interact biochemically, for instance, riboflavin and vitamin B12 are involved in folate metabolism and play a role as cofactors of a folate-metabolising enzyme (Powers, 2005). In Liu and colleagues' study, riboflavin depletion exacerbated a decrease in expression of the Apc induced by isolated folate depletion (Liu *et al.*, 2007).
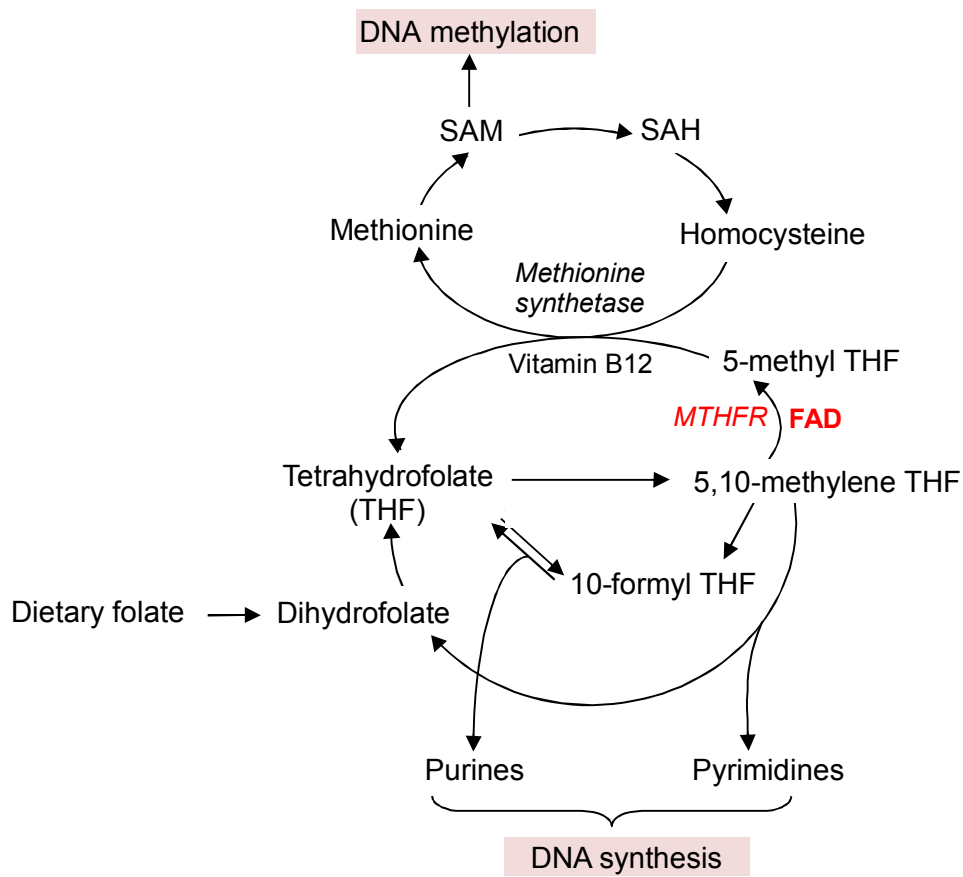
Figure 8 *Simplified diagram of folate metabolism and the association with DNA synthesis and DNA methylation.*

Riboflavin as the form of FAD and vitamin B12 are involved in folate metabolism cycles which mediate DNA synthesis from the de novo synthesis of purines and pyrimidine (dTMP., thymidine deoxymononucleotide) or DNA methylation via methionine synthesis. SAM; S-adenosyl methionine, SAH; S-adenosyl homocysteine, MTHFR; methylene tetrahydrofolate reductase., FAD; flavin adenine dinucleotide.

In addition, riboflavin contributes to the availability and function of folate in the regulation of gene expression of cell cycle proteins through DNA methylation (Crott *et al.*, 2008; Bates and Fuller, 1986). As shown in Figure 8, FAD is a cofactor for 5, 10-methylene tetrahydrofolate reductase (MTHFR) which forms 5-methyl tetrahydrofolate (5-methyl THF) used in methionine synthesis. Folate in the form of 5-methyl THF serves as a methyl donor to remethylation of homocysteine to form methionine, a precursor of SAM (S-adenosylmethionine) which is the primary methyl donor for methylation of DNA (Scott, 1999; Friso and Choi, 2002).

DNA methylation is an important mechanism to regulate expression of genes, including some that are important for regulation of the cell cycle (Razin and Riggs, 1980). For instance, folate deficiency in the human colon cell line SW620 resulted in hypomethylation in tumour suppressor gene p53, thus up-regulated transcription with upregulation of the corresponding mRNA expression (Wasson *et al.*, 2006). In another study, upregulated p53 expression induced by folate depletion in human colonic epithelial cell NCM460, was accompanied by increased expression of cyclin-dependent kinase inhibitors (CKIs); p21 and p16 (Crott *et al.*, 2008). Upregulated p21 blocks transition from G1 to S phase by inhibiting cyclin E-CDK2. Upregulation of p16 consequently arrests the cell cycle in S phase by inhibiting production of cyclin A and thus activation of cyclin A-CDK2 (Johnson and Walker, 1999)

The work of Nakano and colleagues offers a plausible mechanism by which riboflavin deficiency might induce chromosomal instability and DNA aneuploidy, and thereby influence colon cancer risk (Nakano *et al.*, 2011). Aneuploidy implies loss or gain of chromosomes during mitosis thus a result of chromosomal instability (Rao and Yamada, 2013), frequently observed in human diseases such as in most solid tumours (Visscher *et al.*, 1996). Researchers showed that aneuploidy is related to the early stage of colorectal cancer such as ulcerative colitis or adenocarcinoma and the progression of the cancer. A high frequency of aneuploidy and chromosomal instability is a characteristic feature of the cancer, as discussed below. Chromosomal alterations were observed in 36% of non-dysplasia sites and 85% of cancer and dysplasia sites in 14 ulcerative colitis patients (Willenbucher *et al.*, 1999). It is known that ulcerative colitis, which is a chronic inflammatory disease of the colon, is associated with a high risk of colorectal cancer (Ekbom *et al.*, 1990). The progression from ulcerative colitis to colorectal cancer involves genomic instability and progressive accumulation of aneuploidy, evident by highly frequent chromosomal alterations (Willenbucher *et al.*, 1997; 1999). Additionally, ulcerative colitis-related cancers are often developed from flat, dysplastic epithelium. Another study investigating 42 ulcerative colitis patients showed a significant direct correlation between ulcerative colitis duration and extent of aneuploidy. Interestingly, development and extent of aneuploidy in the subjects were significantly related to a decrease in serum level and the expression of p53 which is well known as a tumour suppressor protein, compared with healthy controls (Rosman-Urbach *et al.*, 2004). A further study investigated the incidence of aneuploidy in 57 large bowel adenomas. Aneuploidy was observed in 5 out of 49 low-grade dysplasia adenomas (10%), 7 out of 8 high-grade dysplasia adenomas, intramucous carcinomas or microinvasive carcinomas (87%) (Alcantara Torres *et al.*, 2005). Karaman et al

(2008) performed the micronucleus assay in 21 colorectal cancer patient, 24 patients with colon polyps (10 neoplastic polyps and 14 non-neoplastic polyps) and 20 normal controls. Chromosomal instability was significantly increased in patients with colorectal cancer and neoplastic polyps compared with controls, whereas there was no difference between non-neoplastic polyps and controls (Karaman *et al.*, 2008). Thus, the authors suggested that chromosomal instability and aneuploidy may be a causal factor for the adenoma-carcinoma sequence in early colorectal cancer. Furthermore, recent study with 952 colorectal cancer patients showed the association of high prevalence of DNA aneuploidy with recurrence of the cancer, and they suggested that DNA aneuploidy is a useful predictor of early relapse among stage II colorectal cancer patients (Hveem *et al.*, 2014).

1.1.4. Riboflavin and cell signalling

1.1.4.1. Cell signalling

Cell signalling is the intracellular or intercellular exchange of signals to govern intracellular signal transduction pathways, intercellular communication during development, activation of the immune system and the functioning of the nervous system (Raggiaschi *et al.*, 2005). Intracellular signalling processes are critical for cell function including cell cycle progression, proliferation, differentiation, migration, metabolism and apoptosis (White, 2008). Cell signal transduction pathways are controlled by phosphorylation of proteins involved cellular processes. Series of phosphorylation and dephosphorylation events directly modulate protein enzymatic activity, and affect protein-protein interaction or cellular localization of proteins, thereby cellular signalling networks (Schulze, 2010). Approximately 30% of human proteins are under the counterbalanced controls of kinases and phosphatases. Kinases transfer a phosphate group from ATP to a protein while phosphatases function in dephosphorylation (Macek *et al.*, 2009). Additionally, abnormal phosphorylation of proteins resulting from mutations in particular protein kinases and phosphatases has been linked with an increased risk of developing cancer, diabetes and rheumatoid arthritis (Cohen, 2001).

Phosphorylation of protein pathways may be induced or mediated by ROS such as H_2O_2. For instance, Mitogen-activated protein kinases (MAPKs) cascade pathways, regulate diverse cell functions including the cell cycle, proliferation, and apoptosis, are activated by phosphorylation in response to growth factor or stress stimuli such as oxidative stress and DNA damage (Son *et al.*, 2011). The MAPKs comprise a family of protein kinases that phosphorylate the amino acids serine, threonine and tyrosine thereby leading to sequential transduction of biological signals from cell membrane to the nucleus. MAPK cascades are composed of a three-kinase signalling module; the MAPKs, an MAPK kinase (MAP2K) and an MAP2K kinase (MAP3K). MAP3Ks phosphorylate and activate MAP2Ks, which in turn activate MAPKs through dual phosphorylation on threonine and tyrosine residues. MAPKs consist of three subgroups which are ERKs (growth factor-regulated extracellular signal-related kinases), JNKs (c-jun NH_2-terminal kinases) and p38 MAPKs (Pearson *et al.*, 2001; Son *et al.*, 2011). Some studies have demonstrated that ROS may be required for the activation of MAPK pathways. Sundaresan et al.(1995) reported that when rat vascular smooth muscle cells (VSMC) were stimulated by platelet-derived growth factor (PDGF), the intracellular hydrogen peroxide (H_2O_2) concentration was increased and MAPK pathways particularly ERK1/2 were activated. When the rise in H_2O_2 concentration was blocked by treatment with catalase, the stimulation of MAPKs was inhibited. It suggests that H_2O_2 mediates activation of MAPK pathways in VSMCs and thereby influences PDGF-induced VSMC migration and proliferation which might be early atherogenic changes. Likewise, uncontrolled activation of MAPK pathways may result in excessive production of MAPK-regulated genes and thereby possibly lead to impairments in cell proliferation and apoptosis (Son *et al.*, 2011).

Phosphorylation of proteins is also central to the expression of genes important for protein synthesis, including transcription, mRNA processing including mRNA splicing, mRNA export and translation. Briefly, the first step in gene expression is the transcription of mRNA from DNA by RNA polymerase in the nucleus (Alberts, 2008). Particularly RNA polymerase Ⅱ binds to a single-stranded DNA gene template and transcribes the DNA sequence to mRNA. Pre-mRNA in eukaryotic cells undergoes mRNA processing, including 5′ capping, 3′ cleavage, polyadenylation and mRNA splicing. 7-methylguanosine is added to the 5′ end of pre-mRNA for stability of the RNA. 3′ cleavage and polyadenylation in pre-mRNA are also to protect degradation of RNA. mRNA splicing is the process of removal of non-coding sequences. Then, mature RNA is exported from the nucleus to the cytoplasm. The mRNA sequence is translated and a polypeptide is produced at the ribosome.

An example of a phosphorylation that regulates mRNA processing is phosphorylation of the C-terminal domains (CTD) of RNA polymerase Ⅱ which play an important role in these processes linking to cell cycle regulatory events. When the CTD of RNA polymerase Ⅱ are activated by phosphorylation, the CTD binds to various protein factors and promotes mRNA processing (Hsin and Manley, 2012). RNA polymerase Ⅱ activity is regulated by the CTD phosphorylation depending on the cell cycle. The CTD phosphorylation status can be changed in response to mitogenic signals or cytostatic signals such as growth factor. Some CTD kinases that phosphorylate CTD are cyclin-dependent kinase 7 (CDK 7), CDK8 and CDK9, members of the CDK family, the MAPKs ERK1/2 and the cAbl tyrosine kinase which are involved in cell cycle regulation (Oelgeschlager, 2002; Venetianer *et al.*, 1995).

Phosphorylation of the serine/arginine-rich splicing factor (SR) proteins which are a family of serine, arginine-rich splicing factors is also important for pre-mRNA splicing (Shepard and Hertel, 2009). The SR proteins can be localised into the nucleus by the phosphorylation of the RS domain, allowing functions in mRNA splicing which occurs in the nucleus. Phosphorylation of the RS domain enhances the ability of the SR protein, important for spliceosome assembly in the early step of mRNA splicing. It also facilitates the recruitment of components of the spliceosome such as U1 small nuclear ribonucleoprotein (U1 snRNP) and U2AF35 to intronic splice sites. Also, SR proteins interact with CDK9, a CTD kinase, leading to the phosphorylation of CTD, and SR proteins bind to the phosphorylated site of the CTD of RNA polymerase Ⅱ. This allows the SR protein to recognise pre-mRNA transcript (Long and Caceres, 2009).

Phosphoproteomics is a part of proteomics that identifies and characterises proteins containing a phosphate group, providing the information of changes in activity of candidate proteins or pathways and signalling networks and also the information of phosphorylation sites. These can be achieved by advanced high-throughput phosphoproteomics through phosphoprotein enrichment, identification and relative quantitation by mass spectrometry and bioinformatics tools and biological sequences databases (Macek *et al.*, 2009). Phosphorylation also can be easily detected by 1D or 2D gels-base methods including western blot by probing with phospho-site specific antibodies and phosphoprotein-specific gel staining, however it provides limited information (White, 2008; Macek *et al.*, 2009).

Recent advanced high-throughput proteomics allows the investigation of protein-specific alterations. The isobaric tag for relative and absolute quantification (iTRAQ) is a gel-free

proteomic approach that allows simultaneous identification and quantitation of proteins in multiplexing of up to eight labelled samples (Hultin-Rosenberg *et al.*, 2013). This method has been shown to provide more accurate and reproducible quantification of peptides and proteins through peptides-based detection by mass spectrometry in phosphoproteomics as well (Zhang *et al.*, 2005). Briefly, iTRAQ protocol contains four steps (Gafken and Lampe, 2006). First, prepared protein extracts from each sample are alkylated and proteolytically digested into peptides. Second, the peptides are labelled with a set of iTRAQ reagents individually in a 4 or 8-plex format. Third, labelled peptides are pooled and fractionated by strong cation exchange (SCX) or hydrophilic interaction liquid chromatography (HILIC). Finally, the fractions are analysed by liquid chromatography tandem mass spectrometry (LC-MS/MS) to obtain the mass spectra providing peptide sequence information from peptide fragments and relative quantification from the reporter group ions. The tags consist of three regions; a peptide reactive region, a reporter region and a balance region (Ross *et al.*, 2004). During mass spectrometry (MS), peptide fragments are distinguished according to peptide mass allowing for qualitative analysis, while during MS/MS peptide fragments with equal mass are detected for different intensity of the reporter group ion which corresponds to the relative amount of the peptides.

1.1.4.2. Riboflavin and cell signalling

Yates et al(2003) suggested the putative role of riboflavin as a signalling molecule in the lumen. Luminal absence of riboflavin in the presence of normal systemic riboflavin status in weanling rats resulted in abnormal development of GI tract, which is characteristic of dietary riboflavin depletion. The authors of that study hypothesised that riboflavin plays an important role in intestinal cell proliferation through effects on cell signalling.

A plausible mechanism is through its role as a coenzyme for flavoproteins which are important in the production of reactive oxygen species (ROS) (Bender, 2003). Excessive ROS can cause molecular damage by reacting with DNA, protein and lipids to result in DNA mutation, protein oxidation and lipid peroxidation, all of which are relevant to the pathology of human disease. Nevertheless, ROS also play an important role as signalling molecules (Rhee, 2006). Therefore, redox balance in cells is critically important for the regulation of cell signalling pathways (Fruehauf and Meyskens, 2007).

Riboflavin plays a central role in redox regulation through its influence on the production of reduced glutathione (GSH) (Schafer and Buettner, 2001), which is the most abundant cellular antioxidant (Owen and Butterfield, 2010). Cellular redox buffering capacity can be predicted using the ratio of GSH : oxidised glutathione (GSSG) (Schafer and Buettner, 2001), thus it has been considered as an indicator of oxidative stress (Zitka *et al.*, 2012). One of the enzymes modulating the glutathione redox cycle is glutathione reductase as seen in Figure 9. The enzyme requires FAD as a co-factor. Riboflavin deprivation leads to a significant decrease in activity of the enzyme, thus causing oxidative stress partially due to impaired glutathione redox cycle (Camporeale and Zempleni, 2003; Werner *et al.*, 2005; Beutler, 1969).
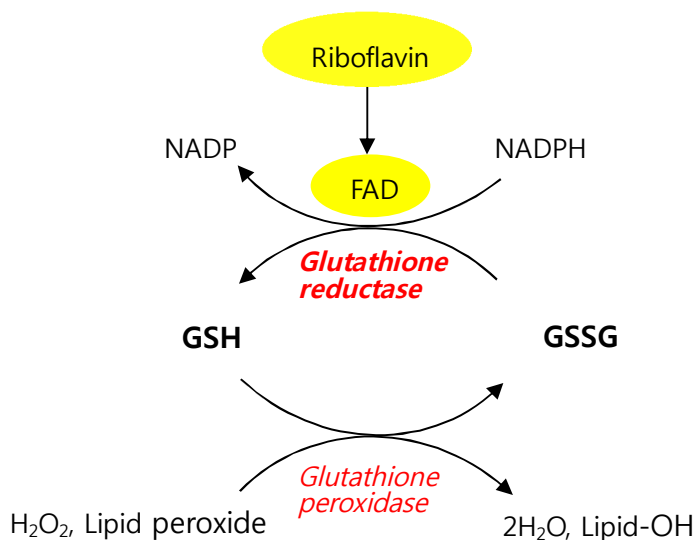
Figure 9 *Glutathione redox cycle*

GSH; reduced glutathione, GSSG; oxidised glutathione. Riboflavin in the form of FAD serves as a cofactor for glutathione reductase which metabolises an oxidised glutathione to a reduced glutathione which is a cellular antioxidant.

NADPH oxidase also requires FAD as a co-factor, and this enzyme generates ROS that function in cell signalling as a part of mechanisms of apoptotic and necrotic cell death (Yazdanpanah *et al.*, 2009). A recent study showed that riboflavin deprivation in macrophage harvested from mice reduced tumour necrosis factor (TNF)-induced ROS production and decreased signalling thereby impairing anti-bacterial ability of macrophages against *Listeria monocytogenes* (Schramm *et al.*, 2014). This can be explained by the FAD-dependence of NADPH oxidase and also the role of riboflavin kinase on NADPH oxidase assembly and

activation. When TNF stimulates TNF receptor 1 (TNFR1), riboflavin kinase mediates bridging of TNFR1 to NADPH oxidase and also generates and provides FAD for NADPH oxidase thereby ROS are produced (Yazdanpanah *et al.*, 2009).

To our knowledge there has been no investigation of the putative role of riboflavin in cell signalling. This study will address this gap in our understanding.

1.1.5. Intestinal epithelial cell model of riboflavin depletion

Nakano *et al.* (2011) developed a human intestinal epithelial cell model of riboflavin depletion by culturing Caco-2 cells in riboflavin-free medium containing dialysed foetal calf serum (FCS). Others have also achieved riboflavin depletion in other cells using a similar approach (Werner *et al.*, 2005; Camporeale and Zempleni, 2003). This is approach has proved effective in achieving different degrees of riboflavin depletion of cells in vitro. In particular, the use of non-dialysed or dialysed FCS can determine whether a severely depleted state is achieved. For instance, intracellular concentrations of riboflavin similar to normal concentrations in human plasma can be achieved using riboflavin-free medium and non-dialysed FCS. However, developing Nakano's cell model was expensive and time-consuming. The cells required 3~4 passages to achieve severely riboflavin-deficient status. Furthermore, dialysation of FCS may lead to a short supply of other essential nutrients which may influence cell proliferation independent of riboflavin status.

This study was designed to develop an improved model of intestinal riboflavin depletion, which could be applied to an investigation of effects of riboflavin depletion on aspects of cell function, but which could also be applied to studies of a putative role of riboflavin in cell signalling. The model required the use of lumiflavin, an inhibitor of riboflavin uptake into cells.

1.1.5.1. Lumiflavin

It is well known that riboflavin is unstable under light exposure, degrading to some structural analogues. Lumiflavin is one of the structural analogues of riboflavin, formed by photodegradation at basic pH (Huang *et al.*, 2006).
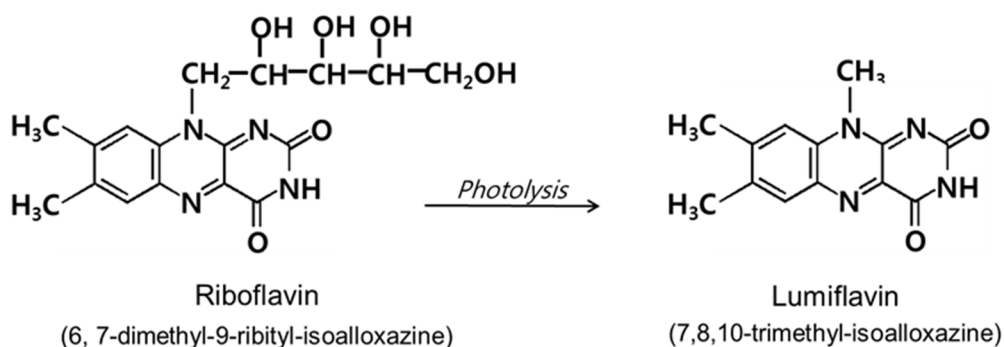
Figure 10 *Structures of riboflavin and lumiflavin.*
Lumiflavin is a structural analogue of riboflavin, obtained by photodegradation of riboflavin. The long ribityl chain of riboflavin binding to the isoalloxazine ring is replaced into a short methyl (Bender, 2003).

Riboflavin uptake studies have shown that lumiflavin competitively saturates the riboflavin transporter, thus leading to significant inhibition of riboflavin uptake into human intestinal cells Caco-2 (Said *et al.*, 1985; Said and Ma, 1994). Lumiflavin shares the same membrane transporter at the apical surface as riboflavin, thus it significantly inhibits the uptake of riboflavin into human intestinal cell line Caco-2, in a lumiflavin concentration-dependent manner. Exposure of Caco-2 cell for 48 hours to 32µM and 97µM of lumiflavin caused a progressive decrease approximately 40% and 70% decrease of riboflavin uptake, respectively (Said and Ma, 1994). Such findings are supported by further recent studies that identified and characterised a human and rat riboflavin transporter in that transporter-mediated riboflavin transport was specifically inhibited by lumiflavin (Yonezawa *et al.*, 2008; Yamamoto *et al.*, 2009). Riboflavin uptake by RFVT3 which is an apically expressed riboflavin transporter that predominantly serves to transport riboflavin uptake into cells was inhibited by lumiflavin and the authors proposed that RFVT3 recognised lumiflavin due to the structural similarity to riboflavin (Fujimura *et al.*, 2010). However, in spite of having a similar structure to riboflavin,

lumiflavin itself is not phosphorylated, thus it cannot be a substrate of riboflavin kinase meaning that cells are unable to utilize it (McCormick, 1962). Therefore, lumiflavin specifically interferes with the uptake of riboflavin into cells. We proposed that the development of a cell model of riboflavin depletion in gastrointestinal cells using lumiflavin would be a useful tool to studying a putative role of riboflavin in cell signalling. Furthermore, this would obviate the need for multiple cell passages and dialysed FCS which are disadvantages of the existing model of Nakano *et al.* (2011). In addition, the cell model was to be used to explore biochemical and functional changes which may be important for the maintenance of regulation of intestinal cell proliferation and cell death.

1.2. Hypothesis, aims and objectives

1.2.1. Hypothesis

- Exposing intestinal cells to lumiflavin depletes the cells of flavins.
- Flavin depletion of intestinal cells has adverse functional effects.
- Lumiflavin induces changes in cell signalling in intestinal cells.

1.2.2. Aim

The overall aim of the study is to examine the biochemical and cellular consequences of modulating riboflavin status of intestinal cells, and to understand the underlying mechanisms.

1.2.3. Objectives

- To develop and to establish an intestinal cell model of riboflavin depletion using lumiflavin, which is a structural analogue of riboflavin.
- To characterise the cell model of riboflavin depletion in terms of specific functions.
- To study alterations in candidate signalling pathways and validate the findings.

CHAPTER 2

MATERIALS AND METHODS

2.1. Materials

2.1.1. Cell lines

Three cell lines Caco-2, HCT116 and HT29 were obtained from The Health Protection Agency, Porton Down, Salisbury, UK. Caco-2 cell are derived from an epithelial colorectal adenocarcinoma of a 72 year old Caucasian male, HCT116 cells from an epithelial colorectal carcinoma of an adult human male and HT29 cells from an epithelial colorectal adenocarcinoma of a 44 years old Caucasian female.

Differentiated Caco-2 and HT29 cell lines are the most similar to the small intestine epithelium in terms of gene expression compared with other colon cancer-derived cell lines including HCT116 (Christensen *et al.*, 2012). As Caco-2 and HT29 cell lines have been widely used for small intestinal cell models of drug and nutrient absorption, they were selected for this study. HCT116 cell line was used for comparison with Caco-2 and HT29 cell lines.

2.1.2. Cell culture

Centrifuge (Sorvall RT6000B refrigerated centrifuge, USA)

Centrifuge (Heraeus PICO17, Thermo Scientific, Germany)

Culture flasks and plates (Nunc)

DMEM (GIBCO, Cat. No. 22320022 & DMEM-F12; Lonza BioWhittake, Cat. No. BE12-719F))

FCS (Biowest, Cat. No. S1810)

Haemocytometer (Improved Neubauer)

Hand tally counter

Microscope (Diaphot: Nikon, Japan)

PBS sterile (Lonza, BioWhittake, Cat. No. BE17-512F)

Penicillin/ streptomycin (1% Penicillin/ streptomycin; GIBCO, Cat. No. 15140-122)

Trypan blue stain 0.4% (GIBCO, Cat. No. 15250-061)

Trypsin-EDTA 0.25% (GIBCO, Cat. No. 15400-054)

2.1.3. Preparation for lumiflavin-containing medium

Lumiflavin (Sigma-Aldrich, Cat. No. L4879)

DMEM (GIBCO, Cat. No. 22320022 & DMEM-F12; Lonza BioWhittake, Cat. No. BE12-719F))

0.2μm non-pyrogenic sterile filter (Nalgene, Cat. No. 83 186.001)

Sodium hydroxide (Sigma Aldrich, Cat. No. S0899)

2.1.4. Intracellular flavin assay

Acetonitrile (Fisher Scientific, Cat. No. 10407440)

Chromsystems (Chromsystems, Germany)

FAD (Sigma-Aldrich, Cat. No. F6625)

FMN (Sigma-Aldrich, Cat. No. F2253)

HPLC system (Fluorescence detector, Jasco FP-920, Japan; autoinjector, Gilson 234; dynamic mixer, Gilson 811C; data module, Gilson 621; pump, Gilson 305 and 306, USA)

PLRP-S column (Polymer labs, Church Stretton, UK)

HPLC vial

Magnesium acetate (Sigma-Aldrich, Cat. No. M2545)

0.2μm nylon membrane filter papers (Whatman, Cat. No. 7402-004)

Orthophosphoric acid (Sigma-Aldrich, Cat. No. 345245)

Potassium phosphate (Sigma-Aldrich, Cat. No. P5379)

Riboflavin (Sigma-Aldrich, Cat. No. R4500)

Sonicator (UCD-200TM: Bioruptor diagenode, Belgium)

Trichloroacetic acid (TCA) (Sigma-Aldrich, Cat. No. T0699)

2.1.5. Glutathione reductase activation coefficient (GRAC)

COBAS Bioanalyser (Roche, Switzerland)

EDTA (Sigma Aldrich, Cat. No. E7889)

FAD (Sigma Aldrich, Cat. No. F6625)

GSSG (Sigma Aldrich, Cat. No. G6654)

NADPH (Sigma Aldrich, Cat. No. N5130)

Potassium phosphate (Sigma Aldrich, Cat. No. P5379)

2.1.6. Adenosine 5′-tryphosphate (ATP) assay

Apoptotic DNA ladder detection kit (abcam, Cat. No. ab66090)

Hydrochloric acid (Fisher Scientific, CAS. No. 7647-10-0, FW=36.46)

Luminometer (Bio-Orbit 1253, Labtech Jade)

0.2μm non-pyrogenic sterile filter (Nalgene, Cat. No. 83 186.001)

Polypropylene reaction vials

2.1.7. Reactive oxygen species (ROS) assay

Culture flasks and plates (Nunc)

DCFDA (2′,7′-dichlorodihydrofluorescein diacetate, Sigma-Aldrich, Cat. No. D6883)

DMEM (GIBCO, Cat. No. 22320022)

DMSO (Sigma Aldrich, Cao. No. D2650)

Fluorescence microplate reader (Fusion plate reader)

PBS sterile (Lonza, BioWhittake, Cat. No. BE17-512F)

2.1.8. MTT assay

Microplate reader (Biotek FLX800, USA)

MTT based Cell growth determination kit (Sigma-Aldrich, Cat .No. CGD-1)

2.1.9. Clonogenic assay

Centrifuge (Soval RT6000B refrigerated centrifuge, USA)

Culture flasks and plates (Nunc)

Haemocytometer (Improved Neubauer)

Methanol (Fisher science, Cat. No. 67-56-1)

Methylene blue (Sigma Aldrich, Cat. No. MB1-25G)

Microscope (Diaphot: Nikon, Japan)

2.1.10. Determination of protein concentration

Bradford reagent (Bio-Rad, Cat. No. 500-0006)

BSA (Sigma Aldrich, Cat. No. P0834)

Microplate reader (Biotek FLX800, USA)

2.1.11. Apoptotic DNA assay

Agarose (Life Technologies, Cat. No. 540-5510UA)

Apoptotic DNA ladder detection kit (abcam, Cat. No. ab66090)

Electrophoresis system (Bio-Rad, UK)

Ethidium bromide (Sigma-Aldrich, Cat. No. E1510)

Isopropanol (Sigma-Aldrich, Cat. No. I9516)

Microwave

Sodium butyrate (Calibochem, Cat. No. 567430)

Quick-Load™ 1kb DNA ladder (BioLabs, UK, Cat. No. N0468G)

2.1.12. Western blot

Acrylamide (National Dignostics, Cat. No. EC890)

Amicon Ultra-0.5 mL Centrifugal Filters (Millipore, Cat. No. UFC500324)

Anti-phospho-tyrosine, clone 4G10 (Millipore, Cat. No. 05-321)

Anti-phospho-serine/threonine (abcam, Cat. No. ab17464)

Anti-phosphoepitope SR proteins clone 1H4 (Millipore, Cat. No. MABE50, Lot. No. 2207243)

Anti-SR protein family (Millipore, Cat. No. MABE126, Lot. No. 2119212)

APS (Sigma Aldrich, Cat. No. A3678)

NaF (Sigma-Aldrich, Cat. No. S1504)

Beta-actin (abcam, Cat. No.ab20272)

B-Glycerophosphate (Sigma-Aldrich, Cat. No. G9891)

ECL (Chemiluminescent HRP substrate, Immobilon Western, Millipore, Cat. No. WBKLS0500)

EDTA (Sigma-Aldrich, Cat. No. E5513)

EGTA (Sigma-Aldrich, Cat. No. E3889)

Electrophoresis system (Bio-Rad, UK)

Filter paper (Chromatography paper, Whatman, Cat. No. 3030672)

Fish gelatin (gelatin from cod water fish skin, Sigma, G7765-250ML)

GeneTools program (SYNGENE, Japan)

Heat block (FALC supplied by Scientific Ltd., UK)

Imaging system (ChemiGenius2 BioImaging system, SYNGENE, Japan)

Loading buffer (Laemmli buffer)

NaVO$_4$ (Sigma-Aldrich, Cat. No. P8340)

Phosphoprotein purification kit (Qiagen, Cat. No. 37101)

PMSF (Sigma-Aldrich, Cat. No. T7626)

Polyoxyethylene sorbitan monolaurate (tween 20) (Sigma-Aldrich, Cat. No. P5927)

Protease Inhibitor cocktail (Sigma-Aldrich, Cat. No. S6508)

Protein standard (Precision Plus protein standard, Bio-Rad, Cat. No. 161-0373)

PVDF membrane (Immonilon Transfer membrane, Millipore, Cat. No. IPVH00010)

Running buffer (0.25M Tris, 1.92M Glycine, 1% SDS, National diagnostic Cat. No. EC870)

SDS (Fisher Scientific, Cat. No. 16416)

Secondary antibodies

Polyclonal rabbit, anti-mouse immunoglobulin, HRP conjugated (DAKO, Cat. No. P0266)

Polyclonal goat, anti-rabbit immunoglobulin, HRP conjugated (DAKO, Cat. No. P0448)

Stripping buffer (Restore Western blot, Thermo Scientific, Cat. No. 21059)

TBST (Sigma Aldrich, Cat. No. T9039)

TEMED (Sigma Aldrich, Cat. No. T9281)

Transfer buffer (0.25M Tris, 1.92M Glycine, National diagnostic Cat. No. EC880)

Tris (Sigma-Aldrich, Cat. No. T1053)

Triton X-100 (BDH lab, UK, Cat. No. 306324N)

2.1.13. High content analysis (HCA)

96-well black-walled clear bottom plate (Nunc)

Anti-phospho-tyrosine, clone 4G10 (Millipore, Cat. No. 05-321)

Anti-phospho-serine/threonine (abcam, Cat. No. ab17464)

Alexa Fluor 488, anti-mouse IgG secondary antibody (Invitrogen, Cat. No. A21202)

Alexa Fluor 555, anti-rabbit IgG secondary antibody (Invitrogen, Cat. No. A31572)

Digitonin (Sigma Aldrich, Poole Dorset, UK)

Hoechst 33342 (Invitrogen, Paisley, UK)

2.1.14. Purification of phosphoproteins

Centrifuge (Soval RT6000B refrigerated centrifuge, USA)

HBSS (Hank's Balanced Salt solution)

Phosphoprotein purification kit (Qiagen, Cat. No. 37101)

Triton X-100 (BDH lab, UK, Cat. No. 306324N)

2.1.15. Pro-Q Diamond phosphoprotein gel stain and SYPRO® ruby stain

Acetic acid (Sigma-Aldrich, Cat. No. 45740)

Acetonitrile (Fisher Scientific, Cat. No. 10407440)

Agitator (SSL4, Stuart, UK)

Methanol (Fisher Scientific, Cat. No. 67-56-1)

Multiplexed Proteomics® Phosphoprotein gel stain kit (Molecular Probes, Cat. No. M33306, Lot. No. 1164331)

PeppermintStick™ phosphoprotein molecular weight standards (Molecular Probes, Cat. No. P27167)

Sodium acetate (Sigma Aldrich, Cat. No. S2889, Lot. 63H079415)

Triton X-100 (BDH lab, UK, Cat. No. 306324N)

Typhoon 9400 Imager (Amersham Biosciences, USA)

2.1.16. Sample concentration by filtration

Amicon® Ultra-0.5 Centrifugal filter devices (Millipore, Cat. No. UFC500324)

Centrifuge (Mikro 22R, Hettich Zentrifugen, Germany)

TEAB buffer (Sigma Aldrich, Cat. No. T7408)

2.1.17. Coomassie blue stain

Agitator (SSL4, Stuart, UK)

Coomassie® stain (InstantBlue™, Expedeon, Cat. No. ISB1L)

2.1.18. Isobaric tag for relative and absolute quantitation (iTRAQ)

Acetonitrile (Fisher Scientific, Cat. No. 10407440)

Agilent 1100-series HPLC (Agilent, Berkshire UK),

Agitator

Ammonium formate (Sigma Aldrich, Cat. No. 70221)

Chromeleon software v.6.50 (Dionex, LC Packing, The Netherlands).

Formic acid (Sigma Aldrich, Cat. No. F0507)

Heat block

HPLC grade H$_2$O (Fisher Chemical, Cat. No. W/0106/17)

Hydrophilic Interaction Liquid Chromatography (HILIC) (Ultimate 3000 from DIONEX, USA)

Incubator

Isopropanol (Sigma Aldrich, Cat. No. 19516)

iTRAQ reagent 8PLEX Multi-plex kit (AB Sciex, Cat. No. P/N4381663, Lot. No. A1222, USA)

LoBind tubes (Sigma Aldrich, Cat. No. Z666505)

Methyl methane ethiosulfonate (MMTS) (Sigma Aldrich. Cat. No. 208795)

Potassium chloride (BDH Chemicals, Cat. No. 10198 아니면 5520090A)

Sequencing Grade Modified Trypsin (Promega, Cat. No. V5111)

SDS-PAGE gel running apparatus (Bio-Rad)

TEAB buffer (Sigma Aldrich, Cat. No. T7408)

Tris-(2-carboxyethyl)phosphine hydrochloride (TCEP) (Sigma Aldrich, Cat. No. 646547)

Trifluoroacetic acid (CHROMAsolv, Sigma Aldrich, Cat. No. 302031)

UltraMicrospin Columns, Silica C18 Vydac (The NEST group, Cat. No. SUM SS18V)

Vacuum concentrator (Scanvac, Lebogene, Denmark)

Ultimate 3000 split flow HPLC system (Dionex, Surrey, UK)

2.1.19. Cell cycle analysis by flow cytometry

Absolute ethanol (BDH, EC 200-578-6)

BD LSR II (BD Biosciences)

Centrifuge (Heraeus PICO17, Thermo Scientific, Germany)

PI/RNase staining solution (Molecular probes, Cat. No. F10797, Lot. No. 1374366)

2.2. Methods

2.2.1. Cell culture

Human intestinal epithelial cells HCT116, Caco-2 and HT29 were used for this project. Cells were cultured in DMEM growth medium containing 10% FCS and 1% penicillin and streptomycin; 100units/ml penicillin and 100μg/ml streptomycin at 37℃ and 5% CO_2.

For cell culture, DMEM growth medium, PBS and trypsin-EDTA were warmed in a water bath at 37℃ for approximately half an hour. A culture hood, micropipettes, a pipette aid, disposal pipettes and 50ml sterile falcon tubes were prepared sterile by cleaning with 70% ethanol before tissue culturing was started.

Thawing cells

Special gloves and a helmet should have been worn for the safety reason. Cells stored in a nitrogen tank were taken out carefully and defrosted rapidly at 37℃ in a water bath. Cell suspension was transferred to 50ml tubes containing 9ml DMEM, mixed well and centrifuged for 5 minutes at 150xg and room temperature. Then, supernatant was removed. 8ml DMEM was added to cell pellet, and cells were resuspended. The cell suspension was seeded into T75 culture flasks with 20ml of DMEM. Cells were observed daily and when it was 80-90% confluent, cells were split.

Splitting cells

Medium was removed with a pipette aid and disposable pipettes, and cells were rinsed gently twice with appropriate volume of sterile PBS; 500 $\mu\ell$/well for a 24well plate, 3ml for T25, 5ml for T75, and 10ml for T175 flasks. Appropriate volume of 0.5% trypsin-EDTA was then treated depending on the confluence and incubated at 37℃ for 5 minutes; for example, 100 $\mu\ell$/well for a 24well plate, 1ml for T25, 3-4ml for T75, and 6-7ml for T175. It was checked if the cells had been detached from a culture flask, and the same volume of growth medium as trypsin-EDTA was added in order to inactivate trypsin-EDTA. Then, cell suspension was split into single cells by mixing well and gently but avoiding causing froth or pipetting too harshly. Cells were counted using a haemocytometer. Cell counting is explained in the following section. After counting, the cell suspension was centrifuged at 150xg and room temperature for 5

minutes. The supernatant was discarded, and the cell pellet was resuspended with appropriate volumes of growth medium. Finally, part of cell suspension was planted into new culture plates or flasks.

Counting cells

Cells were counted whenever cells were split or harvested. A haemocytometer and a coverslip were cleaned with 70% ethanol and wiped. The surface of a coverslip was moisturised very slightly, and the coverslip was laid over the central of the haemocytometer and pressed gently to attach to the haemocytometer. After inactivation of trypsin-EDTA, the cell suspension was mixed thoroughly, and 20 $\mu\ell$ was taken into a microtube containing 20 $\mu\ell$ trypan blue. Trypan blue was used to dye dead cells and cells dyed in blue were excluded from counting. 10 $\mu\ell$ of that was transferred to the edge of one side of the one chamber of the haemocytometer. The slide was then transferred onto the microscope with 10X objective and 10X ocular. The number of cells was counted in 4 corners of 9 major squares, and the counting was repeated for another chamber. Finally, the number of cells was calculated by the following formula.

Cell number/ml = Total cell number in 8 major squares ÷ 8 x 2 x 10⁴

Total cell number = Cell number/ml x volume of cell suspension
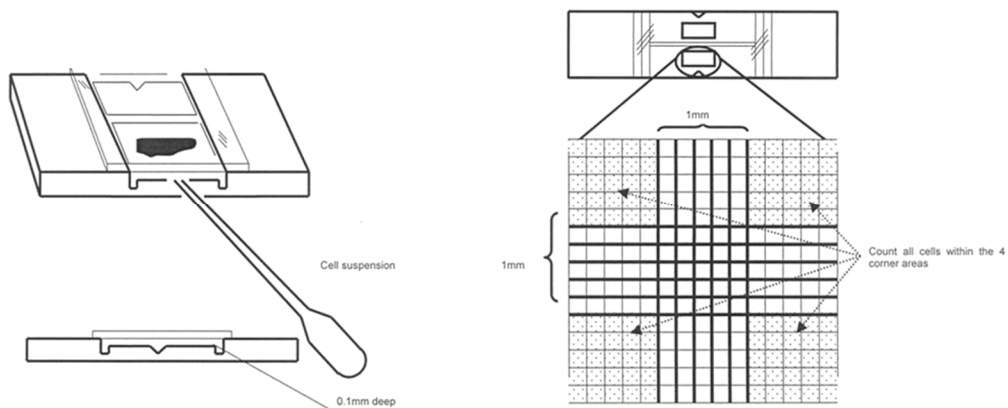
Figure 11 *Counting cells using a haemocytometer.*

(Organization, 2009)

2.2.2. Preparation of lumiflavin-containing media

Lumiflavin was dissolved in 0.1M NaOH and filtered by 0.2μm non-pyrogenic sterile filter to be sterile in the cell culture hood. The concentrated lumiflavin stock (10mM) was aliquoted and stored at -20℃. Lumiflavin was added into DMEM right before used. Final concentration of 0.1M NaOH in lumiflavin-containing DMEM was kept as 2% of the volume of DMEM for all experimental cell groups. Lumiflavin-untreated DMEM also was matched for final concentration of 0.1M NaOH to 2%.

2.2.3. Determination of cell growth

The three intestinal cell lines were planted into a 24well plate and incubated at 37℃ and 5% CO_2 for 1 day to allow cells attached. Cells were then treated with DMEM containing lumiflavin in a range of 0, 10, 25, 40, 60, 75, 90 and 100μM for 24, 48 and 72 hours. At each time points, cells were detached by trypsinisation and counted0. Prior to the main experiment for determination of cell growth, preliminary experiment was performed with Caco-2. The concentrations of lumiflavin used for the preliminary experiment were 0, 0.1, 0.5, 1, 10, 100, 200 and 500μM diluted in DMEM and the time course of lumiflavin treatment was 24, 48 and 72 hours.

2.2.4. Intracellular flavin assay

Intracellular riboflavin, FAD and FMN concentrations were measured using reverse-phase HPLC using a modified method of Capo-chichi et al (Capo-chichi *et al.*, 2000). Flavins are separated by their size and hydrophobicity passing through a column and fluorescence emitted by flavins are detected and converted to flavin concentration.

Preparation of reagents

10% w/v Trichloroacetic acid (TCA) was prepared. 25g TCA was weighed out and dissolved in approximate 200ml of distilled water. It was made up to 250ml with distilled water in a volumetric flask. TCA solution was kept at 4℃ and when used, it was kept on ice.

Flavin buffer was prepared, which consisted of 10mM potassium phosphate and 15mM magnesium acetate buffer, pH2.0. KH_2PO_4 (2.722g) and magnesium acetate (6.435g) were weigh out and dissolved in approximate 200ml distilled water and made up to about 1.8L. This solution was adjusted to pH2.0 with approximate 20ml orthophosphoric acid. Finally, it was made up to 2L in a volumetric flask.

Flavin mobile buffer which is HPLC eluting buffer was prepared as 13% acetonitrile in flavin buffer. 130ml acetonitrile was made up to 1L with flavin buffer. This buffer was filtered to remove gas and dusts using 0.2um nylon membrane filter paper.

Preparation of standards

Stock of combined standard was prepared with 100μM riboflavin, 100μM FMN and 25μM FAD. Riboflavin (18.82mg) was weighed out, dissolved in approximate 100ml of methanol and poured into a 500ml volumetric flask. Weighed FMN (7.13mg) and FAD (44.1225mg) were dissolved in approximate 50ml ddH_2O. The solution was added into riboflavin solution in a volumetric flask and made up to 500ml with ddH_2O. The stock of combined standard was aliquoted with 1.3ml into microtubes and stored at -80℃.

When required, working standards were prepared diluting 100 ㎕ stock of combined standard up to 100ml ddH_2O. Working standard was diluted more with 1 in 2 serial dilutions with ddH_2O. It was kept on ice and in the dark. 200 ㎕ standards were transferred into light-protected tubes, and 100 ㎕ of ice cold TCA was added and mixed well. 150 ㎕ of that was placed into a HPLC vial.

Preparation of cell samples

Cultured cells were harvested and counted. After centrifuged, cells were washed with PBS, transferred into microtubes and centrifuged at 150xg for 5 minutes. Supernatant was removed and cell pellets were stored at -20℃ until analysed.

ddH_2O was added into cell pellet with 200 ㎕/10×10⁶ HCT116, HT29 cells and 150 ㎕/3×10⁶ Caco-2 cells, and mixed well with vortex. Cells in water were lysed by sonication for 5 minutes on ice. 200 ㎕ cell lysate was taken into light-protected tubes. 100 ㎕ ice cold TCA was added into there, mixed well and centrifuged at 20,780xg and 4℃ for 5 minutes. 150 ㎕ of supernatant was taken and placed into a HPLC vial.

Running high performance liquid chromatography (HPLC)

Injection volume was set as 50 $\mu\ell$. Flow rate was 1.5ml/minutes. Florescence was detected at excitation 465nm and emission 530nm and gain 18. Pressure was 2103.1, 2146.6 and 2175.6.

For quality control (QC), whole blood controls; level I and II provided from Chromsystems were used to monitor accuracy of the analysis. 200 $\mu\ell$ of QC was mixed with 100 $\mu\ell$ ice cold TCA and centrifuged. Supernatant was taken and loaded into a HPLC vial. QCs were read before and after running samples. By comparing QCs values of two different times, accuracy of the analysis was able to be monitored.

Calculated flavin concentrations were adjusted by protein concentration. Sonicated cell lysates were centrifuged at 20,780xg and 4℃ for 5 minutes and the supernatant was used to determine protein concentration by Bradford protein assay explained in the section 2.2.10.

2.2.5. Glutathione reductase activation coefficient (GRAC)

Glutathione reductase (GR) is a FAD and NADPH-dependent enzyme which converts oxidised glutathione to the reduced form (Hill *et al.*, 2009).

GRAC is calculated from the ratio between the rate of disappearance of the NADPH in a sample to which an optimal amount of FAD has been added and not added. GRAC is inversely related to intracellular FAD concentration, thus GRAC reflects a functional riboflavin deficiency shown by actual fall in saturation of glutathione reductase with FAD.

Preparation of reagents

GRAC buffer was prepared. Weighed 8.7g K_2HPO_4 was added into 500ml ddH_2O and 6.8g KH_2PO_4 into another flask containing 500ml ddH_2O. Using the KH_2PO_4 solution, the pH of K_2HPO_4 solution was brought to pH7.4. The total volume of the mixture was measured and then EDTA was added to obtain a concentration of 1mg/ml.

Stock of FAD solution was prepared adding 5mg FAD to 33ml buffer and aliquoted 1.5ml to microtubes. Aliquoted FAD stock was wrapped in foil and stored at -20℃. When prepared for use, it is diluted further with the ratio of 1:4 in buffer.

The followings were prepared right before used. 19.6mg GSSG was weighed out and added to 2ml buffer and kept on ice. 6mg NADPH was added to 15ml buffer and kept on ice.

Preparation of cell samples

Cultured cells were harvested and counted by haemocytometer. Cell suspension was centrifuged, wash with PBS and pelleted. Cells were stored at -20℃ until analysed. ddH$_2$O was added into cell pellet with 200 $\mu\ell$/10×10^6 HCT116, HT29 cells and 150 $\mu\ell$/3×10^6 Caco-2 cells, and mixed well with vortex. Cells were then lysed by sonication for 5 minutes on ice. Part of cell lysate was used for determination of intracellular flavins concentration. The remaining cell lysate was centrifuged at 20,780xg and 4℃ for 5 minutes. Supernatant was carefully transferred to new microtubes and kept on ice and in the dark.

Determination of GRAC

5 $\mu\ell$ of a sample were loaded into two blue COBAS sample cups. Into one cup, 135 $\mu\ell$ buffer was added, which was to determine 'unstimulated GR activity'. Into another cup, 115 $\mu\ell$ buffer and 20 $\mu\ell$ FAD solution were added, which was to determine 'stimulated GR activity'. After sample cups were tightly closed and mixed well by inverting 5-6 times, samples were incubated at 37℃ for 30 minutes.

To run COBAS, it should be checked that water in a water bottle on the top is enough. A cuvette ring was properly retained and a lid was correctly covered. It was checked COBAS parameters setting. Sufficient GSSG and NADPH were added into the reagent tray. Glutathione reductase activity was measured by kinetic assay, determining the rate of disappearance of NADPH as the change in absorbance at 340nm. The activation coefficient was calculated as follows.

$$GRAC = \frac{\text{Stimulated GR activity}}{\text{Unstimulated GR activity}}$$

Where GR = glutathione reductase. The assay was run in duplicate for each sample.

2.2.6. Adenosine 5′-triphosphate (ATP) assay

Intracellular ATP concentrations of lumiflavin-treated cells were determined by ATP bioluminescent somatic cell assay kit. This assay is based on the ATP-dependence of firefly luciferase. D-luciferin is oxidised by firefly luciferase emitting light.

$$\text{ATP + Luciferin} \underset{\text{Mg++}}{\overset{\textit{Firefly Luciferase}}{\rightleftarrows}} \text{Adenyl-luciferin + PPi}$$

$$\text{Adenyl-luciferin + O}_2 \longrightarrow \text{Oxyluciferin + AMP + CO}_2 \text{ + Light}$$
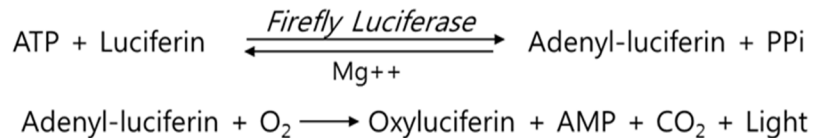
In this study, the light emitted was proportional to the ATP present. The light can be quantified by a luminometer and then converted to ATP concentration using ATP standard curves.

Reagents were prepared by following the preparation instructions of the kit. ddH$_2$O filtered through 0.2μm filter was used to dissolve the reagents. Reaction vials were soaked in 0.1N HCl overnight and rinsed with ddH$_2$O, then left for air dry. This process removed ATP and bacterial contamination. ATP assay mix solution and ATP standard stock solution were aliquoted and stored at -20℃ and in the dark. When used, ATP assay mix was thawed and diluted in to the ratio of 1:25 with ATP assay mix dilution buffer provided. Diluted ATP assay mix was kept in ice and in the dark. ATP standards working solutions were prepared by making serial dilutions of the stock (2μmole).

Cells were cultured in 24-well plates and incubated with DMEM containing 0, 40 and 80μM lumiflavin. At 24, 48 and 72 hours after treatment with lumiflavin, cells were washed with PBS and then PBS was completely removed since PBS can quench the sensitivity. 150 $\mu\ell$ somatic cell ATP releasing reagent per well was dispensed directly into adherent cells and mixed well by gentle pipetting up and down, then detached cells were transferred to a microtube. The samples were kept on ice.

100 $\mu\ell$ ATP assay mix solution were dispensed into a reaction vial and the reaction medium allowed to stand at room temperature for approximately 3 minutes. To stabilize a luminometer, a blank was set up as 0.0, which was prepared as follows: 100 $\mu\ell$ filtered ddH$_2$O were mixed with 100 $\mu\ell$ ATP releasing reagent, and 100 $\mu\ell$ of the mixture was transferred to a

reaction vial already containing 100 $\mu\ell$ ATP assay mix. The reaction vial was mixed well by vortex and the light value of a blank was set as 0.0 in a luminometer.

For ATP standard curves, 100 $\mu\ell$ ATP standards diluted in filtered ddH$_2$O and 100 $\mu\ell$ ATP releasing reagent were mixed together. 100 $\mu\ell$ were taken into a reaction vial containing 100 $\mu\ell$ ATP assay mix. A vial was mixed well by vortex and the light produced in a luminometer measured immediately.

Since ATP extracts from cells had already included ATP releasing reagent, 100 $\mu\ell$ of the extract was mixed with 100 $\mu\ell$ filtered ddH$_2$O. The produced light was determined with the same procedure as done for standards. The light values were converted to ATP concentration using the standard curve. The remains of diluted ATP extracts were used for the measurement of protein concentrations, and finally ATP concentrations were corrected for protein concentration.

2.2.7. Reactive oxygen species (ROS) assay

The intracellular ROS concentration was determined using the cell-permeable and fluorogenic probe 2′,7′-dichlorodihydrofluorescein diacetate (DCFDA) in the three cell lines. DCFDA diffuses into cells and is deacetylated by cellular esterases to non-fluorescent DCFH, which is subsequently oxidised to highly fluorescent DCF by ROS, predominantly H$_2$O$_2$. Fluoregenic probing with DCFDA has been widely used as an indicator of ROS formation and oxidative stress (LeBel *et al.*, 1992).

DCFDA was prepared by dissolving in DMSO. 50mM stock was aliquoted and stored at -20℃ before use. When used, 100μM DCFDA diluted in riboflavin and serum-free DMEM was prepared and kept in dark.

Cells were transferred into a 96-well black-walled clear bottom plate suitable for fluorescence measurements with a seeding density that would lead to 80% confluence after 4 days. After 1 day to allow cells to become attached to the surface of a plate, cells were treated with 0, 40 and 80μM lumiflavin-containing DMEM for 24, 48 and 72 hours.
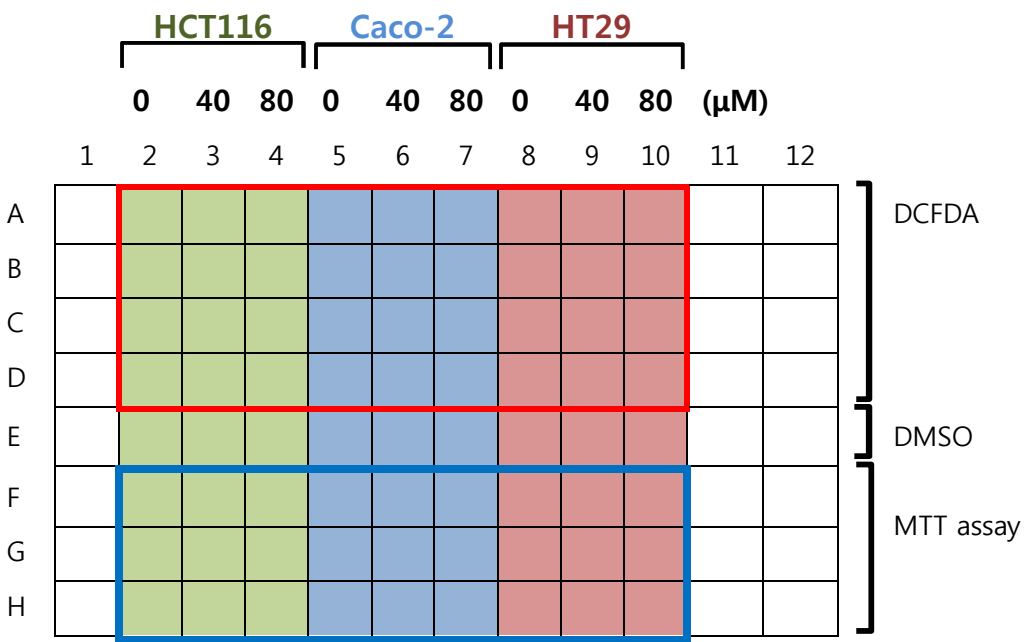
Figure 12 *A 96-well plate layout used for ROS and MTT assay.*

Cells were seeded, and lumiflavin of 0, 40 and 80µM was treated to the cells. Three plates were prepared. At 24, 48 and 72 hours after treatment with lumiflavin, upper half of a plate was used for DCFDA assay. E lane was used for blank of DCFDA assay. Lower half (F~H lane) was used for MTT assay.

At each time point, cells in a half of the plate were washed with PBS twice. 100 ㎕ of 100µM DCFDA diluted in riboflavin and serum-free DMEM was added into cells and the plates were incubated at 37℃ for 30 minutes. For blank of DCFDA, DMSO was treated with the same conditions as DCFDA. Then, DCFDA and DMSO were removed and cells were washed with PBS twice again. 100 ㎕ riboflavin and serum-free DMEM was added to cells. The plate was read by a fluorescence microplate reader with excitation wavelength at 485nm and emission wavelength at 530nm. Fluorescence was recorded right after DCFDA was removed and then every 30 minutes or 1 hour up to 4 hours. Intensity was set as 10 and gain, 1. In parallel wells, MTT assay was performed in order to correct the difference of cell numbers. This will be described in the next section

2.2.8. MTT assay

MTT (3-(4,5-Dimethylthiazol-2-yl)-2,5-diphynyltetrazolium bromide) assay is an alternative method to count viable cells measuring the activity of living cells through mitochondrial dehydrogenase activity. Mitochondrial dehydrogenases of viable cells cleave the tetrazolium ring and form purple MTT formazan crystals which are soluble in acidified isopropanol. The resulting purple formazan solution is spectrophotometrically measured. Absorbances are quantified using an absorbance/cell number curve.

Pre-incubated cells with lumiflavin-containing DMEM were washed with PBS. 50 $\mu\ell$ of 10% MTT solution diluted in lumiflavin-free DMEM was added and incubated at 37℃ for 3 hours. Then, the same amount of MTT solvent (50 $\mu\ell$/well) as 10% MTT solution was directly added into cells and mixed well by pipetting up and down. The plate was read by a plate reader at a wavelength of 562nm and background absorbance measured at 630nm was subtracted.

Absorbance/cell number curves for three cell lines were prepared. Cultured cells were planted in 96-well plate with the different seeding densities in a range of 1000 to 20,000 cells of HCT116 and HT29 and 500 to 10,000 cells of Caco-2 in three replicates. Cells were left to settle down in an incubator. On the next day, MTT assay was performed as described above. Absorbance values and cell numbers were plotted on a graph and obtained equation was used to convert absorbance to cell number.

2.2.9. Clonogenic assay

The clonogenic assay measures the ability of cultured cells to form colonies. Cytotoxic agents may inhibit the clonogenic ability of cells. Thus, the clonogenic assay can determine the proliferative ability of cells and cytotoxicity after incubation with lumiflavin. The reversibility of any effect of lumiflavin also can be determined.

Seeding cells

The three cell lines were seeded into T25 culture flasks and incubated at 37℃ and 5% CO_2 for 1 day to allow cells attached. Cells were treated with 0, 40 and 80μM lumiflavin-

48

containing DMEM. At 24, 48 and 72 hours after treatment, cells were split. After trypsinisation, cell suspension was passed through a 20gage needle 5 times in order to make single cells. Cell numbers were counted by haemocytometer and according to the number of counted cells, cell suspension was diluted. The appropriated number of cells was seeded into a 6 well plate in four replicates, to which 2-3ml lumiflavin-free DMEM was already added. The optimal seeding densities for each three cell lines were selected by preliminary experiments. Then, cells were incubated at 37℃ and 5% CO_2 until a single cell formed the proper size of a colony which consisted of over 50 cells. Thus, a thousand Caco-2 cells were seeded and incubated for 1 week, five hundred HCT116 cells for 12 days, and five hundred HT29 cells for 2 weeks.

Staining and counting colonies

Colonies were stained and counted. Firstly, already existing media were removed. The colonies were then washed once with 2ml PBS per well and fixed with 1ml 70% methanol per well for 5 minutes at room temperature. After methanol was removed, 2ml 1% methylene blue per well was added and incubated at room temperature for 10 minutes. Stained colonies were washed twice with approximate 2ml distilled water per well, and allowed to dry in the air for over half an hour. The colonies composed of over 50cells were counted manually by naked eyes and by viewing under a microscope. The absolute clonogenicity (AC) by following equation and the relative clonogenicity (RC) of lumiflavin-treated cells against control cells (0μM) were calculated.

AC = colony number ÷ seeded cell number × 100

2.2.10. Determination of protein concentration

Bio-Rad Bradford reagent was diluted in to the ratio of 1:5 in ddH_2O, and protein extract samples were diluted in to the ratio of 1:20 in ddH_2O. 4 $\mu\ell$ of standards (BSA 1, 0.75, 0.5, 0.25, 0.125 and 0.0625 mg/ml in ddH_2O) and ddH_2O for blank were loaded into a 96-well plate in duplicate. 4 $\mu\ell$ of diluted samples were dispensed in duplicate or triplicate. Then, 200 $\mu\ell$ of diluted Bio-Rad reagent was dispensed into the wells. After 1minute, the absorbance of them was measured on a microplate reader at 595nm. The absorbance values were subtracted blank from. Mean absorbance of standards was plotted on a graph. An equation was used to convert

absorbance values of samples to protein concentration and finally the result concentration were multiplied by diluted factor.

2.2.11. Apoptotic DNA assay

Apoptosis was investigated using an apoptotic DNA ladder detection kit. Apoptotic DNA laddering assay is the method detecting DNA fragmentation which is caused by apoptosis. Therefore, apoptotic DNA will show multiple bands or a smear on the agarose gel while normal DNA will not.

All required reagents were prepared following the provided manufacturer's instruction. The kit contained TE lysis buffer, enzyme A solution, enzyme B (lyophilised), ammonium acetate solution, and DNA suspension buffer. Enzyme B was dissolved with 275 $\mu\ell$ ddH$_2$O and mixed well before use. The enzyme B solution was aliquoted and stored at -80℃. In addition, ddH$_2$O, PBS and isopropanol were prepared.

As a positive control, sodium butyrate was used to induce apoptotic DNA fragmentation. 1M sodium butyrate stock solution was prepared in sterile ddH$_2$O and aliquoted then stored at -20℃. Three intestinal cell lines; Caco-2, HCT116 and HT29 were exposed to 10mM sodium butyrate for 24 hours, and detached cells as well as adherent cells were separately harvested by gentle trypsinisation. Cells were washed with PBS and centrifuged at 1500xg and 4℃ for 5 minutes. Cell pellets were stored at -20℃ until analysed.

The three cell lines were pre-incubated in lumiflavin-containing DMEM, when harvested, detached cells and adherent cells were separately collected. Floating cells in used media were taken and spun down, and then cell pellets were washed in PBS twice, transferring to microtubes. Cells were centrifuged at 1500xg and 4℃ for 5 minutes. Cell pellets were stored at -20℃ until analysed. Adherent cells were harvested by trypsinisation. Cell numbers were counted using a haemocytometer and trypan blue staining. $0.25 \sim 1 \times 10^6$ cells were pelleted and washed with PBS twice then centrifuged at 150xg and 4℃ for 5 minutes. Cell pellets were stored at -20℃.

Cells were lysed with 35 $\mu\ell$ of TE lysis buffer by gentle pipetting, provided in the kit. 5 $\mu\ell$ of enzyme A solution was added and mixed by gentle vortex. The mixture was incubated at 37℃ for 10 minutes. Then, 5 $\mu\ell$ of enzyme B solution was added and the mixture incubated at 50℃ for 30 minutes. 5 $\mu\ell$ ammonium acetate solution was added to each sample mixture and 50 $\mu\ell$ isopropanol was added and mixed well, and the mixture was kept at -20℃ for 10 minutes. The mixture was spun down at 600xg, 25℃ and for 10 minutes. Supernatant was removed and the DNA pellet was washed with 0.5ml of 70% ethanol. Trace ethanol was removed and dried in the air for longer than 10 minutes at room temperature. Dried DNA pellet was dissolved in 30 $\mu\ell$ DNA suspension buffer. To take images of DNA, 1.2% agarose gel containing 0.5μg/ml ethidium bromide in both gel and running buffer was prepared. 15~30 $\mu\ell$ of the sample was loaded into the gel, and 1kb DNA ladder was also loaded as a standard of DNA size. The gel was run at 50V for 2 hours. Ethidium bromide-stained DNA was visualised by transillumination with UV light.

2.2.12. Western blot

Western blotting is a widely used method for the detection or quantitation of proteins. Proteins are separated according to their size by gel electrophoresis and the proteins can then be identified using specific antibodies against the proteins of interest.

Caco-2 cells were incubated in 40μM lumiflavin-containing DMEM for 3, 6, 17, 24 and 48 hours and then harvested by trypsinisation. Cell number was counted using a haemocytometer and trypan blue staining. After removing trypsin by centrifugation at 150xg and 4℃ for 5 minutes, cells were washed with PBS twice and pelleted.

Cell lysis

Kinase buffer was freshly prepared right before use, whose constituent is presented on Table 2. The volume of kinase buffer was determined with the proportion of 10 $\mu\ell$/0.1×10^6 cells or the volume of cell pellet was roughly determined by eyes, compared with already known volumes of water. Cell pellets were suspended in ice cold kinase buffer by pipetting gently, and stayed on ice for at least 20 minutes with concealment from the sunlight. Then, cell lysates were prepared by cell disruption using a sonicator (high pulse: 5 minutes), keeping staying on ice slush to avoid heat which produced by sonication. They were centrifuged at 20,780xg and 4℃

for 15 minutes. The supernatants were transferred to fresh microtubes, and the protein concentrations were determined and the rest were stored at -80℃.

Cell lysates were taken with the wanted volume depending on the protein concentration and mixed with loading buffer. The mixtures were heated at 95℃ for 5 minutes. Then cooled mixtures were centrifuged down and ready to load to the SDS-PAGE gel.

Table 2 *Preparation of kinase buffer*

Reagent	quantity($\mu\ell$)	Final concentration
1M Tris, pH 7.5	500	50mM
1M NaF	500	50mM
1M B-Glycerophosphate	100	10mM
0.2M EDTA	50	1mM
0.2M EGTA	50	1mM
10% Triton X-100	200	0.2%
ddH$_2$O added up to 10ml		
0.1M PMSF *	10	0.1mM
0.1M NaVO$_4$ *	100	1mM
Protease Inhibitor Cocktail *	100	
***Added directly just before use**		

Table 3 *Preparation of SDS-PAGE gels, running buffer and blotting buffer*

Solution	Stacking gel	Resolving gel			
		7.5%	10%	12%	15%
ddH$_2$O	6.1 ml	7.4	6.1	5.2	3.75
Tris (Stacker) 0.5M pH 6.8 (Resolve) 0.5M pH 8.8	2.5 ml	3.75	3.75	3.25	3.75
Acrylamide	1.3 ml	3.65	4.95	5.8	7.25
10% SDS	100 $\mu\ell$	150	150	150	150
10% APS	100 $\mu\ell$	75	75	75	75
TEMED	20 $\mu\ell$	18	18	18	18
Running buffer(10X)	Diluted to 1X with ddH$_2$O				
Blotting buffer(10X)	Diluted to 1X with the ratio of 3:1:6 of methanol:10X buffer:ddH$_2$O				

To prepare SDS-PAGE gels, the gel apparatus was cleaned and assembled. Following the gel constituents on Table 3, resolving gels were prepared and immediately loaded into the plate and about 1ml of ddH$_2$O was layered on the top, and then left for about 20 minutes to set. After removing ddH$_2$O, prepared stacking gel was loaded and a comb was placed in a gel, and then left for about 20 minutes to set.

The plates were placed in gel running apparatus and the outer tank and 1X running buffer was filled ensuring the wells were covered and about half of the outer tank were filled. After a comb was removed, protein samples and 5 $\mu\ell$ of protein marker were loaded into wells with fine tipped pipette tips. The lid on the tank was placed ensuring the terminals were correctly aligned, red to red and black to black. Gels were run at 100V for 100 minutes.

PVDF membrane, two blotting papers, two sponges, blotting cassettes, methanol and blotting buffer were prepared. PVDF membrane was soaked into methanol for 30 seconds and transferred to a tray that filled with blotting buffer. The blotting cassette (white side down), a sponge were placed ensuring all soaked into the buffer. Then, the plates were removed from the gel running apparatus, and the plates were carefully opened. The stacking gel was removed from the resolving gel. The gel was carefully demounted from the plate, and placed it on a wet blotting paper. A membrane was covered on the gel and then another blotting paper was placed on a membrane and the soaked sponge was on the top. Air bubble between the gel and membrane was removed, which may interrupt transferring proteins of the gel to a membrane. The blotting cassette assembly was closed, locked and placed in the electrophoresis tank with an ice pack. Blotting buffer was filled into the tank until the cassette was covered. It was run at 100V for 90~100 minutes. Ice pack was replaced about an hour later.

Blocking and probing

The membrane was incubated in blocking solution overnight at 4℃ with constant agitation.

- 0.2% gelatin in PBST (0.1% tween 20) for phospho-tyrosine
- 1% BSA in PBST(0.1% tween 20) for phospho-serine/threonine,
- 5% BSA in ddH$_2$O with 0.05% tween 20 for SR and phospho-SR proteins

Then, the membrane was incubated in primary antibody solution overnight at 4℃ with constant agitation.

- Anti-phospho-tyrosine (1:200) in 0.2% fish gelatin in PBST (0.1% tween 20)
- Anti-phospho-serine/threonine (1:300) in 1% BSA in PBST (0.1% tween 20)

- Anti-phospho-SR (1:1500) in 5% BSA in ddH2O with 0.05% tween 20
- Anti-SR (1:500) in 5% BSA in ddH2O with 0.05% tween 20

The membrane was rinsed four times in TBST. Secondary antibody solutions were prepared as following below.

- Polyclonal rabbit anti-mouse IgG HRP conjugated antibody (1:2000) in 0.2% gelatin in PBST (0.1% tween 20) for phospho-tyrosine
- Polyclonal goat anti-rabbit IgG HRP conjugated antibody (1:2000) in 1% BSA in PBST(0.1% tween 20) for phospho-serine/threonine,
- Polyclonal rabbit anti-mouse IgG HRP conjugated antibody (1:5000) in 5% skimmed milk for SR proteins and phospho-SR proteins

The membrane was incubated in the secondary antibody solution at room temperature for 1 hour with constant agitation. And it was rinsed four times in TBST and washed in fresh TBST for 5~10 minutes with constant agitation. The protein bands on the membrane were detected using ECL solution (with mixing the equal volume of each two solutions) and imaging system (ChemiGenius2, Japan). The signals were quantified by densitometry (GeneTools program, Japan).

The signals were normalised by detecting ß-actin as the membrane rinsed four times in TBST were incubated in anti-ß-actin (1 : 5000) in 1% BSA in PBST (0.1% tween 20) at room temperature for 1 hour with constant agitation. Then, the ß-actin bands were detected.

2.2.13. High content analysis (HCA)

High content analysis also known as high content screening or visual screening is a method based on sophisticated and automated image analysis in a fluorescence-stained cell. This method can detect cellular phenotypic changes and quantify them using fluorescence staining of cells which leads to different fluorescence strength and thereby different cellular changes.
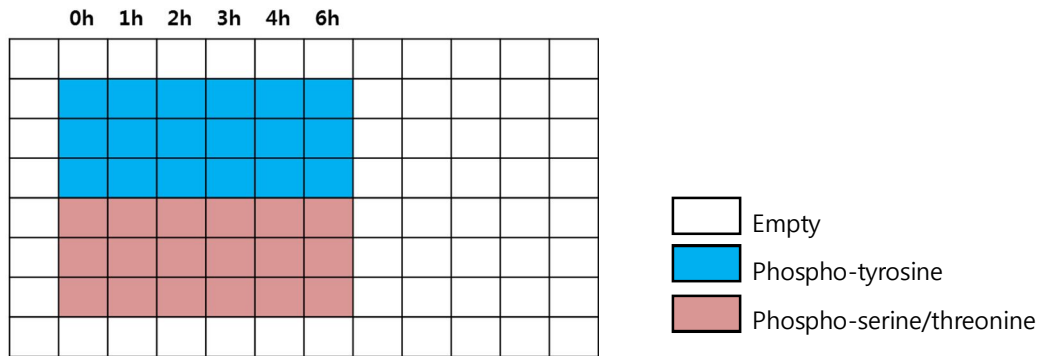
Figure 13 A *96-well plate layout used for HCA.*

Caco-2 cells were used to investigate the effect of lumiflavin in the short term on global phosphorylation using HCA. 7500 cells per well were planted on a 96-well black-walled clear bottom plate suitable for fluorescence measurement. Cells were incubated at 37℃ and 5% CO_2 for 24 hours to settle down on the plate. Prepared 40μM lumiflavin-containing DMEM was added into cells and all cells were washed in PBS and fixed in 10% formaldehyde at the same time.

For staining with primary antibodies, antibody solutions were prepared in digitonin with the different concentrations; the ratio of 1:250 for phospho-tyrosine and 1:100 for phospho-serine/threonine. After washing cells in PBS twice, 50 ㎕ of antibody solution per well was loaded and incubated at room temperature for 1 hour in the dark. For secondary antibody solutions, Alexa Fluor 488, anti-mouse secondary antibody for phospho-tyrosine and Alexa Fluor 555, anti-rabbit secondary antibody for phospho-serine/threonine, Hoechst and PBS were required. The secondary antibodies were diluted in to the ratio of 1:500 and Hoechst was diluted in to the ratio of 1:1250 in PBS. Cells were washed twice with 100 ㎕ of PBS. Prepared 50 ㎕ of secondary antibody solution per well was loaded and incubated at room temperature for 30 minutes in the dark. Then, after washing twice with PBS again, cells were stored in 100 ㎕ of PBS, covered the plate with a sticker and foil to keep cells wet and in the dark. The plate was stored at 4℃ fridge until analysed. Analysis was requested to Imagen Biotech in Manchester, UK.

2.2.14. Purification of phosphoproteins

Phosphorylated proteins are bound with high specificity to phosphoprotein purification resin, while unphosphorylated proteins flow through the resin. And phosphoproteins bound to the resin are eluted and purified. This process thus amplifies the signals of phosphoproteins.

Preparation for reagents provided in the kit

875 $\mu\ell$ CHAPS stock solution (10% [w/v]) was added to 35ml of phosphoprotein lysis buffer to yield ad final concentration of 0.25% (w/v) CHAPS in lysis buffer. One protease inhibitor tablet and 10 $\mu\ell$ of Benzonase Nuclease stock solution were added to a 5ml aliquot of lysis buffer containing CHAPS. Then phosphoprotein lysis buffer was ready. 75 $\mu\ell$ Triton X-100 (10% [w/v]) was added to 3ml of phosphoprotein elution buffer.

Cell lysis

Cell lysis was performed at 4℃. Cell pellets were washed with HBSS and resuspended corresponding to 10×10^6 cells in 5ml of lysis buffer. The cell suspension was incubated at 4℃ for 30 minutes, vortexing briefly every 10 minutes. Then it was centrifuged down at 10,000 xg and 4℃ for 30 minutes. During centrifugation, phosphoprotein purification column was prepared by detaching the top cap, breaking off the bottom closure, and slowing the storage buffer to flow out. 4ml lysis buffer was applied to equilibrate the column and allowed to flow out. When finished centrifugation, the supernatant was taken and the protein concentration was determined. It was taken the volume of cell lysate containing approximately 2.5mg of total protein. Then, protein concentration was adjusted to 0.1mg/ml by adding lysis buffer to yield the final volume of 20ml cell lysate.

Columning

Half of the cell lysate was loaded into the upper reservoir of the column. When almost all lysate had entered the gel bed, the rest of lysate was added and allowed enough time to complete binding of any phosphorylated protein to the affinity column. 6ml of lysis buffer was applied to wash the column and allowed to flow through. Collection tubes were ready under the column. 500 $\mu\ell$ of elution buffer was applied to the column and the eluted fraction was collected. Elution process was repeated six times and the each eluted fractions were separately collected into six tubes. Each eluted fractions were determined for protein concentrations.

10 $\mu\ell$ of each eluted fraction was loaded into a 10% SDS-PAGE gel and the different amount of purified phosphoprotein in each eluted fraction was visualised using Pro-Q Diamond phosphoprotein stain. The rest of eluted tractions were stored at -80℃ until used for concentration by centrifugal filtration.

2.2.15. Staining with Pro-Q Diamond phosphoprotein and SYPRO® ruby

In order to confirm purified phosphoproteins, pooled eluted fraction, flow through fraction and cell lysates were stained on the SPS-PAGE gel with Pro-Q Diamond phosphoprotein stain and also SYPRO® ruby for total protein. PeppermintStick™ phosphoprotein molecular weight standards were also loaded to the gel, provided in the Multiplexed Proteomics® Phosphoprotein gel stain kit. The standards served both as molecular weight markers and as positive and negative controls.

Pro-Q Diamond phosphoprotein gel stain provides a method for selectively staining and detecting phosphate groups attached to tyrosine, serine, or threonine residues without the need for antibodies. SYPRO® Ruby protein gel stain is a total protein stain which is highly sensitive lumiscent staining. According to the instruction, determining the ratio of Pro-Q Diamond dye to SYPRO® Ruby dye signal intensities for each band provides a measure of the phosphorylation level normalised to the total amount of protein.

ProQ-Diamond phosphoprotein gel stain

Fix solution of 50% methanol and 10% acetic acid and destain solution of 20% acetonitrile, 50mM sodium acetate, pH4.0 were prepared. To prepare 1L of destain solution, the followings were combined and mixed thoroughly; 50ml of 1M sodium acetate, pH4.0, 750ml of ddH$_2$O and 200ml of acetonitrile.

The gel was fixed in about 100ml of fix solution and incubated at room temperature with gentle agitation for at least 30 minutes, and fixation step was repeated once more to ensure that all of the SDS was washed out of the gel. Then, the gel was washed in about 100ml of ddH$_2$O with gentle agitation for 10 minutes to remove all of the methanol and acetic acid from the gel. The washing step was repeated twice more. The gel was stained by being incubated in 50ml of Pro-Q Diamond phosphoprotein gel stain, whose volume was equivalent to 10 times the volume of the gel with gentle agitation in the dark for 80 minutes. Then, to destain the gel,

it was incubated in 80ml of destain solution with gentle agitation for 30 minutes at room temperature in the dark. This step was repeated two more times, and then the gel was washed twice in ddH$_2$O at room temperature for 5 minutes per wash. The stained gel was visualised using Typhoon 9400 (Amersham Biosciences) with excitation at 532nm laser and emission at 560nm longpass

SYPRO® Ruby protein stain

Wash solution of 10% methanol, 7% acetic acid in ddH$_2$O was prepared. This stain was performed with the gel which was used for phosphoprotein stain, thus fixation and washing steps were skipped. The gel was rinsed twice in ddH$_2$O for 5 minutes each, and then incubated in 60ml of SYPRO® Ruby gel stain at room temperature overnight with gently agitation, protected from light. Afterwards, the gel was transferred to a clean container and washed in about 100ml of wash solution for 30 minutes. Before imaging, the gel was rinsed in ddH$_2$O two times for 5 minutes each. Proteins were visualised using the imager Typhoon 9400 with an excitation at 457nm and an emission at 610nm blue laser

2.2.16. Sample concentration by filtration

The Millipore spin columns with 3K molecular weight cut off membrane were used to concentrate the eluted fractions of phosphoprotein. Samples were buffer-exchanged by repeated addition of 1M TEAB which is iTRAQ buffer to remove Qiagen elution buffer. This is also an important step to clean up an ionizing contaminant that has caused problems with downstream of mass spectrometry analysis.

The filter device was inserted into the provided microcentrifuge tube and pre-rinsed three times with 0.5ml of ddH$_2$O and spun down at 14,000xg for 10 minutes to remove the glycerol which was contained on the filter membrane. When checked liquid level and just above 50 $\mu\ell$, the liquid in the tube was discarded and further 0.5ml ddH$_2$O was added and spun down.

Four eluted fractions from second to fifth eluted fractions were filtered in two filter devices, and then combined and concentrated in one filter device to be pooled altogether. After pre-rinsing the filter device, up to 500 $\mu\ell$ of sample was added into the filter device.

Capped filter device was placed into the centrifuge rotor, aligning the cap strap toward the center of the rotor, and then centrifuged at 14,000xg and 4℃ for 30 minutes, checking the remaining liquid volume in the filter device every 10 minutes to prevent overspin that may lead to dry out the membrane. Then, for buffer exchange, 0.5ml of 1M TEAB buffer was added and centrifuged at 14,000xg and 4℃ for 15 minutes and this step was performed total four times. The concentrates in the two filter devices were combined to pool all eluted fractions and centrifuged at the same speed for 30 minutes. To recover the concentrated solute, the filter device was placed upside down in a clean microcentrifuge tube, and the tube was placed in the centrifuge, aligning open cap towards the center of the rotor. Then, it was centrifuged at 1,000xg and 4℃ for 2 minutes and the concentrated phosphoprotein was collected into a fresh tube. An aliquot of it was used to determine the protein concentration and to run on the SDS-PAGE gel with Coomassie® blue staining to ensure adequate phosphoprotein concentration. The rest was stored at -80℃ until used for trypsin digestion.

2.2.17. Coomassie® blue stain

After electrophoresis to run protein on SDS-PAGE gel, the gels were transferred to the InstantBlue staining solution and incubated at room temperature overnight with constant agitation, protected from light. Approximate 20ml of the solution was used to ensure enough to cover the gel. Then, the gel was rinsed four times in ddH$_2$O, and taken the images.

2.2.18. Isobaric tag for relative and quantitation (iTRAQ)

2.2.18.1. Trypsin digestion

TCEP which is a reducing agent to break disulfide bonds within and between proteins was prepared, diluting 500mM stock of TCEP in to the ratio of 1:10 with 1M TEAB buffer. MMTS which is an alkylating reagent that reversibly blocks cysteines and other sulfhydryl groups was prepared, diluting 10M stock MMTS with the ratio of 1:50 with isopropanol. Trypsin that contains 20μg in a vial was prepared, adding 5 $\mu\ell$ of trypsin resuspension buffer, which was 50mM acetic acid, and 35 $\mu\ell$ of 1M TEAB buffer to a vial.

Phosphoprotein volumes were calculated to take 85μg. Due to varying volume of each sample, the final volume was filled up to 20 $\mu\ell$ with 1M TEAB buffer. Then, 2 $\mu\ell$ of 20mM TCEP was added to the sample, vortexed well, spun down and incubated for 1 hour at 60℃. Afterwards, 1 $\mu\ell$ of 200mM MMTS was added to a sample, vortexed well, spun down and incubated at room temperature for 10 minutes. An aliquot equivalent to 5μg protein was taken and stored at -20℃, and it was run on the gel later to show 'non-digested proteins'. Then, samples were trypsin-digested at 1:20 ratio (4μg trypsin to 80μg protein) at 37℃ overnight. An aliquot equivalent to 5μg protein was taken to be run on the gel for 'digested sample'. The rests were stored at -80℃ until labelling. The aliquots taken for 'non-digested' and 'digested samples' were run on 10% SDS-PAGE gel and stained with Coomassie® blue for overnight at room temperature with constant agitation, protected from light.

2.2.18.2. Labelling

Peptides were labelled as shown in Table 4, using iTRAQ reagent 8PLEX Multi-plex kit (AB Sciex). Reagents tubes were spun down to make sure the yellow liquids were in the bottom of the tubes. 100 $\mu\ell$ of isopropanol was added to each tube and mixed well and spun down to recover the contents. All content in one tube was taken at once and transferred to one sample. It was then mixed well, spun down and incubated at room temperature for 2 hours in the dark. The samples were stored at -80℃ until used for fractionation.

Table 4 *Samples abbreviation and iTRAQ label*

Treatment details	iTRAQ label
Exp49. 0h	113
Exp50. 0h	116
Exp49. 6h C	114
Exp50. 6h C	117
Exp49. 6h LF	115
Exp50. 6h LF	118
Exp50. 24h C	119
Exp50. 24h LF	121

Exp, experiment; h, hours; C, control; LF, lumiflavin

2.2.18.3. HILIC fractionation

Labelled 8 samples were combined and vacuum-concentrated. The combined peptides were fractionated using high resolution Hydrophilic Interaction Liquid Chromatography (HILIC)-HPLC. Fractionation was performed on an Agilent 1100-series HPLC (Agilent, Berkshire UK), coupled to a PolyHYDROXYETHYL-A (5μm particle size, a column dimension of 200mm, 4.6mm ID, 200Å pore size, PolyLC) analytical HILIC column. This was carried out by Dr. Caroline Evans in the department of chemical and biological engineering at University of Sheffield. The column was run for 60 minuetes at a flow rate of 0.5ml/min with HILIC transfer buffer A: 80% acetonitrile, 10mM ammonium formate, pH 3.0 to remove salts, TCEP and unincorporated iTRAQ reagent. Peptides for analysis were eluted using a 30 minutes elution gradient with increasing HILIC buffer B (HILIC: 5% acetonitrile, 10mM ammonium formate, pH 5.0, 0.5ml/min) from 0-60% buffer B (from 10-40 minutes), followed by 60-100% buffer B (5minutes) and 100% buffer B (10 minutes) at a flow rate of 0.5ml/min. The column was isocratically washed in buffer B for another 5 minutes, and then re-equilibrated in 100% transfer buffer A until 66 minutes. Chromatography was monitored at 280nm using an Agilent 1100 ultraviolet detector module and Chromeleon software v.6.50 (Dionex, LC Packing, The Netherlands). 67 fractions were collected in LoBind tubes in 1 minute intervals and concentrated by a vacuum centrifugal dryer. Then, they were stored at -80℃ until used for sample desalting.

2.2.18.4. Sample desalting

Sample desalting was performed using UltraMicrospin columns (The NEST group) and buffers; buffer A (97% H_2O and 0.1% formic acid), buffer B (97% acetonitrile and 0.1% formic acid) and buffer C (3% acetonitrile and 0.1% trifluoroacetic acid). 100 $\mu\ell$ acetonitrile was added to a column inserted to a tube without bubbles in a column, and spun down at 100xg for 10 seconds. Acetonitrile in the column was washed out twice with 100 $\mu\ell$ HPLC grade H_2O by centrifugation at 100xg for 30 seconds. During second washing, 100 $\mu\ell$ buffer C was loaded to dried sample, mixed well and pulsed. Dissolved sample in buffer C was added into columns and spun down at 100xg for 30 seconds. Then, buffer A was added to the column and centrifuged at 100xg for 30 seconds and this step was repeated so to be total two washings. The column was transferred to a fresh and labeled LoBind tube, and 50 $\mu\ell$ buffer B was added

and spun down at 200xg for 30 seconds. Another 50 $\mu\ell$ buffer B was added and pressed down by pipetting to allow buffer B to go through the column. Thus, desalted sample was collected in a LoBind tube and dried in vacuum centrifugal dryer for approximately 4 hours.

2.2.18.5. Mass spectrometry

Mass spectrometry was performed using a Q-STAR XL Hybrid ESI Quadrupole time-of-flight tandem mass spectrometer (ESI-qQ-TOF-MS/MS) (Applied Biosystems; MDS-Sciex) coupled to an online Ultimate 3000 nano-LC system (Dionex, LC Packings, The Netherlands). These were carried out by Dr. Caroline Evans in the department of chemical and biological engineering at University of Sheffield. Each vacuum-dried peptide fractions were re-dissolved in loading buffer (0.1% formic acid and 3% acetonitrile), injected and captured into a 300µm ID C18-PepMap trap column. Trapped samples were then eluted to a 15cm, 75µm ID C18-PepMap analytical column. The LC gradient was with 3% buffer B (0.1% formic acid and 97% acetonitrile) and 97% buffer A (0.1% formic acid and 3% acetonitrile) for 3 minutes. Then, a 90-minutes LC-MS/MS gradient program with 3-30% buffer B was followed. The mass spectrometer was set to acquire data with a selected mass range of 300-2000m/z. 3 seconds summation of MS/MS scan was followed with pre-selection for peptides with +2 to +4 charge states. The two most abundantly charged peptides above a five count threshold were selected for MS/MS, and dynamically excluded for 60 seconds with a ±50mmu mass tolerance (Glen *et al.*, 2010).

2.2.18.6. Protein identification and relative quantification

MS/MS data generated from the QSTAR® XL was converted to MGF peaklists using Analyst QS v. 1.1 (Applied Biosystems, Sciex; Matrix Science). Swiss-Prot and Trembl *Homo sapiens* protein database (41070, 71449 ORFs respectively) were downloaded from UniProt, (April, 2013). Then peptide sequence and hence protein identification were performed using an in-house Phenyx algorithm cluster (binary version 2.6; Genebio Geneva Bioinformatics SA) at the ChELSI Institute, the University of Sheffield and ProteinPilot Software v2.0 (Applied Biosystems; MDS Sciex). Protein quantification was done using uTRAQ v4.0 which is an iTRAQ-based protein quantification software. Proteins were quantified by determining the iTRAQ reporters'

intensities for peptides, thus producing protein fold changes. Median correction was applied for bias normalization. Protein fold change was analysed statistically using SignifiQuant v4.0 in a paired comparison way to determine alteration in protein level among samples. In order to assess significant pathways altered by an exposure to lumiflavin, overrepresentation analysis by a pathway database, Reactome v45 was carried out, using UniProt accession number of proteins showing a significant fold change compared with controls.

2.2.19. Cell cycle analysis by flow cytometry

Caco-2 cells were treated with 40μM lumiflavin for 6, 24, and 48 hours, and time 0 hour and time-controls were set with 2% (v/v) of 0.1M NaOH in DMEM. Cell were harvested by trysinisation and splitted into single cells by repeated pipetting. Cells were washed with PBS twice. Pelleted 0.2×10^6cells were fixed in 1ml of ice cold 70% ethanol by adding drop by drop, then fixed cells in ethanol were stored at -20℃ until analysed. Cell samples were prepared in three replicates.

Fixed cells were transferred to microtubes and washed in PBS twice. After centrifugation, supernatant was removed, leaving cell pellet. Then, 0.5ml of PI/RNase staining solution was added to cell pellet, and incubated for 30 minutes at room temperature, protected from light. Stained cells were analysed using BD LSR Ⅱ Flow cytometer with 488nm excitation and a 660/20 bandpass filter for emission. Data analysis was run by BD FACSDiva 7.0.

2.2.20. Statistical analysis

Statistical analyses were carried out using SPSS 20.0 statistical software for Windows. Data were examined for distribution characteristics using Shapiro-Wilk and Kolmogorove-Smirnov tests. Depending on the distribution of data, parametric test or non-parametric tests were selected. Data for cell growth, clonogenic assay, ROS and global phosphorylation by western blot and HCA were not normally distributed, and therefore, these variables were analysed using the non-parametric ANOVA, Kruskal-Wallis test. Duncan post hoc test using a rank or Dunnett T3 post hoc test using a rank were followed depending on the raw data homogeneity. A comparison of normal and lumiflavin-treated cells on intracellular flavin concentrations and GRAC was determined using one-way ANOVA followed by the Duncan post

hoc test. For analysis of intracellular ATP concentration and cell cycle analysis by flow cytometry, two-way ANOVA was used since the comparison involved two independent factors such as treatment and more than one time point. When a significant interaction between treatment and incubation time was found, one-way ANOVA followed by post-hoc test was performed to determine the effect of each treatment over incubation time and t-test was used for comparison of treatment. The results were considered significant if P-values were <0.05.

CHAPTER 3

DEVELOPMENT OF INTESTINAL CELL MODELS OF

RIBOFLAVIN DEPLETION

3.1. Introduction

Nakano et al. developed a human intestinal cell model of riboflavin depletion culturing Caco-2 cells in riboflavin-free medium containing dialysed foetal calf serum (FCS) (Nakano *et al.*, 2011). Developing the model was costly and also time-consuming. The cells required 3~4 passages to achieve riboflavin depletion, exposing the cells to gradual reductions from a physiological level of riboflavin to severely depleted level. Furthermore, dialysation of FCS may lead to a depletion of other essential nutrients which may influence cell cycle progression.

This study was therefore conducted to develop an improved model of intestinal riboflavin depletion, using lumiflavin, a structural analogue of riboflavin. As introduced in section 1.1.5.1, there are several reports in the literature that lumiflavin has an inhibitory effect on the uptake of riboflavin into cells, competitively saturating the riboflavin transporter (Said and Ma, 1994; Yonezawa *et al.*, 2008; Yamamoto *et al.*, 2009; Said *et al.*, 2000). Lumiflavin specifically targets riboflavin interrupting uptake of riboflavin into cells. Furthermore, we expected that this would obviate the need for multiple cell passages and the need for dialysed FCS.

Three intestinal cell lines; Caco-2, HCT116 and HT29 were used for this study in order to provide robust data for the effects of riboflavin depletion. All the cell lines are derived from human colon carcinoma, nevertheless they have been extensively used as a cell model to study the absorptive properties of the intestinal epithelium (Thomson *et al.*, 1997; Yonezawa *et al.*, 2008; Hayashi *et al.*, 2007). Indeed, Caco-2 cells have been a useful tool to investigate uptake of nutrients, as the cells behave like duodenal epithelial cells of small intestine (Said and Ma, 1994; Zielinska-Dawidziak *et al.*, 2008). Human riboflavin transporters have recently been identified and characterised using Caco-2 cell lines (Yonezawa *et al.*, 2008), showing further validity to the use of this cell line as a model of human riboflavin depletion. Thus, the three intestinal cell lines were used to develop cell models of riboflavin depletion and they were compared with each other in terms of their proliferative ability and cellular riboflavin status in response to lumiflavin treatment.

3.2. Aims

The overall aim was to develop and validate *de novo* human intestinal cell models of riboflavin depletion using lumiflavin.

3.3. Methods

3.3.1. Cell growth

To identify an appropriate range of lumiflavin concentration, a preliminary experiment was performed using the Caco-2 cell line. After settling down on a culture plate for 24 hours after seeding, cells were incubated in 0.1, 0.5, 1, 10, 100, 200 and 500μM lumiflavin-containing DMEM for 24, 48, and 72 hours. Cells were harvested and the cell numbers were counted daily. Then, three intestinal cell lines; Caco-2, HCT116 and HT29 were treated with 10, 25, 40, 60, 75, 90 and 100μM lumiflavin-containing DMEM for 24, 48 and 72 hours. Cell numbers then were counted daily.

3.3.2. Intracellular flavin assay

Intracellular riboflavin, FAD and FMN concentrations were determined using reverse-phase HPLC as explained in section 2.1.4. For the assay, 40 and 80μM were chosen according to the findings for cell growth. Thus, the three intestinal cell lines were treated with 0, 40 and 80μM lumiflavin-containing DMEM for 48 hours. Calculated flavins concentrations were corrected for protein concentrations.

3.3.3. Glutathione reductase activation coefficient (GRAC)

GRAC was determined using a modified method of erythrocyte GRAC which is a well-established functional measure of riboflavin status (Powers, 1999; Hill *et al.*, 2009). GRAC is the

ratio of stimulated : basal activity of glutathione reductase. Higher GRAC indicates less endogenous FAD. A value of >1.3 GRAC is conventionally considered to reflect poor riboflavin status in human studies (Powers, 1999). The three intestinal cell lines were treated with 0, 40 and 80μM lumiflavin-containing DMEM for 48 hours, and then cells were harvested and GRAC determined as explained in section 2.2.5.

3.3.4. Statistical analysis

Data for cell growth were analysed using Kruskal-Wallis and Duncan post hoc test using a rank for the difference of cell numbers at 72 hours among treatments with various concentrations of lumiflavin. Data for intracellular flavin concentrations and GRAC were analysed using one-way ANOVA followed by the Duncan post hoc test for a comparison of normal and lumiflavin-treated cells. The results were considered significant at $P<0.05$.

3.4.   Results

3.4.1. Effects of lumiflavin on cell growth

As shown in Figure 14, there was a notable difference between the first group; 0 to 1μM and the second group; 100 to 500μM. At low concentrations of lumiflavin such as 0.1~10μM, cell growth was not significantly affected. Caco-2 cells showed arrested cell growth when exposed to 100μM lumiflavin. Cells were unable to survive at very high concentrations of lumiflavin; 200 and 500μM. Therefore, concentrations of lumiflavin for the main experiments used between 10 and 100μM.
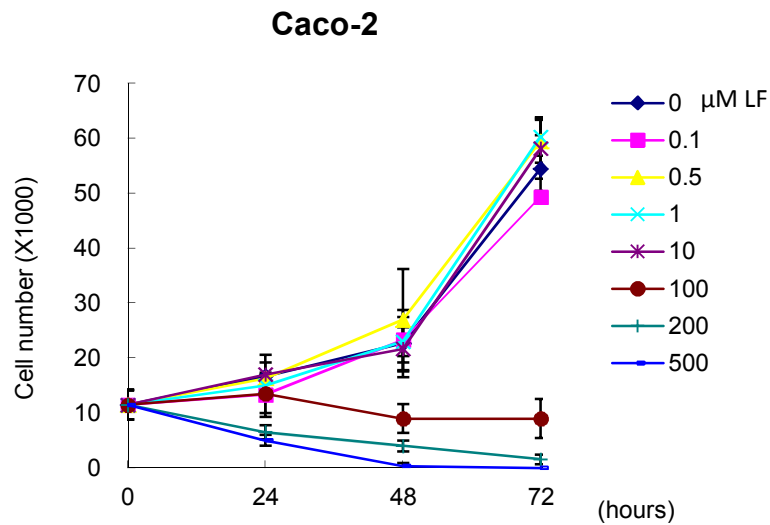
Caco-2

Figure 14 *Preliminary experiment for cell growth in Caco-2 cells treated with lumiflavin in a range of 0 to 500µM.*

Data are presented for a single experiment which was performed in triplicate. Data are expressed as mean±(SEM)

Growth curves for the three cell lines treated with lumiflavin over the range of 0 to 100µM are presented in Figure 15. Cell growth was inhibited by lumiflavin in all three cell lines, in a concentration-dependent manner. Kruskal-Wallis test showed a significant difference among treatments with lumiflavin in Caco-2 ($P<0.05$ at each incubation time), HCT116 and HT29 ($P<0.01$ for 48 and 72 hours incubation). In Caco-2 cells, lumiflavin at a concentration of 60µM or greater led to a lower cell number than 0 to 40µM after only 24 hours ($P<0.05$, Duncan post-hoc test using rank) and effects were sustained. In HCT116 cells, lumiflavin at a concentration of 75µM or greater led a reduction in cell numbers from 48 hours, compared with lower concentrations ($P<0.05$, Duncan post-hoc test using rank), and this effect was sustained. In HT29 cells lumiflavin at a concentration of 60µM or above led to a reduction in cell number from 48 hours, compared with lower concentrations ($P<0.05$, Duncan post-hoc test using rank) and this effect was sustained.

In summary, 40µM lumiflavin led to a 40% decrease in cell numbers in HCT116 and HT29 cells and 25% decrease in Caco-2 cells by 48 hours. This effect increased to a 50% decrease by 72 hours in all three cell lines. Cell growth was arrested by ≥75µM lumiflavin in HCT116 cells and by ≥60µM in Caco-2 and HT29 cells. Therefore, 40 and 80µM were selected for the next experiments.
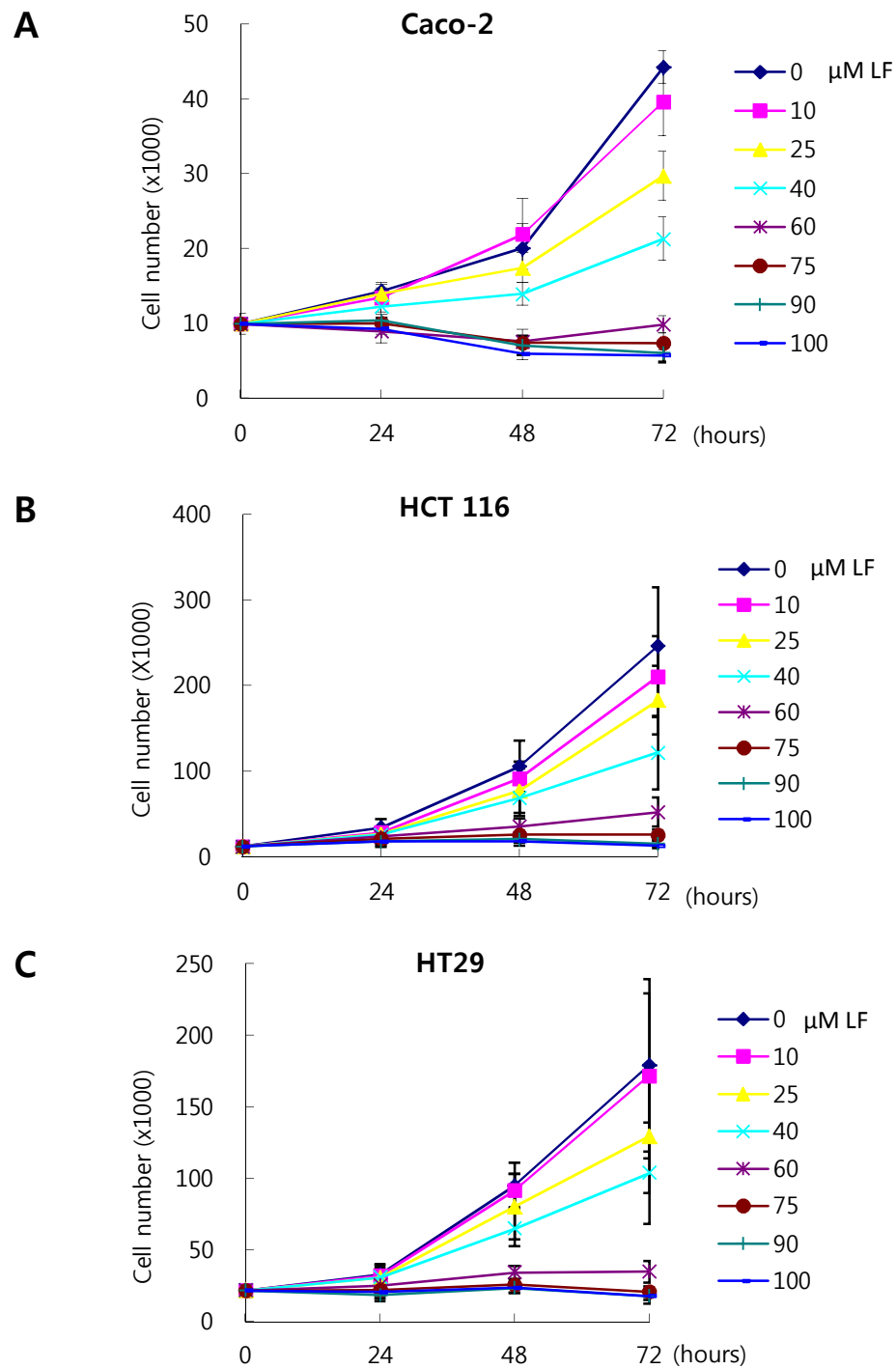
Figure 15 *Cell growth in the three intestinal cell lines treated with lumiflavin in a range of 0 to 100μM.*

Data obtained from three independent experiments in three replicates and expressed as mean (±SEM).

3.4.2. Effects of lumiflavin on intracellular flavins concentration

Intracellular riboflavin, FMN and FAD concentrations were determined by HPLC in cells treated with 0, 40 and 80µM lumiflavin for 48 hours. The data are presented in Figure 16.

Intracellular riboflavin concentrations were significantly decreased in Caco-2 (P=0.002) and HT29 cells (P<0.001) by lumiflavin, compared with untreated cells, in a concentration-dependent manner. Untreated HT29 cells had 1.5~2 fold higher concentration of intracellular riboflavin compared with the other two cell lines. Mean intracellular FAD concentrations showed a progressive fall with increasing lumiflavin concentrations, however effects were not statistically significant. In contrast, intracellular FMN concentrations were unchanged by exposure to lumiflavin, in all cell lines.

A Caco-2
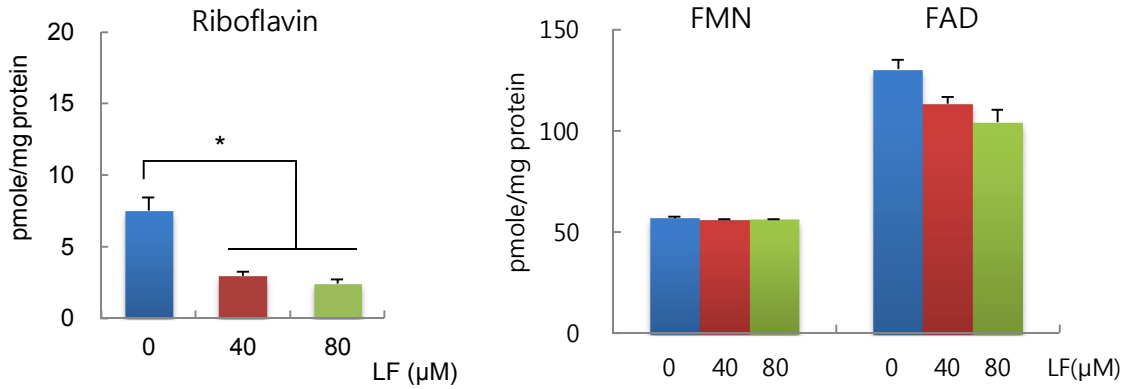
B HCT116
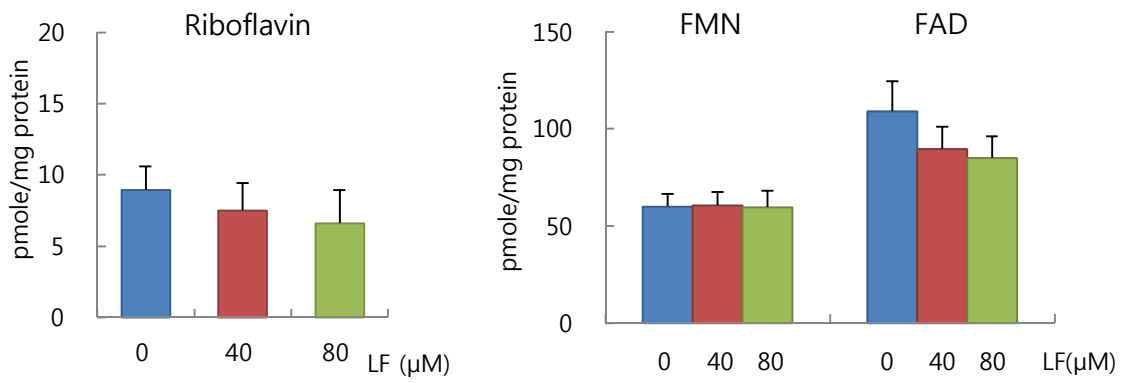
C HT29
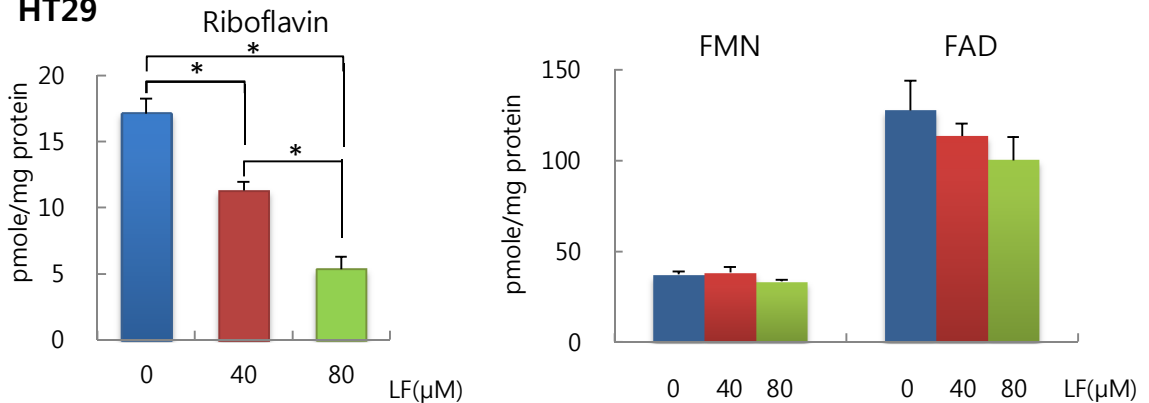
Figure 16 *Effects of lumiflavin on intracellular flavins concentrations determined by HPLC.*

*After incubation of cells with lumiflavin for 48 hours, cells were harvested and lysed. Flavin concentrations were measured in cell lysates and corrected for differences in protein concentration. Data are shown as mean (±SEM) from three independent experiments. One-way ANOVA showed a significant effect of treatment on the concentration of riboflavin in Caco-2 (P=0.002) and HT29 cells (P<0.001). * Significantly different (Duncan post hoc test) P<0.05.*

3.4.3. Effects of lumiflavin on glutathione reductase activation coefficient (GRAC)

Glutathione reductase activation coefficient (GRAC) was determined in cells exposed to 0, 40 and 80μM lumiflavin for 48 hours. This value is inversely related to riboflavin status.

As shown in Figure 17, all three cell lines showed a significant increase in GRAC, in a concentration-dependent manner. The degree of increase in GRAC was higher in Caco-2 cells than in other two cell lines.

A value of <1.30 GRAC reflects poor riboflavin status in human studies (Powers, 1999). Although HCT116 and HT29 cells showed significant increase in GRAC, the values were under 1.30. However, GRAC in Caco-2 cells increased to about 1.50 when cells were exposed to 80μM lumiflavin.
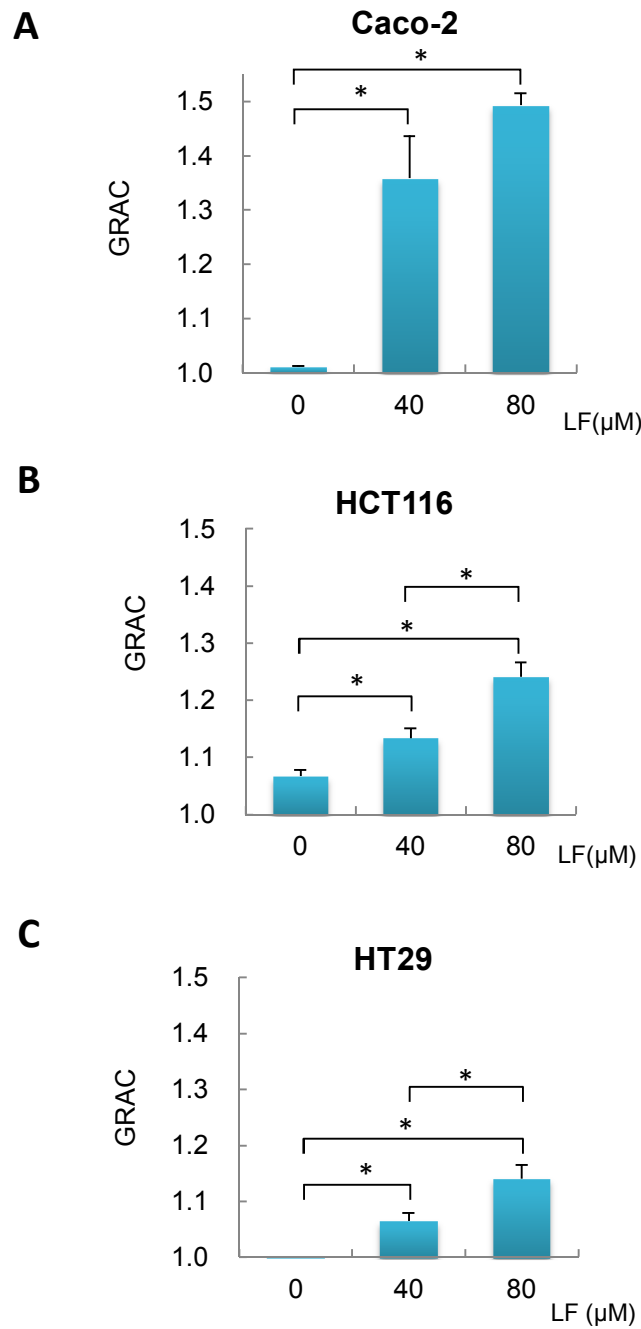
Figure 17 *Glutathione reductase activation coefficient (GRAC).*

*Cells were treated with lumiflavin for 48 hours, and GRAC was determined by kinetic assay. Data shows the mean (±SEM) from three independent experiments; each assay was performed in duplicate. One-way ANOVA showed a significant effect of treatment on GRAC in all cell lines; Caco-2 (P=0.001), HCT116 (P=0.002) and HT29 (P=0.003). * Significantly different (Duncan post hoc test) P<0.05.*

3.5. Discussion

3.5.1. Effects of lumiflavin on cell growth and intracellular flavins status

The preliminary experiment showed that Caco-2 cells were unable to survive in over 200μM lumiflavin. It also appeared that lumiflavin in a range of up to 100μM rapidly inhibited cell growth after only 72 hours in each of three intestinal cell lines in a concentration-dependent manner. Nakano *et al*. (2011) used a protocol which required three passages, meaning approximately 10 days to achieve riboflavin depletion, associated with an arrest in cell growth. Therefore, compared with their model, the lumiflavin-based cell model showed a more rapid inhibition of cell growth. This suggests that lumiflavin competed effectively for sites on riboflavin transporters, consequently leading to its effect on cell growth.

Intracellular riboflavin concentrations were decreased by lumiflavin in Caco-2 and HT29 cells, in a concentration-dependent manner by 48 hours. An *in vitro* study investigated effects of lumiflavin on riboflavin uptake into Caco-2 cells (Said and Ma, 1994). Caco-2 cells were incubated with lumiflavin-containing growth medium at different concentrations for 48 hours. Riboflavin uptake into cells was decreased to 6.4, 3.87 and 1.94pmole/mg protein·3 minutes by 0.055, 32 and 97μM lumiflavin respectively. They measured a rate of uptake of riboflavin into cells rather than intracellular riboflavin concentration. However, their findings are consistent with the results of this study where with the similar experimental condition, in which Caco-2 cells were exposed to 40 and 80μM lumiflavin. Here, we found that intracellular riboflavin concentrations were decreased from 7.51 to 2.95 and 2.39 pmole/mg protein by 0, 40 and 80μM lumiflavin respectively.

Mean intracellular FAD concentration was decreased by lumiflavin in a concentration-dependent manner, but it was modest and statistically not significant. All three cell lines showed only 20~25% fall in intracellular FAD concentration, whereas a fall of 50% in FAD was achieved in Nakano's model (Nakano *et al.*, 2011).
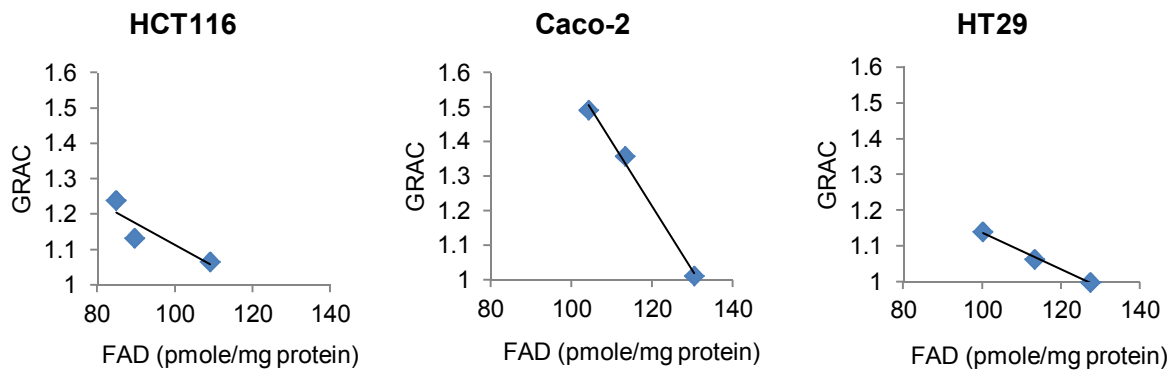
Figure 18 *Correlation between GRAC and intracellular FAD concentration.*

Glutathione reductase (GR) is an FAD-dependent enzyme, and the activation coefficient of the enzyme indicates saturation of the enzyme with FAD, thus fully saturated GR will show 1.0 of GRAC.

There was an inverse relationship between GRAC and intracellular FAD concentrations consistent with the literature (Hustad *et al.*, 2002). As seen in Figure 18, the slope for this relationship in Caco-2 cells was much steeper than that for the other two cell lines, suggesting that GRAC in Caco-2 cells was more sensitive to a reduction in intracellular FAD concentration. Glutathione reductase (GR) is an FAD-dependent enzyme, thus the activation coefficient of the enzyme reflects actual saturation of the enzyme with FAD. GRAC in erythrocytes (EGRAC) is frequently employed to investigate riboflavin deficiency throughout human and animal studies (Powers, 1999), thus in this study, the method was adapted in order to identify functional riboflavin depletion in cells. The value >1.30 is conventionally considered as biochemically functional riboflavin deficiency in humans and animal models of riboflavin deficiency (Powers, 1999).

Exposure of each of three cell lines to lumiflavin for 48 hours led to an increase in GRAC. HCT116 and HT29 cells exposed to lumiflavin exhibited a modest but statistically significant increase in GRAC. In contrast, GRAC increased to over 1.50 in lumiflavin-treated Caco-2 cells suggesting a more severe riboflavin deficiency than the other two cell types. Evidently the sensitivity of cells to riboflavin depletion is cell-line dependent.

GRAC values observed in this study ranged from 1.06±0.08 to 1.49±0.02 across the three cell types, and this is comparable with erythrocyte GRAC values reported in human studies (Bates *et al.*, 2011). This suggests that the cell models of riboflavin depletion may be relevant to human populations.
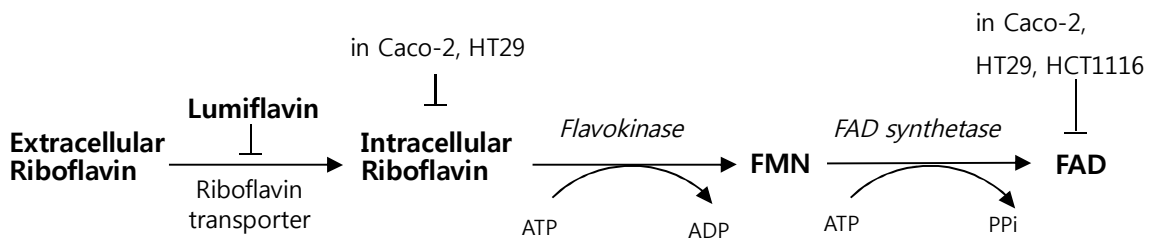
Figure 19 *Summary of results for intracellular flavin concentration*

Uptake of riboflavin into cells is inhibited by lumiflavin, leading to a fall in intracellular riboflavin concentration in Caco-2 and HT29 cells. Not significant fall in intracellular FMN and FAD concentration was observed in any of the three cell lines. Increased GRAC was observed in all three cell lines, reflecting functional FAD depletion

In contrast to riboflavin and FAD, FMN concentrations were unchanged by lumiflavin in all three cell lines. According to an animal study of riboflavin depletion, there is an efficient FAD conservation system (Fass and Rivlin, 1969). FAD is conserved at the expense of FMN as the activity of FAD synthetase is elevated, thus FMN is decreased by riboflavin depletion compared with control. However, in this study, intracellular FMN concentrations were maintained at control values. It is thought there are two possible reasons. The first is that exposure to lumiflavin may have been too short (48 hours) for changes in FMN to be effected. Nakano *et al* (2011) showed that a prolonged depletion elicited a fall in intracellular FMN concentration in Caco-2 cells whereas a short depletion period did not. The second is that lumiflavin may interfere with the conversion of FMN to FAD by influencing the activity of FAD synthetase. This requires further investigation. Alternatively, investigation of effect of lumiflavin on ATP status may support the reason since the enzymes are ATP-dependent (Oka and McCormick, 1987), which will be addressed in the next chapter where determines changes in `intracellular ATP concentration.

Taken together so far, lumiflavin resulted in a modest decrease in the flavin pool, a significant fall of intracellular riboflavin concentration, and this was associated with a significant reduction in cell growth.

3.6. Summary

The study was performed to develop a human intestinal cell model of riboflavin depletion using lumiflavin, a structural analogue of riboflavin. Cell growth was determined in three human epithelial cell lines; Caco-2, HCT116 and HT29 cells, exposed to lumiflavin over the range of 10 to 100µM for up to 72 hours. To confirm riboflavin depletion of the cells, intracellular flavin concentrations and GRAC were determined in the three cell lines exposed to 40 and 80µM lumiflavin for 48 hours.

Cell growth was rapidly inhibited in all three cell lines, in a concentration-dependent manner within 72 hours. Riboflavin depletion was confirmed through a significant decrease in intracellular riboflavin concentration in Caco-2 and HT29 cell lines and a significant increase in GRAC in all three cell lines.

Intestinal cell models of riboflavin depletion by lumiflavin have been developed and established. The next step of this project aimed to characterise the models in terms of various measures of cell function.

CHAPTER 4

CHARACTERISATION OF INTESTINAL CELL MODELS

OF RIBOFLAVIN DEPLETION

4.1.   Introduction

Three intestinal epithelial cell lines were examined for their functional characteristics in response to riboflavin depletion induced by lumiflavin. Manthey et al.(2006) suggested tissue-specific sensitivity of cells for developing riboflavin deficiency. Jurkat lymphoid cells were resistant to severe riboflavin deprivation (0.85 nmole/L) for 5 weeks (Camporeale and Zempleni, 2003), whereas HepG2 liver cancer cells developed signs of riboflavin deficiency after only 4 days in moderately riboflavin-deficient medium (3.1 nmole/L of riboflavin) (Werner *et al.*, 2005). Caco-2 intestinal cells seem to be more resistant to riboflavin depletion compared with HepG2 cells. Nakano *et al* (2011) found that growing Caco-2 cells in moderately riboflavin deficient medium (3.2 nmole/L) for 7days after 4days in a medium containing a physiological concentration of riboflavin led to a significant reduction in flavin concentration together with altered expression of genes that play a role in mitosis leading to cell cycle arrest in mitosis (Nakano *et al.*, 2011). Nakano et al. (2011) suggested efficient flavin conservation mechanisms existed in Caco-2 cells to prevent developing riboflavin deficiency. This might be related to a different expression of riboflavin transporters in different tissues (Yonezawa and Inui, 2013) or a different distribution of riboflavin metabolising enzymes in different tissues (Stipanuk, 2013).

However, others have not examined differences among cell lines derived from the same tissue type, even though studies of enterocytes have used several types of intestinal cell lines such as Caco-2, HCT116 and HT29 cells (Zielinska-Dawidziak *et al.*, 2008; Thomson *et al.*, 1997; Hayashi *et al.*, 2007). Therefore, studies described here may reveal a different sensitivity of three intestinal cell lines to riboflavin depletion, thus providing a robust model showing a stronger case for any effects observed in a single cell line in the same tissue type.

Riboflavin is important in ATP generation mechanisms because it plays a role as a cofactor for enzymes involved in ATP generating reactions. For instance, as described in 1.1.1.4, succinate dehydrogenase catalyses the oxidation of succinate to fumarate using FAD as an electron carrier in the citric acid cycle that is an ATP generating cycle. Riboflavin deficiency affects the activity of these enzymes, leading to accumulation of succinate and a reduction of ATP synthesis. Feeding a riboflavin-deficient diet to weanling rats for 5 weeks led to an increase in succinate and a decrease in fumarate concentration with a fall in ATP concentration in liver (Burch *et al.*, 1970), Furthermore, a study using mitochondrial complex I deficient fibroblast cells derived from a patient reported that riboflavin improved ATP production to

close to normal (Bar-Meir *et al.*, 2001). Another example of redox reactions to which riboflavin is related, is the glutathione redox cycle. Reduced glutathione, which is produced by FAD-dependent glutathione reductase, has been considered as an endogenous antioxidant (Ashoori and Saedisomeolia, 2014). Reduced glutathione serves as a substrate for glutathione peroxidase which transfers hydrogen from reduced glutathione to peroxides such as lipid peroxide or hydroperoxide. Oxidized glutathione is in turn reduced by glutathione reductase to recover intracellular antioxidant status.

Decreased activity of glutathione reductase leads to a fall in reduced glutathione concentration (Manthey *et al.*, 2005; Camporeale and Zempleni, 2003), increasing oxidative stress through uncontrolled ROS. Culture of human lymphoid cells (Jurkat cells) in riboflavin-deficient medium (0.85nmol/L of riboflavin) for 5 weeks led to a reduction in the activity of glutathione reductase and intracellular reduced glutathione concentration (Camporeale and Zempleni, 2003). Riboflavin deprivation for 8 days in human hepatoma cells HepG2 resulted in a reduced activity of glutathione reductase and a decrease in reduced glutathione, leading to an increase in carbonylated proteins, which reflect oxidative damage to protein, and DNA strand breaks (Manthey *et al.*, 2005; 2006). Therefore, riboflavin deficiency could lead to an increased production of ROS and thereby oxidative stress. ROS at physiologically low levels can be beneficial to cells through a function as a signal transporter in cell signalling. However excessive ROS induces oxidative damage in DNA and proteins, promoting altered regulation of cell cycle (Shackelford *et al.*, 2000) and programmed cell death, apoptosis (Circu and Aw, 2010).

We hypothesized that riboflavin depletion induced by lumiflavin will impair intracellular ATP status and result in oxidative stress. Furthermore we examined effects of lumiflavin on clonogenicity indicating proliferative ability with reversibility, and apoptotic cell death.

4.2. Aim

To characterise human intestinal cell models of intracellular riboflavin depletion by lumiflavin in terms of specific functional characteristics including intracellular ATP concentration, ROS production, clonogenicity and apoptotic DNA fragmentation.

4.3. Methods

4.3.1. Intracellular ATP assay

Intracellular ATP concentrations were determined using an ATP bioluminescent somatic cell assay kit, based on ATP-dependence of firefly luciferase (see section 2.2.6). All reagents and apparatus were prepared following the kit instruction. Three cell lines were incubated with 0, 40 and 80μM lumiflavin for 24, 48 and 72 hours. Then, intracellular ATP concentrations were measured daily. ATP concentrations were corrected for differences in cell number by protein concentration. All samples were prepared and analysed in triplicate from three independent experiments.

4.3.2. Measurement of intracellular ROS production

Three intestinal cell lines were pre-incubated in lumiflavin-containing DMEM for 24, 48 and 72 hours at concentrations of 0, 40 and 80μM. ROS production in the three cell lines after incubation with lumiflavin were monitored for up to 4 hours using the DCFDA method as described (see section 2.2.7). Fluorescence is directly proportional to the concentration of oxidised DCFDA thus indicating the level of ROS produced. The data were corrected for the difference in cell numbers (see section 2.2.8). Data presented here obtained from a single experiment in triplicate.. Several preliminary experiments to develop the assay were performed and the same pattern was observed as presented data, thus data for preliminary experiments are not presented.

4.3.3. Clonogenic assay

A clonogenic assay can be used to investigate the proliferative ability of cells by determining cells' ability to form colonies, and can provide information about the cytotoxicity of lumiflavin and its reversibility. Three intestinal cell lines were pre-incubated with 0, 40 and 80μM lumiflavin for 24, 48 and 72 hours. Then cells were split and seeded into 6-well plates

with low seeding densities, and incubated in lumiflavin-free DMEM until a single cell formed the proper size of colony which consists of over 50 cells. Colonies were fixed, stained and counted. Absolute clonogenicities were calculated by dividing colony number by seeded cell number and multiplying 100. Then, absolute clonogenicities were used to calculate relative clonogenicity of lumiflavin-treated cells compared with controls. Data are presented in Figure 22 as relative clonogenicity.

4.3.4. Apoptotic DNA fragmentation assay

As it had been found that exposure to lumiflavin resulted in inhibition of cell growth, experiments were conducted to confirm whether this resulted from cell growth arrest or increased cell death through apoptosis. Apoptotic DNA fragments detection kit can also determine necrotic cell death.

For the apoptotic DNA assay, the three intestinal cell lines were incubated with 0, 40 and 80μM lumiflavin-containing DMEM for 48 hours. Then, floating cells in the used media were collected and adherent cells were harvested. DNA in detached and adherent cells were extracted and visualised as described (see section 2.2.11). Sodium butyrate-treated cells were used for a positive control. DNA was prepared from three independent experiments. The volume of extracted DNA loaded into a gel was adjusted in the second and third repeats in order to avoid too strong signals observed in the first repeat.

4.3.5. Statistical analysis

Intracellular ATP concentration was analysed by two-way ANOVA for comparison of two factors; treatment and time-course. A main effect of treatment was found in Caco-2 and HT29 cells and an interaction of two factors in HCT116 cells was found, thus one-way ANOVA was used to determine the effect of each treatment at each experimental time point. Intracellular ROS concentrations produced at 240 minutes analysed by Kruskal-Wallis test followed by the Duncan post hoc test using a rank to determine the differences in treatments. Data for clonogenic assay were not normally distributed, thus Kruskal-Wallis test was used followed by

Dunnet T3 post hoc test using ranking, for a comparison of relative clonogenicity among treatment and incubation time. The results were considered significant at $P<0.05$.

4.4. Results

Lumiflavin-based intestinal cell models of riboflavin depletion were investigated for specific functional characteristics. Intracellular ATP concentration, intracellular ROS production, clonogenicity and apoptosis were measured.

4.4.1. Effects of lumiflavin on intracellular ATP concentration

The main effect of lumiflavin treatment was on intracellular ATP concentration, in Caco-2 cells ($P<0.001$), HCT116 cells ($P<0.001$) and HT29 cells ($P=0.019$) and a significant effect of incubation time in HCT116 cells ($P=0.012$). There was no interaction between treatment and incubation time in any cell line.

Exposure to lumiflavin resulted in a concentration-dependent decrease in ATP concentration of around 13% and 40% in Caco-2 cells exposed to 40 and 80μM lumiflavin respectively. ATP concentration in 80μM lumiflavin-treated cells was significantly lower than in cells treated with 40μM lumiflavin (Figure 20a). Incubation time did not influence ATP concentration.

Intracellular ATP concentration in HCT116 and HT29 cells was significantly lower in cells incubated with 80μM lumiflavin compared with control. The decrease observed was around 28% and 23% in HCT116 and HT29 cells respectively. HCT116 cells showed a lower ATP concentration after incubation with 80μM lumiflavin for 48 and 72 hours compared with 24 hours (Duncan post-hoc test at $P<0.05$).

The absolute decrease in ATP concentration in cells exposed to 80μM lumiflavin was 0.36~0.41 and 0.28nmole/mg protein in Caco-2 and HCT116 cells respectively, whereas it was about 0.16nmole/mg protein in HT29 cells. Results indicate a different sensitivity of each cell line to lumiflavin exposure.
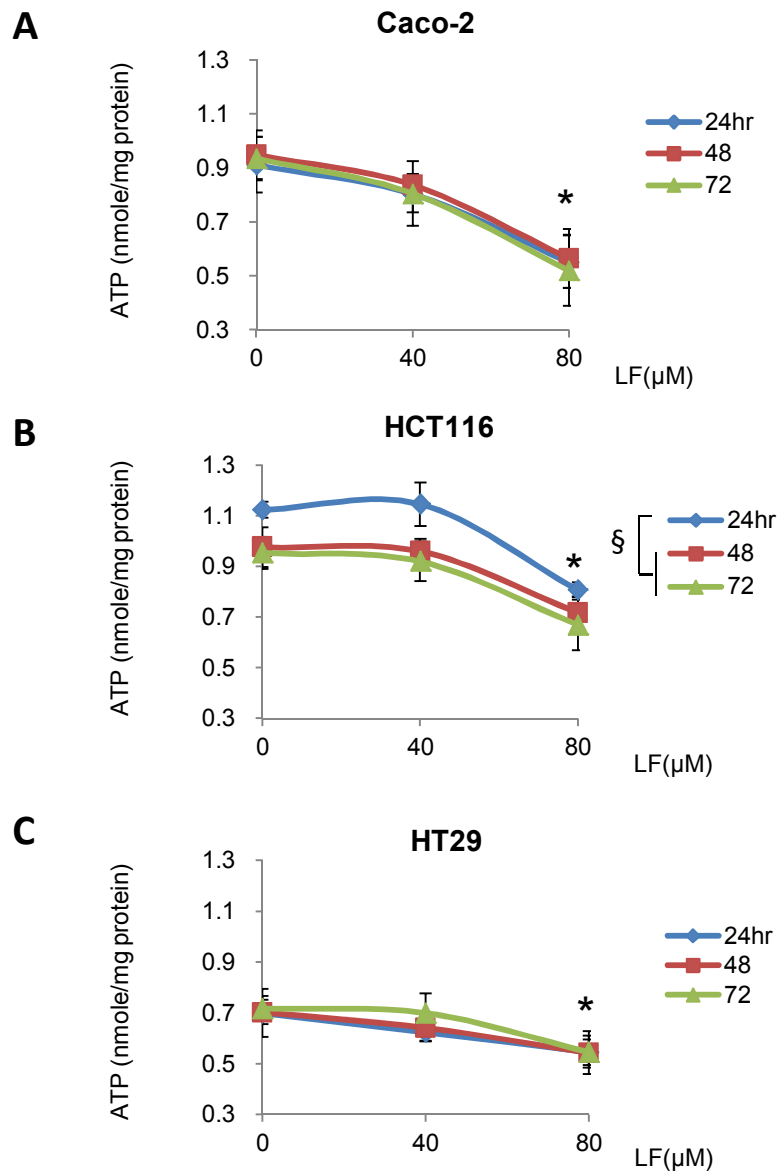
Figure 20 *Effects of lumiflavin on intracellular ATP status*

Cells were incubated with lumiflavin for 24, 48 and 72 hours and ATP concentration measured using an ATP bioluminescent somatic cell assay. ATP concentrations were corrected for differences in protein concentration. Data are shown as means (±SEM) for three independent experiments, each conducted with four replicates. Two way ANOVA showed a significant effect of lumiflavin in Caco-2 (P<0.001), HCT116 (P<0.001) and HT29 cells (P=0.019) and of incubation time in HCT116 cells (P=0.012).

* Significantly lower than control and 40μM lumiflavin (Duncan post-hoc test) P<0.05.

§ Significantly different from 24 hours (Duncan post-hoc test) P<0.05.

4.4.2. Effects of lumiflavin on cellular ROS production

Figure 21 shows the time course of ROS production in three cell lines according to lumiflavin treatment. Overall, there was significant increase in intracellular ROS production at 240 minutes of incubation with 80μM lumiflavin compared with control or 40μM lumiflavin. An increase in ROS concentration was observed in all three cell lines, and the effect was greatest in Caco-2 cells.

All three cell lines clearly showed that 80μM lumiflavin resulted in a significantly higher concentration of ROS compared with controls and 40μM lumiflavin. Exposure of Caco-2 cells to 80μM lumiflavin led to a remarkable increase in ROS concentration, showing a time-dependence; 2, 4.5 and 7 fold ROS concentrations of the control at 24, 48 and 72 hours respectively. Exposure to 40μM lumiflavin did not lead to a consistent effect on ROS concentration compared with the control.

Caco-2 cells produced more ROS than the other two cell lines. Caco-2 cells produced about 5 to 13-fold and 4 to 5-fold more ROS than in HCT116 and HT29 cells respectively in the absence of any lumiflavin. Results implied Caco-2 cells were the most sensitive to lumiflavin exposure.
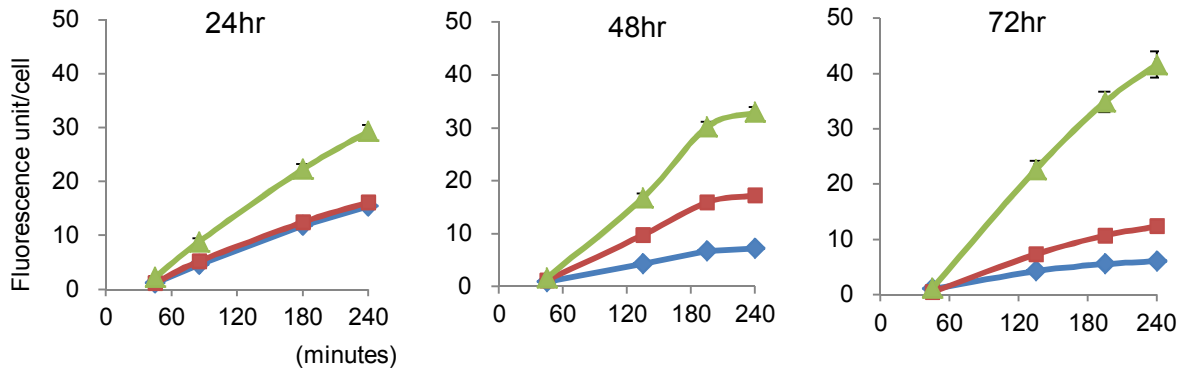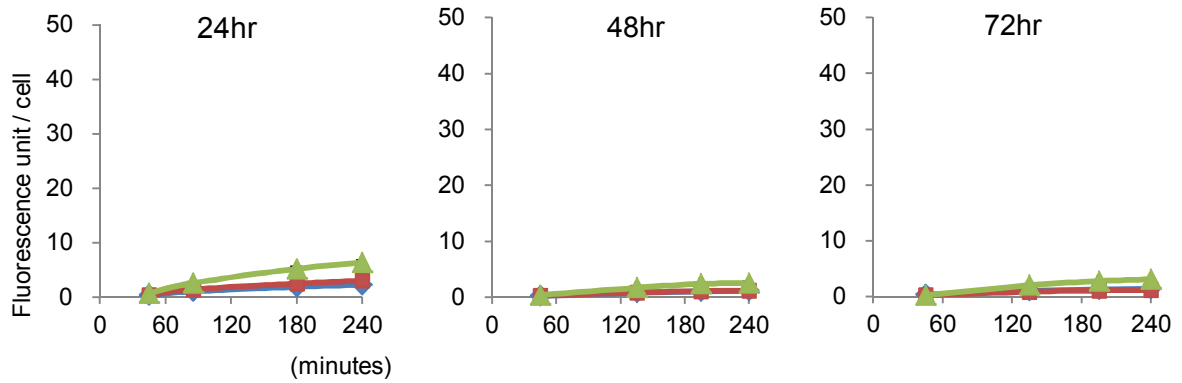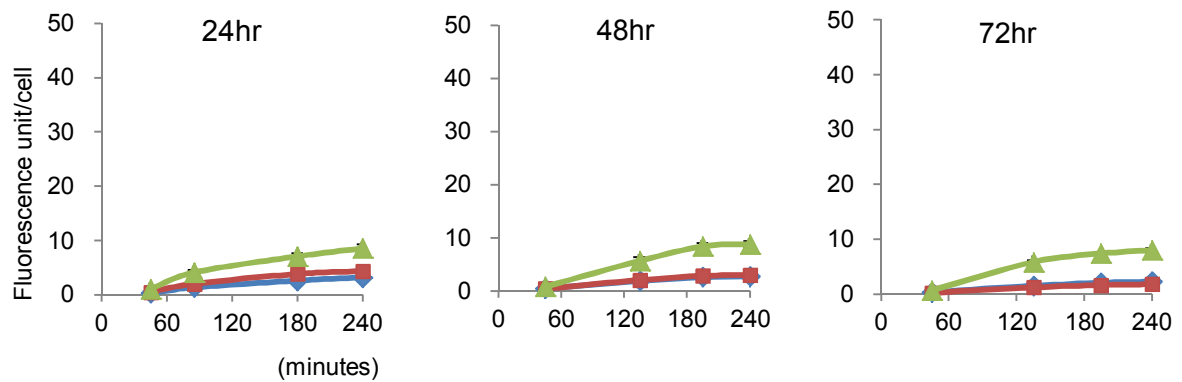
Figure 21 *Time-course of reactive oxygen species (ROS) production.*

hr: hours. Cells pre-incubated with lumiflavin for up to 72 hours were monitored for ROS production over 240 minutes as fluorescence using DCFDA. Data were corrected by cell numbers and expressed as means (±SEM) from a single experiment conducted in triplicate.

4.4.3. Effects of lumiflavin on clonogenicity

Caco-2 cells exposed to lumiflavin showed a highly significant decrease in clonogenicity in a concentration-dependent manner but independent on incubation time (P<0.001, Kruskal-Wallis test). A lot of floating cells were observed after setting up the clonogenic assay. It seemed that some of lumiflavin-treated Caco-2 cells were not attached onto a culture plate.

Clonogenicity of HCT116 was inhibited by only 80μM lumiflavin in a time-dependent manner. In comparison with control (0μM), clonogenicity of 80μM lumiflavin-treated HCT116 cells decreased to about 30, 65 and 70% by 24, 48 and 72 hours pre-incubation respectively (P<0.001, Kruskal-Wallis test).

In contrast, the clonogenic ability of HT29 cells showed a different pattern from the other two cell lines. HT29 cells still showed clonogenic ability following pre-incubation in lumiflavin. Exposure to 40μM lumiflavin resulted in a small increase in clonognicity compared with control.
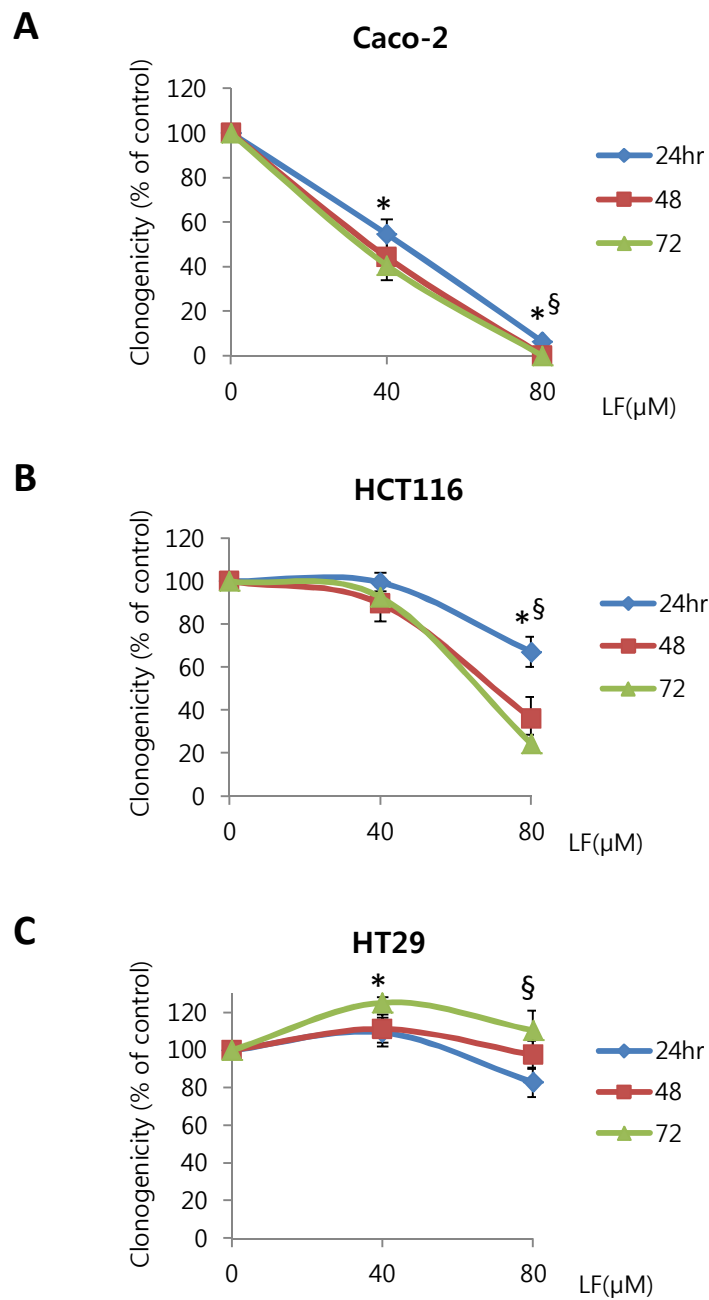
Figure 22 *Effects of lumiflavin on clonogenicity.*

LF: lumiflavin. Cells were pre-incubated with lumiflavin for 24, 48 and 72 hours and then grown in normal DMEM until colonies of >50 cells were formed. Colonies were stained and counted. Data show mean (±SEM) of three independent experiments performed in four replicates. There were significant effects of lumiflavin on clonogenicity in Caco-2 (P<0.001), HCT116 (P<0.001) and HT29 cells (P=0.008) (Kruskal-Wallis test).

* Significantly different from control and § 40µM lumiflavin (Dunnett T3 post-hoc test using ranked data, P<0.05).

4.4.4. Effects of lumiflavin on apoptosis

Three cell lines were incubated with 0, 40 and 80μM lumiflavin for 48 hours or with sodium butyrate which was used for a positive control for apoptotic DNA fragments. Dead cells which were detached and floating in medium and adherent cells were separately collected. Then the apoptotic DNA fragment assay was performed. It is well known that apoptotic DNA fragmentation is a key feature of apoptotic cells, thus distinct multiple bands of DNA fragments of oligonucleosomal size (180~200 bp lengths) can be imaged using DNA laddering assay kit (Bortner *et al.*, 1995).

Figure 23 shows three images of each cell line from three independent experiments. Apoptotic DNA fragment was not found in any detached or adherent Caco-2 cells (Figure 23.A). Only one case of apoptotic DNA fragment was found in detached dead HCT116 cells incubated with 80μM lumiflavin (an arrow of Figure 23.B), showing distinct DNA laddering. However, it was not observed in two other repeats. DNA laddering was not found in HT29 cells (Figure 23.C).

A, Caco-2
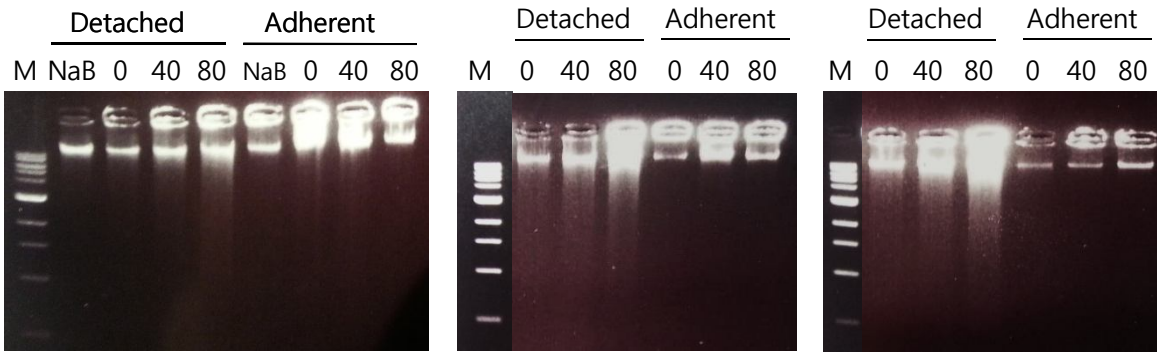
B, HCT116
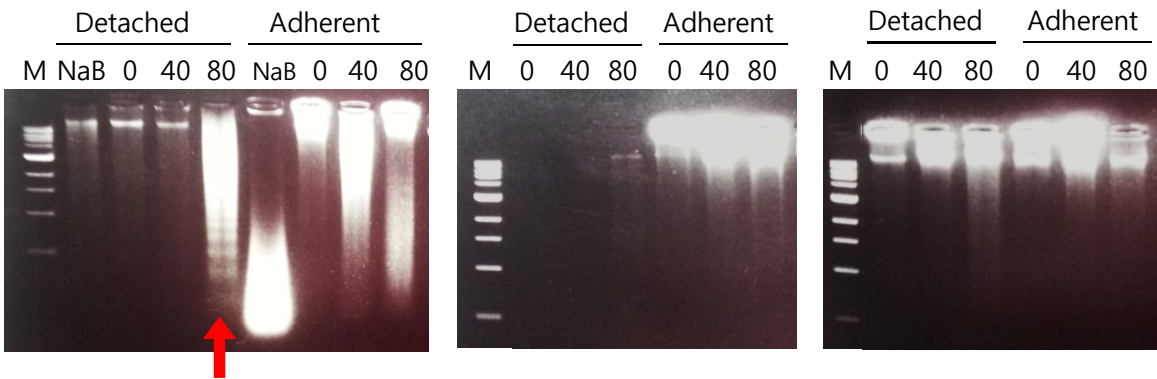
C, HT29
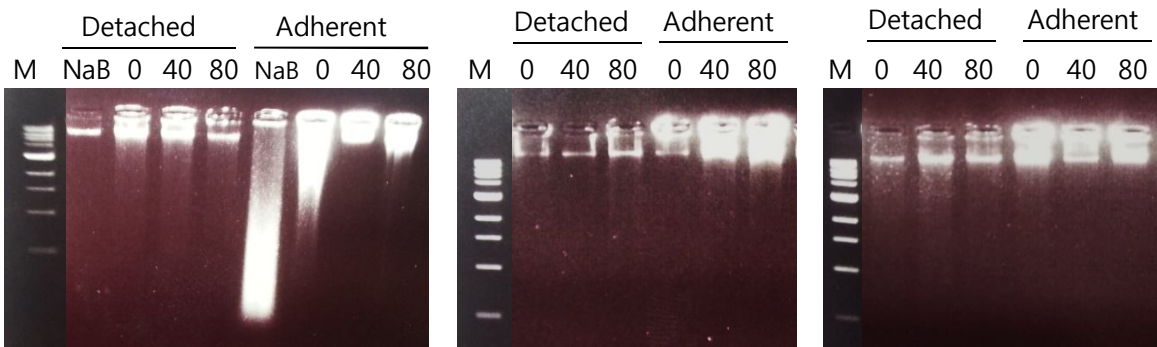
Figure 23 *Determination of apoptotic DNA*

M; DNA marker, NaB; sodium butyrate, 0, 40 and 80; lumiflavin concentrations (µM). DNA were extracted from detached, (dead) cells and adherent cells exposed to sodium butyrate which was a positive control of apoptotic DNA fragment, 40 and 80µM lumiflavin. Three images for each cell line show three repeats from independent experiments.

4.5.   Discussion

In order to characterise the intestinal cell models of riboflavin depletion, intracellular ATP status, ROS production, clonogenicity and apoptotic DNA were investigated in the three intestinal cell lines after incubation with lumiflavin at concentrations of 0, 40 and 80μM for up to 72 hours. Such concentrations of lumiflavin were selected because earlier experiments had shown gradual inhibition and arrest of cell growth at 40 and 80μM (section 3.4.1).

4.5.1. Effects of lumiflavin on intracellular ATP concentration

Intracellular ATP concentrations were significantly decreased at the higher dose of lumiflavin in all three cell lines. Effect of lumiflavin on ATP concentration was greater in Caco-2 cells than the other two cell lines. This finding suggests a different sensitivity to intracellular ATP generation in response to lumiflavin, depending on the cell line.

Riboflavin in the form of FAD plays an important cofactor role for enzymes involved in ATP-yielding reactions such as succinate dehydrogenase and acyl CoA dehydrogenase. The activity of these enzymes is reported to be reduced in riboflavin-deficient animal models (Prentice and Bates, 1981b; 1981a; Olpin and Bates, 1982) leading to a decrease in ATP status (Burch *et al.*, 1970). Burch et al. investigated changes in ATP concentration in the liver of rats fed riboflavin-deficient diet for 5 weeks. They reported riboflavin deficiency caused a 60% decrease in liver ATP concentration compared with weight-matched control animals. Consistent with these findings, this study showed cellular riboflavin depletion led to a significant fall in intracellular ATP in all three cell lines.

The decrease in ATP concentration, reflecting a decrease in the energy status of the riboflavin-deficient cells, may limit the process of DNA synthesis and cell division. Sufficient energy provision influences DNA synthesis and cell progression through the cell cycle. Previous studies showed that an increase in intracellular ATP induced by extraneous stimulation with serum was associated with purine biosynthesis in 3T3 fibroblasts (Grummt *et al.*, 1977), and stimulated ATP generation by hypoxanthine led to purine biosynthesis, regulating the G1/S transition and thereby cell growth (Kondo *et al.*, 2000). Nakano *et al.* (2011) has shown that

severely riboflavin-deficient Caco-2 cells show impaired G2/M transit, and it is thought that this might be due, at least in part, to inadequate energy generation.

4.5.2. Effects of lumiflavin on intracellular ROS production

ROS production was monitored using the DCFDA probe method. Exposure to 80µM lumiflavin resulted in increased ROS production compared with controls in all three cell lines and the effects were greatest in Caco-2 cells. Therefore, a higher concentration of lumiflavin induced oxidative stress. This may have contributed to observed effects on cell proliferation.

According to the literature, ROS are an important factor in the regulation of cell proliferation, playing a role as a signal transporter for cell cycle progression. Indeed, it has been reported that inhibition of ROS production induced cell cycle arrest leading to inhibition of cell proliferation (Scaife, 2004). ROS production was inhibited using the flavoprotein-specific inhibitor, diphenyleneiodonium (DPI) which inhibits the flavoprotein complex NAD(P)H oxidase, in various cancer and non-cancer cell lines such as Rat-1 fibroblasts, HepG2 human hepatoma cell, MCF-7 breast cancer cell lines. Exposure to DPI led to a block of progression of the cells into mitosis with impaired cyclin B1 accumulation which is, as the complex form with cyclin-dependent kinase 1 (CDK1), required for the formation of mitotic spindle and initiation of G2/mitosis transition.

However, excessive ROS production also inhibits cell proliferation influencing the cell cycle checkpoint. Excessive ROS induce oxidative damage in biological molecules including DNA and cell cycle checkpoint functions to prevent replication of damaged DNA, thus allowing additional time to repair it. (Shackelford *et al.*, 2000). Russo et al. (1995) showed that an increase in ROS induced by diethylmaleate (DEM), which depletes the intracellular reduced glutathione (GSH), in Saos-2 human osteosarcoma cells and T98G human brain glioblastoma cells, , resulted in delayed progression of cell cycle in G1 and S phase and G2/M arrest which were mediated by induction of WAF1/CIP1 expression. WAF1/CIP1 family is cyclin-dependent kinase inhibitor proteins (CKIs), including p21, p27, and p57 functioning in most of phases of the cell cycle.

Several *in vitro* and *in vivo* studies showed an association between riboflavin deficiency and oxidative stress measured as an imbalance in the glutathione redox cycle, consequently

leading to cell cycle arrest and apoptosis. According to Manthey *et al* (2005; 2006), HepG2 liver cells cultured in riboflavin-deficient medium exhibited oxidative stress and associated changes that caused cell cycle arrest. They found that riboflavin deficiency was related to a decrease in reduced glutathione (GSH). Protein carbonylation which is a product of protein oxidation and DNA fragmentation was also observed. Such changes led to G1 phase arrest of the cell cycle and an increased proportion of apoptotic cells with an increased expression of gene clusters that play a role in cell stress and apoptosis.

Early-onset apoptosis in intestinal epithelial cells may cause a reduction in the villus population and thereby impair the absorptive function of the intestine. A recent animal study revealed that riboflavin supplementation rescues intestinal epithelial cells from apoptosis and associated changes induced by a chemotherapeutic agent (Bodiga *et al.*, 2012). Riboflavin supplementation improved the causes of and sign of apoptosis in intestinal epithelium. For instance, supplementation of riboflavin individually or as multivitamin led to a decreased incidence of DNA fragmentation which is a key feature of apoptotic cells, a decrease in oxidative damage to lipid and protein, an increase in reduced glutathione, and an increased Bcl-2/Bax ratio. This suggests a protective effect on apoptosis as Bcl-2 is an anti-apoptosis protein and Bax is a stimulator of apoptosis.

Taken together, results show that riboflavin depletion was associated with increased oxidative stress, measured as an increased ROS formation in lumiflavin-treated cells. This might contribute to the observed effect of lumiflavin on cell proliferation.

4.5.3. Effects of lumiflavin on clonogenicity

The effects of lumiflavin on clonogenicity were specific to the cell line. The effect was the most pronounced in Caco-2 and least so in HT29 cells. Clonogenicity of HCT116 cells appeared to be unaffected by 40µM lumiflavin, however it was decreased by 80µM lumiflavin by about 30 to 70% of controls in a time-dependent manner. Thus, a high concentration of lumiflavin (80µM) in HCT116 cells led to irreversible loss of proliferative ability of the cells.

In Caco-2 cells, lumiflavin resulted in a concentration-dependent loss of colony number even by 24 hours. Nakano's in vitro model showed only a 25% decrease in clonogenicity by 72 hours. In contrast, Caco-2 cells in this study showed about 50 and 95% decrease by 40 and

80μM lumiflavin respectively after only 24 hours. Furthermore, since lumiflavin induced a more modest decrease in intracellular flavin concentration than Nakano's model, the results of clonogenic assay in Caco-2 cells may be due to lumiflavin itself rather than riboflavin depletion. When the clonogenic assay for Caco-2 cells was set up, although the same number of cells was seeded, more floating cells were observed at the higher concentration of lumiflavin. The cells seemed to have a problem attaching to the culture plate. Nakano's model of riboflavin-deficient Caco-2 cells also showed that the cell number after 24 hours of seeding was approximately half (Nakano *et al.*, 2011), indicating half of seeded cells successfully attached to the culture plate.

In contrast, clonogenicity of HT29 cells was not affected by lumiflavin. The clonogenic assay is used to investigate effects of drugs on cell proliferative ability. Also this approach can reveal information about the cytotoxicity of a drug and the ability of cells to recover following removal of the drug (Franken *et al.*, 2006). Thus, the fact that clonogenicity was unaffected in HT29 may reflects more efficient detoxification. This may be attributable to better uptake of riboflavin. Indeed intracellular riboflavin concentration in lumiflavin-untreated HT29 cells was approximately two fold higher than in the other two cell lines. Therefore, HT29 cells were less affected and thus more resistant to riboflavin depletion induced by lumiflavin treatment.

4.5.4. Effects of lumiflavin on apoptosis

DNA laddering assay showed distinct DNA fragments in only one case in floating dead HCT116 cells exposed to 80μM lumiflavin for 48 hours, however the finding was not consistent throughout three independent experiments. Furthermore, Caco-2 and HT29 cells did not show DNA laddering. Therefore, in this study, none of the three intestinal cell models of riboflavin depletion induced by lumiflavin showed DNA fragmentation.

This does not necessarily mean that lumiflavin does not cause apoptosis. DNA strand breaks occur at a much later time during discrete stages of surface morphological and nuclear morphological changes in apoptosis. For this reason, it does not mean that an absence of laddering reflects no apoptosis, and thus the possibility of apoptosis cannot be ruled out (Collins *et al.*, 1997). Manthey *et al.* (2006) has reported that severe riboflavin deprivation in liver cancer cells led to an increased incidence of DNA strand breaks and increased proportion

of cells in apoptosis, accompanying increased expression of genes involved in the apoptosis pathway in comparison with riboflavin-sufficient cells.

Therefore, although no DNA fragmentation was found in the models of intestinal cellular riboflavin depletion, it is too early to conclude that there was no association of riboflavin depletion with apoptosis. This study observed a reduction in cell growth and a loss of clonogenicity in Caco-2 cells exposed to lumiflavin, thus the cells may be undergoing cell cycle arrest or an earlier stage of apoptosis prior to DNA strand breaks in the progress of cell death. Further studies should be conducted to explore effects of lumiflavin on the cell cycle and also the earlier stage of apoptosis or throughout apoptosis pathways.

Finally, different responses to lumiflavin were observed between the three cell lines; for instance Caco-2 cells showed the most pronounced effects on intracellular ATP concentration, higher ROS production and biggest loss of clonogenicity. In contrast, HT29 cells produced negligible effects compared with Caco-2 and HCT116 cell lines. This may reflect differences between three cell lines in terms of their efficiency of uptake of riboflavin. As seen in chapter 3 (see section 3.4.2 and 3.4.3), HT29 cells themselves had a higher intracellular riboflavin concentration and lower GRAC than the other two cell lines, probably reflecting a more effective riboflavin handling in HT29 cells thereby enabling these cells to protect themselves against cellular and biochemical dysfunctions. In contrast to HT29 cells, Caco-2 cells, which were the most sensitive to lumiflavin, is thought as the most appropriate cell models to study the putative role of riboflavin on cell signalling.

4.6. Summary

Riboflavin depletion in intestinal cell models induced by lumiflavin resulted in increased oxidative stress and a disruption of energy generation, which may contribute to the observed inhibitory effects on cell proliferation. Exposure to lumiflavin did not lead to DNA fragmentation, which is a key feature of apoptosis.

There were different responses to lumiflavin between cell lines and such differences between cell lines may be related to differences in functional riboflavin depletion and in the efficiency of cells to take up riboflavin.

CHAPTER 5.

LUMIFLAVIN INDUCED CHANGES IN CELL SIGNALLING

5.1.   Introduction

Previous findings in an animal study suggested a role for riboflavin as a signalling molecule for intestinal cell proliferation (Yates *et al*., 2003). They examined the effects of luminal absence of riboflavin on intestinal development in weaning rats fed a riboflavin-deficient diet, but supplied intraperitoneal injection of FMN. Systemic riboflavin status, determined using the EGRAC, liver flavin concentration was not different between luminally deficient rats and rats fed a complete diet. In spite of systemic riboflavin status maintained as much as controls, it appeared impaired gastrointestinal development in luminal riboflavin-deficient weanling rats. Duodenal crypt hypertrophy associated with an increase in crypt depth and cellularity was observed, but crypt cell proliferative index BrdU and crypt bifurcation were lower than controls. A reduction in crypt cell proliferation led to a low incidence of crypt bifurcation, causing increased cellularity and crypt depth. Such abnormal development can affect ensuring villus population. The authors suggested that the binding of riboflavin to an apical riboflavin transporter may influence signalling pathways that drive gene expression which may be associated with enterocyte proliferation and crypt fission. Thus, it hypothesised that riboflavin may act as a signalling molecule, regulating cell proliferation in the lumen.

Based on Yates' study, the simplified diagram for hypothesis of this study is presented in Figure 24. Riboflavin may influence phosphorylation of certain proteins when bound to an apical receptor/transporter in the lumen, bringing signalling cascade which may be responsive to cell proliferation (see the red box in Figure 24). Lumiflavin more specifically targets to riboflavin because it competes for sites on riboflavin transporter thereby inhibits the uptake of riboflavin into cells (see section 1.1.5.1), presumably leading to different patterns in cell signalling pathways. Therefore, lumiflavin was expected to be a useful tool to reveal a role of riboflavin on cell signalling.
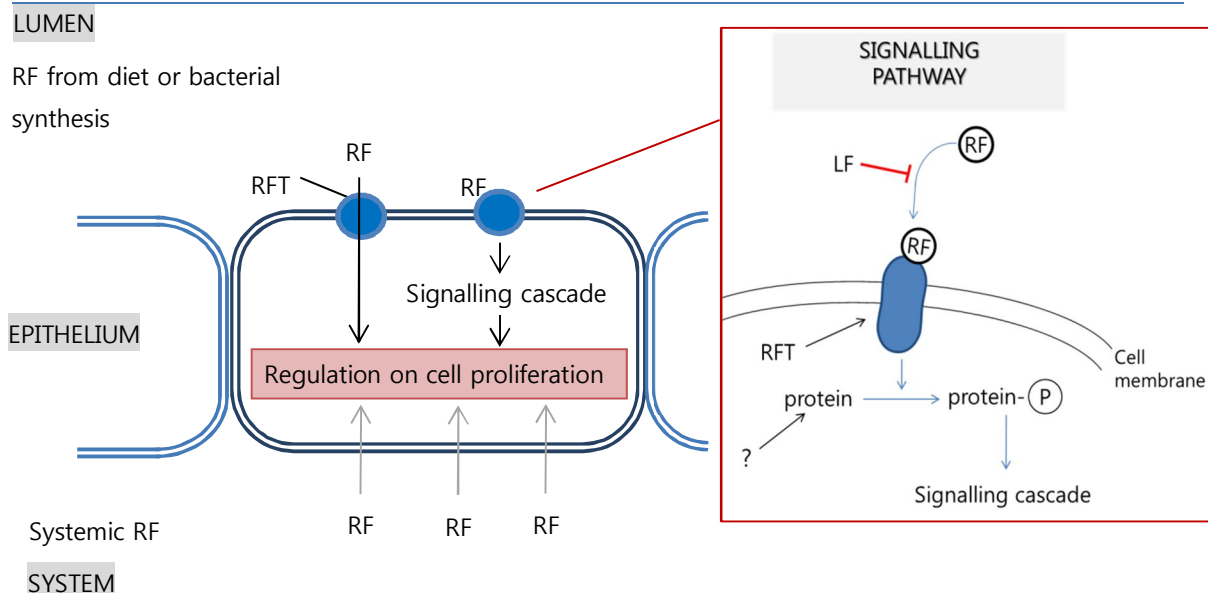
Figure 24 *Diagram of hypothesis based on Yates' animal model of luminal riboflavin depletion*

LF; lumiflavin, p; a phosphate group, RF; riboflavin, RFT; riboflavin transporter. Left side in simplified diagram of an intestinal epithelial cell shows the mechanism of regulation of cell proliferation by riboflavin transported from lumen as its primary role. Right side shows hypothesised mechanism that riboflavin binds to apical riboflavin transporter/receptor, which may affect the phosphorylation of other proteins thus bring signalling cascade to regulate cell proliferation (Yates et al., 2003).

According to Yates' study, it assumed that changes due to riboflavin depletion are not necessary for developing experimental protocols because riboflavin may independently exhibit an effect on cell signalling pathway. Reflecting this point, experimental conditions were developed. Indeed, this study showed that higher dose of lumiflavin resulted in several dysfunctions on energy generation and oxidative stress, however lower dose i.e. 40µM led to effects on cell growth inhibition and a fall in intracellular riboflavin, but not such dysfunctions. Following studies therefore were conducted using the concentration 40µM of lumiflavin. Additionally, the previous part of this study showed most sensitive responses to lumiflavin in Caco-2 cells than HCT116 and HT29. Caco-2 cells exposed to 40µM lumiflavin for a short time period (24 hours) showed impaired proliferation without changes in ROS and ATP status compared with untreated cells. Therefore, Caco-2 cells were used for the following proteomic studies against short treatment with lumiflavin.

Studies were designed to determine whether riboflavin depletion induced by lumiflavin causes an inhibitory effect on cell proliferation through alteration of cell signalling pathways. As described (see section 1.1.4), phosphorylation is an important process for the activation of proteins, initiating downstream cell signalling (Schulze, 2010; White, 2008). Therefore, changes in phosphorylation can be evidence of cell signalling. Phosphorylation occurs mainly on some amino acids of protein; serine, threonine and tyrosine. Conveniently, probing of pan-specific antibodies against the amino acid residues are commonly used for detection of phosphorylated proteins in gel-based methods (Schmelzle and White, 2006; Sawasdikosol, 2010).

Recent advanced high-throughput proteomics enables the investigation of phosphoprotein-specific alterations, such as the isobaric tag for relative and absolute quantification (iTRAQ). iTRAQ allows simultaneous identification of proteins and quantitative comparison of protein abundance in multiplexing of up to eight separately labelled samples (Hultin-Rosenberg *et al.*, 2013). This provides more accurate and reproducible quantification of peptides and proteins through peptide-based detection by tandem mass spectrometry (Zhang *et al.*, 2005). Works were performed to assess changes in global phosphorylation using probes of pan-specific phospho-amino acid residues and also to investigate phosphoprotein profiling using iTRAQ which provided all-encompassing analysis for proteins altered by lumiflavin treatment. Then, studies for validation of findings were followed.

5.2. Aims

To explore changes in phosphorylation and phosphoprotein profiling using proteomic approach by an exposure of Caco-2 cells to lumiflavin and to validate findings.

5.3. Methods

Figure 25 presents overall workflow of chapter 5 including determination of changes in global phosphorylation, phosphoprotein profiling and the cell cycle. Caco-2 cells exposed to 40µM lumiflavin were used. Changes in global phosphorylation were determined by western blot and HCA for the different time periods, focusing on the short term, and then intracellular flavin concentration was determined for the early period up to 24 hours. iTRAQ was used to

determine changes in phosphoprotein profile, followed western blot and cell cycle analysis using HCA and flow cytometry were carried out to confirm the findings.
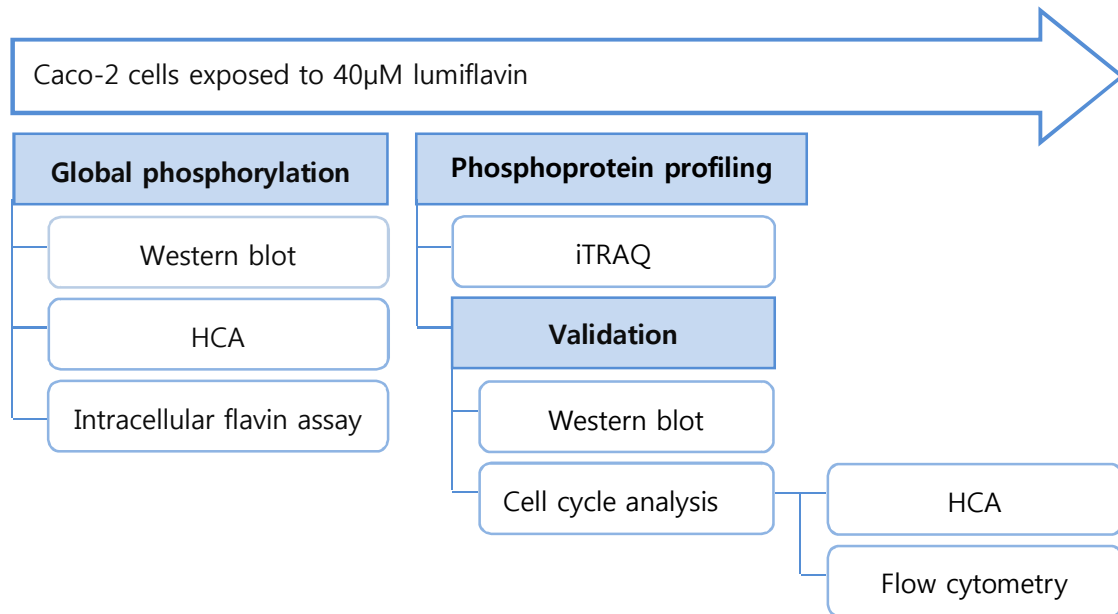
Figure 25 *Experiment scheme in chapter 5.*

HCA; high content analysis, iTRAQ; isobaric tag for relative and absolute quantitation. Caco-2 cells exposed to 40μM lumiflavin were used for investigation of global phosphorylation using western blot and high content analysis (HCA) and intracellular flavin assay was followed for changes in intracellular flavin concentration in the same period. Phosphoprotein profile was determined using iTRAQ and western blot and cell cycle analysis by HCA and flow cytometry were followed to validate iTRAQ findings.

5.3.1. Western blot for global phosphorylation

For global phosphorylation, cell lysates for western blot were prepared as incubated in 40μM lumiflavin-containing DMEM and 2% of 0.1M NaOH in DMEM as a control for 0, 3, 6, 17 and 24 hours. Western blot was performed using probing pan-specific antibodies against phospho-tyrosine and phospho-serine/threonine.

5.3.2. High content analysis

Caco-2 cells in a 96 well plate were treated with 40μM lumiflavin for 0, 1, 2, 3, 4 and 6 hours. For HCA, cells were fixed and immunostained using pan-specific antibodies against

phospho-tyrosine and phospho-serine/threonine. The plate was sent to be analysed by Imagen Biotech. in Manchester, UK.

5.3.3. Intracellular flavin assay in early stage depletion

Intracellular flavin concentrations were monitored following short term exposure to lumiflavin. Caco-2 cells were incubated in 40µM lumiflavin for 3, 6, 17, and 24 hours. Cells were harvested and lysed at each time and stored at -80℃ until analysed. Intracellular riboflavin, FAD and FMN concentrations were determined using reverse-phase HPLC as explained in section 2.2.4.

5.3.4. Preparation of phosphoprotein and iTRAQ
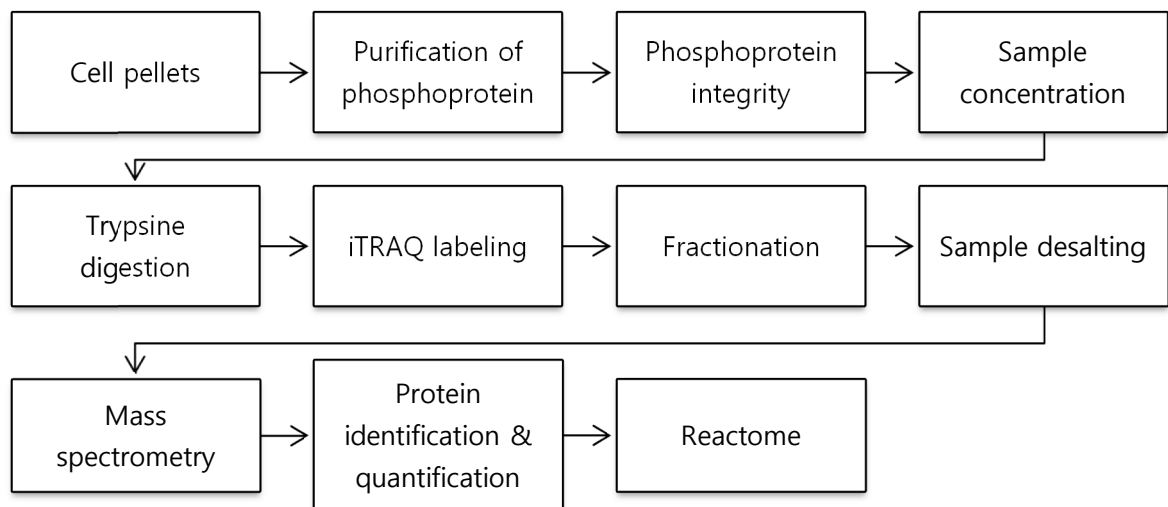
Figure 26 *Workflow of sample preparation and iTRAQ*

Caco-2 cells with different treatments shown in Figure 27 were used to purify phosphoprotein and the integrity of phosphoprotein was identified by phosphoprotein-specific gel stain method. As phosphoprotein was purified as diluted, samples were concentrated and then samples were prepared and run for iTRAQ. Proteins altered by lumiflavin treatment were identified and quantified. Reactome, a pathway database, was used to reveal a change in cell signaling pathway.

Figure 26 shows the workflow of phosphoprotein preparation, iTRAQ and data analysis. As shown in Figure 27, Caco-2 cells were incubated with 40μM lumiflavin for 6 and 24 hours, and 0 hour control and time-controls were also prepared. Cell pellets were harvested and stored in -80℃ until analysed. Cell pellets then were used to purify phosphoproteins using a phosphoprotein purification kit (see section 2.2.14). Purified phosphoproteins were visualised by staining with Pro-Q Diamond phosphoprotein and SYPRO® ruby as described in section 2.2.15.
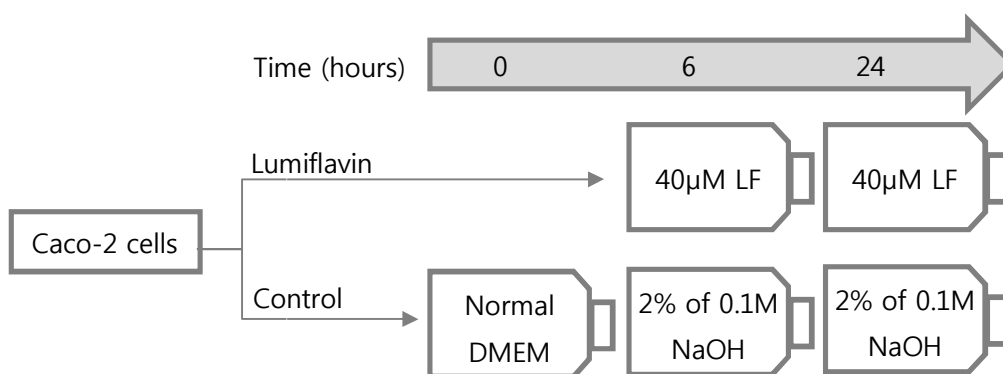
Figure 27 *Cell sample preparation of iTRAQ*

LF; lumiflavin. Five groups with the different treatment and duration were prepared; Caco-2 cells incubated in 40μM lumiflavin-containing DMEM for 6 and 24 hours, in free lumiflavin and free NaOH - DMEM which considered as 0 hour, in 2% (v/v) of 0.1M NaOH in DMEM for 6 and 24 hours as time-controls. Then, three of five groups were used for iTRAQ in replicate; 0 hour, LF and time-control for 6 hours (see Table 4 for iTRAQ labelling in section 2.2.18.2). Thus, total eight samples were used for iTRAQ.

As described in section 2.2.18.2, eight samples were used for sample preparation to proceed to iTRAQ, which were five of 0 hour, 6 hours control, 6 hours lumiflavin, 24 hours control and 24 hours lumiflavin and three of 0 hour, 6 hours control and 6 hours lumiflavin in replicates. Concentrated samples were digested and labelled with iTRAQ reagent. Peptides were fractionated by HILIC and each of fractions was desalted. Samples were run by mass spectrometry (LC-MS/MS). Further data analysis for protein identification and quantification was carried out as described in section 2.2.18.6. Significant pathways that altered by lumiflavin treatment were analysed by overrepresentation analysis using Reactome v45.

5.3.5. Western blot for serine/arginine-rich splicing factor (SR) protein

For validation of the findings of proteomic analysis, SR proteins were examined using western blot. Antibodies against SR proteins family and phospho-SR proteins were used. It can detect multiple SR proteins including SRSF4 at the protein size 75kDa, SRSF6 at 55kDa, SRSF5 at 40kDa, SRSF1 or SRSF 9 at 30kDa, and SRSF3 at 20kDa. Caco-2 cells were prepared by incubation with 40μM lumiflavin for 0, 6, 24 and 48 hours. Time controls were also prepared. Proteins were extracted and western blotting was performed as described.

5.3.6. Cell cycle analysis by HCA

Using the plate which used to investigate global phosphorylation in section 5.3.2, it was requested to Imagen Biotech. for cell cycle analysis. The duration of lumiflavin treatment was for 1, 2, 3, 4, and 6 hours.

5.3.7. Cell cycle analysis by flow cytometry

Caco-2 cells were treated with 40μM lumiflavin for 6, 24, and 48 hours, and time 0hour and time-controls were set with 2% (v/v) of 0.1M NaOH in DMEM. Cells were fixed and stained in PI/RNase staining solution, then cell cycle was analysed by flow cytometer BD LSR II. PI fluorescence dye stains DNA in the cells, and the fluorescence intensity of the stained cells reflects the DNA contents. S phase of the cell cycle leads to double amount of DNA of cells, and the fluorescence of cells in the G2/M phase is around twice as high as that of cells in the subG1/G1 phase. Therefore, the relative amount of cells can be determined (Krishan, 1975).

5.3.8. Statistical analysis

Data for global phosphorylation using western blot was analysed by two-way ANOVA for a comparison of two factors; Treatment and incubation time, followed Mann-Whitney U test was carried out to compare between 0 hour and each time point. HCA data for global

phosphorylation was analysed by Kruskal-Wallis test for a comparison across incubation time points. Data for intracellular flavin concentration and SR proteins using western blot were compared by two-way ANOVA for interaction between treatment and incubation time and the main effect of each factor. Cell cycle data using flow cytometry were analysed by two-way ANOVA for interaction of treatment and incubation time. Following one-way ANOVA was used for main effects of incubation time on each phase in each of treatment, and t-test was used for difference between treatments at each time point. The results were considered significant if P-values were <0.05.

5.4. Results

5.4.1. Global phosphorylation by western blot

Figure 28 shows images of western blots probed using pan-specific phospho-tyrosine (A) and phospho-serine/threonine antibodies (B).
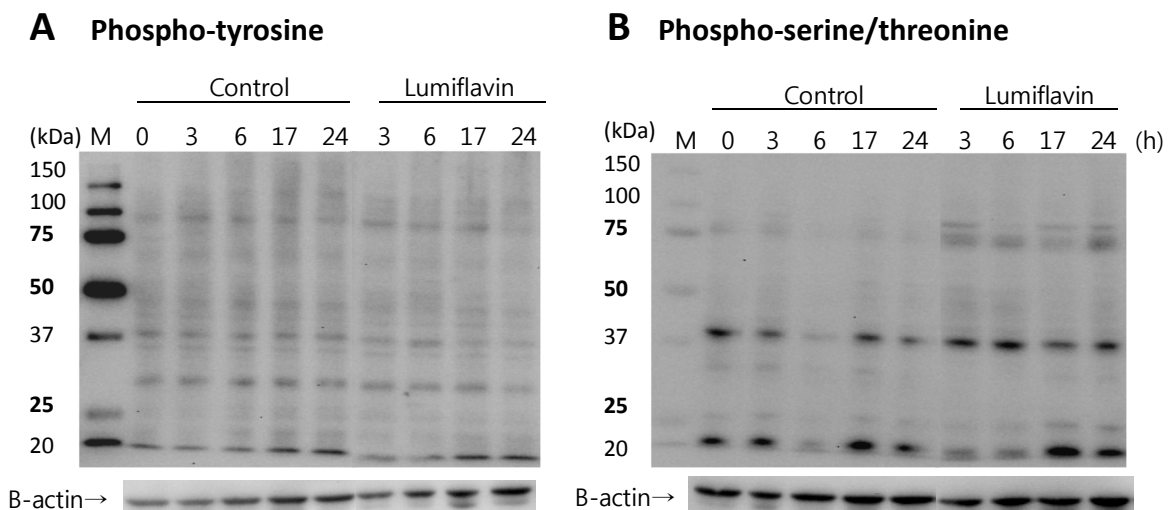
Figure 28 *Western blot for pan-specific phosphorylated tyrosine and serine/threonine.*

Caco-2 cells exposed to 40µM lumiflavin and time-controls were used. Western blot was performed using probing for pan-specific phospho-tyrosine (A) and phospho-serine/threonine (B). Multiple bands in each lane were quantified and presented in Figure 29.

105

In Figure 29, signals on blots were quantified and plotted on graphs and data were obtained from three independent experiments. There was no significant effect of treatment and incubation time, analysed by two-way ANOVA. However, Mann-Whitney U test showed a significant decrease in phospho-tyrosine at 3 and 6 hours compared with 0 hours (P=0.037). No significant difference in phospho-serine/threonine was observed. Relative changes in phosphorylation against controls suggested a modest decrease in phospho-tyrosine and 50% increase in phospho-serine/threonine by short treatment (3 and 6 hours) with lumiflavin, but these changes were not statistically significant. Taken together, Caco-2 cells exposed to 40μM lumiflavin showed a decrease in phosphorylation on tyrosine evident after only 3 and 6 hours.
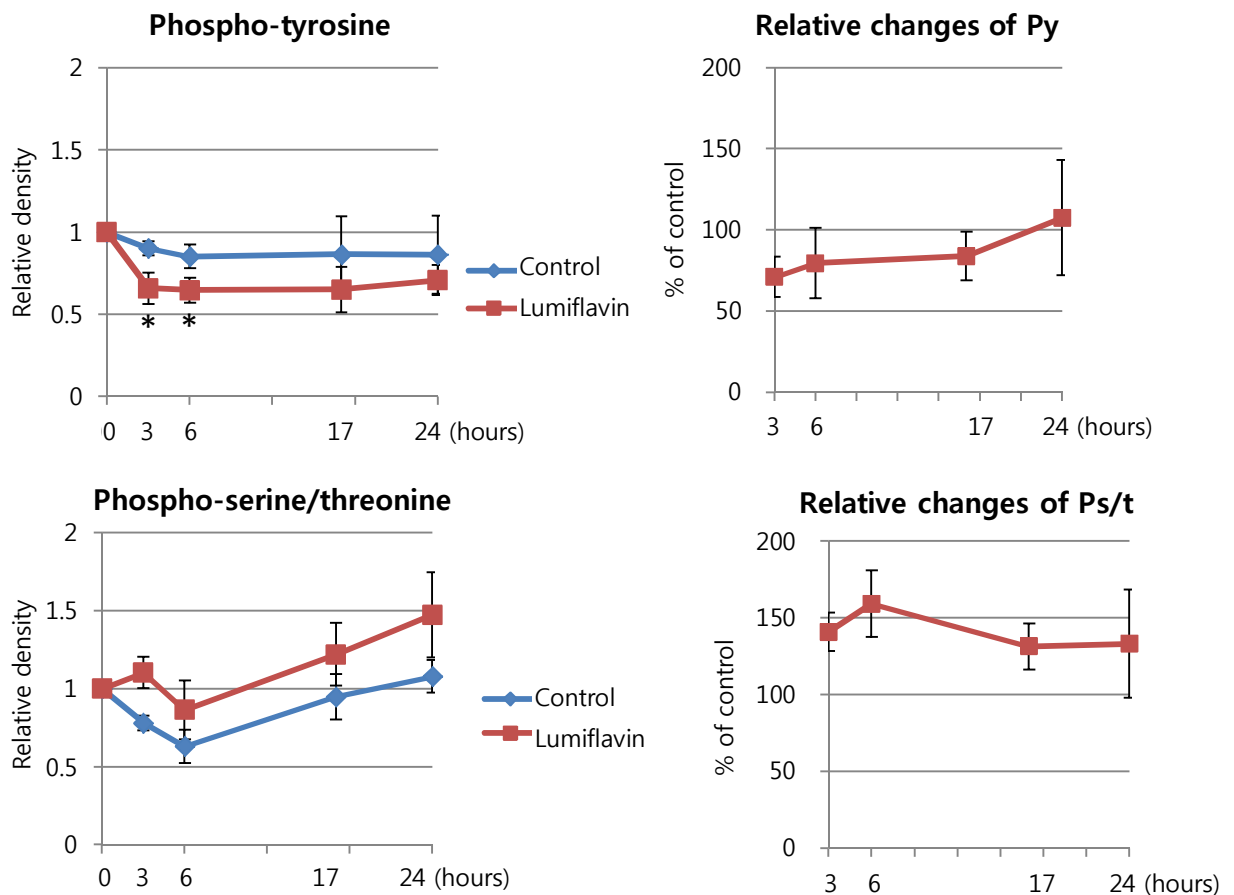
Figure 29 *Quantified signals of western blot by densitometry*

Py; phospho-tyrosine, Ps/t; phospho-serine/threonine. Y axis shows relative signal density against 0 hour. Caco-2 cells exposed to 40μM lumiflavin and time-controls were examined by western blot and multiple bands were quantified for signal strength and corrected by quantified signals of ß-actin. Signal of 0hour was assigned to 1 and others were expressed as relative values. Data were obtained from three independent experiments and expressed as mean±(SEM). Relative changes against time-controls were calculated in each experiments and expressed as mean±(SEM).

* Significant different from 0hour (P<0.05, Mann-Whitney U test)

5.4.2. Global phosphorylation by HCA

There was no significant effect of lumiflavin treatment on phosphor-serine/threonine or phosphor-tyrosine after 3 or 6 hours exposure. Cell numbers on a fixed plate were seen to be uneven (left of each panel in Figure 30), thus it is thought that this might have led to large variations in measuring fluorescence intensity.

A **Phospho-tyrosine**
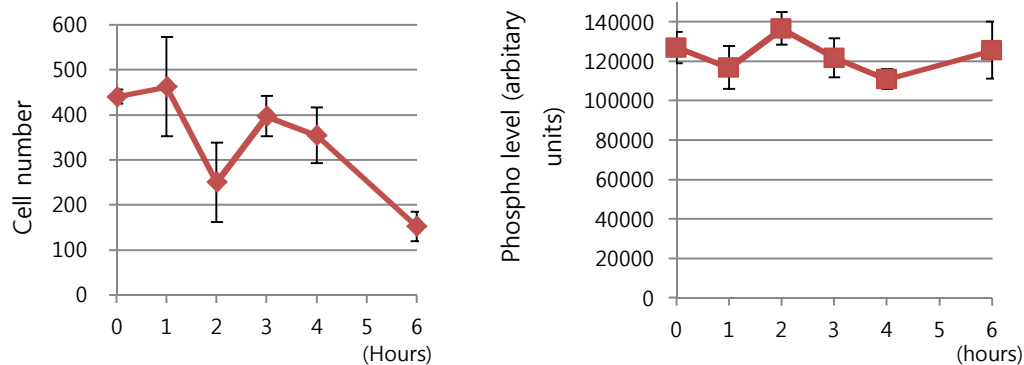
B **Phospho-serine/threonine**
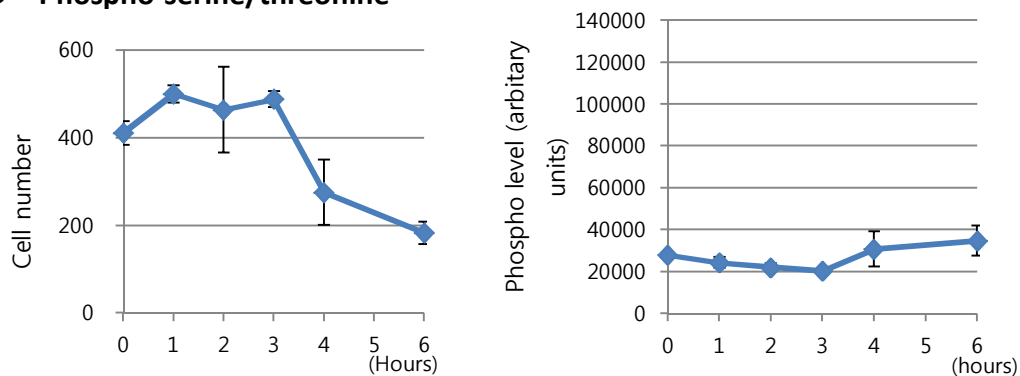
Figure 30 *Cell numbers and fluorescence levels for phospho-tyrosine and phospho-serine/threonine by HCA.*

Caco-2 cells were incubated in 40µM lumiflavin or control for up to 6 hours and then fluorescence-immunostained with pan-specific phospho-tyrosine (A) and phospho-serine/threonine (B). The numbers of cells examined for fluorescence strength (left of each panel) and global phosphorylation level (fluorescence strength) (right of each panel) were presented. Data was obtained from a single experiment in three replicates and expressed as mean (±SEM). Statistical significance was not found in any phospho-levels.

5.4.3. Intracellular flavin concentration in early stage depletion

Effect of lumiflavin on intracellular flavin concentration in early stage depletion was determined. Short term exposure to lumiflavin did not elicit a decrease in intracellular flavins concentrations (two-way ANOVA). It suggests that the observed phosphorylation changes were not linked to riboflavin depletion induced by lumiflavin.
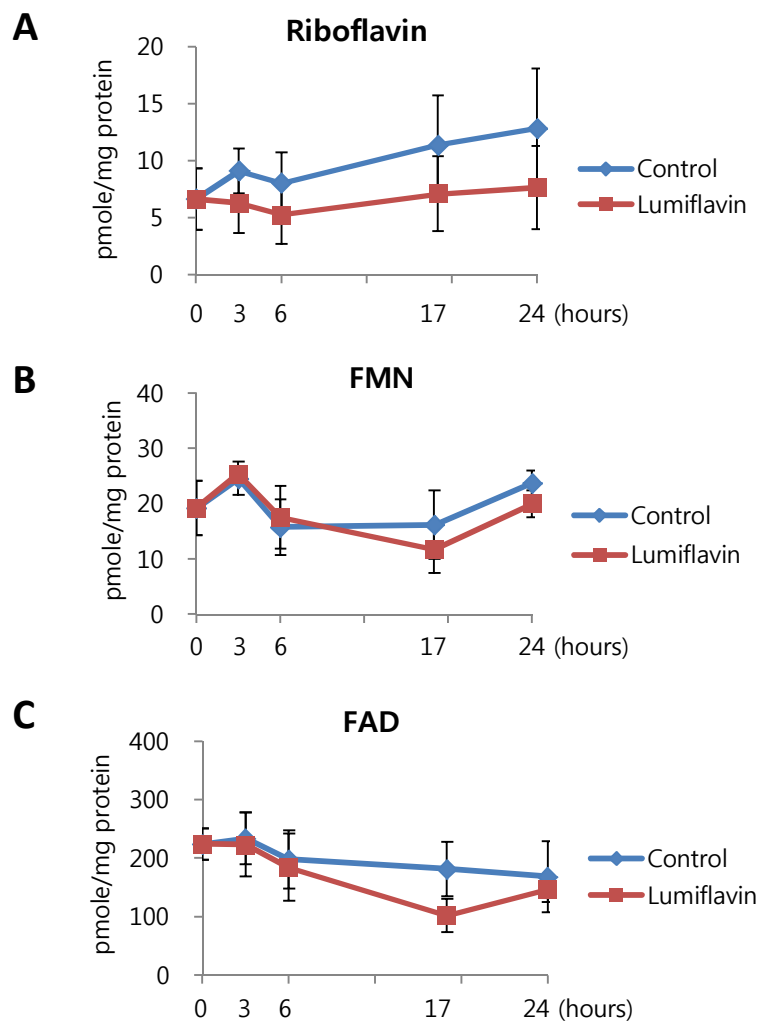
Figure 31 *Effects of lumiflavin on intracellular flavins concentration in early stages of lumiflavin treatment, determined by HPLC.*

Caco-2 cells were incubated in 40µM lumiflavin or control for up to 24 hours. Cells were used for determination of intracellular flavin concentration using HPLC. Data was obtained from three independent experiments and expressed as mean (±SEM). Two-way ANOVA showed no significance on interaction or main effects on treatment and incubation time.

5.4.4. Preparation of phosphoprotein for iTRAQ

Steps of sample preparation

```
┌──────────┐   ┌──────────────┐   ┌──────────────┐   ┌───────────────┐   ┌──────────┐
│   Cell   │ → │ Purification │ → │   Protein    │ → │    Sample     │ → │ Trypsine │
│ pellets  │   │of phosphoprotein│ │  integrity   │   │ concentration │   │ digestion│
└──────────┘   └──────────────┘   └──────────────┘   └───────────────┘   └──────────┘
```
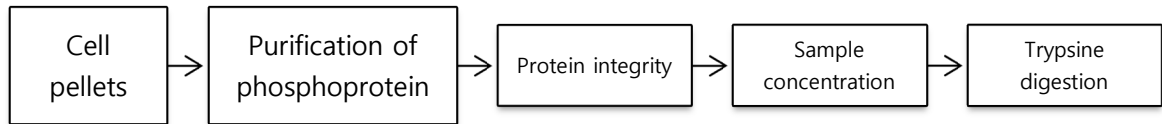
Caco-2 cells treated with 40µM lumiflavin for 6 and 24 hours and controls (0, 6 and 24 hours) were used to prepare phosphoproteins. In order to enrich phosphorylation in samples thereby to increase sensitivity for the proteomic analysis, phosphoproteins were purified from the stored cell pellets as detailed in section 2.2.14. Phosphorylated proteins are bound with high specificity to phosphoprotein purification resin, while unphosphorylated proteins flow through the resin without binding there and thus can be found in the flow-through fraction. Retained Phosphoproteins were eluted and collected in the elution buffer, and this process was repeated for six times. As seen on A of Figure 32, elution of retained proteins in the resin was maximized at 3rd elution as guided by the manufacturer instruction. Each eluted fractions were loaded in the SDS-PAGE gel, stained and visualised, and the strengths of signals were consistent to the graph of protein. Figure 32 confirmed that all phosphoproteins were eluted and collected.
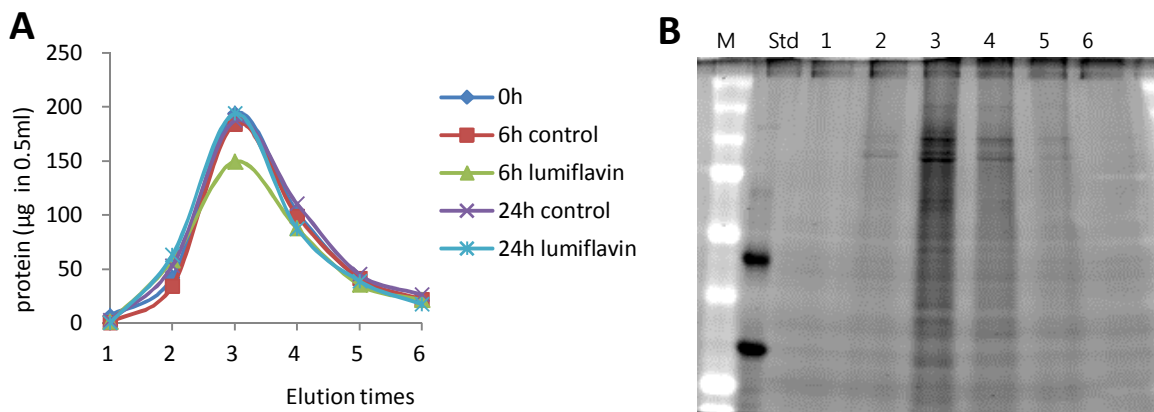
Figure 32 *Protein concentration of purified phosphoprotein in each elution and the SDS-PAGE gel stained with Coomassie blue stain*

h; hours, M; protein marker, Std; phosphoprotein standard, 1~6; first to sixth elution. Protein contents determined for each eluted fraction (A) and the gel stained with coomassie blue for whole proteins (B) are presented. The graph and the image confirmed that almost all phosphoproteins were eluted.

Steps of sample preparation

| Cell pellets | → | Purification of phosphoprotein | → | Protein integrity | → | Sample concentration | → | Trypsine digestion |
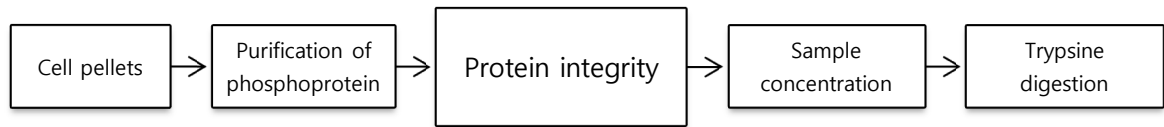
Integrity of purified phosphoproteins were confirmed using staining with Pro-Q Diamond phosphoprotein gel stain and SYPRO® ruby total protein gel stain and western blot probing with pan-specific phospho-serine/threonine antibody (Figure 33). Loaded protein amounts into gels were different; 10μg of cell lysates, 1~1.5μg of 10 $\mu\ell$ flow through fraction and 1.5~2μg of 10 $\mu\ell$ pooled eluted fraction.

Intact protein bands of phosphoproteins were found in eluted fractions (Figure 33, A). Unphosphorylated proteins were in flow-through fraction since no signals on the gel stained with Pro-Q Diamond stain appeared (Figure 33, A), but clear signals were on the gel stained with SYPRO® ruby (Figure 33, B). Clear signals on eluted fractions were observed even though total protein was much less than cell lysate. Furthermore, it needs a caution to interpret the figures because the amounts of loaded protein were different for cell lysates and fractions. Figure 33 (C) shows a confirmation of that using western blot for phospho-serine/threonine. Taken together, the phosphoproteins were successfully enhanced.
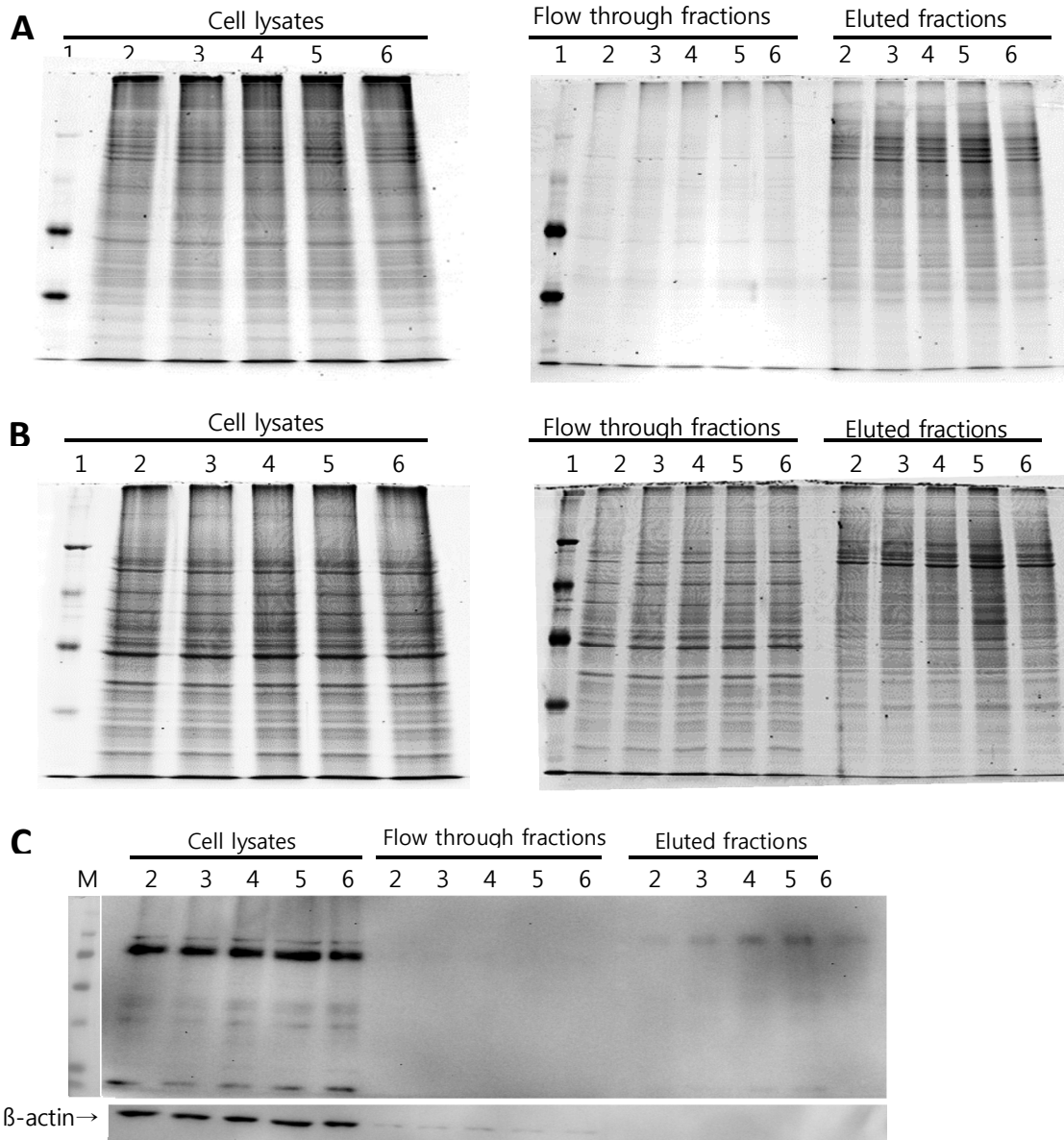
1   Phosphoprotein molecular weight standard, positive and negative controls
2   0h
3   6h control
4   6h lumiflavin
5   24h control
6   24h lumiflavin

Figure 33 *Purified phosphoproteins stained with Pro-Q Diamond phosphoprotein stain and SYPRO® ruby total protein stain and western blot probed with phospho-serine/threonine antibody*

M; protein marker, h; hours. Products of phosphoprotein purification and cell lysates loaded into a gel were stained with Pro-Q Diamond phosphoprotein (A) and SYPRO® ruby total protein (B). (C); further confirmation was done by western blot using phospho-serine/threonine. Loaded protein amounts into gels were 10µg of cell lysates, 1~1.5µg of 10 ㎕ flow through fraction and 1.5~2µg of 10 ㎕ pooled eluted fraction.

111

Steps of sample preparation

Cell pellets → Purification of phosphoprotein → Protein integrity → Sample concentration → Trypsine digestion
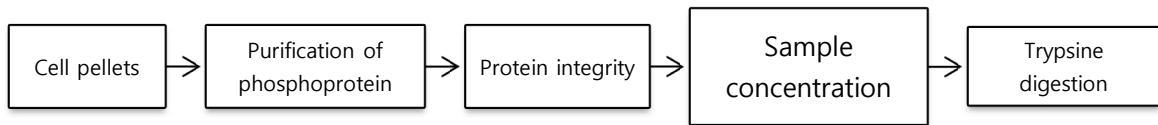
Phosphoprotein was purified as diluted on the process of purification. Thus, each eluted fractions were pooled and concentrated by centrifugal filtration. Eight samples were selected for 8plex of iTRAQ and concentrated. Figure 34 presents coomassie blue gel stain for concentrated phosphoproteins. Strength of signals was similar across the lanes even when compared with the signals of cell lysates. Also, as seen on the additional table of Figure 34, the volumes of concentrated samples equivalent to 10μg protein were approximately around one tenth of cell lysate volume. Therefore, purified phosphoproteins which had been much diluted were successfully concentrated.

A

Treatment	0h	6C	6LF	0h	6C	6LF	24C	24LF	Cell lysate
Protein concentration after filtration (mg/ml)	10.86	7.75	6.78	6.91	7.98	7.54	8.07	7.21	
Volume equivalent to 10μg protein (μl)	0.92	1.29	1.48	1.45	1.25	1.33	1.24	1.39	15

B   M 0h 6C 6LF 0h 6C 6LF 24C 24LF cell lysate
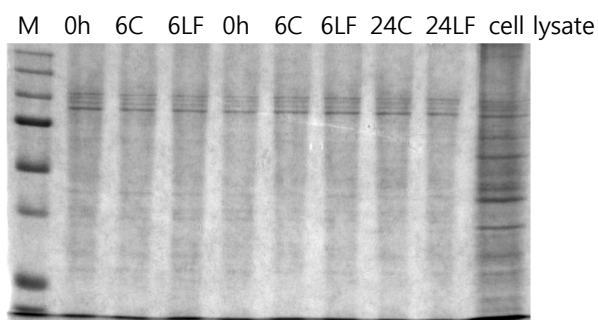
Figure 34 *Concentrated phosphoproteins using filtration*

h; hour, C; control, LF; lumiflavin, M; protein marker. Eight samples were concentrated using centrifugal filtration, and protein concentration was determined. Phosphoprotein equivalent to 10μg was run on a gel and stained with coomassie blue.

<u>Steps of sample preparation</u>

Cell pellets → Purification of phosphoprotein → Protein integrity → Sample concentration → Trypsine digestion
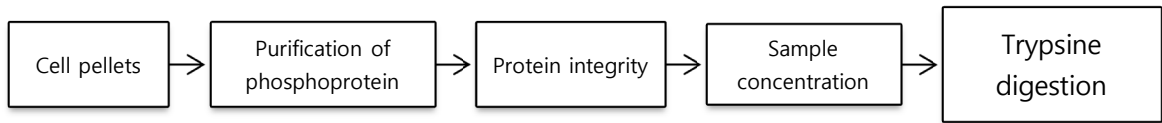
As iTRAQ is a proteomic analysis based on tag-labeling on peptides, concentrated purified phosphoproteins were digested to peptides using trypsin. Before and after digestion, aliquots equivalent to 5μg protein were run on a gel and stained with coomassie blue as presented in Figure 35. Non-digested proteins appeared similar as an image of Figure 34 which is a gel image of concentrated phosphoprotein. Since trypsin-treated proteins were digested to small size peptides, they appeared at the lowest bottom where the bands were stronger than non-digested.
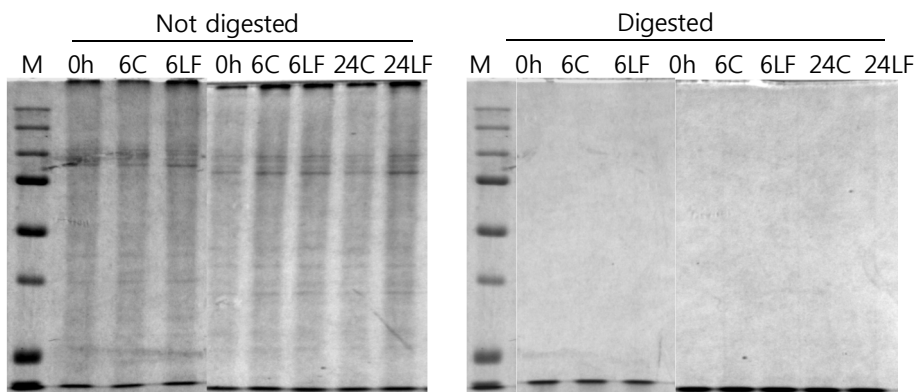
Figure 35 *Trypsin-digested peptides stained with coomassie blue*

M, protein marker; h, hour; C, control; LF, lumiflavin. Phosphoproteins before and after trypsin-digestion, equivalent to 5μg protein, were run on a gel and stained with coomassie blue.

5.4.5. Phosphoprotein profiling by iTRAQ

Trypsin-digested peptides were fractionated by HILIC and analysed by mass spectrometry (LC-MS/MS) for identification of peptide sequence, thereby allowing protein identification and quantification. Results are expressed as fold change compared with control.

300 proteins were identified and quantified, and then the relative fold changes were calculated and subjected to paired comparison analysis using SignifiQuant v4.0. Summaries of proteins that were significantly altered by lumiflavin treatment for 6 and 24 hours compared with the time-controls are presented in Table 5 and Figure 36. Such proteins were sorted through and assessed by overrepresentation analysis in Reactome v45 to investigate relevant pathways represented by identified proteins. Summaries of the number of proteins that were significantly changed in comparison with 0 hour baseline are presented in Table 10.

For the comparisons between treatments, the Venn diagram (Figure 36) shows seven proteins that were significantly altered by lumiflavin over the time course. Four of these proteins which showed increased fold changes (i.e changes in phosphoprotein level) were related to mRNA processing particularly mRNA splicing, and two proteins that decreased in fold changes plays a role on protein synthesis and nucleosome (Table 6). One of seven proteins, drebrin, was excluded due to no relevance because it is a brain protein functioning on the process of neuronal growth and found in brain and also other tissues except the intestine. The fold changes of these six proteins were plotted on graphs, shown in Figure 37.

145 proteins that were significantly altered by 24 hours lumiflavin treatment compared with time-control were analysed by Reactome to identify significant pathways represented by such proteins (Figure 38). Each event is coloured in blue to red according to the probability values from 1.00 to 3×10^{-10}, and probabilities coloured from yellow to red are considered as significant. Significant pathways identified include mRNA processing on gene expression and apoptosis pathway as seen below :

1. mRNA processing on gene expression, relating to processing of capped intron-containing pre-mRNA on mRNA splicing (the last child event P=8.7e-13, 13/112)
2. Post-elongation processing of the transcript, particularly of intron-containing pre-mRNA (the last child event P=8.5e-11, 8/34)
3. RNA polymerase II transcription termination (the last child event P=8.5e-11, 8/43)

4. Apoptosis(P=1.6e-06, 9/154)

Table 7 lists the 13 proteins which matched proteins for mRNA processing and/or RNA polymerase Ⅱ transcription. Table 8 shows the 9 proteins which matched for apoptosis pathway. The fold changes of the proteins were plotted on graphs shown in Figure 39 and Figure 40.

Lumiflavin led to delay or suppression of dephosphorylation on proteins related to gene expression, particularly to mRNA processing and RNA polymerase Ⅱ transcription and on apoptosis-related proteins. In Figure 39, the 6 proteins emphasised in red boxes showed clear differences from controls over the time course. Phosphorylation of such proteins was maintained around baseline (0 hour) or increased approximately 10% by lumiflavin, while cells under the control condition showed a fall in the fold changes of such proteins. The differences between lumiflavin and control were more remarkable at 24 hours up to approximately 30%. Figure 40 presents the fold changes of 9 proteins that matched apoptosis pathway. 5 proteins coloured in red boxes showed greater than 10% changes in fold changes at 24 hours compared with the time-controls. Lumiflavin led to suppress changes in phosphorylation of proteins related to apoptosis. For instance, the fold change of 14-3-3 protein sigma of time-controls cells were increased, while the fold change of the protein in lumiflavin-treated cells was maintained at the level of 0 hour control. Phosphorylation of HMGB1, HMGB2 and PSMB7 was maintained at the control level (0 hour) in cells exposed to lumiflavin, but decreased in time-controls.

Of the 13 and 9 proteins which matched gene expression and apoptosis, proteins with largest changes over the time course were listed according to rank. Proteins showing fold changes less than 10% changes by lumiflavin were excluded in order to select proteins showing clear changes. Finally, the top 15 proteins of interest showing the largest fold changes were selected. The proteins were ranked according to the highest absolute level of fold change against control. Absolute fold changes against time-control at each time point were calculated and ranked. The larger absolute fold change goes to the higher rank. Then, the two ranks at the two time points were summed, and the final ranks were made as the lower sum of ranks goes to the higher rank. The summary and rank of such proteins is listed in Table 9. The top-ranked proteins belonged to serine/arginine-rich splicing factors (SR) proteins family. Therefore, to validate these findings of proteomic analysis was performed using western blot for SR proteins family.

In addition, Table 10 presents the summaries of protein showing significant changes in comparison with 0 hour baseline. It found less phosphorylated proteins in the lumiflavin-treated cells than in the control at 24 hours. This suggests that lumiflavin may suppress phosphorylation on proteins that is normally induced by riboflavin under control conditions. It was sorted through the fold changes of individual proteins, and all proteins showing obvious changes both between treatments and across time course had already been included in the final 15 proteins of interest.

Table 5 *The numbers of proteins showing different fold changes under lumiflavin treatment compared with time-controls.*

(*P*=0.05, MTC off)	6h LF vs 6h C	24h LF vs 24h C
↑	5	82
↓	2	63
Total	7	145

P; probability, MTC; multiple test correction, h; hours, LF; lumiflavin, C; control, ↑/↓; higher or lower in fold change than time-control. 7 proteins were significantly changed by exposure to lumiflavin for 6 hours compared with 6 hour control. Exposure to lumiflavin for 24 hours led to significant changes in phosphorylation of 145 proteins compared with 24 hours control.

6h LF[vs 6h C]   24h LF[vs 24h C]

0   7   138
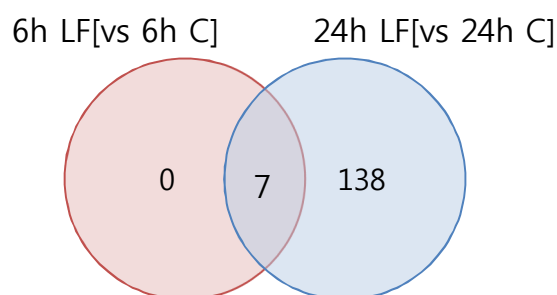
Figure 36 *Venn diagram of proteins showing different fold changes under lumiflavin treatment compared with time-controls.*

h; hours, LF; lumiflavin, C; control. All 7 proteins showing significant difference in comparison between 6 hours treatments were continuously altered over the time course up to 24 hours.

Table 6 *Summaries of seven proteins included in coaggregated part on venn diagram of Figure 36*

Change	Name	UniProt ID	Phospho-site	Related pathways
↑	**HNRNPC** Isoform C1 of Heterogeneous nuclear ribonucleoproteins C1/C2	P07910-2	Ser-260 & 299 in the resting cell, Ser-253, & 238 in the response to hydrogen peroxide	mRNA processing, splicing
↑	**SRSF1** Serine/arginine-rich splicing factor 1	J3KTL2	Ser-2, 199, 201, 205, 231, 234 & 238	mRNA processing, splicing
↑	**SRSF6** Serine/arginine-rich splicing factor 6	Q13247	Extensively phosphorylated on serine residues in the RS domain	mRNA processing, splicing
↑	**DBN1** Drebrin	Q16643	Ser-141, 142, 337, 339 & 342, Thr-331, 335 & 346	A cytoplasmic actin-binding protein, related to neuronal growth. Developmentally-regulated brain protein
↑	**LUC7L3** Cisplatin resistance-associated overexpressed protein, isoform CRA_b /Luc7-like protein 3	J3KPP4 /O95232	Ser-3, 110, 420, 425 & 431	RNA splicing, interacting with SFRS1.
↓	**eEF2** Elongation factor 2	P13639	Thr-54, 57, 59 & 435, Ser-502	Protein biosynthesis Translation elongation; Gene expression; Metabolism of proteins; Translation
↓	**HIST1H2BH** Histone H2B type 1-H	Q93079	Ser-7 & 15 by STK4/MST1, Ser-37 by AMPL, Tyr-43, Ser-79, Ser-113;alternate,	Core component of nucleosome Cell cycle; chromosome maintenance; nucleosome assembly; telomer maintenance

Ser; serine, Thr; threonine, Tyr; tyrosine, ↑/↓; higher or lower in fold change than time-control, STK4/MST1; serine/threonine-protein kinase 4 (EC2.7.11.1), AMPL; cytosol aminopeptidase (EC 3.4.11.1).
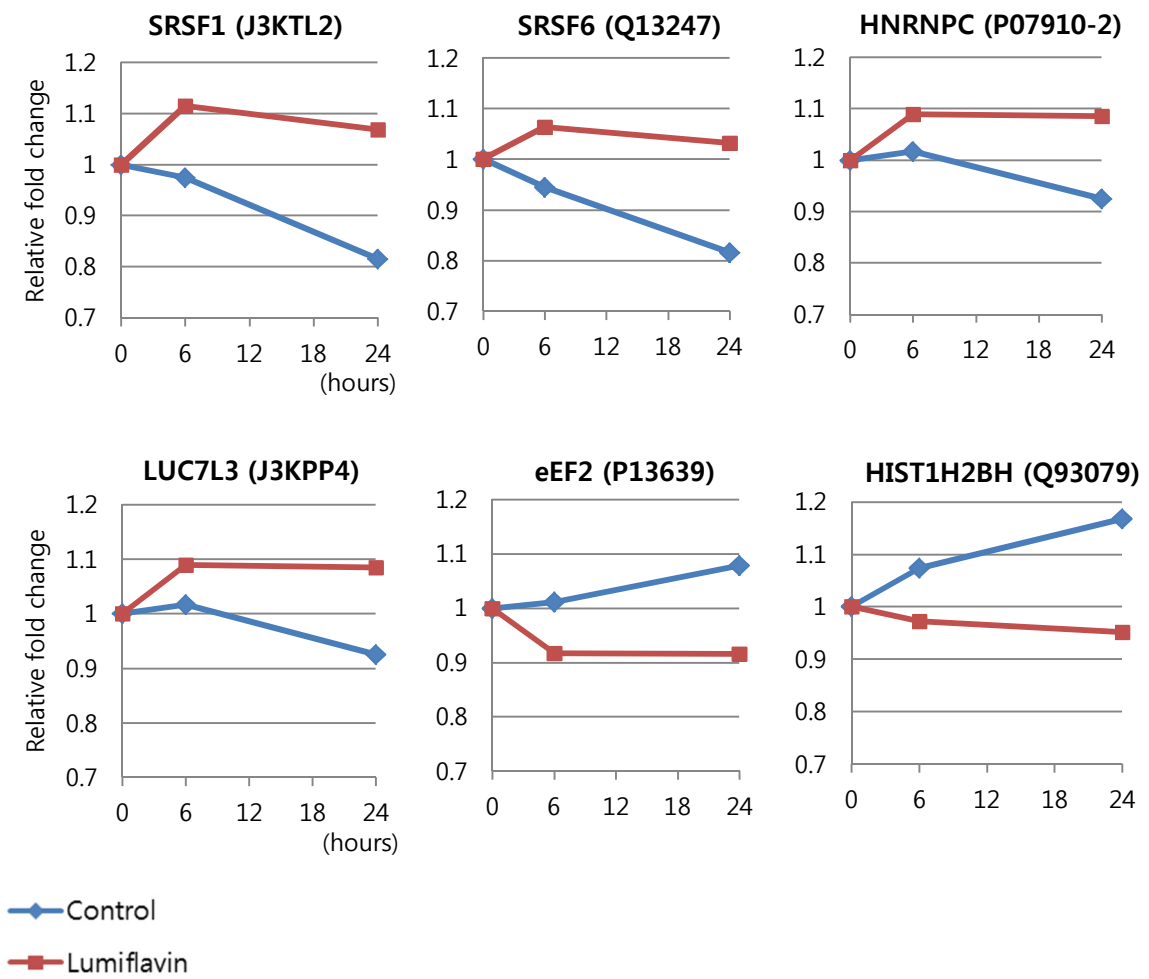
Figure 37 *Fold changes of proteins listed on Table 6.*

For all graphs, X axis shows hours and Y axis shows relative fold changes against 0 hour. Title of each graph shows abbreviated gene name and UniProt accession number. Fold changes of 6 proteins which showed significant changes by exposure to lumiflavin for 6 and also 24 hours compared with time-controls were plotted.

Statistically over-represented events in hierarchy

Each Event is coloured according to the un-adjusted, i.e. not corrected for multiple testing, probability (from hypergeometric test) of seeing given number or more genes in this Event by chance. Only the 'child' events are shown which have a *p*-value lower than the 'parent' event. The top-level (root) Events are ordered according to the lowest p-value of their components. Colour key for probabilities:

| 1e+00 | 3e-01 | 1e-01 | 3e-02 | 1e-02 | 3e-03 | 1e-03 | 3e-04 | 1e-04 | 3e-05 | 1e-05 | 3e-06 | 1e-06 | 3e-07 | 1e-07 | 3e-08 | 1e-08 | 3e-09 | 1e-09 | 3e-10 | > |

- Gene Expression1.1e-08, 25/1031
  - Processing of Capped Intron-Containing Pre-mRNA1.5e-12, 13/117
    - mRNA Splicing8.7e-13, 13/112
- mRNA Processing1.1e-11, 13/136
  - Processing of Capped Intron-Containing Pre-mRNA1.5e-12, 13/117
    - mRNA Splicing8.7e-13, 13/112
- Post-Elongation Processing of the Transcript6.4e-10, 8/43
  - Post-Elongation Processing of Intron-Containing pre-mRNA8.5e-11, 8/34
- Transcription9.9e-06, 8/145
  - RNA Polymerase II Transcription6.5e-07, 8/101
    - RNA Polymerase II Transcription Termination6.4e-10, 8/43
- Apoptosis1.6e-06, 9/154
- Metabolism of proteins8.3e-04, 12/574
  - Translation1.3e-05, 8/151
- Cell Cycle1.5e-04, 12/478
  - Chromosome Maintenance1.0e-04, 6/103
- Meiosis3.0e-03, 4/81
  - Meiotic Synapsis8.1e-04, 4/57
    - Telomere clustering at the nuclear membrane3.9e-04, 4/47
- Binding and Uptake of Ligands by Scavenger Receptors4.3e-01, 2/195
  - Scavenging by Class F Receptors1.1e-03, 2/7

Figure 38 *Reactome analysis of the pathways represented by 145 proteins significantly altered by 24 hours lumiflavin treatment compared with time-control*

119

Statistically over-represented events in hierarchy

Each Event is coloured according to the un-adjusted, i.e. not corrected for multiple testing, probability (from hypergeometric test) of seeing given number or more genes in this Event by chance. Only the 'child' events are shown which have a *p*-value lower than the 'parent' event. The top-level (root) Events are ordered according to the lowest p-value of their components. Colour key for probabilities:

| 1e+00 | 3e-01 | 1e-01 | 3e-02 | 1e-02 | 3e-03 | 1e-03 | 3e-04 | 1e-04 | 3e-05 | 1e-05 | 3e-06 | 1e-06 | 3e-07 | 1e-07 | 3e-08 | 1e-08 | 3e-09 | 1e-09 | 3e-10 | > |

Mitotic M-M/G1 phases 4.7e-02, 5/266
   M Phase 3.0e-02, 5/235
      Mitotic Metaphase and Anaphase 1.2e-02, 5/185
         Mitotic Anaphase 1.2e-02, 5/184
            Nuclear Envelope Reassembly 4.0e-03, 2/13
Disease 3.4e-02, 12/915
   Amyloids 6.3e-03, 3/51
      Serum amyloid P binds DNA and chromatin 1.1e-03, 3/28
   HIV Infection 2.4e-02, 5/221
      Host Interactions of HIV factors 1.8e-02, 4/135
Signal Transduction 1.0e+00, 6/1847
   Signalling by ERBB2 3.3e-01, 2/158
      CHIP (STUB1) mediates ubiquitination of ERBB2 1.9e-03, 2/9
      CUL5 mediates ubiquitination of ERBB2 1.9e-03, 2/9
Metabolism of RNA 2.3e-03, 7/249
3' -UTR-mediated translational regulation 8.6e-03, 4/109
Immune System 9.9e-01, 5/1397
   Adaptive Immune System 9.6e-01, 3/866
      Class I MHC mediated antigen processing & presentation 4.3e-01, 3/320
         Antigen processing-Cross presentation 9.3e-02, 3/145
            ER-Phagosome pathway 7.2e-02, 3/130
               Proteasomal cleavage of substrate 4.9e-02, 2/48

Total number of events assessed: 7726

Number of matching events (i.e. individual hypergeometric tests performed): 250

Number of genes matching submitted identifiers: 52

Figure 38 *Reactome analysis of the pathways represented by 145 proteins significantly altered by 24 hours lumiflavin treatment compared with time-control (continued)*

Table 7 *A summary of 13 proteins which matched mRNA processing and/or RNA polymerase II transcription*

Change	Name	UniProt ID	Phospho-site	Related pathways
↑	**SRSF3** *Serine/arginine-rich splicing factor 3*	P84103	Ser-5, 23 & 148	mRNA processing, splicing in relation with cellular proliferation and/or maturation.
↑	**SRSF9** *Serine/arginine-rich splicing factor 9*	Q13242	Tyr-192 & Ser-193, 195, 204, 208, 211 & 216	mRNA processing, splicing
↑	**SRSF6** *Serine/arginine-rich splicing factor 6*	Q13247	Ser-45, 81, 84, 299, 303, 314 & 316	mRNA processing, splicing
↑	**U2AF1** *Splicing factor U2AF 35 kDa subunit*	Q01081	Ser-61	constitutive and enhancer-dependent splicing by mediating protein-protein interactions and protein-RNA interactions required for accurate 3'-splice site selection.
↑	**U2AF2** *Splicing factor U2AF 65 kDa subunit*	P26368	Ser-2 &79	pre-mRNA splicing.
↑	**SRSF5** *Serine/arginine-rich splicing factor 5*	Q13243	Ser-227, 229, 231, 233, 248, 250, 253, 263, 265, 267 & 270	mRNA processing, splicing
↑	**SNRNP70** *U1 small nuclear ribo-nucleoprotein 70 kDa*	P08621	Ser-268, 320 & 410	Pre-mRNA splicing
↑	**SNRNP200** *U5 small nuclear ribonucleoprotein 200 kDa helicase*	O75643	Ser-26, 225, 2133 & 2135 & Thr-2131	RNA helicase that required for pre-mRNA splicing and involved in spliceosome assembly, activation and disassembly
↑	**SNRPD2** *Small nuclear ribo-nucleoprotein Sm D2*	P62316	Thr-12	pre-mRNA splicing. Required for snRNP biogenesis

Ser; serine, Thr; threonine, Tyr; tyrosine, ↑/↓; higher or lower in fold change than time-control.

Table 7 *A summary of 13 proteins which matched mRNA processing and/or RNA polymerase II transcription (Continued)*

Change	Name	UniProt ID	Phospho-site	Related pathways
↑	**HNRNPK** *Isoform 3 of Heterogeneous nuclear ribonucleoprotein K*	P61978-3	Ser-116, 214, 216, 284 & 379 & Tyr-380	One of the major pre-mRNA-binding proteins
↑	**RBM8A** *RNA-binding protein 8A*	Q9Y5S9	Ser-24, 42, & 56	mRNA processing, splicing, transport, termination of RNA polymerase II transcription
↓	**NUDT21** *Cleavage and poly-adenylation specificity factor subunit 5*	O43809	Tyr-40	Component of the cleavage factor Im (CFIm) complex that plays a key role in pre-mRNA 3'-processing
↓	**SF3B1** *Splicing factor 3B subunit 1*	O75533	Ser-129, 194, 332, 344, 349, 400, 488 & Thr-142, 203, 207, 211, 223, 227, 244, 248, 267, 278, 296, 299, 313, 326, 328, 341, 350, 354, 434 & 436	mRNA processing, splicing

Ser; serine, Thr; threonine, Tyr; tyrosine, ↑/↓; higher or lower in fold change than time-control.

122
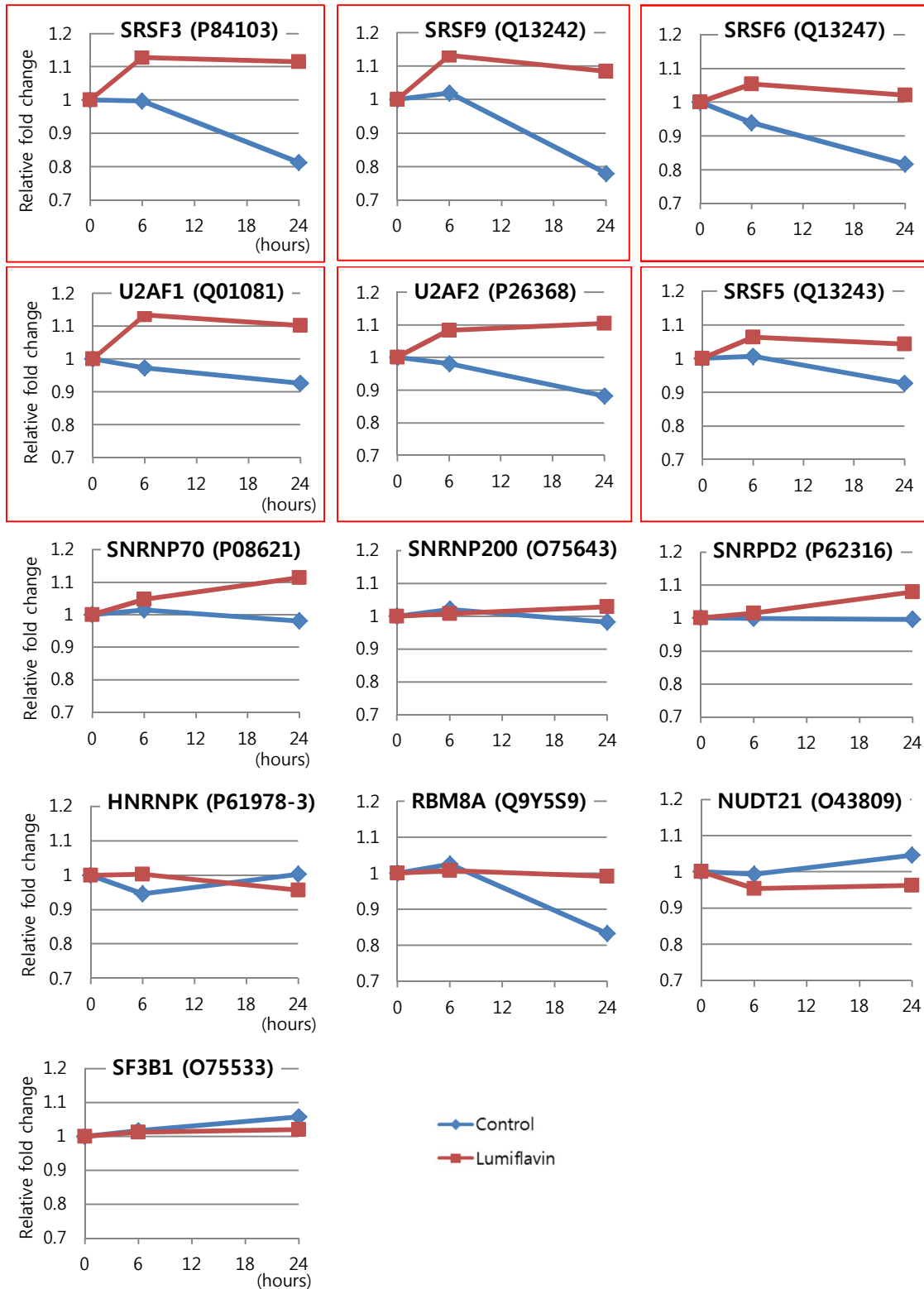
Figure 39 *Fold changes of 13 proteins listed on Table 7, which matched mRNA processing and/or RNA polymerase Ⅱ transcription*

X axis shows hours and Y axis shows relative fold changes against 0 hour. Title of each graph shows abbreviated gene name and UniProt accession number. Fold changes of 13 proteins were plotted on graphs, which showed significant changes by exposure to lumiflavin for 24 hours compared with time-controls and matched mRNA processing and RNA polymerase Ⅱ transcription in gene expression pathway.

Table 8 *A summary of 9 proteins which matched apoptosis*

Change	Name	UniProt ID	Phospho-site	Related pathway
↑	**SFN** *14-3-3 protein sigma*	P31947	Ser-5, 64, 216, 248	Apoptotic signalling pathway in response to DNA damage, Keratinocyte differentiation & proliferation Regulations of cell proliferation & of cyclin-dependent protein serine/threonine kinase activity involved in G1/S transition and/or G2/M transition
↑	**UBA52** *Ubiquitin-60S ribosomal protein L40*	P62987	Ser-57, 65	Apoptotic signalling pathway and related to broad pathways.
↓	**HMGB1** *High mobility group protein B1*	P09429	Ser-35, 100	Apoptotic execution phase Negative regulation of apoptotic cell clearance positive regulation of apoptotic process
↓	**HMGB2** *High mobility group protein B2*	P26583	Ser35	Apoptotic execution phase Positive regulation of protein insertion into mitochondrial membrane involved in apoptotic signalling pathway
↓	**PSMB7** *Proteasome subunit beta type-7*	Q99436	Tyr154	ATP-dependent proteolytic activity
↑	**HIST1H1B** *Histone H1.5*	P16401	Ser-2, 18, 173 & Thr-4, 11, 39, 138	Nucleosome assembly
↑	**HIST1H1C;** *Histone H1.2*	P16403	Ser-2,104 by PKC, & Thr-146	Nucleosome assembly
↓	**NMT1** *Glycylpeptide N-tetradecanoyltransferase 1*	P30419	Ser-31, 47	Intrinsic apoptotic signalling pathway
↓	**LMNA** *Prelamin-A/C*	P02545	Cell cycle regulation; Thr-19, Ser-22 & 392, Cytoskeletal reorganization; Ser-22 & 525, activity, induced; Ser-22, 390, 392, 652 & 657, intracellular localization; Ser-22, 390, 392, 403, 404, 652, & 657	Components of the nuclear lamina, a fibrous layer on the nucleoplasmic side of the inner nuclear membrane. Role in nuclear assembly, chromatic organization, nuclear membrane and telomere dynamics.

Ser; serine, Thr; threonine, Tyr; tyrosine, ↑/↓; higher or lower in fold change than time-control, PKC; protein kinase C (EC 2.7.11.13).
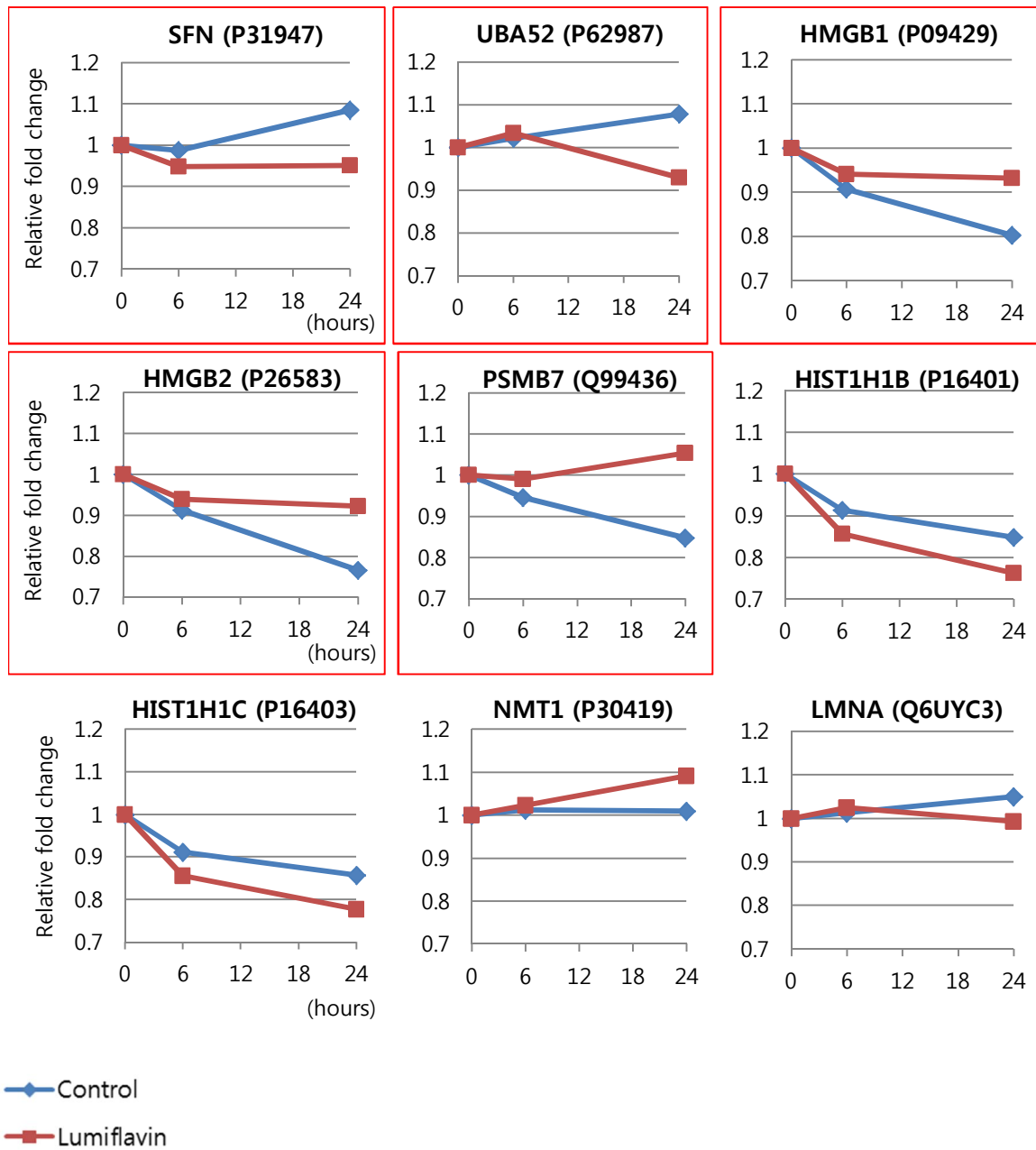
Figure 40 *Fold changes of 9 proteins listed on Table 8 which matched apoptosis pathway*

X axis shows hours and Y axis shows relative fold changes against 0 hour. Title of each graph shows abbreviated gene name and UniProt accession number. Fold changes of 9 proteins were plotted on graphs, which showed significant changes by exposure to lumiflavin for 24 hours compared with time-control and matched apoptosis pathway.

Table 9 *Rank of fold changes of final 15 proteins altered by lumiflavin*

Rank	Comparison with control	UniProt ID	Name	
1	↑	P84103	SRSF3	*Serine/arginine-rich splicing factor 3*
1	↑	Q07955	SRSF1	*Serine/arginine-rich-splicing factor 1*
3	↑	Q13242	SRSF9	*Serine/arginine-rich splicing factor 9*
4	↑	Q13247	SRSF6	*Serine/arginine-rich splicing factor 6*
5	↑	Q01081	U2AF1	*Splicing factor U2AF 35 kDa subunit,*
6	↑	P26368	U2AF2	*Splicing factor U2AF 65 kDa subunit*
8	↑	Q99436	PSB7	*Proteasome subunit beta type-7*
9	↑	P07910-2	hnRNP C1/C2	*Isoform C1 of Heterogeneous nuclear ribonucleoproteins C1/C2*
12	↑	Q13243	SRSF5	*Serine/arginine-rich splicing factor 5*
14	↑	P31947	SFN	*14-3-3 protein sigma*
15	↑	P62987	UBA52	*Ubiquitin-60S ribosomal protein L40*
7	↓	Q93079	HIST1H2BH	*Histone H2B type 1-H*
10	↓	P13639	eEF2	*Elongation factor 2*
11	↓	P26583	HMGB2	*High mobility group protein B2*
12	↓	P09429	HMGB1	*High mobility group protein B1*

↑/↓; higher or lower in fold change than time-control. Upper 11 protein showed higher fold changes than time-control and bottom 4 protein showed lower fold changes than time-controls.

Table 10 *The number of proteins showing different fold changes under lumiflavin treatment in comparison with 0 hour*

(P=0.05, MTC off)	Comparison with 0 hour	6 hours	24 hours
Control	↑	1	46
	↓	0	57
Lumiflavin	↑	5	14
	↓	9	15

P; probability, MTC; multiple test correction, ↑/↓; higher or lower in fold change than time-control. Table shows the number of proteins changed under each condition compared with 0 hour. For example, 103 proteins were significantly changed under 24 hours control condition compared with 0hour, while 29 proteins were changed by 24 hours lumiflavin compared with 0 hour.

5.4.6. Validation of proteomic analysis by western blot

Out of 15 proteins of interest, some of serine/arginine-rich splicing factor proteins (SR protein) showed biggest changes by treatment of Caco-2 cells with lumiflavin. Members of SR protein family contain the same SR domain on their sequences, thus multiple proteins can be detected using the same antibody. Hence, western blotting of both whole cell lysates and the phosphoprotein used for iTRAQ was performed using antibodies against SR proteins and phosphorylated SR proteins.

Cell lysates were prepared from Caco-2 cells treated with 40μM lumiflavin for 6, 24 and 48 hours, and time-controls and 0 hour control were set up. The signals of phospho-SR proteins found at 40, 30 and 20kDa were identified as SRSF5, SRSF1 or 9, and SRSF3 respectively (Figure 41 A). Also, the corresponding SR proteins were found at the same sizes, even though the bands at 40 and 30kDa were weak (Figure 41 B). Protein expression was quantified by densitometry (Figure 42), and the proportion of phospho-SR protein to total SR protein was calculated. Contrary to the iTRAQ data, there were no significant differences between treatments on these SR proteins and their phosphorylated proteins in the cell lysates.

Purified phosphoproteins were the same samples used for iTRAQ, thus samples consisted of 8 samples in total; 0 hour, 6 hour control, 6 hour lumiflavin in duplicate, 24 hour control and 24 hour lumiflavin.

Due to limited volumes of purified phosphoproteins, the blot was stripped after probing for the total SR protein and reused for phosphor-SR proteins. It is possible that insufficient stripping may have interfered with the phospho-SR protein signal. Nevertheless, an increase in phospho-SRSF1/9 with lumiflavin treatment was detected at 30kDa, while the total SRSF1/9 protein was unaffected by treatment. Therefore, such an increase in phospho-SRSF1/9 was not from increased expression of SRSF1/9 but increased phosphorylation itself, as supported by the proportion (Figure 44 A).

A **Anti-phospho-SR**
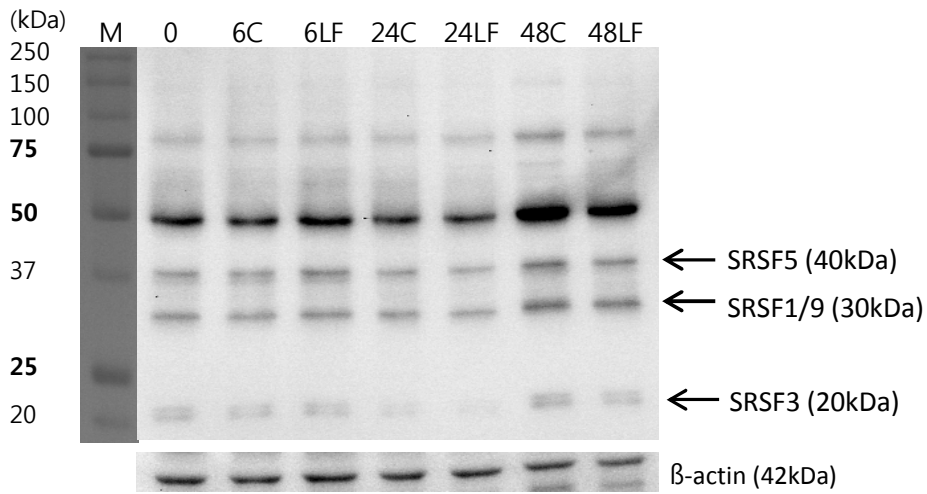
B **Anti-SR**
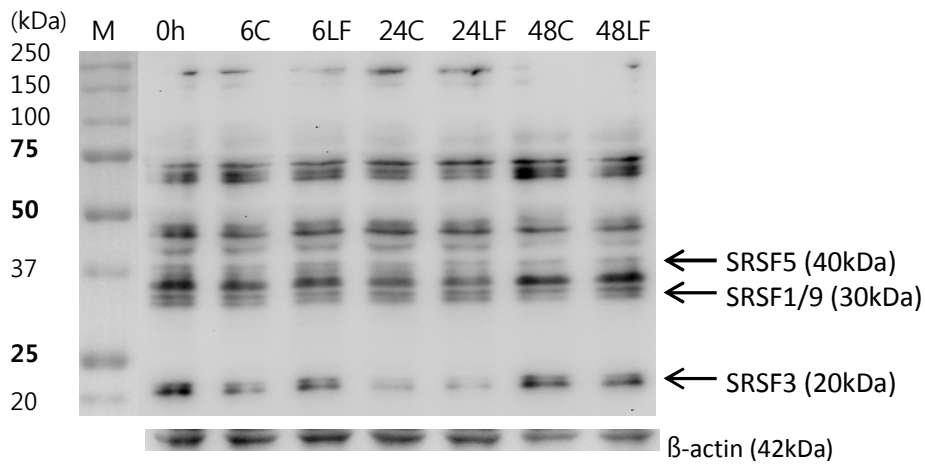
Figure 41 *Western blot for SR and phospho-SR proteins using cell lysates*

M; protein marker, h; hour, C; control, and LF; lumiflavin-treated. The numbers show durations of treatment (hours). Caco-2 cells exposed to 40µM lumiflavin for 6, 24 and 48 hours, time-controls and 0hour control were used to prepare cell lysates. Western blot was performed using antibodies for anti-SR protein family and anti-phospho-SR proteins clone 1H4.

A   SRSF5_40kDa
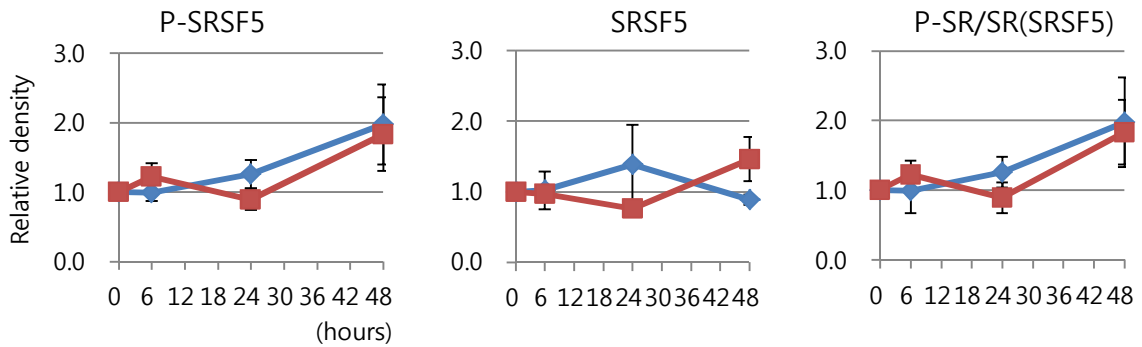
B   SRSF1/9_30kDa
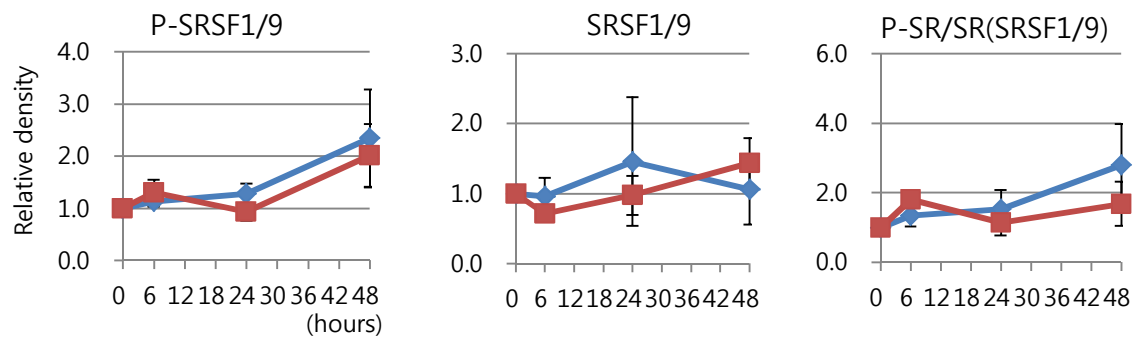
C   SRSF3_20kDa
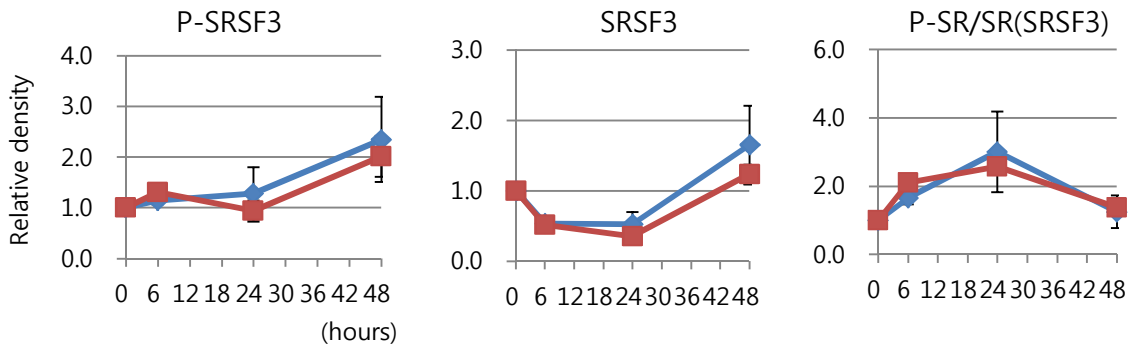
Figure 42 *Quantified western blot bands for phospho-SR protein and whole SR protein and the proportions of phospho-proteins using cell lysates*

X axis shows incubation time (hours) and Y axis shows relative signal density against 0 hour. Caco-2 cells exposed to 40µM lumiflavin for 6, 24 and 48 hours, time-controls and 0 hour control were used to prepare cell lysates. Western blot was performed using antibodies for anti-SR protein family and anti-phospho-SR proteins clone 1H4. Signals were quantified by densitometry and the ratio of phospho-SR protein to total SR proteins was calculated.

A **Anti-phospho-SR**
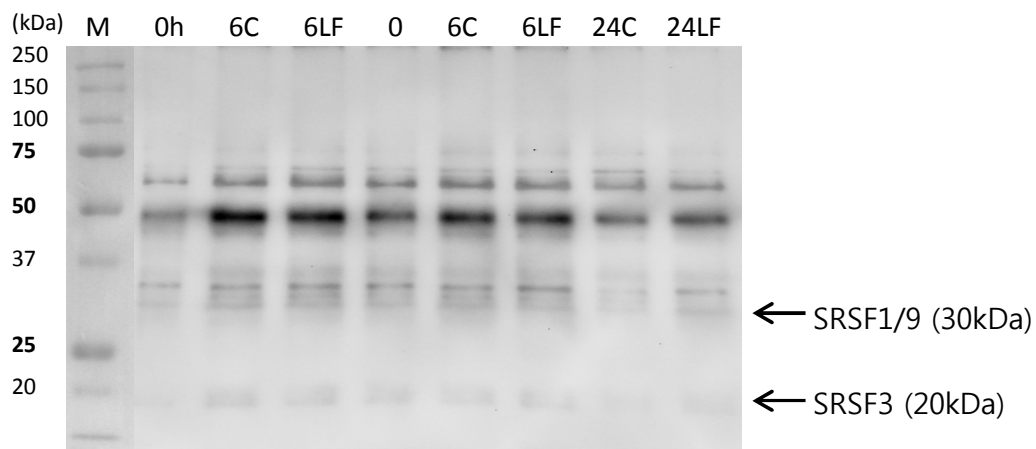
B **Anti-SR**
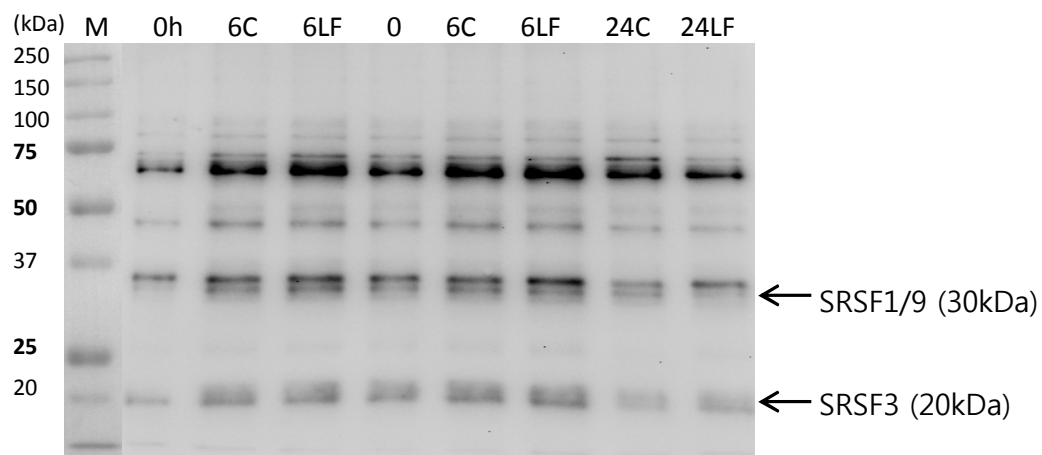
Figure 43 *Western blot for SR and phospho-SR proteins using purified phospho-proteins*

M means protein marker, h; hour, C; control, and LF; lumiflavin-treated. The numbers show incubation time. Western blot was performed using antibodies for anti-SR protein family and anti-phospho-SR proteins clone 1H4 in phosphoproteins which were used for iTRAQ.

A **SRSF1/9_30kDa**
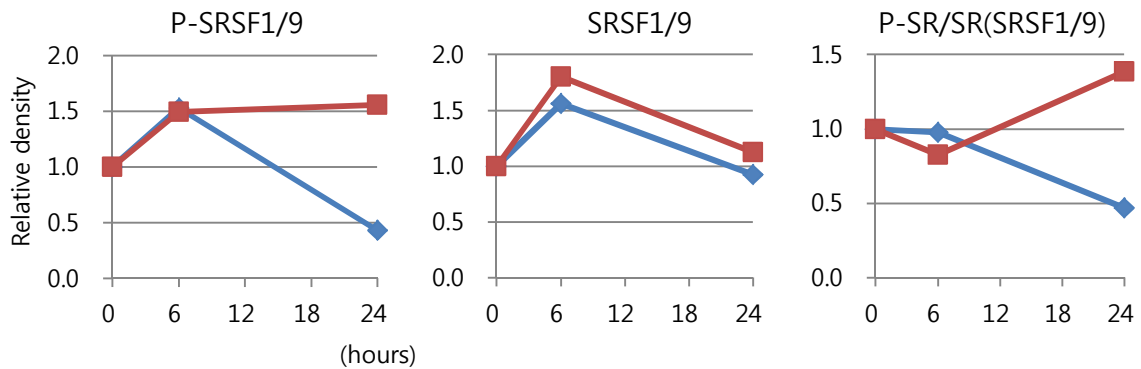
B **SRSF3_20kDa**
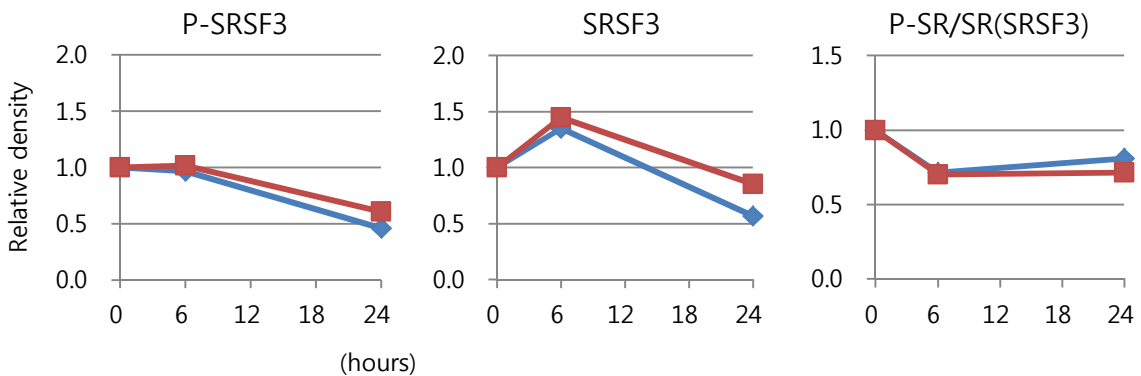
Figure 44 *Quantified western blot bands for phospho-SR protein and whole SR protein and the proportions of phospho-proteins using purified phospho-protein*

X axis shows incubation time (hours) and Y axis shows relative signal strength against 0 hour. Phosphoproteins which were used for iTRAQ were used for confirmation of iTRAQ data performed by western blot. Western blot was performed using antibodies for anti-SR protein family and anti-phospho-SR proteins clone 1H4. Signals were quantified by densitometry and the ratio of phospho-SR protein to total SR proteins was calculated.

5.4.7. Effect of lumiflavin on the cell cycle

Proteomic analysis revealed that lumiflavin treatment resulted in changes in gene expression pathways, particularly mRNA processing and the apoptosis pathway. Cell cycle analysis was performed to confirm these findings. Changes in mRNA processing in gene expression pathways may be associated with changes in the cell cycle. Also, cell cycle analysis allows an investigation of apoptotic cells and aneuploidy cells observed in Nakano's model (Nakano *et al.*, 2011). Thus, the effect of lumiflavin on each stage of the cell cycle in Caco-2 cells was investigated using two methods; HCA for the effect of short treatment up to 6 hours and flow cytometry for longer treatment up to 48 hours.

Figure 45 shows the percentage of cells in each stage of the cell cycle analysed by HCA. Lumiflavin led to a progressive reduction in cells in S phase in a time-dependent manner. Although not statistically significant, cells in G1 phase were slightly increased by 3 hours then decreased, while cells in G2 and above G2 phase were increased at 4 and 6 hours. In addition, it is known that apoptotic cells can be detected in sub G1 phase however there was no clear pattern in the time course.

Figure 46 shows the cell cycle data analysed by flow cytometry in Caco-2 cells treated with 40 μM lumiflavin for 6, 24 and 48 hours. A progressive decrease in cells in G1 phase by lumiflavin across all time points was observed (P=0.04 by one-way ANOVA). Duncan post-hoc analysis showed a significant reduction of cells in G1 phase at 48 hours compared to 0 and 6 hours. Two-way ANOVA showed that there was interaction effect between treatment and incubation time at only S phase (P=0.006). Analysis to determine the main effects, showed that the proportion of cells in S phase was significantly increased by lumiflavin treatment at 24 and 48 hours (P=0.006 by one-way ANOVA), and was also increased compared with time controls (P<0.05 by t-test). Lumiflavin led to a significant decrease of cells in G1 phase compared with the time control at 48 hours (P=0.001, t-test), while it resulted in an increase of cells in G2/M phase (P=0.014, t-test). There were no differences in sub G1, where apoptotic cells are detected. Slightly more polyploidy cells were found in lumiflavin-treated cells however, this did not reach statistical significance. In contrast to lumiflavin-treated cells, controlled cells showed no differences across incubation time in all phases, as analysed by one-way ANOVA. Taken together, the data suggests that lumiflavin impaired the progress of the cell cycle, leading to slow progression of the cell cycle, particularly in S phase.

In addition, the data from HCA showed a decrease of cells in S phase, whereas flow cytometry data showed no changes by lumiflavin treatment by 6 hours. However, due to missing of time-controls on HCA experimental set, there was limitation to interpreting the effect of lumiflavin itself on the cell cycle.
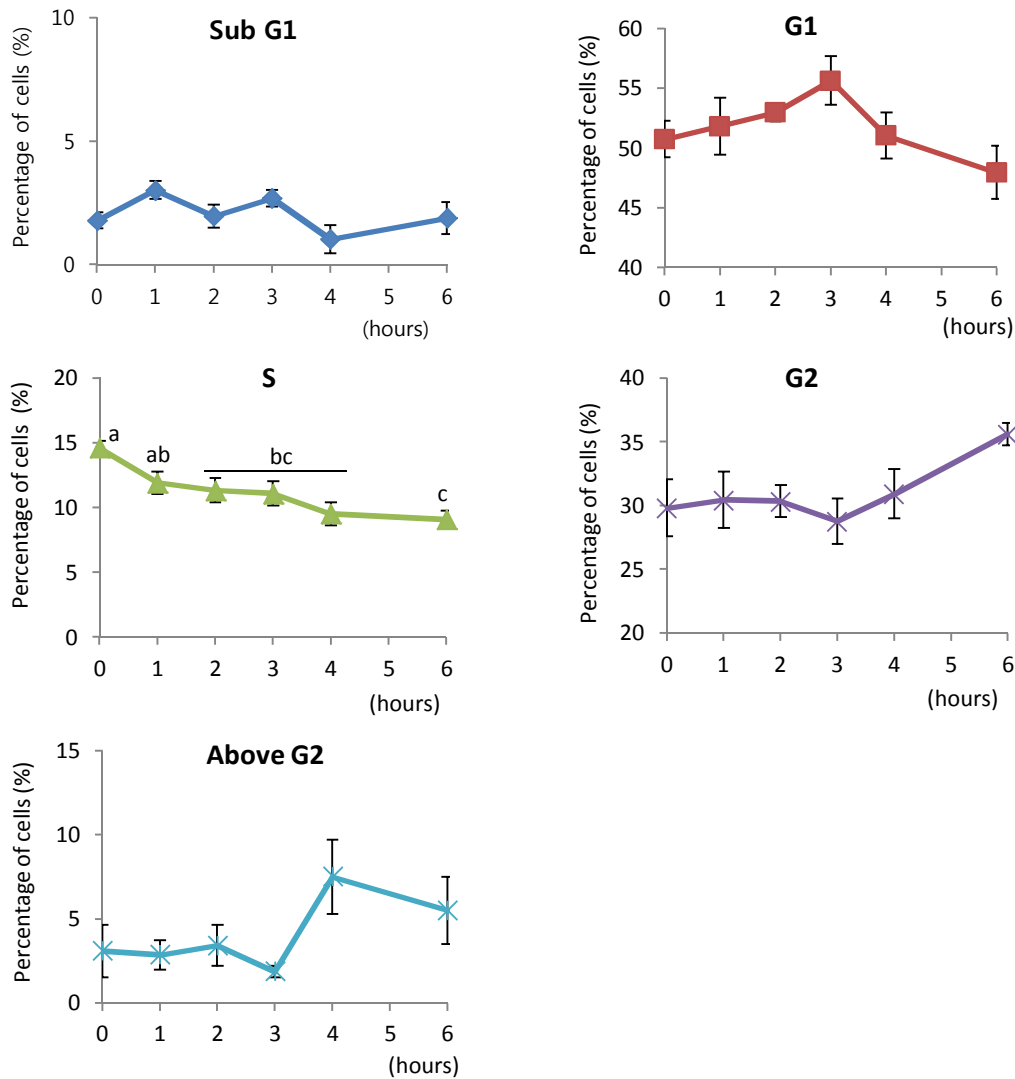
Figure 45 *Cell cycle analysis by HCA*

X axis shows hours, and Y axis shows percentage (%) of cells in each phase. Data are shown as mean (± SEM) from three wells of a single experiment. Percentage of cells in S phase were statistically significantly different over the time course (P=0.037, Kruskal-Wallis). Points not sharing the same letter were significantly different (P<0.05 by Duncan post-hoc using rank).
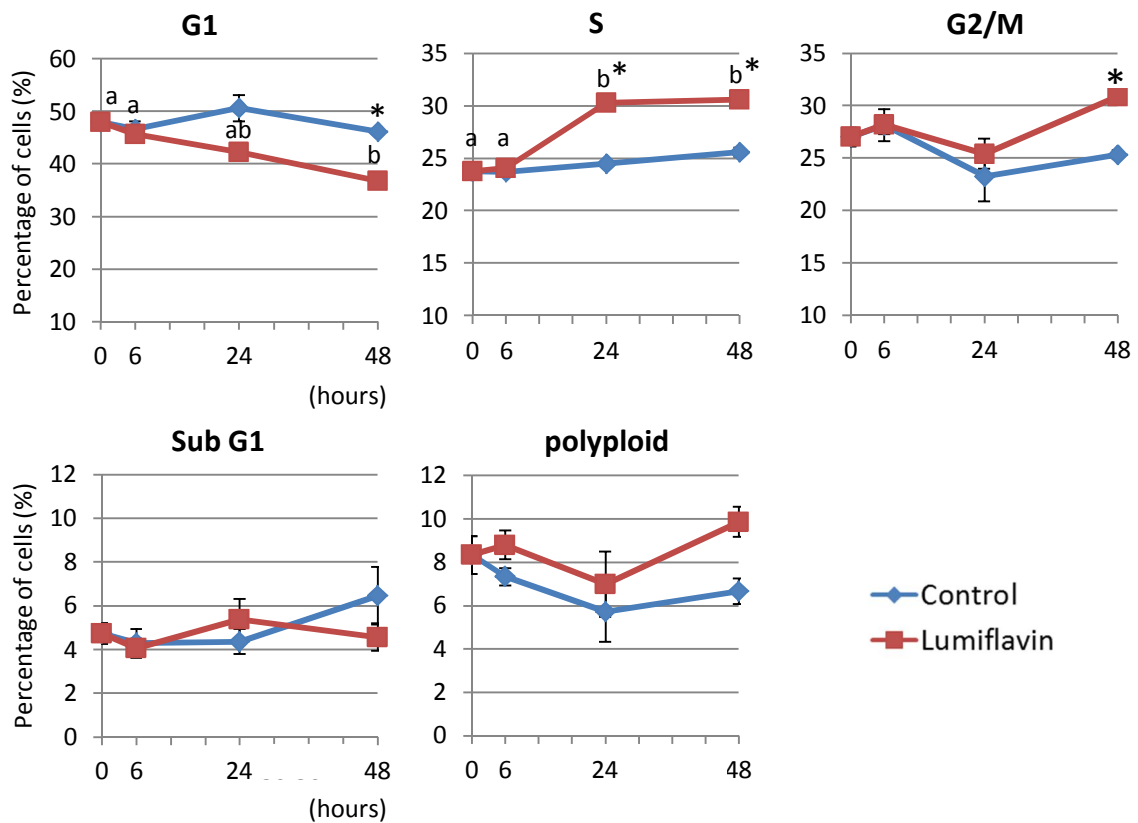
Figure 46 *Cell cycle analysis by flow cytometry*

X axis shows hours and Y axis, percentage (%) cells in each phase. Two-way ANOVA showed significant interaction between treatment and incubation time at only S phase (P=0.006). To determine main effects, it compared the differences between treatment at each time points by t-test and across incubation time in separated groups by one-way ANOVA. Asterisk Shows significant difference between control and lumiflavin at each time point by t-test (P=0.001 at G1, P<0.05 at S, P=0.014 at G2/M phase). Letters shows significant difference across time points (P=0.04 at G1, P=0.006 at S by one-way ANOVA). Points not sharing the same letter were significantly different (P<0.05 by Duncan post-hoc test).

5.5. Discussion

5.5.1. Effects of lumiflavin on global phosphorylation

Caco-2 cells exposed to 40μM lumiflavin were examined for global phosphorylation. There was a significant decrease in phosphorylation on tyrosine after only 3-6 hours of lumiflavin treatment, but there was no significant effect on global phospho-serine/threonine. Therefore, global phosphorylation results indicate a limited effect of lumiflavin-induced riboflavin depletion on cell signalling.

It was then required to investigate whether changes to global phosphorylation resulted from riboflavin depletion or from lumiflavin itself. Intracellular flavins concentrations in all the forms of riboflavin were not significantly changed by lumiflavin over a short time period; up to 24 hours. It suggests that such changes in global phosphorylation were not linked to riboflavin depletion induced by lumiflavin.

5.5.2. Effects of lumiflavin on phosphoprotein profile by iTRAQ

Caco-2 cells exposed to 40μM lumiflavin for 6 and 24 hours were examined for phosphoprotein profile. Phosphoproteins were purified and validated for successful purification of phosphoproteins and their intact integrity through various staining methods for phosphoproteins and western blotting.

Proteomic analysis allowed the identification of alterations in the phosphorylation of the 15 key proteins affected by lumiflavin treatment. These proteins were related to pathways of mRNA processing (splicing) on gene expression, protein synthesis or apoptosis that were significantly altered by exposure to lumiflavin. Top ranked proteins were related to pre-mRNA splicing, which were of the serine/arginine-rich splicing factor (SRSF) family showing higher fold change than 0 hour and also time-controls. In contrast, the fold change in control cells was decreased with time. This suggests that lumiflavin treatment led to delay or suppression of the process of pre-mRNA splicing, mRNA transcription and further protein synthesis, which is supported by the lower fold changes in proteins related to protein synthesis compared with

135

time controls. In addition, the fold change described here indicates changes in phosphoprotein level rather than changes in the level of phosphorylation. Furthermore, it has found that when all treatment groups were compared with 0 hour baseline, lumiflavin-treated cells had fewer phosphorylated proteins than time-controls, suggesting inhibitory effects of lumiflavin on pathways that are normally induced by riboflavin. In other words, in comparison with 0 hour baseline, more phosphoproteins were significantly different in the 24 hour control than in 24 hour lumiflavin treatment. This may be due to changes in cell growth and cell density thus increasing density of cell signalling transducers and accumulation of signalling events, thereby changing the proteome. For instance, an *in vitro* study reported that phosphorylation of signal transducers and activators of transcription 3 (STAT3), which is involved in cytokine signalling, was increased with cell density resulting in binding to DNA and activation of transcription thereby enhancing cell proliferation in melanoma cells (Kreis *et al.*, 2007).

Lumiflavin is thought to alter the regulation of apoptosis that should occur in riboflavin-rich condition through impaired phosphorylation of proteins related to apoptosis. For example, phosphorylation of 14-3-3 protein sigma (SFN, UniProt accession No. P31947) was inhibited by lumiflavin. 14-3-3 protein sigma promotes cell survival as it binds to BAD phosphorylated by AkT, disrupting the binding of BAD to Bcl2 thus inhibiting apoptosis (Datta *et al.*, 2000; Won *et al.*, 2003). High mobility group box 1 & 2 complex (HMGB1 and HMGB2 complex, UniProt accession No. P09429 & P26583) stimulates DNA cleavage in apoptosis pathway (Kalinowska-Herok and Widlak, 2008). Proteasome subunit beta type-7 (PSMB7, UniProt accession No. Q99436) is related to ATP-dependent trypsin-like proteolytic activity (Rho *et al.*, 2008). Lumiflavin led to maintain the phosphorylation of these proteins at the control level (0 hour), but they were decreased under control condition. This suggests that cells under normal condition were primed to undergo cell proliferation with suppression of apoptosis, whereas lumiflavin suppressed such normal responses of cells under riboflavin-rich condition. In other words, these findings may contribute to the observed inhibitory effect of lumiflavin on cell proliferation.

In an iTRAQ-based proteomic analysis using human prostate cancer cells, Glen *et al.* (2008) considered a 50% fold change (±0.50) as biologically significant in up or down regulation of proteins, to identify candidate proteins involved in prostate cancer progression and metastasis. We also showed a range of fold change from 0.34 to 1.54 (see Appendix 3). However, the cut-off fold change 50% may not be applicable to this study since extracted

phosphoproteins rather than entire proteins were used. There have been very few studies using iTRAQ for phosphoproteins extracted from Caco-2 or other colon-cancer cell lines, thus there was no available information on fold changes to be expected. However, since this study was designed to lead to modest effects of riboflavin depletion preceding biochemical dysfunctions, a moderate range of fold change was expected.

This study used only phosphoproteins for iTRAQ analysis which resulted in limited outcomes to changes in phosphorylation, however if whole proteins were used, more information would have been produced such as protein expression levels. To take into account this limitation, a validation analysis using western blot with phospho-SR and also total SR proteins was performed.

In addition, an alternative method of iTRAQ could have been 2D DIGE (difference gel electrophoresis) method followed by phosphorylated-protein expression profiling, where up to two different protein samples can be labelled separately and run in two-dimensional electrophoresis (Raggiaschi *et al.*, 2005).

There may be some potential off-target effects of lumiflavin. It is known that riboflavin in milk can be photodegraded to lumiflavin or lumichrome and the resultants catalyse the oxidation of lipids to lipid peroxides and methionine to methional which result in milk odour (Bender, 2003). It has not been studied influence of lumiflavin on oxidation of lipids from foetal calf serum in cell culture medium. Only a few studies have reported effects of irradiation of riboflavin-containing culture medium. In one such *in vitro* study, riboflavin-containing normal growth medium in µM concentrations was irradiated and used to culture leukaemia cells (de Souza *et al.*, 2006). They reported leukaemia cell-specific induction of apoptosis with activation of Fas cascade; Fas and FasL overexpression followed by activation of caspase 8 and mitochondrial amplification mechanisms, involving the stimulation of ceramide production. These cascades led to an inhibition of mitogen activated protein kinases: JNK, MEK and ERK and the survival mediators PKB and IAP1, and upregulation of cell cycle progression regulators such as p21. These effects of irradiated riboflavin were not found in normal human lymphocytes. However, their study did not consider the potential side-effects of undetermined materials produced by irradiation of riboflavin. Here, an alternative method to overcome potential confounding effect of lumiflavin and to confirm that the findings of this study are true effects on signalling via riboflavin transporter is the reduction of apical riboflavin

transporter expression by gene knockdown. It has been reported recently that mutation of cysteine residues, particularly on C463 and C467 of human riboflavin transporter-2 (hRFT-2) ablated riboflavin uptake (Subramanian *et al.*, 2011a). Their group also investigated effects of hRFT-2 gene-specific siRNA knockdown on intestinal riboflavin uptake driving the similar adverse effect on riboflavin uptake (Subramanian *et al.*, 2011b).

5.5.3. Effects of lumiflavin on SR proteins

Proteomic analysis showed that some of serine/arginine-rich splicing factor proteins were ranked as biggest effects of lumiflavin on the phosphorylated SR proteins, compared with control treatment. For this reason, SR proteins were selected to validate the findings of the proteomic analysis by probing SR proteins and their corresponding phospho-SR proteins using western blot. Difference between treatments on phosphorylation status of SR proteins against their corresponding SR proteins; SRSF5, SRSF1/9 and SRSF3 was not found in whole cell lysates. However, increased phosphorylation in SRSF1/9 detected at 30kDa by lumiflavin was found in purified phosphoproteins, in agreement with iTRAQ data. It is supposed because purification of phosphoprotein amplifies such significance.

Serine/arginine-rich splicing factor proteins family, called as SR protein, play an important role in alternative pre-mRNA splicing. Briefly, RNA splicing is a RNA-processing step during which the entire length of the gene, including exons and introns, is transcribed into RNA and intron sequences are removed from the long RNA by RNA splicing, producing much shorter RNA, and then RNA as mRNA directs the synthesis of a particular protein (Alberts, 2008). Alternative pre-mRNA splicing is an important process during RNA transcription and further synthesis of different proteins from the same gene. SR proteins are involved in constitutive and alternative RNA splicing (Shepard and Hertel, 2009).

The phosphorylation status of the SR proteins is key to the role in alternative pre-mRNA splicing (Shepard and Hertel, 2009). Phosphorylation enhances the ability of the SR protein, important for early steps of spliceosome assembly in the alternative splicing. Phosphorylation of the SR protein facilitates the recruitment of components of the spliceosome such as U1 small nuclear ribonucleoprotein (U1 snRNP) and U2AF35 to intronic splice sites, whilst dephosphorylation causes negative regulation of spliceosome assembly. Walsh *et al.* (2013) suggested the regulation of nutrients in alternative pre-mRNA splicing. Phosphorylation and also abundance of SRSF3 protein was increased in response to insulin and arachidonic acid

138

during culture of rat hepatomacytes in high glucose-containing medium. These changes were related to enhanced splicing and expression of glucose-6-phosphate dehydrogenase RNA.

However, this study is not able to identify target proteins of these SR proteins altered by lumiflavin treatment influence. From the proteomic analysis data, it is possible that alteration in SR protein may target apoptosis-related proteins which observed as significantly altered by lumiflavin treatment. Therefore, further study is required to investigate the association of SR proteins and proteins involved in apoptosis pathway.

5.5.4. Effects of lumiflavin on the cell cycle

Cell cycle analysis was performed to confirm the findings of proteomics analysis, in which exposure to lumiflavin resulted in an impairment in mRNA processing and apoptosis pathway, associated with progression of the cell cycle. In addition, aneuploidy cells observed in Nakano's model (Nakano *et al.*, 2011) and apoptotic cells were investigated by cell cycle analysis. Thus, the cell cycle was anlaysed in Caco-2 cells exposed to 40μM lumiflavin for a short period up to 6 hours and longer up to 48 hours by HCA and flow cytometry respectively. There is a limitation on interpretation due to missing of time-controls on HCA. However, when referred flow cytometry data up to 6 hours, we can suppose that lumiflavin was related to impaired progression of the cell cycle even only up to 6 hours. There was a progressive fall in S phase by lumiflavin treatment for up to 6 hours and cells in G2/M phase were slightly increased, suggesting impaired progression of S and G2/M phase.

Flow cytometry data revealed significant changes in cell cycle progression by longer exposure to lumiflavin. The proportion of cells in G1 phase was progressively decreased, but cells in S phase were accumulated by lumiflavin and a subsequent G2/M phase arrest.

These findings suggest that lumiflavin caused slow progression of the cell cycle particularly in S phase. According to literatures, it is possible that arrest of cells in S phase may be as a result of DNA damage, driving cells to apoptosis. Incompletely replicated DNA leads to cell arrest in S phase and delayed onset of mitosis (Alberts, 2008), and apoptosis can coincide with an accumulation of cells in S phase and a subsequent G2/M phase block in folate-deficient HepG2 liver cells (Huang *et al.*, 1999).

An increased proportion of cells in G2/M phase was observed in lumiflavin-treated cells at 48 hours, suggesting longer exposure of Caco-2 cells to lumiflavin led to impaired G2/M phase progression. However, further analysis is required to distinguish between arrest in G2 and M phase. Proteomic analysis found a decreased fold change of approximately 35% in histone H3 (UniProt accession No. K7EK07) at 24 hours exposure to lumiflavin compared with the time-control (Appendix 3, Appendix 6). Phosphorylated histone H3 is considered as a marker of mitosis, appearing at high levels in mitotic nuclei (Hendzel *et al.*, 1997; Tsuta *et al.*, 2011). Therefore, it can be suggested that the observed G2/M phase arrest is likely to be in G2 rather than in mitosis, however this requires further confirmation.

Such cell cycle arrest can result in physiologically important implications, in that the resultant impaired cell proliferation can decrease the renewal of tissues particularly the small intestine that depends on rapid cell proliferation (Heath, 1996).

5.6.   Summary

1. Lumiflavin led to small but significant fall in the global phosphorylation of tyrosine after only 3~6 hours.

2. Such changes occurred without a significant fall in intracellular flavins concentrations.

3. Proteomic analysis showed that lumiflavin may suppress phosphorylation of some proteins that should occur in riboflavin-rich condition. Also, it found that significant pathways altered by lumiflavin were related to gene expression particularly in mRNA processing and apoptosis pathway. The key 15 proteins were found, showing significant changes by exposure to lumiflavin.

4. On validation of the findings of proteomic analysis, there were no significant changes caused by exposure to lumiflavin on SR proteins and phospho-SR proteins in cell lysates. However changes on phospho-SRSF1 and 9 were found in purified phosphoproteins, which is consistent with the proteomic analysis.

5. Cell cycle analysis revealed that lumiflavin caused slow progression of the cell cycle particularly in S phase with progressive fall in cells in G1 across incubation time but increased cells in G2/M phase at 48 hours.

CHAPTER 6.

DISCUSSION AND CONCLUSION

6.1. Conclusions

It was hypothesised that lumiflavin leads to a depletion of flavins in intestinal cells associated with adverse functional effects and an interruption of the putative role of riboflavin as a signalling molecule in the regulation of intestinal cell proliferation. Investigation of the hypothesis entailed four elements of research; development of intestinal epithelial cell models of riboflavin depletion using lumiflavin; characterisation of the models; investigation of alterations in cell signalling in terms of candidate signalling pathways and related proteins; validation of findings in terms of SR proteins and the cell cycle. Three intestinal epithelial cell lines; Caco-2, HCT116 and HT29 were used for development and characterisation of the cell models, and Caco-2 cells were used for the signalling studies. The findings were as follows;.

1. Lumiflavin led to a rapid inhibition of cell growth in a concentration-dependent manner in all three cell lines exposed to lumiflavin over a concentration up to 100μM.
2. Exposure of three cell lines to 40 and 80μM lumiflavin led to a fall in intracellular riboflavin concentration but not in FMN and FAD concentrations, and an increase in GRAC, an indicator of functional riboflavin deficiency.
3. Riboflavin depletion induced by lumiflavin resulted in a reduction in intracellular ATP concentration and enhanced ROS production, suggesting disruption of energy generation and enhanced oxidative stress.
4. A cell-specific irreversible loss of clonogenicity was observed.
5. Such biochemical and cellular consequences of riboflavin depletion induced by lumiflavin were cell-specific. Overall, Caco-2 cells were relatively sensitive, whereas HT29 cells were more resistant to riboflavin depletion.
6. No effect of lumiflavin on apoptotic DNA fragmentation was found in any of the three cell lines.
7. 40μM lumiflavin in Caco-2 cells caused changes in the global phosphorylation of tyrosine at 3 and 6 hours, which is suggestive of an effect on cell signalling. Such changes preceded cellular riboflavin depletion.
8. Exposure of Caco-2 cell to 40μM lumiflavin led to a suppression in phosphorylation of some proteins, suggesting that lumiflavin interrupts cell signalling that occurs under conditions of riboflavin adequacy.

9. Exposure to lumiflavin led to an alteration in mRNA processing in gene expression pathway and apoptosis pathway, delaying or suppressing the process of pre-mRNA splicing, mRNA transcription and further protein synthesis and also stimulating apoptosis pathway which may contribute to observed effects on cell proliferation.

10. Phosphorylation of SRSF1/9 was consistent with the proteomics analysis data, validated in purified phosphoproteins.

11. Lumiflavin resulted in accumulation of cells in S phase with subsequent G2/M phase arrest.

6.2. Discussion

Caco-2 and HT29 cell lines were chosen to develop intestinal cell models of riboflavin depletion in order to study roles of riboflavin on cell proliferation and HCT116 was used for the comparison with the two cell lines. Caco-2 and HT29 cell lines are considered to be useful models of human small intestinal epithelial cell function. Recently Christensen et al. (2012) concluded that Caco-2 cells are the most suitable *in vitro* model for oral drug absorption, following *in vitro* model HT29 cells. They are the most similar to small intestinal enterocytes with respect to expression of transporters important to absorptive function. Also, the most dominant gene expression profile in differentiated Caco-2 and HT29 cells was similar to that of normal small intestinal epithelium. Such similarities were greater in differentiated Caco-2 and HT29 than other colon cancer-derived cell lines including HCT116, HCT15 and SW620. Indeed, the Caco-2 cell line is the most frequently used cell line as a model of small intestinal cell function (Said and Ma, 1994; Zielinska-Dawidziak *et al.*, 2008; Subramanian *et al.*, 2011b), and the HT29 cell lines has been suggested as a useful alternative cell model to Caco-2 (Collett *et al.*, 1996).

Considering the available evidence it was decided that undifferentiated Caco-2 and HT29 cells would provide useful alternative cell models to normal small intestinal cells. Undifferentiated state of the cell lines is on proliferative status implying the different regulation from differentiation. In addition, we have reported the consistent results of intracellular flavins concentration with an *in vitro* study used differentiated Caco-2 monolayer exposed to lumiflavin (Said and Ma, 1994) mentioned in section 3.5.1. This suggests that undifferentiated Caco-2 cells may also show the similar effects on riboflavin uptake with differentiated Caco-2

cellls. Finally, the cell lines present several advantages such as availability, proliferability, homogeneity and reproducibility (Bourgine *et al.*, 2012).

However, it must be noted that undifferentiated Caco-2 and HT29 cell lines are not fully representative of the normal small intestinal epithelium. There have been inconsistent similarities on gene expression among differentiated and undifferentiated Caco-2 and HT29 cells and normal small intestinal epithelium. Christensen et al.(2012) performed principal component analysis of gene expression data with human colon cell lines, laser-dissected tissues of normal human colonocytes, tumour cells and small intestinal enterocytes. Undifferentiated Caco-2 and HT29 were less similar to normal small intestinal enterocytes in most dominant gene expression but closer to HCT116 which was most different from small intestinal enterocytes. In contrast, Tremblay *et al.*(2006) showed the inconsistency between differentiated and undifferentiated Caco-2 cells on some particular gene expression involved in cell proliferation. For instance, cell division cycle 34 showed the similar expression between undifferentiated and differentiated Caco-2 cells, however BRCA2 and CDKN1A interacting protein (TOK1) showed different expression.

Taken together, undifferentiated Caco-2 and HT29 cell lines would be useful cell models for this study, however there is a limitation which they are not fully representative of the normal small intestinal epithelium particularly in that they may show the difference on gene expression.

We compared these three cell lines in terms of their response to lumiflavin treatment and riboflavin depletion. The effects of riboflavin depletion induced by lumiflavin were different between the three cell lines. The effects on clonogenicity, ROS production and ATP concentration were the most pronounced in Caco-2 cells and least so in HT29 cells. This may reflect differences in functional riboflavin depletion (elevated GRAC) and in the efficiency of uptake of riboflavin.. While Caco-2 cells showed the greatest change in GRAC by lumiflavin and the lowest concentration of intracellular riboflavin, HT29 cells were the most resistant to lumiflavin. HT29 cells maintained GRAC in the range of non-functional deficiency under lumiflavin treatment and furthermore the cells possessed the highest intracellular riboflavin concentration, implying less vulnerability to riboflavin deficiency. Additionally, Caco-2 cells produced more ROS than the other two cell lines under normal conditions, suggestive of cell-specific differences for ROS requirement for ordinary cell signal transduction. As mentioned in section 4.5.2, ROS play an important role as signal transporters for the regulation of cell cycle progression, as suggested by Scaife's study (2004). ROS production was inhibited using the

flavoprotein-specific inhibitor, DPI in *in vitro* models, and this led to cell cycle arrest in G2 phase thereby inhibiting cell proliferation. Taken together, this study suggests that Caco-2 cells are the most appropriate tool for studying the role of riboflavin on intestinal cell proliferation.

Effects of lumiflavin on cell growth were rapid and marked in all three cell lines, with a clear dose response, even though lumiflavin resulted in modest intracellular flavin depletion and a decline in functional flavins status. In spite of the modest riboflavin depletion, lumiflavin resulted in a more pronounced decrease in clonogenicity than that shown after 72 hours of growth of Caco-2 cells in a riboflavin-depleted medium in Nakano's model (Nakano *et al.*, 2011). These findings suggest that lumiflavin competed effectively for sites on the riboflavin transporter, hence resulting in effective interruption of cell proliferation with appearance of more rapid inhibition of cell proliferation than growth in a riboflavin-deficient medium alone.

Exposure of cells to lumiflavin influenced flavin homeostasis. While intracellular riboflavin concentration was decreased by lumiflavin, an observed gradual decrease in mean FAD concentration did not reach statistical significance, and intracellular FMN concentrations were unchanged by exposure to lumiflavin in all three cell lines. This result is consistent with our previous study in Caco-2 cells grown in riboflavin-depleted medium, in which FMN concentrations were maintained at control values within the same duration of treatment (Nakano *et al.*, 2011). The maintenance of FMN concentration in our model may be related to the observed reduction in intracellular ATP concentration in response to lumiflavin. It has been reported that riboflavin depletion leads to a decreased expression of mRNA for both riboflavin kinase and FAD synthetase in HepG2 cells (Werner *et al.*, 2005) and a reduction in activities of both enzymes was observed in the liver of riboflavin-deficient rats (Lee and McCormick, 1983). Both enzymes are ATP-dependent, however riboflavin kinase has a K_m about 20-fold lower than that for FAD synthetase. This indicates a strong affinity of riboflavin kinase for ATP substrate and thus relative insensitivity to changes in intracellular ATP status. The disruption of ATP conservation in our lumiflavin-based model of riboflavin depletion may have compromised activity of FAD synthetase, whilst having less effect on riboflavin kinase. This would have maintained the FMN concentration.

Riboflavin depletion induced by lumiflavin compromised antioxidant status. In this study, GRAC was significantly increased by exposure to lumiflavin, reflecting a decreased activity of glutathione reductase due to a compromised supply of FAD to the enzyme. This would limit

the production of the antioxidant glutathione. FAD-dependent glutathione reductase is an important enzyme in the glutathione redox cycle, producing a reduced glutathione, which is an endogenous antioxidant. *In vitro* studies used hepatoma cancer cells showed that riboflavin deficiency led to a decrease in activity of glutathione reductase, reflecting a decrease in reduced glutathione content, and an increase in carbonylated protein, the product of oxidative damage in proteins, and DNA strand breaks (Manthey *et al.*, 2005; 2006). Furthermore, an *in vitro* study reported that enhanced oxidative stress also affects activity and mRNA expression of glutathione reductase, diminishing an anti-apoptotic role against oxidative stress (Kim *et al.*, 2010). Exposure of human hepatoma cells to hydrogen peroxide (H_2O_2) resulted in a fall in activity and mRNA expression of glutathione reductase. This led to a decrease in reduced glutathione status, measured as a fall in the ratio of GSH/GSSG and a decrease in total GSH content. There was an associated increased incidence of apoptosis with an increased activity of caspase-3. However, induction of overexpression of glutathione reductase restored these apoptotic changes in cell viability, ROS level, total GSH content, caspase-3 activity and the proportion of apoptotic cells.

Exposure to lumiflavin led to an enhanced production of ROS in all cell types, which may have contributed to arrest of cells in S phase and thus the observed effect on cell proliferation. As described, excessive ROS production can induce oxidative damage to cellular substrates, including DNA, and impair cell cycle checkpoint function to prevent replication of damaged DNA, thus allowing additional time for DNA repair namely arrest of the cell cycle in S phase (Shackelford *et al.*, 2000). Indeed, this study found that lumiflavin led to arrest of cells in S phase with subsequent G2/M phase arrest.

Dysregulation of control over the cell cycle, whenever or wherever acquired in foetal and early neonatal life or adulthood, is likely to be strongly associated with developmental or differentiating defects in certain tissues including the GI tract. Previous studies have produced evidence that riboflavin depletion leads to abnormal development of the GI track and that this may be modulated by aberrant mitosis of its cells. In a rat model of riboflavin deficiency during the postnatal period, crypt hypertrophy and decreased proliferation were observed in the small intestine, implying a failure to secure normal development of the villus (Powers, 2003; Williams *et al.*, 1995; Yates *et al.*, 2001). Furthermore, a more recent study found fewer crypt cell divisions with significantly shorter and less cellular crypts in the colon of adult gastroscopy patients with low riboflavin status, compared with normal controls (Nakano *et al.*, 2011). In the subsequent *in vitro* study using Caco-2 cells, riboflavin deficiency led to inhibition of cell

proliferation by the arrest of cell cycle in mitosis and a significant increase in the proportion of aneuploid cells, with alterations in genes involved in the regulation of mitosis.

A difference in effects on the cell cycle between this model and Nakano's cell model was found. S phase arrest was observed in this lumiflavin-induced riboflavin depletion model but arrest in mitosis was observed in Nakano's model (Nakano *et al.*, 2011). However, it may be unwise to make a direct comparison of the two models because of the very different protocols used to achieve riboflavin deficiency and differences in the degree of riboflavin deficiency. This lumiflavin-based model resulted in modest riboflavin depletion within the shorter period; only 72 hours, compared with Nakano's model. Nakano *et al.* (2011) used a protocol of culturing cells with a gradual depletion from medium with physiological level of riboflavin to riboflavin-free medium for approximately 10 days. The prolonged depletion of riboflavin induced severe degree of riboflavin deficiency meaning significantly falls in the concentrations of FAD and FMN; approximately 80% fall in intracellular FMN concentration and approximately 50% fall in intracellular FAD concentration. Therefore, the different effects on the cell cycle between the two models may be caused from the different degrees of riboflavin deficiency achieved.

This study found changes in phosphorylation of proteins through determination of global phosphorylated amino acid residues and phosphoprotein profiling by proteomic analysis. Such changes were not linked to riboflavin depletion. Lumiflavin is known to inhibit the uptake of riboflavin into cells by competing for sites on the riboflavin transporter (Said and Ma, 1994; Fujimura *et al.*, 2010). Therefore, in this cell signalling study, the term 'riboflavin depletion induced by lumiflavin' actually means obstruction of lumiflavin in the role of riboflavin itself rather than exhausting flavins pool.

Phosphoproteomic analysis revealed that lumiflavin may suppress cell signalling pathways that normally occur in riboflavin-rich condition. Pathways that significantly altered by lumiflavin were gene expression pathway particularly in mRNA processing and apoptosis pathway. Exposure to lumiflavin led to sustained phosphorylation in some of serine/arginine-rich splicing factor proteins family (the SR protein).

According to literatures, observed changes in the SR protein may be related to regulation of the cell cycle and apoptosis. Recent studies suggested that alternative splicing network is closely related to from cell cycle control to apoptosis. An in vitro study reported that SRSF1 downregulation or knockout promoted proapoptotic splicing of pre-mRNAs of Bcl2

family; Bcl-x, Mcl1 and caspase-9, and SRSF1 directly binds to mRNAs of these proteins and regulates expression (Moore *et al.*, 2010). Another showed that SRSF3 played an important role in the regulation of G1 to S phase progression and apoptosis through association with Bcl2 in HCT116 colon cancer cells (Kurokawa *et al.*, 2014). HCT116 cells were treated with siRNA for SRSF3 for 24 hours, synchronised in the G1 phase by serum starvation for the next 48 hours, and then stimulated with 10% FCS for 24 hours. SRSF3 knockdown reduced mRNA and protein levels of G1/S checkpoint such as cyclins (D1, D3 and E1), E2F1 and E2F7, and led to hypophosphorylation of retinoblastoma protein (Rb), thereby resulting in G1 phase arrest and an increase in apoptotic cells. Rb is a tumour suppressor protein, inhibiting progression of G1/S transit when dephosphorylated by cyclin-dependent kinases (CDKs) which consisted of cyclin D and E. When Rb is dephosphorylated, it binds to E2F and restricts the function of E2F complex on G1/S transit. Also, they showed that siRNA knockdown for SRSF3 for 24, 48 and 72 hours led to a time-dependent increase in apoptotic cells with a reduction in expression of Bcl-2.

Exposure of Caco-2 cells to lumiflavin led to a change in the cell cycle. An increased proportion of cells in S phase were observed in Caco-2 cells exposed to lumiflavin with subsequent accumulation of cells in G2/M phase. Therefore iTRAQ analysis might be expected to produce changes in phosphorylation of DNA damage/repair-linked proteins or proteins involved in S phase progression. For instance, CDK2 (cyclin-dependent kinase) acts at the G1/S transition and also in DNA replication and transition from S phase to G2/M phase. CDK2 regulates early and late stage of DNA replication by interacting with cyclin E and cyclin A to permit G1/S transition and to regulate S phase (De Boer *et al.*, 2008; Flores *et al.*, 2010). CDK2 activity is changed during S and G2 phase by phosphorylation and dephosphorylation on different sites (Gu *et al.*, 1992). CDK2 phosphorylates some proteins in response to DNA damage for instance BRCA2, p53 and so on. CDK2 phosphorylates the carboxy-terminal region of BRCA2, where the essential recombination protein RAD51 directly interacts, and blocks the interactions between BRCA2 and RAD51 (Esashi *et al.*, 2005). DNA damage stimulates dephosphorylation of BRCA2 and increasing interactions with RAD51 which binds to single and double-stranded DNA and initiates DNA strand exchange (Baumann *et al.*, 1996). CDK2 is also required for p53-independent G2/M checkpoint activation by balancing S phase regulatory proteins such as Cdc6 (cell division control protein 6) (Chung and Bunz, 2010). Cdc6 acts in the initiation of DNA replication and is associated with the DNA damage sensor ATR

(serine/threonine-protein kinase ATR (Ataxia telangiectasia and Rad3-related protein)) to control completion of DNA replication before initiation of mitosis. (Ayad, 2005).

Unfortunately, the proteomic analysis in this study revealed no significant pathways in which such proteins are involved. This may be due to insufficient exposure time to lumiflavin to emerge accumulated effects on changes in such proteins, thus it requires further study using longer time periods.

However, significant changes in various types of histones were observed in this study. Fewer phosphorylated histone proteins were found in lumiflavin-treated cells compared with time-controls; Histone H2, H3 and H4 (HIST1H2BH, UniProt accession No. Q93079; HIST1H2AJ, UniProt accession No. Q99878; H3F3B, UniProt accession No. K7EK07; HIST1H4A, UniProt accession No. P62805). Purposes of phosphorylation of histone are histone deposition and chromatin decondensation during S phase and chromatin condensation during mitosis. Thus, phosphorylation of histones may be induced in response to DNA damage for DNA repair (Banerjee and Chakravarti, 2011). In this study, histone H4 showed approximately 40% lower fold change by lumiflavin compared with time-control. The fold changes of histone H4 were increased by time in control conditions, but not changed by lumiflavin. This suggests that phosphorylation of histone H4 may naturally occur in riboflavin-rich condition and lumiflavin may suppress the normal response. DNA breaks can be formed in normal conditions by endogenous ROS that are produced as a result of metabolic processes (Podhorecka *et al.*, 2010). Approximately 99% of DNA breaks are repaired, whilst approximately 1% of DNA breaks become DNA double-strand breaks (DSBs) during DNA replication, which is the most dangerous type of DNA damage resulting in severe consequences for chromosome aberrations, genomic instability and severe clinical implications such as cancer. A study using yeast has reported that phosphorylation on Ser1 of histone H4 occurs for the repair of DNA damage independent of cell-cycle stage (Cheung *et al.*, 2005). This modification has been found in mammals as well (Banerjee and Chakravarti, 2011). DNA damage stimulates casein kinase II (CK II) leading to phosphorylation on Ser1 of histone H4 (H4S1) in regions close to double-strand breaks (Cheung *et al.*, 2005). Rossetto *et al* (2012) suggested that phosphorylation of H4S1 may act to stabilise nucleosomes that are newly reassembled during restoration of chromatin structure by preventing the acetylation of the histone H4 tail by the NuA4 HAT. However, this study revealed no information of phosphorylation sites on peptide sequences so it is not clear whether the observed changes in histone H4 is derived from phosphorylation of the specific site Serine 1 of histone H4.

Apoptotic DNA fragment, which is a key feature of apoptosis, was not found in cells exposed to lumiflavin. However, phosphoproteomic analysis revealed that apoptosis pathway was significantly altered by exposure to lumiflavin with changes in the related genes. As described, DNA fragmentation is a late event during apoptosis, therefore further study may confirm the finding through investigation of early changes represented as a predictor of apoptosis such as caspases (McIlwain *et al.*, 2013).

In conclusion, results were compatible with the first two hypotheses in that exposing intestinal cells to lumiflavin resulted in riboflavin depletion and functional riboflavin deficiency. Also, lumiflavin-treated, thus flavin-depleted, cells showed cellular and biochemical dysfunction associated with a reduced capacity to generate energy, a reduced antioxidant status and enhanced production of ROS. Lumiflavin-induced changes in cell signalling included modest changes in global phosphorylation. No specific candidate pathways were identified, however we found that lumiflavin induced suppression of normal cell signalling of riboflavin-rich condition, induction of apoptosis pathway and changes in mRNA processing.

6.3. Limitations

1. An attempt was made to measure FAD-dependent succinate dehydrogenase activity, in order to strengthen the finding that exposure to lumiflavin disrupted ATP generation. However this proved unsuccessful and an alternative protocol needs to be developed. For example, determination of substrate or products of succinate dehydrogenase; succinate or furmarate may be useful.

2. A comparison of response to lumiflavin between the cell lines in terms of phosphorylation using western blot and proteomic analysis could not be made because of cost limitations. HT29 cells which were resistant to lumiflavin could behave differently from Caco-2 cells used for signalling study.

3. Phosphoprotein profiling by iTRAQ in cells exposed to lumiflavin for 24 hours and time-control was determined in a single experiment, due to limitations of cost and number of labelling. Determination in replicate would increase reliability of results.

6.4. Future work

In order to build on the finding of the results described in this study, the following studies are proposed.

1. Early events in apoptosis should be measured to determine effects of exposure to lumiflavin in the apoptosis pathway, despite a lack of evidence for DNA fragmentation. For example, determination of caspases may be useful.

2. Determination of mitosis-specific markers could reveal a distinct effect of exposure to lumiflavin on mitosis. Cell cycle data using flow cytometry provided the combined proportion of cells in both G2 and mitosis phase. For example, phosphorylated histone H3 (pHH3) is widely used as a mitosis marker.

3. Total protein profiling using proteomic analysis might reveal effects of exposure to lumiflavin on SR protein and gene expression of certain proteins which may be consequently regulated through aberrant phosphorylation in SR proteins.

4. Investigation of apoptosis-related proteins in cells exposed to lumiflavin and induced for overexpression of SR protein may reveal the association.

REFERENCES

Adams, R. R., Carmena, M. &Earnshaw, W. C. (2001). Chromosomal passengers and the (aurora) ABCs of mitosis. *Trends in Cell Biology* 11(2): 49-54.

Ainiwaer, J., Tuerhong, A., Hasim, A., Chengsong, D., Liwei, Z. &Sheyhidin, I. (2013). Association of the plasma riboflavin levels and riboflavin transporter (C20orf54) gene statuses in Kazak esophageal squamous cell carcinoma patients. *Molecular Biology Reports* 40(5): 3769-3775.

Alberts, B. (2008). *Molecular biology of the cell.* New York: Garland Science.

Alcantara Torres, M., Rodriguez Merlo, R., Repiso Ortega, A., de Lucas Veguillas, A., Valle Munoz, J., Sanchez Simon, R. &Martinez Potenciano, J. L. (2005). DNA aneuploidy in colorectal adenomas. Role in the adenoma-carcinoma sequence. *Revista Espanola de Enfermedades Digestivas* 97(1): 7-15.

Arachchige Don, A. S., Dallapiazza, R. F., Bennin, D. A., Brake, T., Cowan, C. E. &Horne, M. C. (2006). Cyclin G2 is a centrosome-associated nucleocytoplasmic shuttling protein that influences microtubule stability and induces a p53-dependent cell cycle arrest. *Experimental Cell Research* 312(20): 4181-4204.

Ashoori, M. &Saedisomeolia, A. (2014). Riboflavin (vitamin B2) and oxidative stress: a review. *The British Journal of Nutrition*: 1-7.

Ayad, N. G. (2005). CDKs give Cdc6 a license to drive into S phase. *Cell* 122(6): 825-827.

Banerjee, T. &Chakravarti, D. (2011). A peek into the complex realm of histone phosphorylation. *Molecular and Cellular Biology* 31(24): 4858-4873.

Bar-Meir, M., Elpeleg, O. N. &Saada, A. (2001). Effect of various agents on adenosine triphosphate synthesis in mitochondrial complex I deficiency. *The Journal of Pediatrics* 139(6): 868-870.

Bates, B., Lennox, A., Prentice, A., Bates, C. &Swan, G. (2011).National Diet and Nutrition Survey:Headline results from Years 1, 2 and 3 (Combined) of the Rolling Programme (2008/2009-2010/11). Department of Health
The Food Standards Agency.

Bates, C. J. &Fuller, N. J. (1986). The effect of riboflavin deficiency on methylenetetrahydrofolate reductase (NADPH) (EC 1.5.1.20) and folate metabolism in the rat. *The British Journal of Nutrition* 55(2): 455-464.

Bates, C. J., Prentice, A., Cole, T. J., van der Pols, J. C., Doyle, W., Finch, S., Smithers, G. &Clarke, P. C. (1999). Micronutrients: highlights and research challenges from the 1994-5 National Diet and Nutrition Survey of people aged 65 years and over. *The British Journal of Nutrition* 82(1): 7-15.

Bates, C. J., Prentice, A. M., Paul, A. A., Prentice, A., Sutcliffe, B. A. &Whitehead, R. G. (1982). Riboflavin status in infants born in rural Gambia, and the effect of a weaning food supplement. *Transactions of the Royal Society of Tropical Medicine and Hygiene* 76(2): 253-258.

Baumann, P., Benson, F. E. &West, S. C. (1996). Human Rad51 protein promotes ATP-dependent homologous pairing and strand transfer reactions in vitro. *Cell* 87(4): 757-766.

Bender, D. A. (2003). *Nutritional biochemistry of the vitamins.* Cambridge, UK ; New York, N.Y.: Cambridge University Press.

Beutler, E. (1969). Effect of flavin compounds on glutathione reductase activity: in vivo and in vitro studies. *The Journal of Clinical Investigation* 48(10): 1957-1966.

Blot, W. J., Li, J. Y., Taylor, P. R., Guo, W., Dawsey, S., Wang, G. Q., Yang, C. S., Zheng, S. F., Gail, M., Li, G. Y. &et al. (1993). Nutrition intervention trials in Linxian, China: supplementation with specific vitamin/mineral combinations, cancer incidence, and disease-specific mortality in the general population. *Journal of the National Cancer Institute* 85(18): 1483-1492.

Bodiga, V. L., Bodiga, S., Surampudi, S., Boindala, S., Putcha, U., Nagalla, B., Subramaniam, K. &Manchala, R. (2012). Effect of vitamin supplementation on cisplatin-induced intestinal epithelial cell apoptosis in Wistar/NIN rats. *Nutrition* 28(5): 572-580.

Bohnsack, B. L. &Hirschi, K. K. (2004). Nutrient regulation of cell cycle progression. *Annual Review of Nutrition* 24: 433-453.

Bortner, C. D., Oldenburg, N. B. &Cidlowski, J. A. (1995). The role of DNA fragmentation in apoptosis. *Trends in Cell Biology* 5(1): 21-26.

Bourgine, J., Billaut-Laden, I., Happillon, M., Lo-Guidice, J. M., Maunoury, V., Imbenotte, M. &Broly, F. (2012). Gene expression profiling of systems involved in the metabolism and the disposition of xenobiotics: comparison between human

intestinal biopsy samples and colon cell lines. *Drug Metabolism and Disposition: The biological fate of chemicals* 40(4): 694-705.

Burch, H. B., Lowry, O. H., Bradley, M. E. &Max, P. F., Jr. (1970). Hepatic metabolites and cofactors in riboflavin deficiency and calorie restriction. *The American Journal of Physiology* 219(2): 409-415.

Camporeale, G. &Zempleni, J. (2003). Oxidative folding of interleukin-2 is impaired in flavin-deficient jurkat cells, causing intracellular accumulation of interleukin-2 and increased expression of stress response genes. *Journal of Nutrition* 133(3): 668-672.

Capo-chichi, C. D., Gueant, J. L., Feillet, F., Namour, F. &Vidailhet, M. (2000). Analysis of riboflavin and riboflavin cofactor levels in plasma by high-performance liquid chromatography. *Journal of Chromatography. B, Biomedical Sciences and Applications* 739(1): 219-224.

Cheung, W. L., Turner, F. B., Krishnamoorthy, T., Wolner, B., Ahn, S. H., Foley, M., Dorsey, J. A., Peterson, C. L., Berger, S. L. &Allis, C. D. (2005). Phosphorylation of histone H4 serine 1 during DNA damage requires casein kinase II in S. cerevisiae. *Current biology : CB* 15(7): 656-660.

Christensen, J., El-Gebali, S., Natoli, M., Sengstag, T., Delorenzi, M., Bentz, S., Bouzourene, H., Rumbo, M., Felsani, A., Siissalo, S., Hirvonen, J., Vila, M. R., Saletti, P., Aguet, M. &Anderle, P. (2012). Defining new criteria for selection of cell-based intestinal models using publicly available databases. *BMC genomics* 13: 274.

Chung, J. H. &Bunz, F. (2010). Cdk2 is required for p53-independent G2/M checkpoint control. *PLoS genetics* 6(2): e1000863.

Circu, M. L. &Aw, T. Y. (2010). Reactive oxygen species, cellular redox systems, and apoptosis. *Free Radical Biology & Medicine* 48(6): 749-762.

Cohen, P. (2001). The role of protein phosphorylation in human health and disease. The Sir Hans Krebs Medal Lecture. *European Journal of Biochemistry / FEBS* 268(19): 5001-5010.

Collett, A., Sims, E., Walker, D., He, Y. L., Ayrton, J., Rowland, M. &Warhurst, G. (1996). Comparison of HT29-18-C1 and Caco-2 cell lines as models for studying intestinal paracellular drug absorption. *Pharmaceutical Research* 13(2): 216-221.

Collins, J. A., Schandl, C. A., Young, K. K., Vesely, J. &Willingham, M. C. (1997). Major DNA fragmentation is a late event in apoptosis. *The Journal of Histochemistry and Cytochemistry : Official Journal of the Histochemistry Society* 45(7): 923-934.

Crosio, C., Fimia, G. M., Loury, R., Kimura, M., Okano, Y., Zhou, H., Sen, S., Allis, C. D. &Sassone-Corsi, P. (2002). Mitotic phosphorylation of histone H3: spatio-temporal regulation by mammalian Aurora kinases. *Molecular and Cellular Biolology* 22(3): 874-885.

Crott, J. W., Liu, Z., Keyes, M. K., Choi, S. W., Jang, H., Moyer, M. P. &Mason, J. B. (2008). Moderate folate depletion modulates the expression of selected genes involved in cell cycle, intracellular signaling and folate uptake in human colonic epithelial cell lines. *The Journal of Nutrirional Biochemistry* 19(5): 328-335.

Dahly, E. M., Guo, Z. &Ney, D. M. (2002). Alterations in enterocyte proliferation and apoptosis accompany TPN-induced mucosal hypoplasia and IGF-I-induced hyperplasia in rats. *Journal of Nutrition* 132(7): 2010-2014.

Datta, S. R., Katsov, A., Hu, L., Petros, A., Fesik, S. W., Yaffe, M. B. &Greenberg, M. E. (2000). 14-3-3 proteins and survival kinases cooperate to inactivate BAD by BH3 domain phosphorylation. *Molecular Cell* 6(1): 41-51.

De Boer, L., Oakes, V., Beamish, H., Giles, N., Stevens, F., Somodevilla-Torres, M., Desouza, C. &Gabrielli, B. (2008). Cyclin A/cdk2 coordinates centrosomal and nuclear mitotic events. *Oncogene* 27(31): 4261-4268.

de Santa Barbara, P., van den Brink, G. R. &Roberts, D. J. (2003). Development and differentiation of the intestinal epithelium. *Cellular and Molecular Life Sciences* 60(7): 1322-1332.

de Souza, A. C., Kodach, L., Gadelha, F. R., Bos, C. L., Cavagis, A. D., Aoyama, H., Peppelenbosch, M. P. &Ferreira, C. V. (2006). A promising action of riboflavin as a mediator of leukaemia cell death. *Apoptosis: An international journal on programmed cell death* 11(10): 1761-1771.

de Vogel, S., Dindore, V., van Engeland, M., Goldbohm, R. A., van den Brandt, P. A. &Weijenberg, M. P. (2008). Dietary folate, methionine, riboflavin, and vitamin B-6 and risk of sporadic colorectal cancer. *Journal of Nutrition* 138(12): 2372-2378.

do Carmo Avides, M. &Glover, D. M. (1999). Abnormal spindle protein, Asp, and the integrity of mitotic centrosomal microtubule organizing centers. *Science* 283(5408): 1733-1735.

Ekbom, A., Helmick, C., Zack, M. &Adami, H. O. (1990). Ulcerative colitis and colorectal cancer. A population-based study. *The New England Journal of Medicine* 323(18): 1228-1233.

Esashi, F., Christ, N., Gannon, J., Liu, Y., Hunt, T., Jasin, M. &West, S. C. (2005). CDK-dependent phosphorylation of BRCA2 as a regulatory mechanism for recombinational repair. *Nature* 434(7033): 598-604.

Fass, S. &Rivlin, R. S. (1969). Regulation of riboflavin-metabolizing enzymes in riboflavin deficiency. *American Journal of Physiology* 217(4): 988-991.

Flores, O., Wang, Z., Knudsen, K. E. &Burnstein, K. L. (2010). Nuclear targeting of cyclin-dependent kinase 2 reveals essential roles of cyclin-dependent kinase 2 localization and cyclin E in vitamin D-mediated growth inhibition. *Endocrinology* 151(3): 896-908.

Fodde, R., Smits, R. &Clevers, H. (2001). APC, signal transduction and genetic instability in colorectal cancer. *Nature Review. Cancer* 1(1): 55-67.

Franken, N. A., Rodermond, H. M., Stap, J., Haveman, J. &van Bree, C. (2006). Clonogenic assay of cells in vitro. *Nature protocols* 1(5): 2315-2319.

Friso, S. &Choi, S. W. (2002). Gene-nutrient interactions and DNA methylation. *Journal of Nutrition* 132(8 Suppl): 2382S-2387S.

Fruehauf, J. P. &Meyskens, F. L., Jr. (2007). Reactive oxygen species: a breath of life or death? *Clinical Cancer Research: An official journal of the American Association for Cancer Research* 13(3): 789-794.

Fujimura, M., Yamamoto, S., Murata, T., Yasujima, T., Inoue, K., Ohta, K. Y. &Yuasa, H. (2010). Functional characteristics of the human ortholog of riboflavin transporter 2 and riboflavin-responsive expression of its rat ortholog in the small intestine indicate its involvement in riboflavin absorption. *Journal of Nutrition* 140(10): 1722-1727.

Gafken, P. R. &Lampe, P. D. (2006). Methodologies for characterizing phosphoproteins by mass spectrometry. *Cell Communication & Adhesion* 13(5-6): 249-262.

Galderisi, U., Jori, F. P. &Giordano, A. (2003). Cell cycle regulation and neural differentiation. *Oncogene* 22(33): 5208-5219.

Gavet, O. &Pines, J. (2010). Activation of cyclin B1-Cdk1 synchronizes events in the nucleus and the cytoplasm at mitosis. *Journal of Cell Biology* 189(2): 247-259.

Glen, A., Evans, C. A., Gan, C. S., Cross, S. S., Hamdy, F. C., Gibbins, J., Lippitt, J., Eaton, C. L., Noirel, J., Wright, P. C. &Rehman, I. (2010). Eight-plex iTRAQ analysis of variant metastatic human prostate cancer cells identifies candidate biomarkers of progression: An exploratory study. *The Prostate* 70(12): 1313-1332.

Glen, A., Gan, C. S., Hamdy, F. C., Eaton, C. L., Cross, S. S., Catto, J. W., Wright, P. C. &Rehman, I. (2008). iTRAQ-facilitated proteomic analysis of human prostate cancer cells identifies proteins associated with progression. *Journal of Proteome Research* 7(3): 897-907.

Gregory, J., Lowe, S., Bates, C., Prentice, A., Jacson, L., Smithers, G. &Farron, H. (2000).National Diet and Nutritional Survey (NDNS): young people aged 4 to 18 years., Vol. Volume 1: Report of the diet and nutrition surveyLondon: The Stationery Office.

Grummt, F., Paul, D. &Grummt, I. (1977). Regulation of ATP pools, rRNA and DNA synthesis in 3T3 cells in response to serum or hypoxanthine. *European Journal of Biochemistry / FEBS* 76(1): 7-12.

Gu, Y., Rosenblatt, J. &Morgan, D. O. (1992). Cell cycle regulation of CDK2 activity by phosphorylation of Thr160 and Tyr15. *The EMBO journal* 11(11): 3995-4005.

Hayashi, I., Sohn, K. J., Stempak, J. M., Croxford, R. &Kim, Y. I. (2007). Folate deficiency induces cell-specific changes in the steady-state transcript levels of genes involved in folate metabolism and 1-carbon transfer reactions in human colonic epithelial cells. *Journal of Nutrition* 137(3): 607-613.

Hayes, J. D. &McLellan, L. I. (1999). Glutathione and glutathione-dependent enzymes represent a co-ordinately regulated defence against oxidative stress. *Free Radical Research* 31(4): 273-300.

Heath, J. P. (1996). Epithelial cell migration in the intestine. *Cell Biology International* 20(2): 139-146.

Hendzel, M. J., Wei, Y., Mancini, M. A., Van Hooser, A., Ranalli, T., Brinkley, B. R., Bazett-Jones, D. P. &Allis, C. D. (1997). Mitosis-specific phosphorylation of histone H3 initiates primarily within pericentromeric heterochromatin during G2 and spreads in an ordered fashion coincident with mitotic chromosome condensation. *Chromosoma* 106(6): 348-360.

Hill, M. H., Bradley, A., Mushtaq, S., Williams, E. A. &Powers, H. J. (2009). Effects of methodological variation on assessment of riboflavin status using the erythrocyte glutathione reductase activation coefficient assay. *The British Journal of Nutrition* 102(2): 273-278.

Hsin, J. P. &Manley, J. L. (2012). The RNA polymerase II CTD coordinates transcription and RNA processing. *Genes & Development* 26(19): 2119-2137.

Huang, R., Kim, H. J. &Min, D. B. (2006). Photosensitizing effect of riboflavin, lumiflavin, and lumichrome on the generation of volatiles in soy milk. *Journal of Agricultural and Food Chemistry* 54(6): 2359-2364.

Huang, R. F., Ho, Y. H., Lin, H. L., Wei, J. S. &Liu, T. Z. (1999). Folate deficiency induces a cell cycle-specific apoptosis in HepG2 cells. *Journal of Nutrition* 129(1): 25-31.

Huang, S. N. &Swaan, P. W. (2000). Involvement of a receptor-mediated component in cellular translocation of riboflavin. *The Journal of Pharmacology and Experimental Therapeutics* 294(1): 117-125.

Hultin-Rosenberg, L., Forshed, J., Branca, R. M., Lehtio, J. &Johansson, H. J. (2013). Defining, comparing, and improving iTRAQ quantification in mass spectrometry proteomics data. *Molecular & Cellular Proteomics : MCP* 12(7): 2021-2031.

Hustad, S., McKinley, M. C., McNulty, H., Schneede, J., Strain, J. J., Scott, J. M. &Ueland, P. M. (2002). Riboflavin, flavin mononucleotide, and flavin adenine dinucleotide in human plasma and erythrocytes at baseline and after low-dose riboflavin supplementation. *Clinical chemistry* 48(9): 1571-1577.

Hveem, T. S., Merok, M. A., Pretorius, M. E., Novelli, M., Baevre, M. S., Sjo, O. H., Clinch, N., Liestol, K., Svindland, A., Lothe, R. A., Nesbakken, A. &Danielsen, H. E. (2014). Prognostic impact of genomic instability in colorectal cancer. *The British Journal of Cancer* 110(8): 2159-2164.

Jankowski, J. A., Goodlad, R. A. &Wright, N. A. (1994). Maintenance of normal intestinal mucosa: function, structure, and adaptation. *Gut* 35(1 Suppl): S1-4.

Johnson, D. G. &Walker, C. L. (1999). Cyclins and cell cycle checkpoints. *Annual review of pharmacology and toxicology* 39: 295-312.

Kalinowska-Herok, M. &Widlak, P. (2008). High mobility group proteins stimulate DNA cleavage by apoptotic endonuclease DFF40/CAD due to HMG-box interactions with DNA. *Acta Biochimica Polonica* 55(1): 21-26.

Karaman, A., Binici, D. N., Kabalar, M. E. &Calikusu, Z. (2008). Micronucleus analysis in patients with colorectal adenocarcinoma and colorectal polyps. *World journal of gastroenterology : WJG* 14(44): 6835-6839.

Katayama, H., Brinkley, W. R. &Sen, S. (2003). The Aurora kinases: role in cell transformation and tumorigenesis. *Cancer Metastasis Reviews* 22(4): 451-464.

Kee, N., Sivalingam, S., Boonstra, R. &Wojtowicz, J. M. (2002). The utility of Ki-67 and BrdU as proliferative markers of adult neurogenesis. *Journal of neuroscience methods* 115(1): 97-105.

Kim, S. J., Jung, H. J., Hyun, D. H., Park, E. H., Kim, Y. M. &Lim, C. J. (2010). Glutathione reductase plays an anti-apoptotic role against oxidative stress in human hepatoma cells. *Biochimie* 92(8): 927-932.

Kondo, M., Yamaoka, T., Honda, S., Miwa, Y., Katashima, R., Moritani, M., Yoshimoto, K., Hayashi, Y. &Itakura, M. (2000). The rate of cell growth is regulated by purine biosynthesis via ATP production and G(1) to S phase transition. *Journal of biochemistry* 128(1): 57-64.

Kreis, S., Munz, G. A., Haan, S., Heinrich, P. C. &Behrmann, I. (2007). Cell density dependent increase of constitutive signal transducers and activators of transcription 3 activity in melanoma cells is mediated by Janus kinases. *Molecular cancer research : MCR* 5(12): 1331-1341.

Krishan, A. (1975). Rapid flow cytofluorometric analysis of mammalian cell cycle by propidium iodide staining. *J Cell Biol* 66(1): 188-193.

Kurokawa, K., Akaike, Y., Masuda, K., Kuwano, Y., Nishida, K., Yamagishi, N., Kajita, K., Tanahashi, T. &Rokutan, K. (2014). Downregulation of serine/arginine-rich splicing

factor 3 induces G1 cell cycle arrest and apoptosis in colon cancer cells. *Oncogene* 33(11): 1407-1417.

LeBel, C. P., Ischiropoulos, H. &Bondy, S. C. (1992). Evaluation of the probe 2',7'-dichlorofluorescin as an indicator of reactive oxygen species formation and oxidative stress. *Chemical research in toxicology* 5(2): 227-231.

Lee, S. S. &McCormick, D. B. (1983). Effect of riboflavin status on hepatic activities of flavin-metabolizing enzymes in rats. *The Journal of Nutrition* 113(11): 2274-2279.

Li, H. &Clagett-Dame, M. (2009). Vitamin A deficiency blocks the initiation of meiosis of germ cells in the developing rat ovary in vivo. *Biology of Reproduction* 81(5): 996-1001.

Lindqvist, A., Kallstrom, H., Lundgren, A., Barsoum, E. &Rosenthal, C. K. (2005). Cdc25B cooperates with Cdc25A to induce mitosis but has a unique role in activating cyclin B1-Cdk1 at the centrosome. *J Cell Biol* 171(1): 35-45.

Liu, T., Soong, S. J., Wilson, N. P., Craig, C. B., Cole, P., Macaluso, M. &Butterworth, C. E., Jr. (1993). A case control study of nutritional factors and cervical dysplasia. *Cancer epidemiology, biomarkers & prevention : a publication of the American Association for Cancer Research, cosponsored by the American Society of Preventive Oncology* 2(6): 525-530.

Liu, Z., Choi, S. W., Crott, J. W., Keyes, M. K., Jang, H., Smith, D. E., Kim, M., Laird, P. W., Bronson, R. &Mason, J. B. (2007). Mild depletion of dietary folate combined with other B vitamins alters multiple components of the Wnt pathway in mouse colon. *Journal of Nutrition* 137(12): 2701-2708.

Long, J. C. &Caceres, J. F. (2009). The SR protein family of splicing factors: master regulators of gene expression. *The Biochemical Journal* 417(1): 15-27.

Macek, B., Mann, M. &Olsen, J. V. (2009). Global and site-specific quantitative phosphoproteomics: principles and applications. *Annual review of pharmacology and toxicology* 49: 199-221.

Manthey, K. C., Chew, Y. C. &Zempleni, J. (2005). Riboflavin deficiency impairs oxidative folding and secretion of apolipoprotein B-100 in HepG2 cells, triggering stress response systems. *The Journal of Nutrition* 135(5): 978-982.

Manthey, K. C., Rodriguez-Melendez, R., Hoi, J. T. &Zempleni, J. (2006). Riboflavin deficiency causes protein and DNA damage in HepG2 cells, triggering arrest in G1 phase of the cell cycle. *The Journal of Nutritional Biochemistry* 17(4): 250-256.

McCormick, D. B. (1962). The Intracellular localization, partial purification, and properties of flavokinase from rat liver. *The Journal of biological chemistry* 237(3): 959-962.

McIlwain, D. R., Berger, T. &Mak, T. W. (2013). Caspase functions in cell death and disease. *Cold Spring Harbor perspectives in biology* 5(4): a008656.

Moat, S. J., Ashfield-Watt, P. A., Powers, H. J., Newcombe, R. G. &McDowell, I. F. (2003). Effect of riboflavin status on the homocysteine-lowering effect of folate in relation to the MTHFR (C677T) genotype. *Clinical chemistry* 49(2): 295-302.

Moore, M. J., Wang, Q., Kennedy, C. J. &Silver, P. A. (2010). An alternative splicing network links cell-cycle control to apoptosis. *Cell* 142(4): 625-636.

Murata-Hori, M. &Wang, Y. L. (2002). The kinase activity of aurora B is required for kinetochore-microtubule interactions during mitosis. *Current biology : CB* 12(11): 894-899.

Nakano, E., Mushtaq, S., Heath, P. R., Lee, E. S., Bury, J. P., Riley, S. A., Powers, H. J. &Corfe, B. M. (2011). Riboflavin depletion impairs cell proliferation in adult human duodenum: identification of potential effectors. *Digestive diseases and sciences* 56(4): 1007-1019.

Oelgeschlager, T. (2002). Regulation of RNA polymerase II activity by CTD phosphorylation and cell cycle control. *Journal of Cellular Physiology* 190(2): 160-169.

Oka, M. &McCormick, D. B. (1987). Complete purification and general characterization of FAD synthetase from rat liver. *The Journal of biological chemistry* 262(15): 7418-7422.

Olpin, S. E. &Bates, C. J. (1982). Lipid metabolism in riboflavin-deficient rats. 1. Effect of dietary lipids on riboflavin status and fatty acid profiles. *British Journal of Nutrition* 47(3): 577-596.

Organization, W. H. (2009).Cell culture procedures.

Owen, J. B. &Butterfield, D. A. (2010). Measurement of oxidized/reduced glutathione ratio. *Methods in Molecular Biology* 648: 269-277.

Pasteur, L. (2008).Louis Pasteur Biology 3 (http://thiscooldude.blogspot.com/2008/01/cell-division-chromatid-centromere.html).

Pearson-Education (2009).Mitosis (http://royaleb.wordpress.com/2009/04/27/mitosis/). Benjamin Cummings.

Pearson, G., Robinson, F., Beers Gibson, T., Xu, B. E., Karandikar, M., Berman, K. &Cobb, M. H. (2001). Mitogen-activated protein (MAP) kinase pathways: regulation and physiological functions. *Endocrine Reviews* 22(2): 153-183.

Poddar, R., Sivasubramanian, N., DiBello, P. M., Robinson, K. &Jacobsen, D. W. (2001). Homocysteine induces expression and secretion of monocyte chemoattractant protein-1 and interleukin-8 in human aortic endothelial cells: implications for vascular disease. *Circulation* 103(22): 2717-2723.

Podhorecka, M., Skladanowski, A. &Bozko, P. (2010). H2AX Phosphorylation: Its Role in DNA Damage Response and Cancer Therapy. *Journal of Nucleic Acids* 2010.

Powers, H. J. (1999). Current knowledge concerning optimum nutritional status of riboflavin, niacin and pyridoxine. *The Proceedings of the Nutrition Society* 58(2): 435-440.

Powers, H. J. (2003). Riboflavin (vitamin B-2) and health. *The American Journal of Clinical Nutrition* 77(6): 1352-1360.

Powers, H. J. (2005). Interaction among folate, riboflavin, genotype, and cancer, with reference to colorectal and cervical cancer. *The Journal of Nutrition* 135(12 Suppl): 2960S-2966S.

Powers, H. J., Bates, C. J. &Duerden, J. M. (1983). Effects of riboflavin deficiency in rats on some aspects of iron metabolism. *International Journal for Vitamin and Nutrition Research.* 53(4): 371-376.

Powers, H. J., Weaver, L. T., Austin, S. &Beresford, J. K. (1993). A proposed intestinal mechanism for the effect of riboflavin deficiency on iron loss in the rat. *The British Journal of Nutrition* 69(2): 553-561.

Powers, H. J., Weaver, L. T., Austin, S., Wright, A. J. &Fairweather-Tait, S. J. (1991). Riboflavin deficiency in the rat: effects on iron utilization and loss. *The British Journal of Nutrition* 65(3): 487-496.

Preedy, V. R. (2013). *B vitamins and folate : chemistry, analysis, function and effects.* Cambridge: RSC Publishing.

Prentice, A. M. &Bates, C. J. (1981a). A biochemical evaluation of the erythrocyte glutathione reductase (EC 1.6.4.2) test for riboflavin status. 1. Rate and specificity of response in acute deficiency. *The British Journal of Nutrition* 45(1): 37-52.

Prentice, A. M. &Bates, C. J. (1981b). A biochemical evaluation of the erythrocyte glutathione reductase (EC 1.6.4.2) test for riboflavin status. 2. Dose-response relationships in chronic marginal deficiency. *The British Journal of Nutrition* 45(1): 53-65.

Raggiaschi, R., Gotta, S. &Terstappen, G. C. (2005). Phosphoproteome analysis. *Bioscience Reports* 25(1-2): 33-44.

Rao, C. V. &Yamada, H. Y. (2013). Genomic instability and colon carcinogenesis: from the perspective of genes. *Frontiers in Oncology* 3: 130.

Razin, A. &Riggs, A. D. (1980). DNA methylation and gene function. *Science* 210(4470): 604-610.

Rhee, S. G. (2006). Cell signaling. H2O2, a necessary evil for cell signaling. *Science* 312(5782): 1882-1883.

Rho, J. H., Qin, S., Wang, J. Y. &Roehrl, M. H. (2008). Proteomic expression analysis of surgical human colorectal cancer tissues: up-regulation of PSB7, PRDX1, and SRP9 and hypoxic adaptation in cancer. *Journal of Proteome Research* 7(7): 2959-2972.

Ripoll, P., Pimpinelli, S., Valdivia, M. M. &Avila, J. (1985). A cell division mutant of Drosophila with a functionally abnormal spindle. *Cell* 41(3): 907-912.

Rohner, F., Zimmermann, M. B., Wegmueller, R., Tschannen, A. B. &Hurrell, R. F. (2007). Mild riboflavin deficiency is highly prevalent in school-age children but does not increase risk for anaemia in Cote d'Ivoire. *The British Journal of Nutrition* 97(5): 970-976.

Rosman-Urbach, M., Niv, Y., Birk, Y., Smirnoff, P., Zusman, I., Morgenstern, S. &Schwartz, B. (2004). A high degree of aneuploidy, loss of p53 gene, and low soluble p53 protein serum levels are detected in ulcerative colitis patients. *Diseases of the Colon and Rectum* 47(3): 304-313.

Ross, P. L., Huang, Y. N., Marchese, J. N., Williamson, B., Parker, K., Hattan, S., Khainovski, N., Pillai, S., Dey, S., Daniels, S., Purkayastha, S., Juhasz, P., Martin, S., Bartlet-Jones, M., He, F., Jacobson, A. &Pappin, D. J. (2004). Multiplexed protein quantitation in Saccharomyces cerevisiae using amine-reactive isobaric tagging reagents. *Molecular & Cellular Proteomics : MCP* 3(12): 1154-1169.

Rossetto, D., Avvakumov, N. &Cote, J. (2012). Histone phosphorylation: a chromatin modification involved in diverse nuclear events. *Epigenetics : official journal of the DNA Methylation Society* 7(10): 1098-1108.

Russo, T., Zambrano, N., Esposito, F., Ammendola, R., Cimino, F., Fiscella, M., Jackman, J., O'Connor, P. M., Anderson, C. W. &Appella, E. (1995). A p53-independent pathway for activation of WAF1/CIP1 expression following oxidative stress. *The Journal of biological chemistry* 270(49): 29386-29391.

Said, H. M., Hollander, D. &Duong, Y. (1985). A dual, concentration-dependent transport system for riboflavin in rat intestine in vitro. *Nutrition research* 5(11).

Said, H. M. &Ma, T. Y. (1994). Mechanism of riboflavine uptake by Caco-2 human intestinal epithelial cells. *Am J Physiol* 266(1 Pt 1): G15-21.

Said, H. M., Ortiz, A., Moyer, M. P. &Yanagawa, N. (2000). Riboflavin uptake by human-derived colonic epithelial NCM460 cells. *Am J Physiol Cell Physiol* 278(2): C270-276.

Sawasdikosol, S. (2010). Detecting tyrosine-phosphorylated proteins by Western blot analysis. *Current protocols in immunology / edited by John E. Coligan ... [et al.]* Chapter 11: Unit 11 13 11-11.

Scaife, R. M. (2004). G2 cell cycle arrest, down-regulation of cyclin B, and induction of mitotic catastrophe by the flavoprotein inhibitor diphenyleneiodonium. *Molecular Cancer Therapeutics* 3(10): 1229-1237.

Schafer, F. Q. &Buettner, G. R. (2001). Redox environment of the cell as viewed through the redox state of the glutathione disulfide/glutathione couple. *Free Radical Biology & Medicine* 30(11): 1191-1212.

Schmelzle, K. &White, F. M. (2006). Phosphoproteomic approaches to elucidate cellular signaling networks. *Current Opinion in Biotechnology* 17(4): 406-414.

Schramm, M., Wiegmann, K., Schramm, S., Gluschko, A., Herb, M., Utermohlen, O. &Kronke, M. (2014). Riboflavin (vitamin B2) deficiency impairs NADPH oxidase 2

(Nox2) priming and defense against Listeria monocytogenes. *European Journal of Immunology* 44(3): 728-741.

Schulze, W. X. (2010). Proteomics approaches to understand protein phosphorylation in pathway modulation. *Current opinion in plant biology* 13(3): 280-287.

Scott, J. M. (1999). Folate and vitamin B12. *The Proceedings of the Nutrition Society* 58(2): 441-448.

Shackelford, R. E., Kaufmann, W. K. &Paules, R. S. (2000). Oxidative stress and cell cycle checkpoint function. *Free Radical Biology & Medicine* 28(9): 1387-1404.

Shepard, P. J. &Hertel, K. J. (2009). The SR protein family. *Genome biology* 10(10): 242.

Shi, Z., Zhen, S., Wittert, G. A., Yuan, B., Zuo, H. &Taylor, A. W. (2014). Inadequate riboflavin intake and anemia risk in a Chinese population: five-year follow up of the Jiangsu Nutrition Study. *PloS one* 9(2): e88862.

Smith, M. W. (1985). Expression of digestive and absorptive function in differentiating enterocytes. *Annual review of physiology* 47: 247-260.

Son, Y., Cheong, Y. K., Kim, N. H., Chung, H. T., Kang, D. G. &Pae, H. O. (2011). Mitogen-Activated Protein Kinases and Reactive Oxygen Species: How Can ROS Activate MAPK Pathways? *Journal of Signal Transduction* 2011: 792639.

St Clair, W. H. &Osborne, J. W. (1985). Crypt fission and crypt number in the small and large bowel of postnatal rats. *Cell and Tissue Kinetics* 18(3): 255-262.

Stipanuk, M. H. (2013). *Biochemical, physiological and molecular aspects of human nutrition.* Philadelphia, Pa. ; London: W.B. Saunders.

Subramanian, V. S., Rapp, L., Marchant, J. S. &Said, H. M. (2011a). Role of cysteine residues in cell surface expression of the human riboflavin transporter-2 (hRFT2) in intestinal epithelial cells. *American Journal of Physiology. Gastrointestinal and Liver Physiology* 301(1): G100-109.

Subramanian, V. S., Subramanya, S. B., Rapp, L., Marchant, J. S., Ma, T. Y. &Said, H. M. (2011b). Differential expression of human riboflavin transporters -1, -2, and -3 in polarized epithelia: a key role for hRFT-2 in intestinal riboflavin uptake. *Biochimica et biophysica acta* 1808(12): 3016-3021.

Sundaresan, M., Yu, Z. X., Ferrans, V. J., Irani, K. &Finkel, T. (1995). Requirement for generation of H2O2 for platelet-derived growth factor signal transduction. *Science* 270(5234): 296-299.

Takizawa, C. G. &Morgan, D. O. (2000). Control of mitosis by changes in the subcellular location of cyclin-B1-Cdk1 and Cdc25C. *Current Opinion in Cell Biology* 12(6): 658-665.

Terada, Y., Tatsuka, M., Suzuki, F., Yasuda, Y., Fujita, S. &Otsu, M. (1998). AIM-1: a mammalian midbody-associated protein required for cytokinesis. *The EMBO journal* 17(3): 667-676.

Thomas, C. G., Vezyraki, P. E., Kalfakakou, V. P. &Evangelou, A. M. (2005). Vitamin C transiently arrests cancer cell cycle progression in S phase and G2/M boundary by modulating the kinetics of activation and the subcellular localization of Cdc25C phosphatase. *Journal of Cellular Physiology* 205(2): 310-318.

Thomson, A. B., Doring, K., Keelan, M. &Armstrong, G. (1997). Nutrient uptake into undifferentiated and differentiated HT-29 cells in culture. *Canadian Journal of Physiology and Pharmacology* 75(5): 351-356.

Totafurno, J., Bjerknes, M. &Cheng, H. (1987). The crypt cycle. Crypt and villus production in the adult intestinal epithelium. *Biophysical Journal* 52(2): 279-294.

Tremblay, E., Auclair, J., Delvin, E., Levy, E., Menard, D., Pshezhetsky, A. V., Rivard, N., Seidman, E. G., Sinnett, D., Vachon, P. H. &Beaulieu, J. F. (2006). Gene expression profiles of normal proliferating and differentiating human intestinal epithelial cells: a comparison with the Caco-2 cell model. *Journal of Cellular Biochemistry* 99(4): 1175-1186.

Tsuta, K., Liu, D. C., Kalhor, N., Wistuba, II &Moran, C. A. (2011). Using the mitosis-specific marker anti-phosphohistone H3 to assess mitosis in pulmonary neuroendocrine carcinomas. *American Journal of Clinical Pathology* 136(2): 252-259.

Vagnarelli, P., Hudson, D. F., Ribeiro, S. A., Trinkle-Mulcahy, L., Spence, J. M., Lai, F., Farr, C. J., Lamond, A. I. &Earnshaw, W. C. (2006). Condensin and Repo-Man-PP1 co-operate in the regulation of chromosome architecture during mitosis. *Nature Cell Biology* 8(10): 1133-1142.

van den Donk, M., Buijsse, B., van den Berg, S. W., Ocke, M. C., Harryvan, J. L., Nagengast, F. M., Kok, F. J. &Kampman, E. (2005). Dietary intake of folate and riboflavin, MTHFR C677T genotype, and colorectal adenoma risk: a Dutch case-control study. *Cancer Epidemiology, Biomarkers & Prevention* 14(6): 1562-1566.

van der Flier, L. G. &Clevers, H. (2009). Stem cells, self-renewal, and differentiation in the intestinal epithelium. *Annual review of physiology* 71: 241-260.

Venetianer, A., Dubois, M. F., Nguyen, V. T., Bellier, S., Seo, S. J. &Bensaude, O. (1995). Phosphorylation state of the RNA polymerase II C-terminal domain (CTD) in heat-shocked cells. Possible involvement of the stress-activated mitogen-activated protein (MAP) kinases. *European Journal of Biochemistry / FEBS* 233(1): 83-92.

Visscher, D. W., Wallis, T. L. &Crissman, J. D. (1996). Evaluation of chromosome aneuploidy in tissue sections of preinvasive breast carcinomas using interphase cytogenetics. *Cancer* 77(2): 315-320.

Walsh, C. M., Suchanek, A. L., Cyphert, T. J., Kohan, A. B., Szeszel-Fedorowicz, W. &Salati, L. M. (2013). Serine arginine splicing factor 3 is involved in enhanced splicing of glucose-6-phosphate dehydrogenase RNA in response to nutrients and hormones in liver. *The Journal of biological chemistry* 288(4): 2816-2828.

Wasson, G. R., McGlynn, A. P., McNulty, H., O'Reilly, S. L., McKelvey-Martin, V. J., McKerr, G., Strain, J. J., Scott, J. &Downes, C. S. (2006). Global DNA and p53 region-specific hypomethylation in human colonic cells is induced by folate depletion and reversed by folate supplementation. *Journal of Nutrition* 136(11): 2748-2753.

Weichselbaum, E. &Buttriss, J. (2014). Diet, nutrition and schoochildren:An update. *British Nutrition Foundation Nutrition Bulletin* 39: 9-73.

Werner, R., Manthey, K. C., Griffin, J. B. &Zempleni, J. (2005). HepG2 cells develop signs of riboflavin deficiency within 4 days of culture in riboflavin-deficient medium. *The Journal of Nutritional Biochemistry* 16(10): 617-624.

White, F. M. (2008). Quantitative phosphoproteomic analysis of signaling network dynamics. *Current Opinion in Biotechnology* 19(4): 404-409.

Willenbucher, R. F., Aust, D. E., Chang, C. G., Zelman, S. J., Ferrell, L. D., Moore, D. H., 2nd &Waldman, F. M. (1999). Genomic instability is an early event during the

progression pathway of ulcerative-colitis-related neoplasia. *The American Journal of Pathology* 154(6): 1825-1830.

Willenbucher, R. F., Zelman, S. J., Ferrell, L. D., Moore, D. H., 2nd &Waldman, F. M. (1997). Chromosomal alterations in ulcerative colitis-related neoplastic progression. *Gastroenterology* 113(3): 791-801.

Williams, E. A., Powers, H. J. &Rumsey, R. D. (1995). Morphological changes in the rat small intestine in response to riboflavin depletion. *The British Journal of Nutrition* 73(1): 141-146.

Williams, E. A., Rumsey, R. D. &Powers, H. J. (1996a). Cytokinetic and structural responses of the rat small intestine to riboflavin depletion. *The British Journal of Nutrition* 75(2): 315-324.

Williams, E. A., Rumsey, R. D. &Powers, H. J. (1996b). An investigation into the reversibility of the morphological and cytokinetic changes seen in the small intestine of riboflavin deficient rats. *Gut* 39(2): 220-225.

Won, J., Kim, D. Y., La, M., Kim, D., Meadows, G. G. &Joe, C. O. (2003). Cleavage of 14-3-3 protein by caspase-3 facilitates bad interaction with Bcl-x(L) during apoptosis. *The Journal of biological chemistry* 278(21): 19347-19351.

Wong, W. M. &Wright, N. A. (1999). Cell proliferation in gastrointestinal mucosa. *Journal of Clinical Pathology* 52(5): 321-333.

Yamamoto, S., Inoue, K., Ohta, K. Y., Fukatsu, R., Maeda, J. Y., Yoshida, Y. &Yuasa, H. (2009). Identification and functional characterization of rat riboflavin transporter 2. *Journal of biochemistry* 145(4): 437-443.

Yates, C. A., Evans, G. S., Pearson, T. &Powers, H. J. (2003). Absence of luminal riboflavin disturbs early postnatal development of the gastrointestinal tract. *Digestive diseases and sciences* 48(6): 1159-1164.

Yates, C. A., Evans, G. S. &Powers, H. J. (2001). Riboflavin deficiency: early effects on post-weaning development of the duodenum in rats. *The British Journal of Nutrition* 86(5): 593-599.

Yazdanpanah, B., Wiegmann, K., Tchikov, V., Krut, O., Pongratz, C., Schramm, M., Kleinridders, A., Wunderlich, T., Kashkar, H., Utermohlen, O., Bruning, J. C.,

Schutze, S. &Kronke, M. (2009). Riboflavin kinase couples TNF receptor 1 to NADPH oxidase. *Nature* 460(7259): 1159-1163.

Yen, T. H. &Wright, N. A. (2006). The gastrointestinal tract stem cell niche. *Stem cell reviews* 2(3): 203-212.

Yonezawa, A. &Inui, K. (2013). Novel riboflavin transporter family RFVT/SLC52: identification, nomenclature, functional characterization and genetic diseases of RFVT/SLC52. *Molecular Aspects of Medicine* 34(2-3): 693-701.

Yonezawa, A., Masuda, S., Katsura, T. &Inui, K. (2008). Identification and functional characterization of a novel human and rat riboflavin transporter, RFT1. *American journal of physiolgy. Cell Physiology* 295(3): C632-641.

Zhang, Y., Wolf-Yadlin, A., Ross, P. L., Pappin, D. J., Rush, J., Lauffenburger, D. A. &White, F. M. (2005). Time-resolved mass spectrometry of tyrosine phosphorylation sites in the epidermal growth factor receptor signaling network reveals dynamic modules. *Molecular and cellular proteomics : MCP* 4(9): 1240-1250.

Zielinska-Dawidziak, M., Grajek, K., Olejnik, A., Czaczyk, K. &Grajek, W. (2008). Transport of high concentration of thiamin, riboflavin and pyridoxine across intestinal epithelial cells Caco-2. *Journal of nutritional Science and vitaminology (Tokyo)* 54(6): 423-429.

Zitka, O., Skalickova, S., Gumulec, J., Masarik, M., Adam, V., Hubalek, J., Trnkova, L., Kruseova, J., Eckschlager, T. &Kizek, R. (2012). Redox status expressed as GSH:GSSG ratio as a marker for oxidative stress in paediatric tumour patients. *Oncology Letters* 4(6): 1247-1253.

APPENDIX

APPENDIX

Appendix 1 *Reactome analysis of the pathways represented by 145 proteins significantly altered under 24hours lumiflavin treatment compared with time-control with matching proteins.*

Statistically over-represented events in hierarchy

Each Event is coloured according to the un-adjusted, i.e. not corrected for multiple testing, probability (from hypergeometric test) of seeing given number or more genes in this Event by chance. Only the 'child' events are shown which have a p-value lower than the 'parent' event. The top-level (root) Events are ordered according to the lowest p-value of their components. Colour key for probabilities:

| 1e+00 | 3e-01 | 1e-01 | 3e-02 | 1e-02 | 3e-03 | 1e-03 | 3e-04 | 1e-04 | 3e-05 | 1e-05 | 3e-06 | 1e-06 | 3e-07 | 1e-07 | 3e-08 | 1e-08 | 3e-09 | 1e-09 | 3e-10 | > |

⊟ ⁘ **Gene Expression** 1.1e-08, 25/1031

　　⊟ Matching identifiers
　　　Q13247 SRSF6
　　　P20042 EIF2S2
　　　Q13242 SRSF9
　　　P62316 SNRPD2
　　　P26368 U2AF2
　　　P05387 RPLP2
　　　Q9NZI8 IGF2BP1
　　　P62753 RPS6
　　　Q01081 U2AF1
　　　Q01105 SET
　　　Q9Y5S9 RBM8A
　　　P13639 EEF2
　　　P84103 SRSF3
　　　P61978-3 HNRNPK
　　　Q9Y5M8 SRPRB
　　　O75643 SNRNP200
　　　P08621 SNRNP70
　　　Q13263-2 TRIM28
　　　O43809 NUDT21
　　　P24534 EEF1B2
　　　O76094 SRP72
　　　Q99436 PSMB7
　　　Q13243 SRSF5
　　　P62987 UBA52
　　　O75533 SF3B1

⊟ ⁘ **Processing of Capped Intron-Containing Pre-mRNA** 1.5e-12, 13/117

　　⊟ Matching identifiers
　　　Q13247 SRSF6
　　　P84103 SRSF3
　　　Q13242 SRSF9
　　　P61978-3 HNRNPK
　　　P62316 SNRPD2
　　　P26368 U2AF2
　　　P08621 SNRNP70
　　　O75643 SNRNP200

Appendix 1 *(continued)*

　O43809 NUDT21
　Q01081 U2AF1
　Q13243 SRSF5
　Q9Y5S9 RBM8A
　O75533 SF3B1

mRNA Splicing8.7e-13, 13/112

Matching identifiers
　Q13247 SRSF6
　P84103 SRSF3
　Q13242 SRSF9
　P61978-3 HNRNPK
　P62316 SNRPD2
　P26368 U2AF2
　P08621 SNRNP70
　O75643 SNRNP200
　O43809 NUDT21
　Q01081 U2AF1
　Q13243 SRSF5
　Q9Y5S9 RBM8A
　O75533 SF3B1

mRNA Processing1.1e-11, 13/136

Matching identifiers
　Q13247 SRSF6
　P84103 SRSF3
　Q13242 SRSF9
　P61978-3 HNRNPK
　P62316 SNRPD2
　P26368 U2AF2
　P08621 SNRNP70
　O75643 SNRNP200
　O43809 NUDT21
　Q01081 U2AF1
　Q13243 SRSF5
　Q9Y5S9 RBM8A
　O75533 SF3B1

Processing of Capped Intron-Containing Pre-mRNA1.5e-12, 13/117

Matching identifiers
　Q13247 SRSF6
　P84103 SRSF3
　Q13242 SRSF9
　P61978-3 HNRNPK
　P62316 SNRPD2
　P26368 U2AF2
　P08621 SNRNP70
　O75643 SNRNP200
　O43809 NUDT21
　Q01081 U2AF1
　Q13243 SRSF5
　Q9Y5S9 RBM8A
　O75533 SF3B1

Appendix 1 *(continued)*

mRNA Splicing 8.7e-13, 13/112

Matching identifiers
Q13247 SRSF6
P84103 SRSF3
Q13242 SRSF9
P61978-3 HNRNPK
P62316 SNRPD2
P26368 U2AF2
P08621 SNRNP70
O75643 SNRNP200
O43809 NUDT21
Q01081 U2AF1
Q13243 SRSF5
Q9Y5S9 RBM8A
O75533 SF3B1

Post-Elongation Processing of the Transcript 6.4e-10, 8/43

Matching identifiers
Q13247 SRSF6
P84103 SRSF3
Q13242 SRSF9
P26368 U2AF2
O43809 NUDT21
Q01081 U2AF1
Q13243 SRSF5
Q9Y5S9 RBM8A

Post-Elongation Processing of Intron-Containing pre-mRNA 8.5e-11, 8/34

Matching identifiers
Q13247 SRSF6
P84103 SRSF3
Q13242 SRSF9
P26368 U2AF2
O43809 NUDT21
Q01081 U2AF1
Q13243 SRSF5
Q9Y5S9 RBM8A

Transcription 9.9e-06, 8/145

Matching identifiers

RNA Polymerase II Transcription 6.5e-07, 8/101

Matching identifiers
Q13247 SRSF6

Appendix 1 *(continued)*

P84103 SRSF3
Q13242 SRSF9
P26368 U2AF2
O43809 NUDT21
Q01081 U2AF1
Q13243 SRSF5

    Q9Y5S9 RBM8A

RNA Polymerase II Transcription Termination 6.4e-10, 8/43

    Matching identifiers
      Q13247 SRSF6
      P84103 SRSF3
      Q13242 SRSF9
      P26368 U2AF2
      O43809 NUDT21
      Q01081 U2AF1
      Q13243 SRSF5
      Q9Y5S9 RBM8A

Apoptosis 1.6e-06, 9/154

    Matching identifiers
      Q6UYC3 LMNA
      P31947 SFN
      P16403 HIST1H1C
      P26583 HMGB2
      P09429 HMGB1
      P16401 HIST1H1B
      P62987 UBA52
      Q99436 PSMB7
      P30419 NMT1

Metabolism of proteins 8.3e-04, 12/574

    Matching identifiers
      Q6UYC3 LMNA
      P51858 HDGF
      P20042 EIF2S2
      P13639 EEF2
      Q9Y5M8 SRPRB
      P05387 RPLP2
      P62753 RPS6
      O00567 NOP56
      P24534 EEF1B2
      P27797 CALR
      O76094 SRP72
      P62987 UBA52

Translation 1.3e-05, 8/151

    Matching identifiers
      P62753 RPS6
      P24534 EEF1B2
      P20042 EIF2S2
      P13639 EEF2
      Q9Y5M8 SRPRB
      O76094 SRP72
      P62987 UBA52

Appendix 1 *(continued)*

      P05387 RPLP2

Cell Cycle 1.5e-04, 12/478

    Matching identifiers

Q6UYC3 LMNA
P07437 TUBB
O75531 BANF1
O60832 DKC1
P06748 NPM1
Q99878 HIST1H2AJ
P62805 HIST1H4A
Q93079 HIST1H2BH
Q9Y266 NUDC
P07900 HSP90AA1
Q99436 PSMB7
P62987 UBA52

Chromosome Maintenance1.0e-04, 6/103

Matching identifiers
Q6UYC3 LMNA
O60832 DKC1
P06748 NPM1
Q99878 HIST1H2AJ
P62805 HIST1H4A
Q93079 HIST1H2BH

Meiosis3.0e-03, 4/81

Matching identifiers
Q6UYC3 LMNA
Q99878 HIST1H2AJ
P62805 HIST1H4A
Q93079 HIST1H2BH

Meiotic Synapsis8.1e-04, 4/57

Matching identifiers
Q6UYC3 LMNA
Q99878 HIST1H2AJ
P62805 HIST1H4A
Q93079 HIST1H2BH

Telomere clustering at the nuclear membrane3.9e-04, 4/47

Matching identifiers
Q6UYC3 LMNA
Q99878 HIST1H2AJ
P62805 HIST1H4A
Q93079 HIST1H2BH

Binding and Uptake of Ligands by Scavenger Receptors4.3e-01, 2/195

Matching identifiers
P27797 CALR
P07900 HSP90AA1

Appendix 1 *(continued)*

Scavenging by Class F Receptors1.1e-03, 2/7

Matching identifiers
P27797 CALR
P07900 HSP90AA1

- Mitotic M-M/G1 phases 4.7e-02, 5/266

  - Matching identifiers
    - Q6UYC3 LMNA
    - O75531 BANF1
    - Q9Y266 NUDC
    - Q99436 PSMB7
    - P62987 UBA52

  - M Phase 3.0e-02, 5/235

    - Matching identifiers
      - Q6UYC3 LMNA
      - O75531 BANF1
      - Q9Y266 NUDC
      - Q99436 PSMB7
      - P62987 UBA52

    - Mitotic Metaphase and Anaphase 1.2e-02, 5/185

      - Matching identifiers
        - Q6UYC3 LMNA
        - O75531 BANF1
        - Q9Y266 NUDC
        - Q99436 PSMB7
        - P62987 UBA52

      - Mitotic Anaphase 1.2e-02, 5/184

        - Matching identifiers
          - Q6UYC3 LMNA
          - O75531 BANF1
          - Q9Y266 NUDC
          - Q99436 PSMB7
          - P62987 UBA52

        - Nuclear Envelope Reassembly 4.0e-03, 2/13

          - Matching identifiers
            - Q6UYC3 LMNA
            - O75531 BANF1

- Disease 3.4e-02, 12/915

  - Matching identifiers
    - O75531 BANF1
    - P06748 NPM1
    - Q99878 HIST1H2AJ
    - P62805 HIST1H4A
    - Q93079 HIST1H2BH
    - P05387 RPLP2

Appendix 1 *(continued)*

- P07686 HEXB
- P62753 RPS6
- P07900 HSP90AA1
- Q99436 PSMB7
- P62987 UBA52
- P30419 NMT1

Amyloids 6.3e-03, 3/51

Matching identifiers
Q99878 HIST1H2AJ
P62805 HIST1H4A
Q93079 HIST1H2BH

Serum amyloid P binds DNA and chromatin 1.1e-03, 3/28

Matching identifiers
Q99878 HIST1H2AJ
P62805 HIST1H4A
Q93079 HIST1H2BH

HIV Infection 2.4e-02, 5/221

Matching identifiers
O75531 BANF1
P06748 NPM1
Q99436 PSMB7
P62987 UBA52
P30419 NMT1

Host Interactions of HIV factors 1.8e-02, 4/135

Matching identifiers
O75531 BANF1
P06748 NPM1
Q99436 PSMB7
P62987 UBA52

Signal Transduction 1.0e+00, 6/1847

Matching identifiers
P62753 RPS6
P08254 MMP3
P07900 HSP90AA1
Q99436 PSMB7
P62987 UBA52
P30419 NMT1

Signaling by ERBB2 3.3e-01, 2/158

Matching identifiers
P07900 HSP90AA1
P62987 UBA52

CHIP (STUB1) mediates ubiquitination of ERBB2 1.9e-03, 2/9

Matching identifiers
P07900 HSP90AA1

Appendix 1 *(continued)*

P62987 UBA52

CUL5 mediates ubiquitination of ERBB2 1.9e-03, 2/9

Matching identifiers
P07900 HSP90AA1
P62987 UBA52

Metabolism of RNA 2.3e-03, 7/249

- Matching identifiers
    - P62753 RPS6
    - P62316 SNRPD2
    - Q01105 SET
    - Q99436 PSMB7
    - P62987 UBA52

    - Q9Y5S9 RBM8A
    - P05387 RPLP2

3' -UTR-mediated translational regulation 8.6e-03, 4/109

- Matching identifiers
    - P62753 RPS6
    - P20042 EIF2S2
    - P62987 UBA52
    - P05387 RPLP2

Immune System 9.9e-01, 5/1397

- Matching identifiers
    - P09429 HMGB1
    - P27797 CALR
    - P07900 HSP90AA1
    - Q99436 PSMB7
    - P62987 UBA52

    Adaptive Immune System 9.6e-01, 3/866

    - Matching identifiers
        - P27797 CALR
        - Q99436 PSMB7
        - P62987 UBA52

    Class I MHC mediated antigen processing & presentation 4.3e-01, 3/320

    - Matching identifiers
        - P27797 CALR
        - Q99436 PSMB7
        - P62987 UBA52

    Antigen processing-Cross presentation 9.3e-02, 3/145

    - Matching identifiers
        - P27797 CALR
        - Q99436 PSMB7
        - P62987 UBA52

Appendix 1 *(continued)*

ER-Phagosome pathway 7.2e-02, 3/130

- Matching identifiers
    - P27797 CALR
    - Q99436 PSMB7
    - P62987 UBA52

    Proteasomal cleavage of substrate 4.9e-02, 2/48

Matching identifiers
  Q99436 PSMB7
  P62987 UBA52

Total number of events assessed: 7726

Number of matching events (i.e. individual hypergeometric tests performed): 250

Number of genes matching submitted identifiers: 52

Appendix 2 *List of proteins altered by lumiflavin treatment for 6 hours compared with time-control*

UniProt ID	6h Name	Fold change
P07910-2	**HNRNPC** *Isoform C1 of Heterogeneous nuclear ribonucleoproteins C1/C2*	*1.072*
J3KTL2	**SRSF1** *Serine/arginine-rich-splicing factor 1*	*1.143*
Q13247	**SRSF6** *Serine/arginine-rich splicing factor 6*	*1.126*
D6R9W4	**DBN1** *Drebrin (Fragment)*	*1.107*
J3KPP4	**LUC7L3** *Cisplatin resistance-associated overexpressed protein, isoform CRA_b*	*1.101*
P13639	**EEF2** *Elongation factor 2*	*0.907*
Q93079	**HIST1H2BH** *Histone H2B type 1-H*	*0.906*

Fold changes against 1 of control (P<0.05, MTC off)

Appendix 3 *List of proteins altered by lumiflavin treatment for 24 hours compared with time-control*

UniProt ID	24h Name	Fold change	UniProt ID	24h Name	Fold change
Q9H1E3	**UCKS1** *Nuclear ubiquitous casein and cyclin-dependent kinase substrate 1*	*1.538*	M0QXS5	**HNRNPL** *Heterogeneous nuclear ribonucleoprotein L (Fragment)*	*0.342*
Q13242	**SRSF9** *Serine/arginine-rich splicing factor 9*	*1.390*	P62805	**HIST1H4A** *Histone H4*	*0.607*
P84103	**SRSF3** *Serine/arginine-rich splicing factor 3*	*1.372*	K7EK07	**H3F3B** *Histone H3 (Fragment)*	*0.646*
E7ET93	**GABRE** *REVERSED Gamma-aminobutyric acid receptor subunit epsilon*	*1.354*	P07437	**TUBB** *Tubulin beta chain*	*0.705*
C9JAB2	**SRSF7** *Serine/arginine-rich-splicing factor 7*	*1.328*	Q99878	**HIST1H2AJ** *Histone H2A type 1-J*	*0.719*
J3KTL2	**SRSF1** *Serine/arginine-rich-splicing factor 1*	*1.315*	B4DTG2	**EEF1G** *Elongation factor 1-gamma*	*0.737*
B8ZZQ6	**PTMA** *Thymosin alpha-1*	*1.297*	Q15233	**NONO** *Non-POU domain-containing octamer-binding protein*	*0.739*
P19338	**NCL** *Nucleolin*	*1.259*	J3QK90	**NSFL1C** *NSFL1 cofactor p47*	*0.740*
P26368	**U2AF2** *Splicing factor U2AF 65 kDa subunit*	*1.253*	F5H5D3	**TUBA1C** *Tubulin alpha-1C chain*	*0.755*
Q13247	**SRSF6** *Serine/arginine-rich splicing factor 6*	*1.250*	P07237	**P4HB** *Protein disulfide-isomerase*	*0.759*
E7EX17	**EIF4B** *Eukaryotic translation initiation factor 4B*	*1.246*	P23246	**SFPQ** *Splicing factor, proline- and glutamine-rich*	*0.761*

Fold changes against 1 of control (P<0.05, MTC off)

Appendix 3 *List of proteins altered by lumiflavin treatment for 24 hours compared with time-control (continued)*

UniProt ID	24h Name	Fold change	UniProt ID	24h Name	Fold change
E7ES08	**HMGB3** *High mobility group protein B3 (Fragment)*	*1.243*	Q93079	**HIST1H2BH** *Histone H2B type 1-H*	*0.817*
Q99436	**PSMB7** *Proteasome subunit beta type-7*	*1.243*	P20042	**EIF2S2** *Eukaryotic translation initiation factor 2 subunit 2*	*0.823*
P62995	**TRA2B** *Transformer-2 protein homolog beta*	*1.242*	Q16555	**DPYSL2** *Dihydropyrimidinase-related protein 2*	*0.833*
H7BYM6	**HMGA1** *High mobility group protein HMG-I/HMG-Y*	*1.229*	E9PB51	**RBM4** *RNA-binding protein 4 (Fragment)*	*0.843*
P49006	**MARCKSL1** *MARCKS-related protein*	*1.227*	F8VXL2	**DYNLL1** *Dynein light chain 1, cytoplasmic*	*0.850*
P20290	**BTF3** *Transcription factor BTF3*	*1.227*	P13639	**EEF2** *Elongation factor 2*	*0.851*
P07686	**HEXB** *Beta-hexosaminidase subunit beta*	*1.227*	P62987	**UBA52** *Ubiquitin-60S ribosomal protein L40*	*0.862*
M0QXD6	**GTF2F1** *General transcription factor IIF subunit 1 (Fragment)*	*1.217*	Q9NZI8	**IGF2BP1** *Insulin-like growth factor 2 mRNA-binding protein 1*	*0.862*
Q14498	**RBM39** *RNA-binding protein 39*	*1.209*	J3QLI9	**SNRPD1** *Small nuclear ribonucleoprotein Sm D1*	*0.869*
F5H7R9	**PTMS** *Parathymosin (Fragment)*	*1.207*	P31947	**SFN** *14-3-3 protein sigma*	*0.876*
P26583	**HMGB2** *High mobility group protein B2*	*1.204*	Q8NC51	**SERBP1** *Plasminogen activator inhibitor 1 RNA-binding protein*	*0.877*
Q92688	**ANP32B** *Acidic leucine-rich nuclear phosphoprotein 32 family member B*	*1.197*	G8JLB6	**HNRNPH1** *Heterogeneous nuclear ribonucleoprotein H*	*0.878*
Q9Y5S9	**RBM8A** *RNA-binding protein 8A*	*1.191*	P27797	**CALR** *Calreticulin*	*0.884*
Q01081	**U2AF1** *Splicing factor U2AF 35 kDa subunit*	*1.189*	Q9Y2X3	**NOP58** *Nucleolar protein 58*	*0.889*
Q5JWU6	**TPD52L2** *Tumor protein D52-like 2, isoform CRA_e*	*1.178*	F8WA83	**PDIA6** *Protein disulfide-isomerase A6*	*0.889*
P07910-2	**HNRNPC** *Isoform C1 of Heterogeneous nuclear ribonucleoproteins C1/C2*	*1.176*	O43143	**DHX15** *Putative pre-mRNA-splicing factor ATP-dependent RNA helicase DHX15*	*0.894*
P05387	**RPLP2** *60S acidic ribosomal protein P2*	*1.169*	Q9Y5M8	**SRPRB** *Signal recognition particle receptor subunit beta*	*0.896*
B4E135	**LIG1** *DNA ligase 1*	*1.164*	O60884	**DNAJA2** *DnaJ homolog subfamily A member 2*	*0.899*
P09429	**HMGB1** *High mobility group protein B1*	*1.161*			
D6R9W4	**DBN1** *Drebrin (Fragment)*	*1.158*			
E9PM92	**C11orf58** *Protein C11orf58 (Fragment)*	*1.158*			

Fold changes against 1 of control (P<0.05, MTC off)

Appendix 3 *List of proteins altered by lumiflavin treatment for 24 hours compared with time-control (continued)*

UniProt ID	24h Name	Fold change
G3V1X9	**CBX5** *Chromobox homolog 5 (HP1 alpha homolog, Drosophila), isoform CRA_a*	*1.155*
O75531	**BANF1** *Barrier-to-autointegration factor*	*1.150*
P08254	**MMP3** *Stromelysin-1*	*1.144*
P62753	**RPS6** *40S ribosomal protein S6*	*1.143*
Q7Z6L1	**TECPR1** *REVERSED Tectonin beta-propeller repeat-containing protein 1*	*1.141*
B1AKZ5	**PEA15** *Astrocytic phosphoprotein PEA-15*	*1.139*
A8MYV2	**LUC7L** *LUC7-like (S. cerevisiae)*	*1.136*
P08621	**SNRNP70** *U1 small nuclear ribonucleoprotein 70 kDa*	*1.136*
J3KPP4	**LUC7L3** *Cisplatin resistance-associated overexpressed protein, isoform CRA_b*	*1.132*
H0YN26	**ANP32A** *Acidic leucine-rich nuclear phosphoprotein 32 family member A*	*1.131*
Q13243	**SRSF5** *Serine/arginine-rich splicing factor 5*	*1.126*
Q5QPL9	**RALY** *RNA-binding protein Raly (Fragment)*	*1.117*
H7C2Q8	**EBNA1BP2** *EBNA1 binding protein 2, isoform CRA_d*	*1.116*
F5H8H3	**STARD10** *PCTP-like protein*	*1.114*
P51858	**HDGF** *Hepatoma-derived growth factor*	*1.114*
Q9BR76	**CORO1B** *Coronin-1B*	*1.112*
Q9Y266	**NUDC** *Nuclear migration protein nudC*	*1.112*
Q9Y383-2	**LUC7L2** *Isoform 2 of Putative RNA-binding protein Luc7-like 2*	*1.108*
K7ELL7	**PRKCSH** *Glucosidase 2 subunit beta*	*1.105*
Q9UHB6	**LIMA1** *LIM domain and actin-binding protein 1*	*1.105*
E7EUT4	**GAPDH** *Glyceraldehyde-3-phosphate dehydrogenase*	*1.103*

Fold changes against 1 of control (P<0.05, MTC off)

184

Appendix 4 *List of proteins altered by 6 hours lumiflavin compared with 0hour control*

UniProt ID	6h LF Name	Fold change
Q13242	**SRSF9** *Serine/arginine-rich splicing factor 9*	1.135
F5GWN7	**SNAP91** *Clathrin coat assembly protein AP180*	1.131
P84103	**SRSF3** *Serine/arginine-rich splicing factor 3*	1.130
J3KTL2	**SRSF1** *Serine/arginine-rich-splicing factor 1*	1.111
P07910-2	**HNRNPC** *Isoform C1 of Heterogeneous nuclear ribonucleoproteins C1/C2*	1.083
P16401	**HIST1H1B** *Histone H1.5*	0.859
P16403	**HIST1H1C** *Histone H1.2*	0.859

Fold changes against 1 of control (P<0.05, MTC off)

Appendix 5 *List of proteins altered by 24 hours control compared with 0hour control*

UniProt ID	24h control Name	Fold change	UniProt ID	24h control Name	Fold change
P62805	**HIST1H4A** *Histone H4*	1.432	Q9H1E3	**NUCKS1** *Nuclear ubiquitous casein and cyclin-dependent kinase substrate 1*	0.714
P07437	**TUBB** *Tubulin beta chain*	1.366	B8ZZQ6	**PTMA** *Thymosin alpha-1*	0.733
Q99878	**HIST1H2AJ** *Histone H2A type 1-J*	1.337	P49006	**MARCKSL1** *MARCKS-related protein*	0.751
P07237	**P4HB** *Protein disulfide-isomerase*	1.325	E7ES08	**HMGB3** *High mobility group protein B3 (Fragment)*	0.766
Q15233	**NONO** *Non-POU domain-containing octamer-binding protein*	1.318	Q13242	**SRSF9** *Serine/arginine-rich splicing factor 9*	0.783
P23246	**SFPQ** *Splicing factor, proline- and glutamine-rich*	1.308	P05387	**RPLP2** *60S acidic ribosomal protein P2*	0.784
J3QK90	**NSFL1C** *NSFL1 cofactor p47*	1.244	C9JAB2	**SRSF7** *Serine/arginine-rich-splicing factor 7*	0.787
Q93079	**HIST1H2BH** *Histone H2B type 1-H*	1.233	P53999	**SUB1** *Activated RNA polymerase II transcriptional coactivator p15*	0.787
F5H5D3	**TUBA1C** *Tubulin alpha-1C chain*	1.229	P19338	**NCL** *Nucleolin*	0.794
Q9NZI8	**IGF2BP1** *Insulin-like growth factor 2 mRNA-binding protein 1*	1.214	P28074	**PSMB5** *Proteasome subunit beta type-5*	0.797
M0R2B8	**SNRPA** *U1 small nuclear ribonucleoprotein A (Fragment)*	1.200	P84103	**SRSF3** *Serine/arginine-rich splicing factor 3*	0.802

Fold changes against 1 of control (P<0.05, MTC off)

Appendix 5 *List of proteins altered by 24 hours control compared with 0hour control (continued)*

UniProt ID	24h control Name	Fold change	UniProt ID	24h control Name	Fold change
P34931	**HSPA1L** *Heat shock 70 kDa protein 1-like*	*1.181*	P16401	**HIST1H1B** *Histone H1.5*	*0.808*
F8VXL2	**DYNLL1** *Dynein light chain 1, cytoplasmic*	*1.162*	E9PM92	**C11orf58** *Protein C11orf58 (Fragment)*	*0.812*
P20042	**EIF2S2** *Eukaryotic translation initiation factor 2 subunit 2*	*1.150*	Q92688	**ANP32B** *Acidic leucine-rich nuclear phosphoprotein 32 family member B*	*0.813*
G8JLB6	**HNRNPH1** *Heterogeneous nuclear ribonucleoprotein H*	*1.142*	P26583	**HMGB2** *High mobility group protein B2*	*0.815*
E9PRY8	**EEF1D** *Elongation factor 1-delta*	*1.142*	E7ET93	**GABRE** *REVERSED Gamma-aminobutyric acid receptor subunit epsilon*	*0.816*
E9PJF4	**CLNS1A** *Methylosome subunit pICln*	*1.138*	F5H7R9	**PTMS** *Parathymosin (Fragment)*	*0.817*
Q8NC51	**SERBP1** *Plasminogen activator inhibitor 1 RNA-binding protein*	*1.127*	P16403	**HIST1H1C** *Histone H1.2*	*0.819*
Q12906-4	**ILF3** *Isoform 4 of Interleukin enhancer-binding factor 3*	*1.124*	J3KTL2	**SRSF1** *Serine/arginine-rich-splicing factor 1*	*0.822*
O43143	**DHX15** *Putative pre-mRNA-splicing factor ATP-dependent RNA helicase DHX15*	*1.124*	Q01105	**SET** *Protein SET*	*0.826*
I3L4N8	**ACTG1** *Actin, cytoplasmic 2, N-terminally processed (Fragment)*	*1.119*	Q13247	**SRSF6** *Serine/arginine-rich splicing factor 6*	*0.827*
P24534	**EEF1B2** *Elongation factor 1-beta*	*1.116*	D6R9W4	**DBN1** *Drebrin (Fragment)*	*0.837*
Q9Y5M8	**SRPRB** *Signal recognition particle receptor subunit beta*	*1.115*	P09429	**HMGB1** *High mobility group protein B1*	*0.842*
H3BRV0	**EIF3C** *Eukaryotic translation initiation factor 3 subunit C*	*1.111*	Q9Y5S9	**RBM8A** *RNA-binding protein 8A*	*0.843*
B7TY16	**ACTN1** *Actinin alpha 1 isoform 3*	*1.110*	G3V1X9	**CBX5** *Chromobox homolog 5 (HP1 alpha homolog, Drosophila), isoform CRA_a*	*0.844*
F8WA83	**PDIA6** *Protein disulfide-isomerase A6*	*1.106*	P62995	**TRA2B** *Transformer-2 protein homolog beta*	*0.845*
P13667	**PDIA4** *Protein disulfide-isomerase A4*	*1.103*	Q99436	**PSMB7** *Proteasome subunit beta type-7*	*0.849*
			E7EX17	**EIF4B** *Eukaryotic translation initiation factor 4B*	*0.850*
			B1AKZ5	**PEA15** *Astrocytic phosphoprotein PEA-15*	*0.851*
			P07686	**HEXB** *Beta-hexosaminidase subunit beta*	*0.858*
			P26368	**U2AF2** *Splicing factor U2AF 65 kDa subunit*	*0.862*
			Q5JWU6	**TPD52L2** *Tumor protein D52-like 2, isoform CRA_e*	*0.863*
			H0YN26	**ANP32A** *Acidic leucine-rich nuclear phosphoprotein 32 family member A*	*0.865*

Fold changes against 1 of control (P<0.05, MTC off)

Appendix 5 *List of proteins altered by 24 hours control compared with 0hour control (continued)*

UniProt ID	24h control Name	Fold change
O14737	**PDCD5** *Programmed cell death protein 5*	*0.876*
B5MD17	**CBX1** *Chromobox protein homolog 1 (Fragment)*	*0.876*
M0QXD6	**GTF2F1** *General transcription factor IIF subunit 1 (Fragment)*	*0.880*
P51858	**HDGF** *Hepatoma-derived growth factor*	*0.887*
Q9BQ61	**C19orf43** *Uncharacterized protein C19orf43*	*0.889*
H7BYM6	**HMGA1** *High mobility group protein HMG-I/HMG-Y*	*0.891*
P08254	**MMP3** *Stromelysin-1*	*0.893*

Fold changes against 1 of control (P<0.05, MTC off)

Appendix 6 *List of proteins altered by 24 hours lumiflavin compared with 0hour control*

UniProt ID	24h LF Name	Fold change
P16401	**HIST1H1B** *Histone H1.5*	*0.724*
P16403	**HIST1H1C** *Histone H1.2*	*0.739*
K7EK07	**H3F3B** *Histone H3 (Fragment)*	*0.763*
P28074	**PSMB5** *Proteasome subunit beta type-5*	*0.780*
P53999	**SUB1** *Activated RNA polymerase II transcriptional coactivator p15*	*0.837*
P14625	**HSP90B1** *Endoplasmin*	*0.896*
B4DN89	**SRSF2** *Serine/arginine-rich-splicing factor 2*	*1.136*
E7ET93	**GABRE** *REVERSED Gamma-aminobutyric acid receptor subunit epsilon*	*1.100*

Fold changes against 1 of control (P<0.05, MTC off)